MODELING VARIATIONS OF THE SEASONAL CYCLE OF PLANKTON PRODUCTION: THE LABRADOR SEA, LABRADOR SHELF AND HAMILTON INLET

DIANA CARDOSO

MODELING VARIATIONS OF THE SEASONAL CYCLE OF PLANKTON PRODUCTION: THE LABRADOR SEA, LABRADOR SHELF AND HAMILTON INLET

By

© Diana Cardoso

A thesis submitted to the school of Graduate Studies in partial fulfillment of the requirements for the degree of Masters of Science

Environmental Science Graduate Program

Memorial University of Newfoundland

April, 2004

St. John's **Newfoundland** **Canada**

Abstract

Changes in phytoplankton production can have a profound impact on the marine ecosystem. One factor that can affect phytoplankton populations is change in stratification of the water column. Climate changes over the Labrador Sea and Labrador Shelf have significantly altered the stratification of these regions. Regulation of the Churchill River flow, due to hydroelectric development, has influenced the stratification of Hamilton Inlet of coastal Labrador. Observations in the Labrador region are inadequate to determine the influence of stratification variability on the marine ecosystem. The goal of this research was to integrate the available data with simplified ecosystem models to enhance our understanding. To investigate the sensitivity of seasonal plankton dynamics to climate-induced changes in stratification of the Labrador Sea and Shelf, distinct periods of natural variability were used to force the model. The model was also used to investigate the impact of altering freshwater flow into Hamilton Inlet before and after hydroelectric development. The model exhibited distinct seasonal plankton dynamics that match the existing chlorophyll measurements from each region reasonably well. It was found that in the Labrador Sea and Shelf, when the North Atlantic Oscillation index was positive the spring bloom was delayed. The total annual phytoplankton biomass in the Sea increased while on the Shelf it remained unchanged. In Hamilton Inlet after hydroelectric development, the model showed that the timing of the spring bloom remained unchanged but the total annual biomass decreased. The primary production in the Inlet also decreased after 1976 by about 25%, while for the Shelf there was little difference in primary production.

Acknowledgements

I would like to thank Dr. Brad deYoung and Dr. Joe Wroblewski for offering me this opportunity to participate in a challenging and exciting research project as part of my graduate degree program. I am grateful for their patience, insight and guidance during the course of this thesis. Several scientists at the Bedford Institute of Oceanography provided useful data: Brain Petrie provided SeaWiFS and biological and physical oceanographic data. Igor Yashayaev provided an extensive physical data set averaged yearly from 1948 to 2001 and Ken Drinkwater provided Hamilton Inlet data. I am grateful to Newfoundland and Labrador Hydro for sharing data and insight. I Also thank Chris Stevenson for the continuous computer support and assistance.

Support for this research was provided by the Coasts Under Stress project (J. Wrobleski) funded by The Social Sciences and Humanities Research Council of Canada (SSHRC) and the Natural Sciences and Engineering Research Council (NSERC) through the SSHRC Major Collaborative Research Initiatives program and the Office of the Vice-President (Research and International Relations) of Memorial University and NSERC (B. deYoung). Personal support included the Wild Things Scholarship from the National History Society of Newfoundland and Labrador, a Graduate Study Fellowship and teaching assistantships from the Department of Physics and Physical Oceanography.

I would like to thank Michael Elliott for supporting me and coming with me to Newfoundland. His love, understanding and patience was much appreciated and kept me focused on my goals. My parents, Maria and Tony Cardoso, for their continuous support, their positive outlook and weekly phone calls.

Table of Contents

List of Tables

List of Figures

List of Abbreviations

BIO	Bedford Institute of Oceanography
CIL	Cold Intermediate Layer
CPR	Continuous Plankton Recorder
CZCS	Coastal Zone Color Scanner
DFO	Department of Fisheries and Oceans
DSOW	Denmark Strait Overflow Water
ISW	Irminger Sea Water
LSW	Labrador Sea Water
LS1	Labrador Sea sub-region 1
MESD	Marine Environmental Science Division
NAFO	North Atlantic Fisheries Organization
NAO	North Atlantic Oscillation
NASA	National Aeronautics and Space Administration
NEADW	North East Atlantic Deep Water
NOAA	National Oceanic and Atmospheric Administration
NOCD	National Oceanographic Center
NODC	National Oceanographic Data Center
NPZD	Nutrient-Phytoplankton-Zooplankton-Detritus
NPZ	Nutrient-Phytoplankton-Zooplankton
NWADW	North West Atlantic Deep Water

OLABS	Offshore Labrador Biological Studies Program
OWS-P	Ocean Weather Station Papa
OWS-B	Ocean Weather Station Bravo
SeaWiFS	Sea-viewing Wide Field-of-view Sensor

CHAPTER 1

Introduction

1.1. Overview

Phytoplankton, are the principal source of organic matter that sustains the food chain in the ocean. Changes in abundance or distribution of phytoplankton can have a profound impact on the ecosystem, causing changes in zooplankton and larger predator populations. Phytoplankton production is mainly regulated by the depth of the mixed-layer, the intensity of the solar radiation which penetrates the mixed-layer and the concentration of dissolved nutrients with depth (Sverdrup, 1953, Wroblewski *et al.*, 1988). In general the mixing time of water in the mixed-layer is fast relative to plankton motility and population response. For example, surface gravity waves which circulate plankton in the upper few meters have periods of several seconds while the turnover times of algal populations are one to several days (Denman and Powell, 1984). Therefore, when the mixed-layer is deeper than a certain critical depth known as "the Sverdrup depth" the rate of photosynthesis is light limited. The mixed-layer depth sets the light level which each phytoplankton cell is exposed to as it is mixed from the base of the mixed-layer to the surface. When the depth of the mixed-layer shallows above the critical depth in spring due to the thermal stratification, primary production is increased leading to a spring bloom (Sverdrup, 1953). Though primary production can be high when solar radiation increases in spring and summer, nutrients are also essential for primary production. Since phytoplankton grow in the surface layer, transport and

entrainment of nutrients to the surface layer is essential. Strong stratification limits the vertical transfer of nutrients from layers below the euphotic zone and sustaining productivity becomes reliant on regeneration of nutrients within the mixed-layer. Once nutrients are depleted, which occurs following a phytoplankton bloom, primary production is reduced. This is the typical situation found in tropical oceans; however, seasonal changes in temperature and winds reduce the stratification and vertical transport of nutrients to the mixed-layer occurs (Mann and Lazier, 1996). At mid-latitudes nutrient concentration is high in the winter due to the deep convection, and production is at a minimum because of the reduced solar radiation and the great depth of the mixed-layer. In spring, the water column stabilizes, nutrients become trapped in the surface layer, solar radiation increases and production reaches a maximum. When phytoplankton deplete the nutrients in the mixed-layer by late summer, grazing is maximized leading to a peak in zooplankton. In autumn, mixing increases and stratification begins to breakdown, nutrients are replenished in the surface layer, and primary production often increases depending on whether there is sufficient solar input. The density gradient determines the mixed-layer depth and density is dependent on temperature and salinity. At the surface, salinity is affected by precipitation, evaporation and temperature by solar heating and cooling. Below the surface, salinity and temperature change by mixing with other water masses (Raymont, 1980). In the open ocean, salinity changes are usually small and density is mainly controlled by temperature. In coastal regions there are large salinity gradients due to continental run off, river discharge and tides (Pickard and Emery, 1982). Coastal inlets with freshwater inflow form an estuarine environment in which fresh river

water interacts directly with saline coastal waters forming strong vertical and horizontal salinity gradients.

The Labrador Sea in the Northwest Atlantic (Figure 1.1) is a region with high nitrate and chlorophyll concentrations, a pronounced spring bloom in phytoplankton, and depletion of nitrate in the surface layer in summer (Siegel *et al.*, 2002). Intense winter storms cause vertical mixing and deep convection, eliminating the surface mixed-layer and minimizing primary production. This allows nutrients to be advected to the surface waters and leads to high rates of biological productivity in spring and early summer (Tian *et al.*, 2004). However, the intensity of this deep convection during winter is regulated by climate variations, which in turn cause variations in biological productivity (Tian *et al.*, 2004). There have been distinct climate change events in the Labrador Sea over the last 50 years that have altered the deep convection (Lazier *et al.*, 2002; Pickart *et al.*, 2003; Yashayaev, 2002). In the late 1960s, warmer weather over the Northwest Atlantic increased the surface freshwater content by the equivalent of 1.4 m, an event known as the Great Salinity Anomaly (Dickson et al., 1988b). The winter convection depth was reduced to 200 m in 1969 to 1971 from deeper than approximately 800 m in other years (Tian *et al.*, 2004; Lazier *et al.*, 2002). In the first half of the 1990s cold weather prevailed and increased the intensity and frequency of winter storms, which lead to the deepest convection (2300 m) recorded over the last 50 years in the winter of 1992 (Yashayaev, 2002).

Hamilton Inlet is made up of Goose Bay, Lake Melville, and Groswater Bay that opens onto the Labrador Shelf. Along with being the largest inlet along the Labrador

coast it is also the point of discharge for the largest river in Labrador, the Churchill River. Study of Hamilton Inlet is important for the economic development of the area and determining the environmental risk of these developments. There is currently one hydroelectric generating station at Churchill Falls, completed in 1971. As a result, hundreds of existing lakes and bogs were linked to form the Smallwood Reservoir from which water is released. This alteration increased the drainage area into Lake Melville and has the potential to change the Lake circulation, nutrient transport, and stratification and could therefore affect the coastal ecosystem. It is now proposed to build further hydroelectric stations in the lower Churchill River at Gull Island and Muskrat Falls (Hydro Lower Churchill Development Corporation Ltd., Environmental Impact Statement, 1980). This development could cause greater changes in the water circulation and properties of Hamilton Inlet and affect the fishing industry.

This study investigated the sensitivity of seasonal plankton dynamics to changes in stratification on the open ocean of the Labrador Sea, the continental Labrador Shelf south of 55°N and the coastal Hamilton Inlet along the Labrador coast (Figure 1.1). To investigate the sensitivity in the Labrador Sea and Shelf of seasonal plankton dynamics in the mixed-layer to climate induced changes in stratification, the data from the distinct periods of natural variability are used to force an ecosystem model. The model was run with historical data collected at Ocean Station Bravo in the central Labrador Sea (56°30 ° N, 52 ° 30 ° W) during the warm period (1968) and from Bravo and the surrounding sea during the cold period (1991 to 1999). The model was also run for the Labrador Shelf during the same warm and cold periods, however, the Shelf data were sparser. To

investigate the sensitivity in Hamilton Inlet of the plankton dynamics in the mixed-layer to changes in freshwater flow, data from before and after the hydroelectric development was used to force the ecosystem model. The model was run for both Hamilton Inlet and the Labrador Shelf over the same time periods. The models were verified against biological and chemical data obtained from the Bedford Institute of Oceanography (BIO) database, the Continuous Plankton Recorder program (CPR), the Coastal Zone Colour Scanner program (CZCS), studies by industry, and results from other similar model studies.

This modeling investigation will attempt to determine the sensitivity of the seasonal plankton dynamics to changes in salinity gradients as a result of climate change in the Labrador Sea and Shelf and as a result of freshwater flow changes in Hamilton Inlet. The model estimate of plankton production can then be used to predict possible impacts on fish production. However, the relationship between primary production and fishery production remains poorly understood (Tian *et al.*, 2001). Generally high phytoplankton production in the Labrador Shelf region supports important marine ecosystems and commercial fisheries. The coastal zone which only makes up 20% of the global oceans accounts for half of the global marine primary production (Tian *et al.*, 2001). As a result, most of the world fisheries are located on the coasts (Tian *et al.*, 2001). Recent dramatic declines of ground fish stocks have highlighted the need to understand natural and anthropogenic variations on the Labrador coast (Loder *et al.*, 1995). Several studies have investigated the affect of climate changes in the Labrador Sea and Shelf on fish production (e.g. deYoung and Rose, 1993; Drinkwater, 1994;

Taggart *et al.*, 1994, Rose *et al.* 2000). There were also concerns about hydropower development on the Churchill River affecting fish stocks in Groswater Bay (Saunders, 1981). It is hypothesized that increased freshwater discharge to Lake Melville and regulation of Churchill River discharge resulting from hydropower development may result in significant changes to the nutrient budget, to the circulation and to entrainment of nutrients, which may therefore alter the plankton ecosystem in Hamilton Inlet. There was one study completed by Bobbitt and Akenhead (1982) to investigate the influence of changes in discharge from Churchill River on the oceanography of Groswater Bay. They concluded that variations in freshwater flow did not significantly alter the water properties in Groswater Bay. This conclusion was based on measurements from June to August in early 1950s and August 1981. However, the question remains how does the plankton ecosystem respond to the variability in freshwater flow? Also, it is hypothesized that the climate changes over the Labrador Sea that significantly altered the temperature, salinity and the mixed-layer, will affect the seasonal plankton dynamics. In summary this modeling study will attempt to determine whether:

i. The Churchill River significantly contributes to the nutrient budget of Hamilton Inlet, which may affect the abundance and seasonal dynamics of the planktonic ecosystem in Hamilton Inlet and the Labrador Shelf.
ii. The Churchill River flow significantly contributes to the circulation and entrainment of nutrients in Hamilton Inlet, which may affect the abundance and seasonal dynamics of the planktonic ecosystem in Hamilton Inlet and the Labrador Shelf.
iii. Past climate change events affect the abundance and seasonal dynamics of the planktonic ecosystem in the Labrador Sea and Shelf.

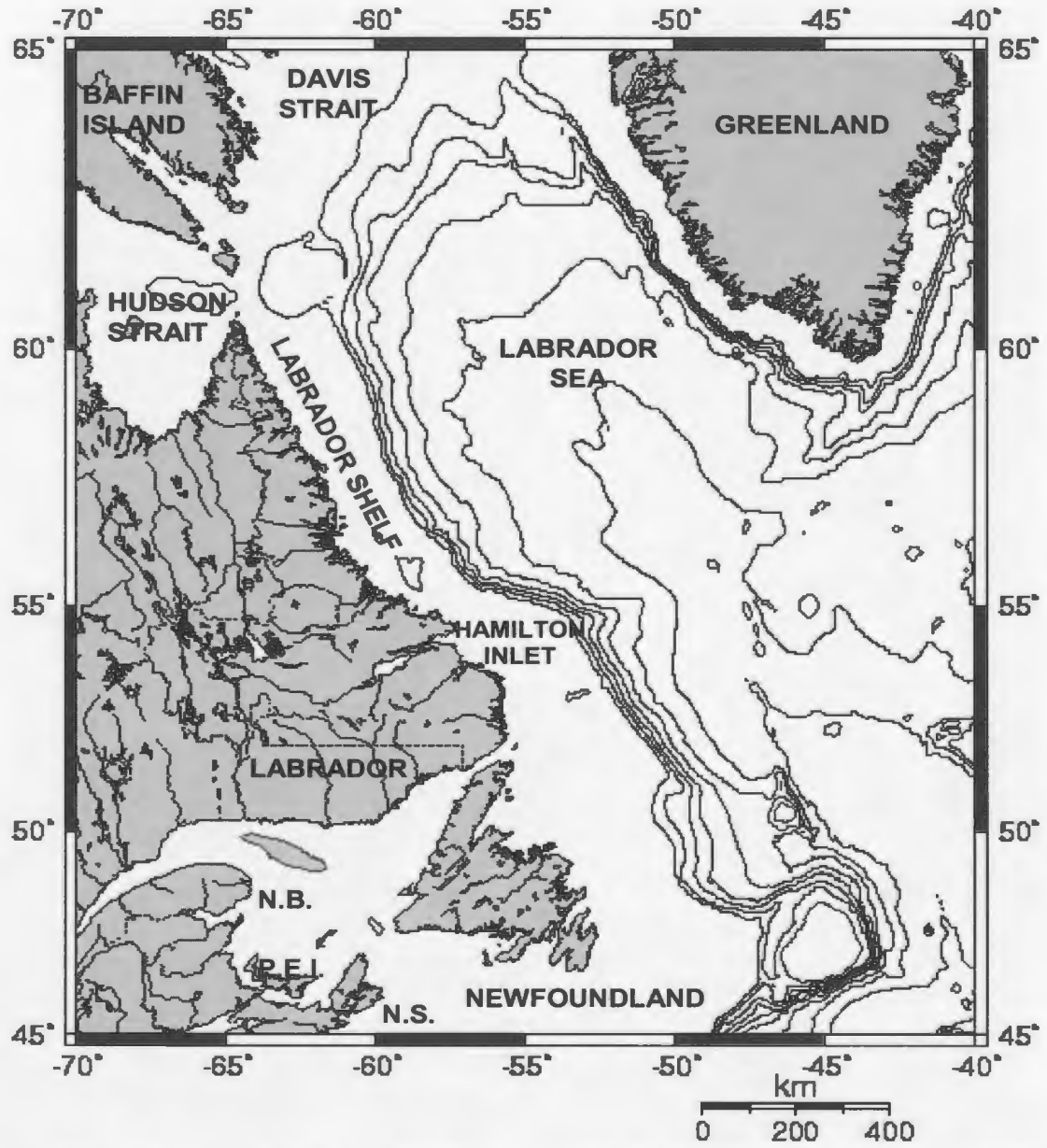

Figure 1.1: A map of the Labrador Sea region in the Northwest sub Arctic Atlantic Ocean between Labrador and Greenland. Contour lines are every 500 m.

1.2. Physical and Biological Processes: Each Region

1.2.1. Labrador Sea

The Labrador Sea is located south of the Davis Strait, between the Canadian east coast and Greenland, and north of the oceanic polar front. The Sea is bounded on almost all sides by; the West Greenland Current, the Labrador Current and the North Atlantic Current (Figure 1.2). The West Greenland and Labrador Currents are narrow (~100 km), strong (~40 cm/s at the surface) and travel along the continental slopes (Lazier, 1982; Myers *et al.*, 1990; Lazier and Wright, 1993; Colbourne, 2000). The North Atlantic Current, to the south, is an eastward extension of the northern branch of the Gulf Stream (Lazier, 1980). Away from the boundary currents, in the center of the Labrador Sea, flow is much slower and is on average cyclonic. The top 1500 m water mass is a mixture of cold, fresh, polar water transported south by the Labrador Current and warmer, saltier water transported by the West Greenland Current (Lazier, 1980) from the Irminger Sea. The surface layer of the Labrador Sea has relatively high temperature and salinity values, despite the significant freshwater inputs to the sea from precipitation, ice melt, and river runoff. At depths below 1500 m, the North Atlantic Current transports warmer water to the Labrador Sea. There are three major water masses in the Labrador Sea; two are in the deep layer, the North West Atlantic Deep Water (NWADW) and the North East Atlantic Deep Water (NEADW) and in the intermediate layer, the Labrador Sea Water (LSW) (Figure 1.3). The NWADW is the deepest and densest water mass in the Labrador Sea and it is composed mainly of Denmark Strait Overflow Water (DSOW). The NEADW

lies above the NWADW and has warmer temperatures and a local salinity maximum. The LSW occurs at mid depths across the North Atlantic north of 40°N and can reach depths of 2000 m (Myers *et al*, 1990). The LSW is weakly stratified, fresher, and colder at 34.83 ppt and 2.8 °C respectively and has a low potential vorticity relative to its surroundings (Figure 1.3). The LSW is formed in the Labrador Sea as a result of deep winter convection, which is discussed in detail in the next section. However, Pickart *et al.* (2003) contested this statement and showed evidence that LSW can also be formed in the Irminger Sea.

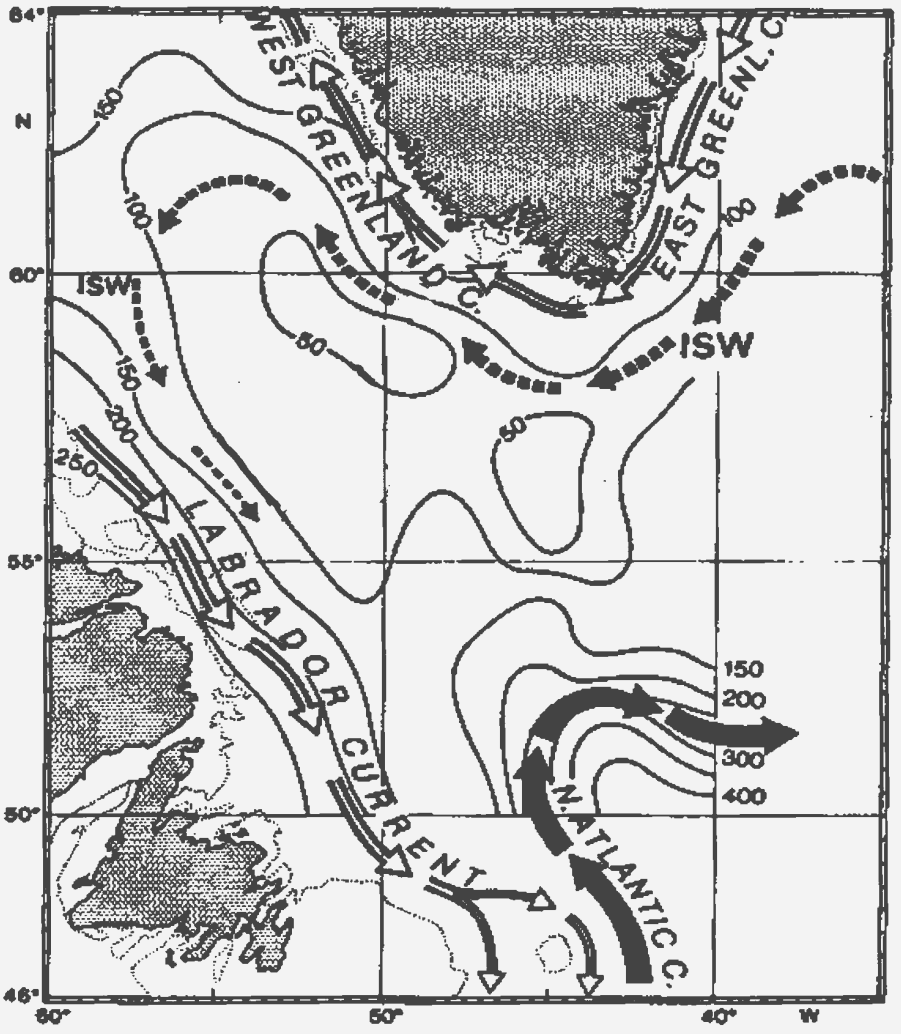

Figure 1.2: Circulation schematic with the depth of the 27.6 isopycnal in the early winter. Includes: The warm and salty circulation branches of the North Atlantic Current (solid arrows) and Irminger Sea Water (ISW) (dashed arrows), and the near surface, cold and fresh East/West Greenland and Labrador Current (open arrows) (Modified from The Labrador Sea Deep Convection Experiment, 1998).

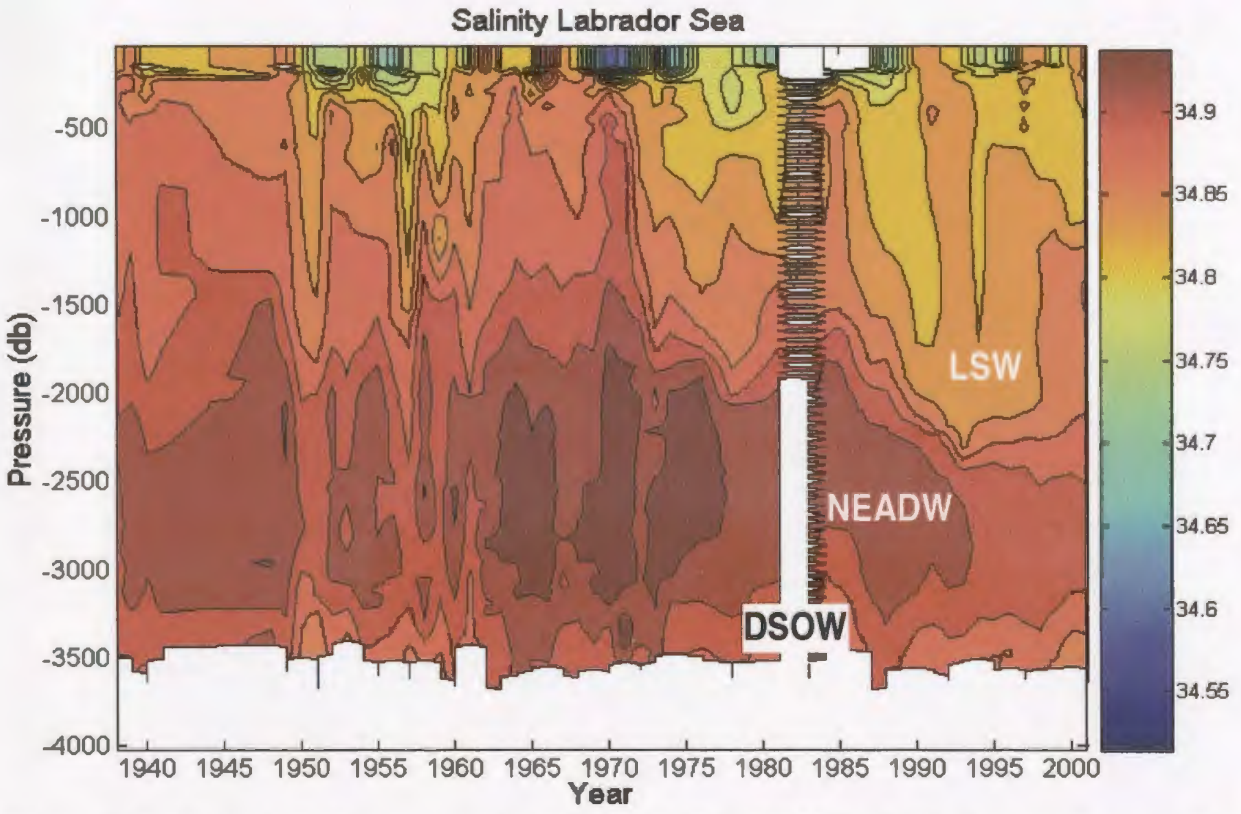

Figure 1.3: Historical data summarized from 1940 to 2000 by I. Yashayaev (personal communication, BIO). Salinity (colours and black contour lines) in pressure-time coordinates.

a) Convection in the Labrador Sea

Weather conditions in the Labrador Sea region can be extreme, especially in the winter. During the winter, cold, dry Arctic air passes over the Sea causing heat loss at the surface, which leads to convection. Convection and the resulting mixing occurs in the mixed-layer at the surface of the ocean, but such convection differs distinctly from deep convection where the surface forcing, which eliminates the thermocline, enables mixing to occur to uncommonly great depths. Convection occurs when meteorological conditions become sufficiently intense to overcome the vertical density stratification and

the surface buoyancy forcing exceeds a critical level. This leads to mixing of the water column and the surface layer deepens, forming a homogeneous column of water to a certain depth. Once the surface forcing subsides, convection ceases and the deep column of water begins to decay, breaking into fragments and restratification occurs. There can be surface restratification after just a few days, while the column volume as a whole can restratify within a few weeks (The Labrador Sea Deep Convection Experiment, 1998). Surprisingly there are very few locations where open-ocean deep convection is known to occur. The locations for offshore deep water formation are the Northwest Mediterranean and in the polar regions; in the southern hemisphere in the Weddell and Ross Seas off the Antarctic coast (where Antarctic Bottom Water is formed) and in the northern hemisphere in the Labrador and Greenland Seas (where North Atlantic Deep Water is formed) (The Labrador Sea Deep Convection Experiment, 1998).

The Labrador Sea is an ideal site for convection since there is strong atmospheric forcing, the stratification beneath the surface mixed-layer is weak, there is no ice cover, and the deeper water is brought towards the surface by cyclonic circulation where it can be directly exposed to the surface forcing. In the Labrador Sea, convection occurs during late winter (February/March) and in recent years has penetrated down to 2000 m, which makes this Sea one of the most extreme deep ocean convection sites in the world (The Labrador Sea Deep Convection Experiment, 1998). The most intense deep convection is probably near the Labrador Shelf slope where heat loss from the cold continental winds is most intense.

b) Annual Cycle

There are annual variations of salinity and temperature in the Labrador Sea. The greatest variation is near the surface, where as below 200 m the annual variation decreases rapidly. The annual cycle of surface salinity and temperature tends to stabilize the water column in summer and destabilize it in winter (Lazier, 1980). The magnitude of the seasonal variation in temperature in the central region of the Labrador Sea is approximately 6 °C at 10 m, 1.5 °C at 100 m and 0.2 °C at 1000 m (The Labrador Sea Deep Convection Experiment, 1998; Yashayaev, 2002). The salinity changes from summer and winter at 10 m is 0.2 - 0.3‰ (Lazier, 1980). The surface mixed-layer, which is related to surface heat flux, stratification, and sea-ice, increases through the winter reaching a maximum in late March but by the end of April it is reduced to 50 m (Tang *et al.*, 1999).

c) Climate Changes and the Labrador Sea

The Labrador Sea is an important location for monitoring climate change since in winter there is a large upward heat flux at the sea surface. The Labrador Sea plays a key role in the climate dynamics of the North Atlantic since; i) it has the freshest and coldest water conditions relative to the surrounding waters; ii) it is a major source of intermediate water for the North Atlantic; iii) its great volume makes it a more stable reservoir for climate monitoring; and iv) the two deep layer water masses NWADW and NEADW carry signals from their source in the Nordic Seas (Yashayaev, 2002). The North Atlantic Oscillation (NAO) is used as a climate change indicator and is a measure of the strength of the cyclonic circulation and climate variability (The Labrador Sea Deep Convection

Experiment, 1998). The NAO measures the wintertime sea level pressure difference between Iceland and the Azores. When the NAO index is high, this indicates there is greater cyclonic flow over the North Atlantic and therefore greater circulation of cold Arctic air, stronger storms and hence more heat loss from the sea surface. When the NAO index is low, the opposite is true with an expected reduced heat loss from the sea surface. The NAO index shows a minimum in the 1960s, after which there have been strong oscillations with approximately a 10 year period trend. The peaks in the NAO index occurred in the late 1940s, early 1970s, the mid 1980s, and the 1990s. Between 1948 and 1950 the severe winters lead to extreme heat loss of the ocean and deep convection to approximately 2000 m (Myers *et al.*, 1990). In 1957 and 1972 a similar event occurred in the central Labrador Sea in which convection occurred to about 1500 m. Again during the 1990s the NAO was at an all time high over the last 50 years, the LSW mass became quite large and convection reached depths of 2300 m in 1993 and 1994, the deepest convection ever recorded (The Labrador Sea Deep Convection Experiment, 1998; Yashayaev, 2002). During the 1990s, the Labrador Sea became 0.6°C colder and 0.05 % fresher relative to the late 1960s (Yashayaev, 2002). Yashayaev (2002) reported a long-term cooling of the top 300 m between the1930s and 1980s of 1°C, and warming between 1984 and 1999. The warming trend was interrupted by a period of cooling between 1988 and 1994. Dickson *et al.* (1988b) reported on the Great Salinity Anomaly, a freshening of the upper about 500 m of the North Atlantic in the mid 1960s. He concluded that atmospheric conditions caused the transport of a significant amount of Arctic ice out of the Arctic, which combined with melting, resulted in low salinity values in the Labrador

Sea between 1969 and 1972. This addition of freshwater to the surface layer of water restricted the deep winter convection to 200 m in 1969-1971 (Lazier *et al.*, 2002). Lazier and Wright (1988) reported on a great salinity anomaly of the deep waters of the Labrador Sea in 1967 and 1968. The lowering of salinity, due to the increased freshwater volume, led to stronger stratification thereby reducing vertical mixing and preventing deepening of the mixed-layer and deep convection. Therefore, the strong convection may partially be due to severe winter weather indicated by the NAO index, but may also be due to the currents and the freshwater cycle. Tang *et al.* (1999) reported that a decrease in surface salinity by 1% reduces the mixed-layer depth by 17 to 55%. An increase in wind speed by 40% and decrease in air temperature by up to 4°C, typical of severe winter conditions, doubles the mixed-layer depth.

1.2.2. Labrador Shelf

The Labrador Shelf extends approximately between 200 and 300 km from the coast and the maximum depth varies from 400 to 500 m. The major influences on the Shelf are the Labrador Current, surface heating, and ice. Other important influences include winds and freshwater (Loder *et al.*, 1998). The Labrador Current is concentrated over the break and upper slope of the Shelf with a small branch on the inner Shelf. About 80% of the flow past Labrador is concentrated over the 600-800 m isobaths on the slope and acts as a barrier between the Shelf and offshore waters beyond the 2000 m isobaths (Lazier, 1982). The Labrador Current is made up of subpolar water from three sources; i) the East-West Greenland Current which flows westward; ii) the Baffin Island Current flowing south through the Davis Strait and a small volume through the Hudson Strait; and

iii) outflow from the Hudson Strait. The heat source for the Shelf water varies seasonally; in summer surface heating is dominated from solar radiation while in winter cooling is dominated by heat loss to the cold atmosphere (Loder *et al.*, 1995).

Sea-ice forms on the Shelf and alters the hydrodynamics, temperature, salinity and deep-water formation and serves to partially insulate the ocean. Sea-ice on the Shelf is enhanced by winter cooling, wind, and the Labrador Current, which carries cold water, sea-ice, and icebergs (Loder *et al.*, 1998). Sea-ice begins to appear on the northern Labrador coast in November and remains throughout the winter and early spring. Before the ice arrives the mixed-layer deepens due to the winds and surface cooling. The mixed-layer shallows when the ice cover begins due to the increased buoyancy created by ice melt (Tang and DeTracey, 1998). However, there is little change in mixed-layer depth once the water is covered by ice. Tang and DeTracey (1998) showed that for a 120 m transect across the Newfoundland Shelf the mixed-layer decreased from 80 m in the interior of the pack ice towards the inner Shelf to 25 m at the eastern edge of the Shelf and ice edge. In comparison the open ocean mixed-layer depth with no ice coverage was 150 to 200 m.

The freshwater input to the Shelf comes from the Hudson Strait, continental runoff, melting of Greenland ice cap and ice flows. There have been a few studies on the influence of freshwater input on the Shelf. Tang and DeTracey (1998) investigated the variation in the mixed-layer, heat and salt fluxes, and ice melt across the Shelf caused by ice conditions. Sutcliffe *et al.* (1983) investigated the nutrient flux from the Hudson Strait and the biological consequences. A recent study expanded on Sutcliffe's work to

investigate the effects of the Hudson Strait outflow on the biology of the Labrador Shelf (Drinkwater and Harding, 2001). Drinkwater and Harding (2001) tested whether the Hudson Strait influences primary production on the northern Shelf and if this production initiated a food chain that is advected southward. They found that production on the southern Shelf is more supported by local upwelling and on the northern Shelf, the intense mixing in the Hudson Strait of several water currents elevated the surface nutrient concentrations.

Similar to the Labrador Sea intermediate layer water, the Shelf also has a fresher, colder intermediate layer water (CIL). The CIL is water below 0°C found on the Shelf during late spring to the fall. This CIL extends from the shore to the Shelf break (Figure 1.4). This layer of water remains isolated between the seasonally heated upper layer and the warmer slope water near the bottom from the offshore. The CIL water is separated from the warmer saltier water of the continental slope by a frontal region denoted by a strong horizontal temperature and salinity gradient near the edge of the Shelf (Colbourne and Fitzpatrick, 2002). During the early 1970s and 1990s, corresponding to the cold period and deep convection in the Labrador Sea, the area of the CIL on the Shelf reached record highs. Also, lower salinities were reported in the Labrador Current in 1971 and 1972 at the same time that they were also reported for the Labrador Sea at OWS Bravo (Lazier and Wright, 1993).

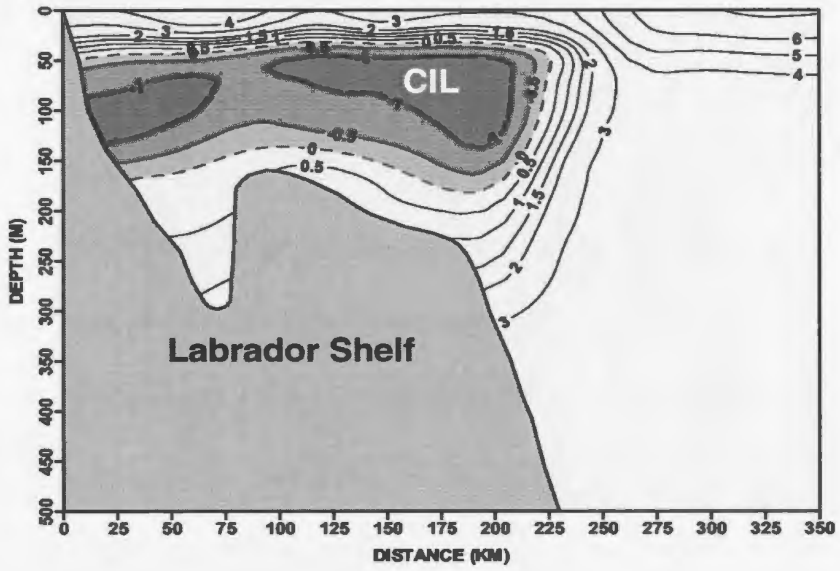

Figure 1.4: Contours of temperature along Seal Island transect (off southern Labrador, Figure 2.1) showing the colder intermediate layer water (CIL) in July 2001. (Modified from Colbourne, 2002).

d) Annual Cycle

Lazier (1982), investigated seasonal variability of temperature and salinity in the Labrador Current. He found that horizontal temperature and salinity gradients are small in the waters over the Shelf relative to the gradients across the slope where the strongest part of the Labrador Current flows. There existed seasonal changes in temperature and salinity to depths of 200 m. He suggested that most of the seasonal changes were a result of advection by the Labrador Current. However, in the summer near the shore on the inner Shelf the horizontal salinity gradient above 30 m is large and, though smaller, still present at 50 and 100 m. On the middle Shelf the horizontal salinity gradient is small at all depths, which indicates that the freshwater influences are restricted to the inner Shelf. For other seasons there is a lack of data due to the harsh weather conditions over the Shelf in winter. Lazier (1982) found in December the horizontal temperature on the

slope changed very little from summer values at 50 m. The salinity gradients in December over the surface layer on the Shelf were much smaller than in summer, most likely due to the reduced run-off. The vertical gradients of temperature and salinity show a distinct annual cycle. Salinity increased with depth over the entire year with a minimum in July and August at the surface below 31 psu as compared to over 33 psu in winter. Seasonal changes in temperature are more complex, the surface temperature reaches a minimum of $-1.5^{\circ}C$ in winter and a maximum of around $7^{\circ}C$ in August. The temperature at 50 m follows the same pattern but with a time delay where the maximum occurs in October and the minimum in March (Lazier, 1982). In the winter the mixed-layer can reach 200 m (Lazier and Wright, 1993). In summer, the mixed-layer depth is quite shallow due to the solar heating and the ice melt, thereby lowering salinity.

1.2.3. Hamilton Inlet

Hamilton Inlet is the largest inlet along the Labrador coast situated at $54^{\circ}N$ and between $60.5^{\circ}W$ and $57^{\circ}W$ (Figure 1.5). Three bodies of water, Goose Bay, Lake Melville and Groswater Bay make up the Hamilton Inlet. Groswater Bay is open to the Labrador Shelf. It is about 55 km in length and constricts into a narrow shallow area about 2.8 km in width, 30 m in depth and 22 km long, called The Narrows at the entrance to Lake Melville. The Lake is approximately 170 km long with a maximum width of over 35 km and average depth of 86 m with a maximum basin depth of over 200 m. Goose Bay is 22 km long, with a basin depth of over 60 m. There are 4 major rivers which discharge into the Inlet, Northwest River, Kenamu River, Goose River and the largest river, the Churchill River (Bobbitt and Akenhead, 1982) (Figure 1.6).

Figure 1.5: Location of Hamilton Inlet along the Labrador Coast highlighted by the blue box (Adapted from www.Mapquest.com).

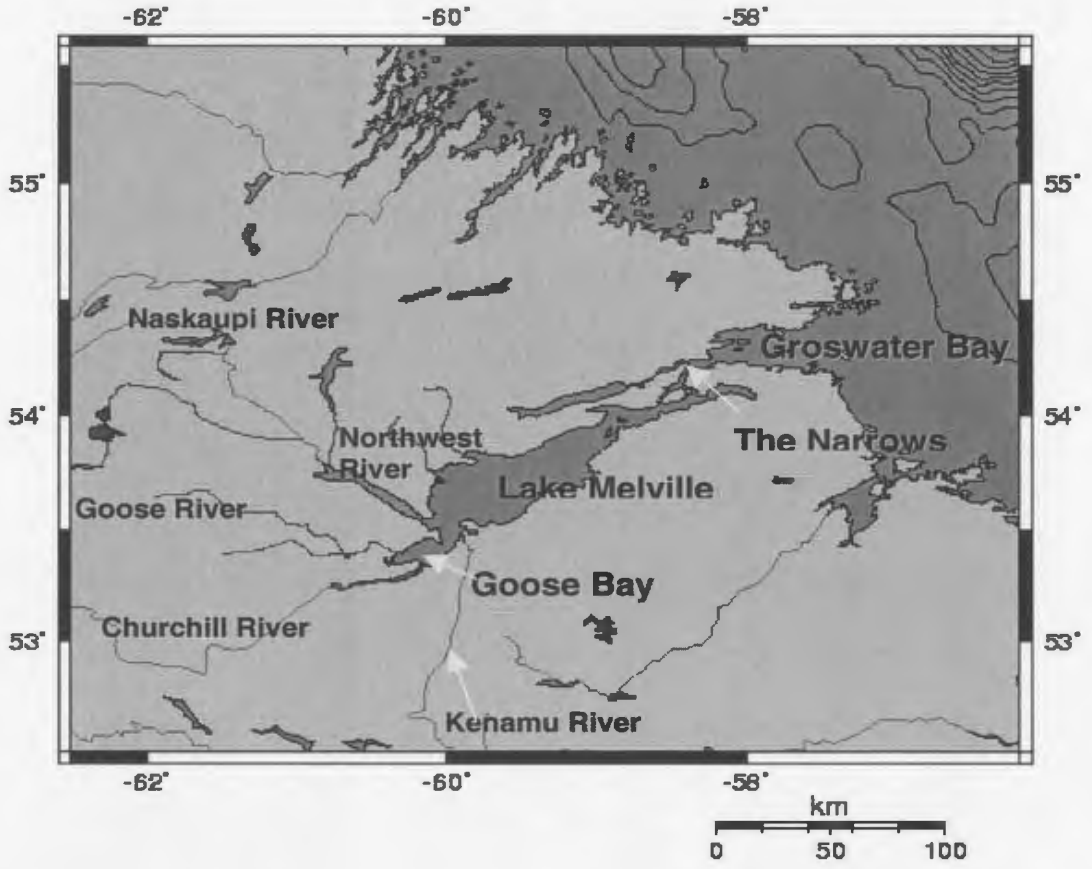

Figure 1.6 Hamilton Inlet, located along the Labrador Coast at 54°N and between 60.5°W and 57°W, and the major rivers that discharge into the Inlet.

a) Description of Estuarine Circulation

Lake Melville is an estuary. Estuaries are defined as semi-enclosed coastal area where fresh water drains into the sea (Dyer, 1979). The interaction of fresh and saline water sets up a complex circulation pattern that varies with several factors such as winds, tides, seasons, and basin morphology. The driving force behind estuarine circulation is the pressure of the freshwater inflow that generates gradients, both horizontal and vertical, of salinity and density. The upper layer of freshwater flows seaward, this outflow is compensated by an inward flow at some deeper level. The compensating flow is

controlled by the amount of seawater transferred to the upper layer by entrainment. This seaward flow of fresher water and the compensation current below is referred to as estuarine circulation (Figure 1.7). Typically strong stratification exists where the salinity increases with depth. The freshwater inflow tends to cause greater stratification while winds and tidal currents tend to break down stratification. The strong stratification resists the exchange of momentum and reduces the vertical mixing. Mixing and entrainment between layers is often the result of internal waves.

There are several classifications of estuaries. Lake Melville is a fjord due to the combination of the Lake deep basin and The Narrows, which creates a sill restricting the water flow between the Lake and Groswater Bay. The small cross sectional area of The Narrows in relation to the large size of the Lake causes the Inlet to be classified as a landlocked fjord (Bobbitt and Akenhead, 1982). One major influence on Lake Melville circulation is expected to be internal tidal motion since the sill extends to the stratified layer. The Narrows causes a choking effect of the Lake, reducing the height of the tide in the Lake; the tides in Groswater Bay are 1.3-2 m and the tides in Lake Melville are 0.2-0.5 m (Bobbitt and Akenhead, 1982). In a fjord, estuarine circulation resulting in nutrient entrainment is restricted to the shallow surface layer above the sill. There are typically three distinct layers in a fjord; the upper layer with a mix of freshwater over seawater, the middle layer is seawater influenced by tides and the bottom layer contains stagnant water, or water that is periodically renewed. The deep water is replaced when water flowing in over the sill is denser than the water in the basin. The water density coming over the sill fluctuates with tidal current, wind, and runoff. In the spring for

example, a time of increased drainage into the Lake, a rapid surface water flow forms, which reduces inflow over the sill. In the winter, when runoff is minimal the tides dominate and may lead to complete mixing or renewal of deeper waters. Bobbitt and Akenhead (1982) discussed a few characteristics of the Inlet. They found that the deep water in the Lake basin was completely renewed during the study period in 1980, and predicted that renewal should continue to take place in other years. The Lake Melville surface layer had consistent salinity across the whole Lake due to the large discharge rates. There was also minimal vertical exchange between the upper and lower layers by entrainment, and the depth and salinity of the surface layer was strongly influenced by wind.

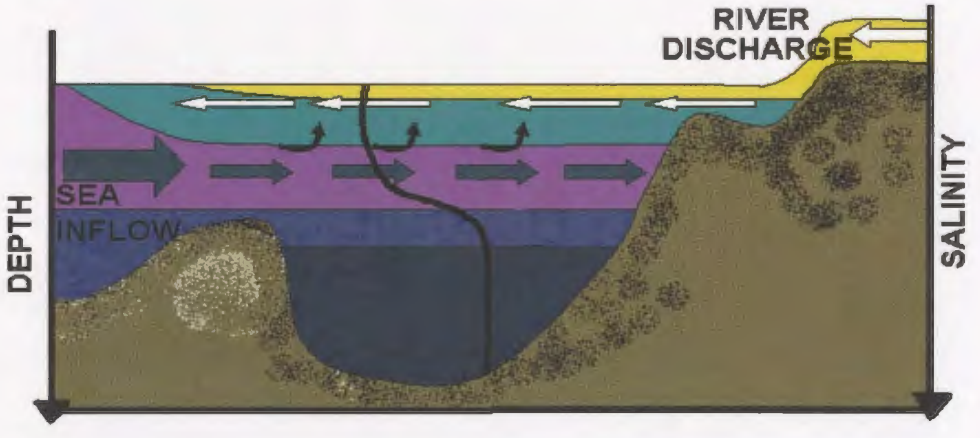

Figure 1.7: Estuarine circulation and salinity gradient in a fjord.

The balance between freshwater discharge and ocean currents is important to primary production since it results in strong stratification and upwelling of nutrients, this relationship is discussed in the next section.

b) Description of Productivity of an Estuary

Without dissolved nutrients in the surface layer, phytoplankton production could not occur. Estuary circulation causes a nutrient flux, which traps nutrients in the estuary. The freshwater runoff alone usually provides little nutrients to the estuary. The major contribution to the nutrient content is most often from ocean currents. Tides carry oxygen and nutrients into the estuary. If vertical mixing occurs, some nutrients become trapped, and the nutrients are not carried back out to sea and instead they circulate within the estuary. The turbulence or counter current that occurs between the two layers of sea and fresh water causes the two layers to mix and therefore entrainment of nutrients occurs in the surface layer. Also, the renewal of deeper waters during winter in the estuary causes nutrients to become suddenly available again in the surface layer. Thus, it is important to have a balance between freshwater discharge and ocean currents, resulting in stratification and entrainment of nutrients, which contribute to primary production. Estuaries are considered areas of high productivity since they trap nutrients making them important to the fishery industry. It has been shown that larvae can adapt to the circulation pattern in an estuary in order to maximize food intake and survival (Mann and Lazier, 1996). For example, in the St Lawrence River a correlation was found between river run-off and lobster and halibut landings (Sutcliffe, 1972, 1973). He showed that as discharge increased, entrainment increased, increasing primary production and causing

greater survival of larvae. A greater survival of the larvae resulted in an increase of halibut and lobster catch 9 to 10 years later.

River discharge is therefore important to productivity in estuaries in the following ways:

- Rivers may contain certain important substances for productivity
- Rivers contribute to entrainment and surface layer mixing, making nutrients available for primary production in the surface layer
- Rivers may regulate the thickness of the surface layer, controlling the available light for primary production

c) Annual Cycle

There are few studies of the seasonal cycle of physical and biological conditions for Hamilton Inlet. There have also been a few studies in winter of the Lake ice conditions and studies of river flow. FENCO Newfoundland Ltd. completed the Lake Melville Freeze Up study during 1981 to 1982. They found that the Lake begins to freeze in late December and was completely frozen over by December 29, 1981. The Lake remained ice covered until early April when the spring thaw commenced, and the Lake was free of ice by June 11, 1982. The ice cover causes changes in the water properties since the surface waters are no longer exposed to wind, solar input is reduced and ice melt occurs. The Memorial University, Lake Melville Ice Research study in 1973 found that after ice cover the upper 20 m of Lake Melville had become fresher, colder and the thermocline was reduced by a half from 18.3 m to 9 m.

The river flow into the Inlet has a distinct seasonal cycle. In January the river flow is less than 1000 m^3/s, in April the flow begins to increase and reaches a maximum in June, after which it decreases back to below 1000 m^3/s by end of December. This seasonal cycle has been changed due to hydroelectric development, which has regulated the river flow. The regulated river flow increases the flow in winter and decreases the flow over spring and summer resulting in a less pronounced seasonal cycle (Hydro Lower Churchill Development Corporation Ltd., Environmental Impact Statement, 1980). The details of the hydroelectric development are described in detail in the next section.

1.3. Churchill Falls Hydroelectric Development and Impacts

The study of Hamilton Inlet is helpful in the economic development of the area and determining the environmental risk of these developments. Currently there exists one hydroelectric generating station at Churchill Falls, which was completed in 1971. There was no dam constructed but instead a series of dykes to divert water. Hundreds of existing lakes and bogs were linked with dykes to form the Smallwood Reservoir from which water is released through control structures. A section of the Churchill River was diverted in a new course along a series of lakes parallel to the original riverbed in order to supply the power plant, descending over 300 m (Bobbitt and Akenhead, 1982). Excess water is released through the Jacopie spillway and allowed to flow along the original route. The drainage area into the Inlet was increased by approximately 11,400 km^2 through the construction of dykes at Orma and Sail Lakes. These dykes divert water

from the Naskaupi River, which eventually flows into Lake Melville, and Kanairiktok River which does not flow into Lake Melville. Therefore, the diversion of the water from Kanairiktok River increased the total amount of freshwater inflow to Lake Melville (Bobbitt and Akenhead, 1982). This increased inflow has the potential to change the Lake circulation and therefore the coastal ecosystem. Bobbitt and Akenhead (1982) showed that even though the freshwater content increased, the salinity in the upper 30 m actually increased by 1 to 2 ppt when comparing results from before and after the development in August 1952 and 1981. This increased salinity was caused by lower discharge rate from the Churchill River, resulting in lower discharge from Lake Melville into Groswater Bay.

It is now proposed to build further hydroelectric stations in the lower Churchill River at Gull Island and Muskrat Falls (Hydro Lower Churchill Development Corporation Ltd., Environmental Impact Statement, 1980). This could cause greater changes in the water circulation and properties of Hamilton Inlet and has the potential to influence the fish and fisheries. Hydroelectric developments have impacted the environment worldwide. For example, on the Dnieper River, which flows to the Black Sea, construction of a dam caused a change in the pattern of seasonal discharge (Tolmazin, 1985). The spring discharge rate was reduced and the discharge became sporadic throughout the year. This resulted in a $3.8 billion loss to the fishery industry. Saunders (1981) showed that codfish and capelin were present in Groswater Bay, however, 70% of the fisherman interviewed felt changes of flow of the Churchill River was to blame for the cod stock decline in Groswater Bay.

1.4. Fish Populations

Historically northern cod spawns from Hamilton Bank south to the Grand Banks (Hutchings, 1996). In the past there have been reports of northern cod present in Groswater Bay (Saunders, 1981; Bobbitt and Akenhead, 1982; deYoung & Rose, 1993; Hutchings, 1996). The fish species present in Hamilton Inlet are mostly in early stages of development from spawning in offshore waters. Northern cod are one of the most important fish to the fisheries industry in the area. The Labrador cod spawn on the Labrador Shelf and migrate in the summer to the Labrador coast. It is believed the Labrador population is the most important to the fisheries because its more northerly distribution provides the best location from which to generate high levels of recruitment. It may also be the most vulnerable location to changing ocean conditions (deYoung and Rose, 1993).

Over the past fifty years, many fish stocks have declined in the North Atlantic. Over fishing is the primary cause for the declines, however, climate variability has also been proposed as a factor (deYoung and Rose, 1993; Hutchings and Myers, 1994; Rose *et al.*, 2000). Over fishing has been widespread since 1950 and caused a severe decline in northern cod. Over fishing reduced the harvestable stock in the North Atlantic by 3 million tons from 1960 to 1992. The spawning biomass declined from 1.6 million tons in 1962 to 22,000 tons in 1992 (Hutchings and Myers, 1994). Adult cod shifted their distribution southward in the late 1980s and early 1990s and northern cod have become commercially extinct in the most northerly portion of their former range off Labrador since the 1960s (deYoung and Rose, 1993; Rose *et al.*, 2000). The period of decline of

northern cod has been accompanied by substantial changes and variability in the environment in the Northwest Atlantic (Rose *et al.*, 2000). Over the last 30 yrs there was a -0.25°C per decade change in Northwest Atlantic temperatures (deYoung and Rose, 1993). deYoung and Rose (1993) proposed that the decline of northern cod is unlikely to have been caused solely by fishing and there may be a link between ecosystem changes and population response due to the disproportionate decline in abundance in the Labrador region. It is believed that cold-water temperatures influenced the spatial patterns of cod movements, spawning locations, and the resultant survival of their progeny. For example, there was a major decline in capelin, the major food for cod, off Labrador in 1989 just before the southern shift of cod (Rose *et al.*, 2000). However, Hutchings and Myers (1994) rejected the hypothesis that cod collapse is due to environmental change. They found water temperature was not associated with cod abundance or with adult distribution by depth and concluded that cod collapse was due solely to overexploitation. Drinkwater (1994) concluded that the decrease in spawning stock biomass of several commercially important fish species is largely attributed to over fishing, but is also related to environmental conditions.

The interest for this study is in the effect of climate change and river flow changes on the ecosystem, in particular plankton and fish, which spawn on the Labrador Shelf. There are two ways to look at fish population response to climate variability. Are fish populations affected directly by changes in the ocean conditions or are the effects propagated through the foodweb? Most likely, both effects are important and studies have shown examples of both (e.g. Denman *et al.*, 1998). This study will focus on fish

population response to climate variability by propagation through the foodweb. The longest record of changes in marine life is associated with commercial fishing. Interpreting changes in fish populations is difficult since both natural causes and over fishing affect abundance. Also, the life span of many fish species is such that variations in abundance must be investigated over several years of environmental forcing (Planque and Taylor, 1998). On the other hand, plankton species have shorter life cycle and are not yet commercially exploited, which makes the study of their response to climate change more feasible. Also, the effects of climate on plankton can be transferred from plankton to higher trophic levels like fish (Aebisher *et al.*, 1990). For example, changes in plankton of the North Sea have been used to forecast repeatedly the conditions for the growth pelagic fishes (Pavshtiks, 1968; Carlotti and Radach, 1996). Long-term connections between climate and plankton have been studied in the North Atlantic with the Continuous Plankton Recorder Program (e.g., Colebrook, 1978; Cushing, 1990; Taylor, 1995). Also, Planque and Taylor (1998) investigated links to changes in the Gulf Stream signal and the relationship of the NAO index to variation in zooplankton in the North Atlantic.

1.5. NPZ Models

Existing observations throughout the Labrador Sea and Shelf are inadequate to determine the effects that oceanic and climate variability have on the marine ecosystem. Therefore, it is necessary to apply biological and physical models. To simulate the seasonal response of the planktonic ecosystem to river flow and climate variability, a one

dimensional coupled mixed-layer and planktonic ecosystem model is used. The ecosystem model used is the 4 compartment nutrient-phytoplankton-zooplankton-detritus, NPZD, model of Denman and Pena (1999) forced with solar radiation, initial nitrate concentration and mixed-layer depth determined from historical salinity, temperature and density. The NPZD model is coupled with a one-dimensional mixed-layer model. The NPZ model was developed to study biogeochemistry in the ocean after methods to measure photosynthetic pigments and concentrations of chemicals in the ocean were developed (Steele, 1998). NPZ models were first applied by Riley (1946) and are considered a common tool in oceanographic research (Franks, 2002). They use a set of coupled differential equations to represent planktonic ecosystems. The main criteria in order to accept the model simulation as a description of the system in question is to obtain good agreement with observations. In recent years satellite derived data has provided more opportunities to apply NPZ models, offering data both to initialize and to verify the models. For example, Fasham *et al.* (1990) expanded on the simple NPZ model using 7 state variables coupled with a model of Atlantic circulation and simulated the productivity, and compared the output as chlorophyll with remotely sensed ocean colour. There have been few ecosystem models developed for the Labrador Sea and fewer for coastal Labrador, perhaps due in part to the lack of a continuous, long term data series. Recently Tian *et al.* (2004) have developed a physical-biological coupled model for the Labrador Sea, which included winter convection, food web dynamics, chemical fluxes and active export through zooplankton vertical migration. The model was used to investigate export of biogenic carbon and nitrogen and found that DOC export by vertical

convection dominated over sinking particulate and active export. In another study by Tian *et al.* (2004) a physical-biological coupled model was used for the Labrador Sea which included microbial food web dynamics (phytoplankton, microzooplankton, detritus, DOM and bacteria), and mesoplankton food web (phytoplankton, mesoplankton and large sinking particles). The model was used to examine the sensitivity of biogenic carbon export to oceanic climate in the Labrador Sea. Trela (1996) developed an ecosystem model to simulate the annual cycles of mixed-layer properties that control the air-sea exchanges of CO_2. These controlling properties included temperature, salinity, alkalinity, dissolved inorganic carbon, nutrients, phytoplankton and zooplankton. The results reveal that the annual cycles of N, P, and Z have a single peak bloom period of P and Z, and nutrients are mostly constant until summer when they are almost depleted corresponding to the spring bloom.

1.6. Approach to Problem

This modeling investigation will attempt to determine the sensitivity of the seasonal plankton dynamics as a result of climate change in the Labrador Sea and Shelf, and freshwater discharge changes in Hamilton Inlet and Labrador Shelf. This work is motivated by the correlation that has been found between the climate variability and fish stock fluctuations in coastal Labrador (deYoung and Rose, 1993; Rose *et al.*, 2000). There has also been concern that the change of freshwater discharge to Hamilton Inlet was to blame for the cod stock decline in Groswater Bay (Saunders, 1981). In order to investigate how changes in the physical environment affect fishery production at high

trophic levels it is necessary to understand the effects on production at the lower trophic levels since plankton are a major food source for juvenile fish (Li *et al.*, 2000). Therefore, this study will focus on the lower trophic level, the plankton. Because of the complexity of the foodweb system and the lack of long-term continuous biological observations in the Labrador region, it is necessary to use a coupled biological-physical model to predict plankton response to the physical forcing. The model estimate of plankton production can then be used to predict the fish production. The biological model is a four compartment NPZ model consisting of nutrients N, phytoplankton P, zooplankton Z, and detritus D developed by Denman and Pena (1999). This model was coupled with a one-dimensional mixed-layer model driven by solar radiation, density and nitrogen concentration in deep water. The model was run in the Labrador Sea and Shelf for periods that had different environmental conditions due to climate variability. The model was also run for Hamilton Inlet for the period before and after the hydroelectric development to determine the effects of changing freshwater discharge. Historical temperature, salinity, density, nitrate, chlorophyll, ice thickness, and cloud cover data were collected from the three regions, the Labrador Sea, Labrador Shelf and Hamilton Inlet, for these periods. The Labrador Shelf and Sea have more historical data available including satellite data and other model studies. The Labrador Sea 1968 data were used to determine parameter values and model sensitivity to the parameters. Due to the lack of data in the Inlet it was decided to run the model just outside Groswater Bay on the Labrador Shelf to help verify the modeled plankton dynamics. The model is verified

using results from other models from the literature, historical observations of chlorophyll and satellite-derived data for each region.

1.7. Outline of Thesis

Chapter 2 gives a description of the meteorological and oceanographic data from each region required for the model simulations and model validation. Chapter 3 describes the models used, the parameters used, and the sensitivity of the model to the parameters. Model simulations and results for each region are presented in Chapter 4 as well as a discussion of model results in relation to observations and a comparison of the results from each region. Chapter 5 presents a summary of the findings.

CHAPTER 2

Data for model runs and model validation

Physical and biological data were obtained from various sources for the three study regions: The Labrador Sea, Labrador Shelf and Hamilton Inlet. Historical data were primarily obtained from studies completed by industry and from the Bedford Institute of Oceanography (BIO) database. The studies by industry are generally specific to each region and described in the sections below. The BIO database is currently being expanded to include biological and chemical data building on the primarily physical data archive begun by the Marine Environmental Science Division (MESD). This database not only contains data collected by the MESD, but also those sent to the Marine Environmental Data Service in Ottawa, the National Oceanographic Center (NODC) in Washington, as well as data recovered from universities, consulting firms, and other groups. The database includes nitrate, nitrite, ammonium, urea, total nitrogen, silicate, phosphate, chlorophyll, phaeophytin, dissolved oxygen, temperature, salinity, particulate organic carbon, particulate organic nitrogen and suspended particulate matter data. The geographic limits for the database are from 35^{o} – 90^{o} N and 40^{o} – 90^{o} W, thus incorporating all three region for this study (Petrie *et al.*, 1999). By far the most extensive data are for nitrate, phosphate, temperature and salinity, which are used in this study. The chlorophyll data is less extensive. The data obtained from the database includes the years 1928 to 2001 for depths up to 4000 m in the Labrador Sea. This database is available in part to the public through the Department of Fisheries and Oceans (DFO) website (www.mar.dfo-mpo.gc.ca/science/ocean/home.html). Data for each region

was obtained from this website and also from personal communication with B. Petrie and K. Drinkwater (BIO). Some of the studies in the Labrador region that are a part of this database include temperature and salinity time series from 1951 to 2001 on Hamilton Bank on the Labrador Shelf (Colbourne, 2002).

In 1976 the International Commission for the Northwest Atlantic Fisheries (ICNAF) established standard oceanographic stations along transects in the Northwest Atlantic from Cape Cod (USA) to Egedesminde (Greenland). Several of these stations in Newfoundland have annual oceanographic surveys conducted by the DFO. The transects included in this study are the Makkovik Bank and Seal Island transects on the Labrador Shelf (Figure 2.1) (Colbourne, 2002; Pepin and Maillet, 2002). Another study starting in the early 1960s by BIO conducted experiments on photosynthetic production versus light intensity for natural phytoplankton populations in the Northwest Atlantic north of 50° N on the Labrador Shelf and in the Labrador Sea (Irwin *et al.*, 1978, 1986, 1989, 1990). Additionally, an oceanographic sampling program was conducted at the Ocean Weather Station Bravo (OWS-B) located near the center of the Labrador Sea at 56°30N, 51°00W (Figure 2.1). Extensive temperature and salinity data were collected from January 1964 to January 1974 down to 1500 m (Shuby, 1969, 1974; Lazier, 1980).

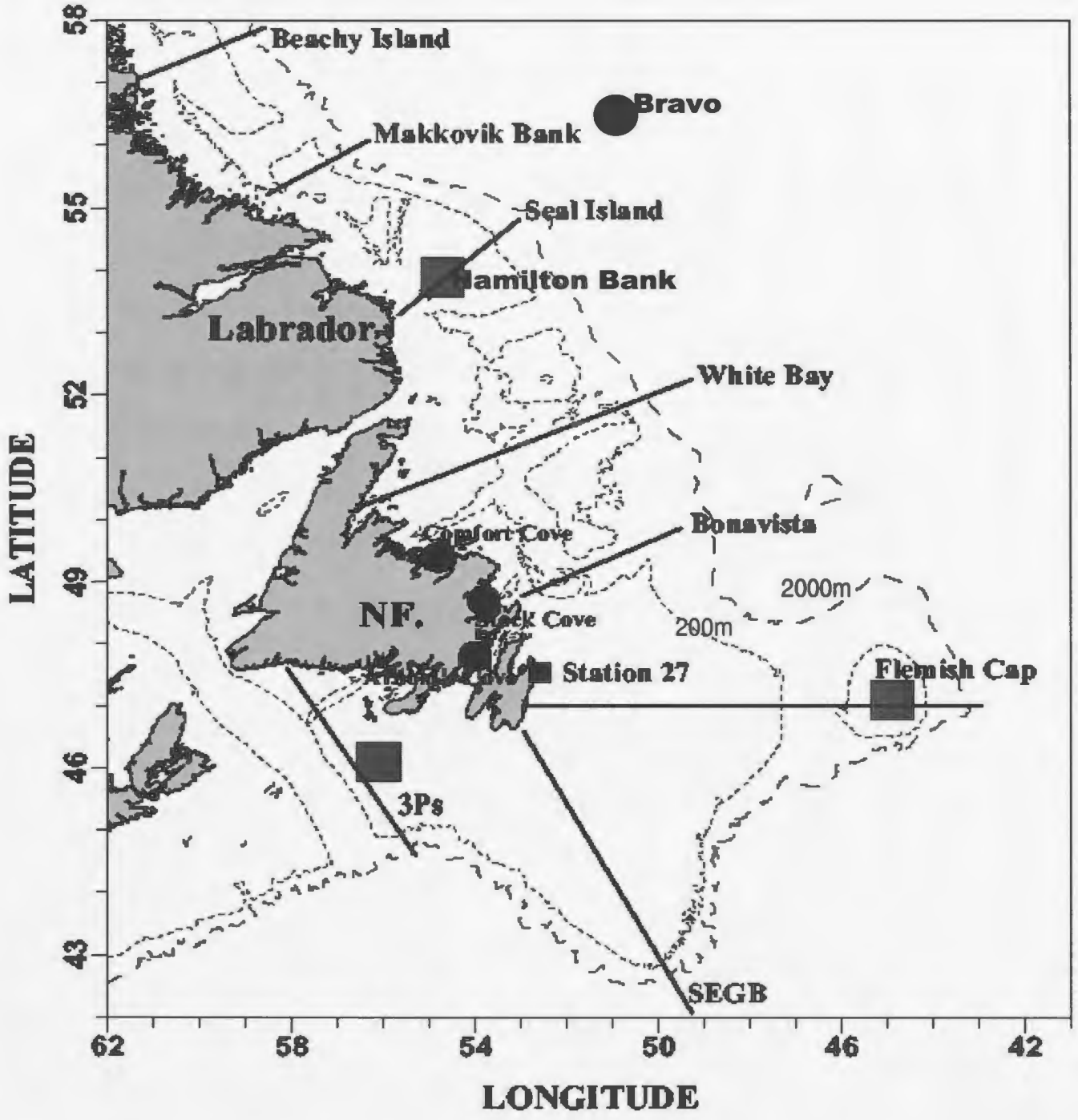

Figure 2.1: The standard regions, transects and stations in Newfoundland and Labrador established by the International Commission for the Northwest Atlantic Fisheries in 1976 and other studies.

2.1. Continuous Plankton Recorder

An important source of phytoplankton bloom data was from the Continuous Plankton Recorder Program from 1959 until 1986 in the Northwest Atlantic (Myers *et al.*, 1994). This study determined long term biological changes in the ocean. There were an enormous number of samples collected, more than 17000 west of 40°. The recorder sampled at an average depth of 6.7 $\pm$ 1.7 m along standard routes while towed by a ship. One route passed through the Labrador Shelf region corresponding to the NAFO division 2J and the other route was in the Labrador Sea in a region called LS1 (Figure 2.2). The data are reported as phytoplankton colour (Myers *et al.*, 1994), therefore absolute abundance cannot be determined. However, the data do show the seasonal pattern of the phytoplankton cycle in the Labrador Sea. The seasonal cycle for phytoplankton in LS1 is a single sharp spring peak with a smaller fall peak, and copepods have only the spring peak (Figure 2.3). The phytoplankton bloom begins in April and reaches a maximum in June. The copepod cycle also begins in April but reaches a maximum slightly later, in July.

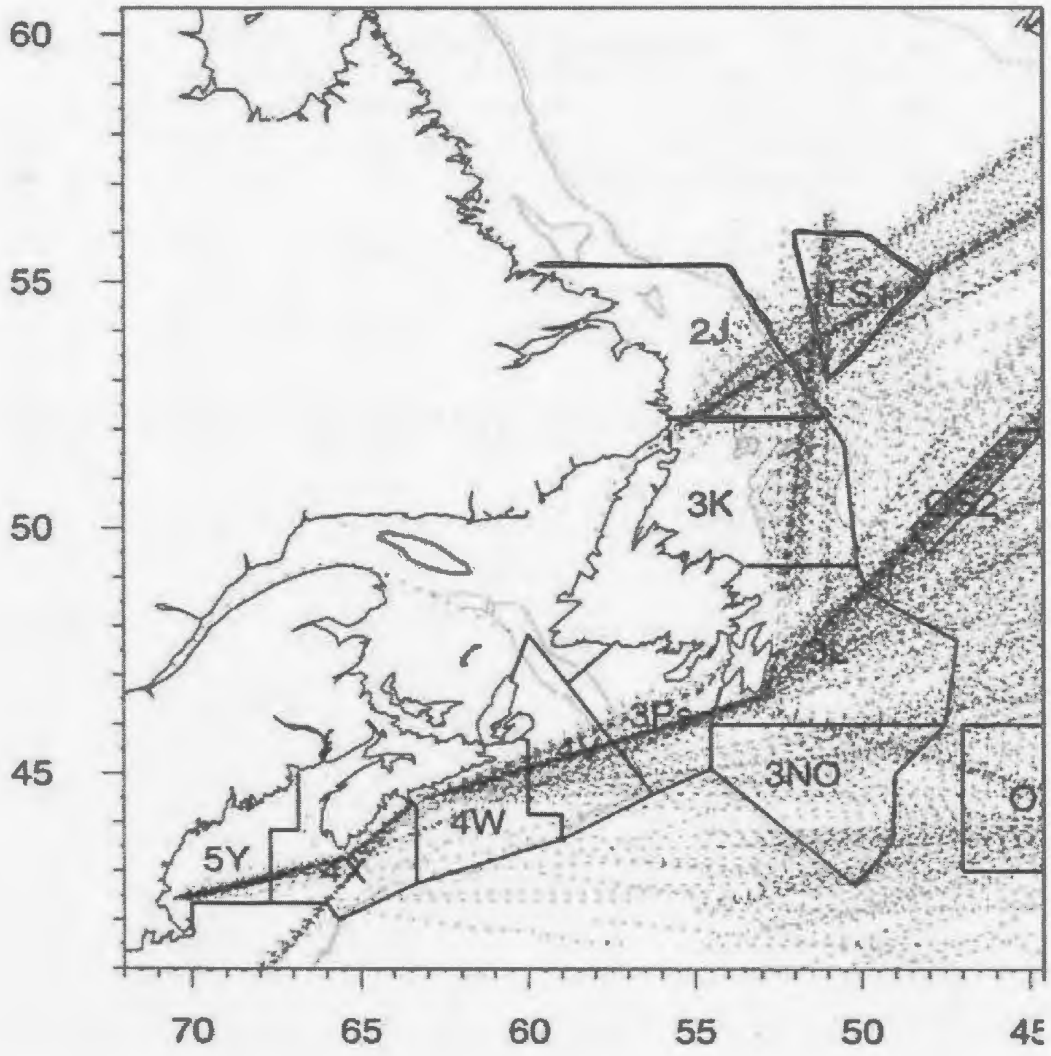

Figure 2.2: Map showing Continuous Plankton Recorder Program sample locations during the period of 1959 to 1992, sections outlined in bold are those used relevant to this study (Modified from Myers *et al.*, 1994).

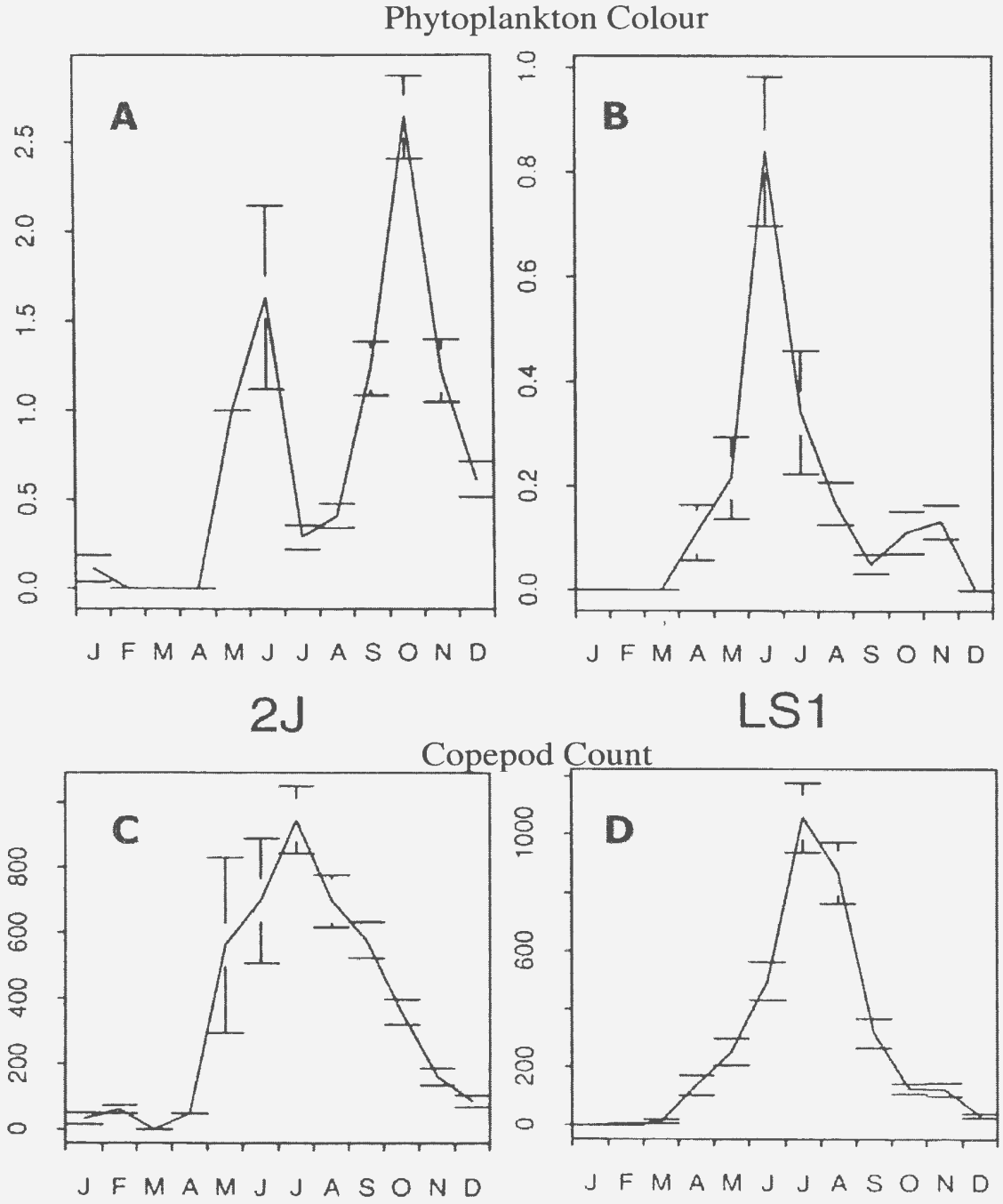

Figure 2.3: Monthly mean of phytoplankton colour and total copepod count from the Continuous Plankton Recorder Program from 1959 to 1986 in the NAFO 2J and LS1 regions on the Labrador Shelf and in the Labrador Sea respectively. A) Phytoplankton colour 2J, B) phytoplankton colour LS1, C) total copepod count 2J, D) total copepod count LS1. Error bars represent the standard error of each mean. (Modified from Myers *et al.*, 1994).

2.2. Satellite Derived Data

The development of satellite ocean-colour sensors provided estimates of surface chlorophyll concentrations by measurement of chloropigments (Hooker *et al.*, 1992; McClain *et al.*, 1992; Aiken *et al.*, 1995). This data made it possible to compare model predictions of phytoplankton with remotely sensed ocean colour and has improved validity of models. In addition, the sensors have provided data for large special regions over the entire year. The data from the satellite are analyzed for ocean colour to determine phytoplankton chlorophyll concentrations, a green pigment in phytoplankton important in photosynthesis. Analysis of the spectral data from the satellite sensors allows the concentration of phytoplankton to be determined. In the image, as the concentration of phytoplankton pigments increases, ocean color shifts from blue to green to red. In order to compute chlorophyll concentrations from remotely sensed ocean colour, algorithms have been developed and are continuously refined (Hooker *et al.*, 1992; McClain *et al.*, 1992; Aiken *et al.*, 1995). However, satellite derived data have been reported to over estimate and under estimate chlorophyll concentrations when the standard algorithms are used, especially at high latitudes. This is due to the varying absorption coefficients of phytoplankton caused by changes in species composition, light, and nutrient conditions (Stuart *et al.*, 2000). Therefore, caution should be taken when relying solely on satellite derived chlorophyll concentrations to validate models.

For this study, two satellite ocean-colour sensors are used: the historical Coastal Zone Colour Scanner (CZCS) and the newer, more sophisticated Sea-viewing Wide Field-of-view Sensor (SeaWiFS). The data are available for the Labrador Sea and Shelf

and not Hamilton Inlet. NASA developed the CZCS, which was launched on the Nimbus-7 satellite in October 1978 and was the first Ocean Color space sensor. The CZCS is no longer in use but during its 7 1/2 year lifetime (October 1978 - June 1986), the satellite acquired nearly 68,000 images, each covering up to 2 million square kilometers of ocean surface. The accuracy of each chlorophyll concentration computed from the CZCS as compared to actual ship observations is roughly 30% (Campbell and Aarup, 1992). To validate the model, the summarized CZCS data by Campbell and Aarup (1992) is used. Campbell and Aarup (1992) used a series of 60 images between January 1979 and December 1983 to produce monthly averages to represent one year. The maximum chlorophyll concentration between winter and late summer in the Labrador Sea varies between 1 and 10 mg/m^3 (Figure 2.4 a). The Labrador Shelf has a slightly higher concentration, between 3 and 10 mg/m^3. The months in which these maxima occur are July and August for the Labrador Sea and June or July on the southern Labrador Shelf (Figure 2.4 b).

The second satellite ocean-colour sensor, which replaced the CZCS, also developed by NASA, is SeaWiFS from which images are available for the Labrador Sea and Shelf during the years 1997-present. SeaWiFS images and data were obtained from BIO (B. Petrie, personal communication, BIO) for the Makkovik Bank Transect, Seal Island Transect on the Labrador Shelf and the Labrador Sea Transect (Figure 2.5). The chlorophyll is computed as bi-monthly means from 1997 to 2000. There are several gaps in these data; there are virtually no data early and late in each year, especially for the Makkovik Bay transect in which January to April is missing. The maximum chlorophyll

concentration is up to 16 mg/m^3, which occur in June along the slope region of the Labrador Sea and Seal Island Transect. The chlorophyll bloom seems to start in May and finished by July. Certain years in Figure 2.5 also show a second chlorophyll bloom in the fall between September and October.

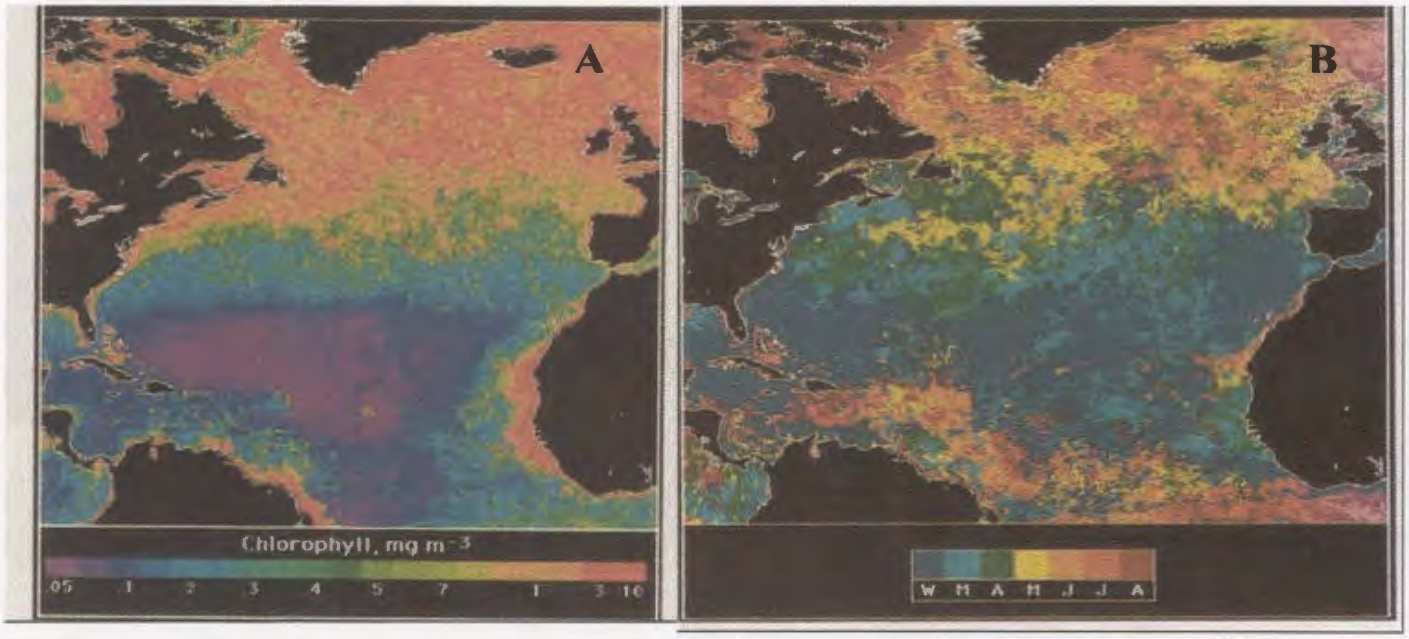

Figure 2.4: Coastal Zone Colour Scanner images adapted from Campbell and Aarup (1992). A) Maximum surface chlorophyll concentration between January and August based on a 5-year monthly average between January 1979 and December 1983 of CZCS images. The colour scale depicts chlorophyll concentrations as mg/m^3. B) Month in which the maximum chlorophyll concentration occurs. The colour scale depicts months.

Figure 2.5: Bi-weekly composite images of satellite derived sea surface concentrations of chlorophyll from BIO (B. Petrie, personal communication, BIO). The colour scale depicts the chlorophyll concentration as mg/m^3. A) Labrador Sea transect, B) Seal Island transect, C) Makkovik Bank transect.

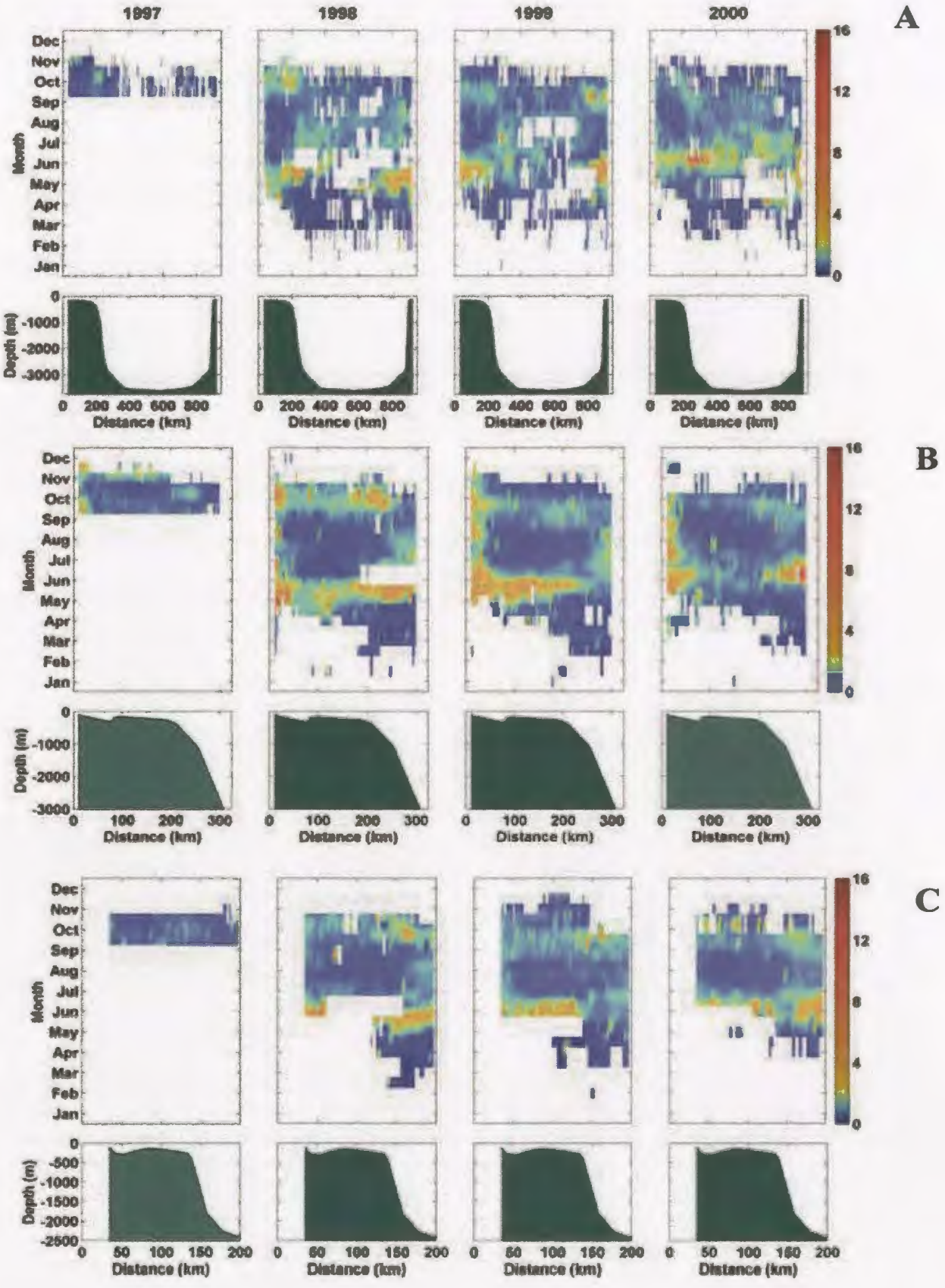
1997
1998
1999
2000
A
B
C
Month
Dec
Nov
Oct
Sep
Aug
Jul
Jun
May
Apr
Mar
Feb
Jan
Depth (m)
Distance (km)

2.3. Bloom Timing and Mixed-Layer Depth

Another study by Siegel *et al.* (2002) averaged the SeaWiFS data for the years 1998, 1999, and 2000 to study the bloom timing. This study determines the day the bloom is initiated, the day the chlorophyll maximum concentration occurs and the corresponding mixed-layer depth (Figure 2.6 and Table 2.1). The day of the bloom initiation is between days 150 and 200 for the Labrador Sea and Shelf region. The corresponding mixed-layer depth is highly variable with an average value of 146-147 m. A summary of other reported maximum chlorophyll concentration timing from the literature is summarized in Table 2.2. The day of maximum chlorophyll concentration varies from days 158 to 180.

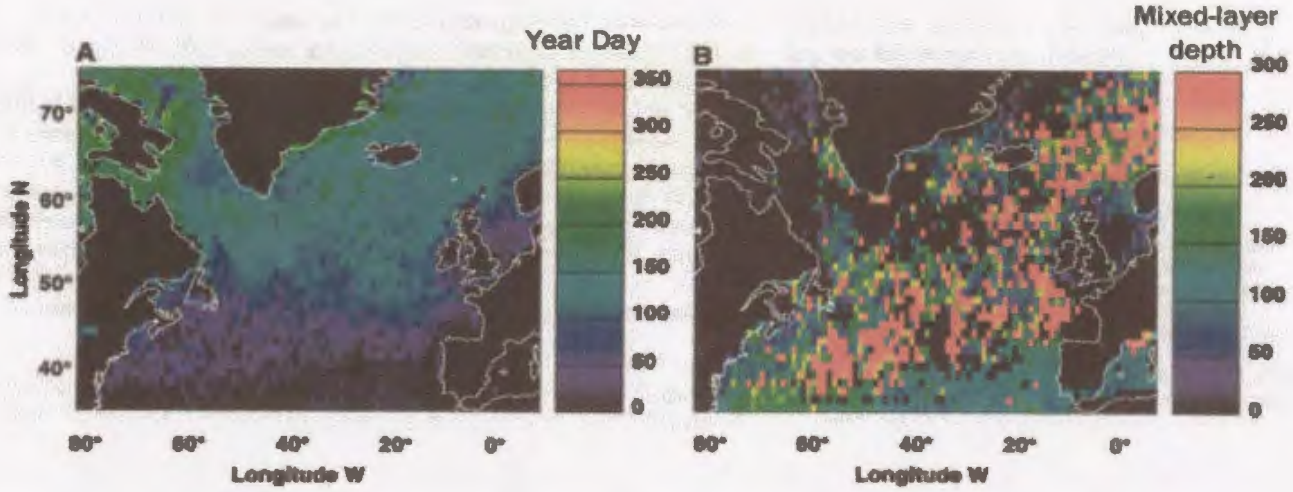

Figure 2.6: SeaWiFS image averages for the years 1998, 1999, 2000, (Modified from Siegel *et al.*, 2002). A) Year day of bloom initiation, the colour scale indicates Julian day of the year starting with January 1. B) Mixed-layer depth at year day of bloom initiation, colour scale is the mixed-layer depth in meters.

Table 2.1: Bloom timing and mixed-layer depth in the North Atlantic. Observations from inland seas and coastal regions are not included. Median values are estimated for each range (Siegel *et al.*, 2002).

Region (°N)	Day of bloom initiation (day)	Day of maximum chl. concentration (day)	Depth of mixed-layer at time of bloom initiation (m)
35-40	13	99	127
40-45	33	117	181
45-50	82	143	205
50-55	112	163	146
55-60	129	173	147
60-65	134	178	185
65-70	137	173	22
70-75	143	172	192

Table 2.2: Timing of maximum chlorophyll concentration for the Labrador Sea and Shelf from the literature.

Day of maximum chl. concentration (day)	Period of data observation	Reference from Literature
173	Simulated and measured by Continuous Plankton Recorder over several years	Tian *et al.*, 2004
160	Simulated for 1966-1968	Tian *et al.*, 2004
158	Simulated for 1969-1971	Tian *et al.*, 2004
178	Simulated for the 1990s	Tian *et al.*, 2004
160-180 (June)	SeaWiFS, 1997-2000	Afanasyev, 2001 and B. Petrie (personal communication, BIO)
160-180 (June)	Simulated over several years	Trela, 1996
June, July, August	CZCS, monthly average, Jan. 1979 to Dec. 1983 of	Campbell and Aarup, 1992

2.4. Solar Radiation

Solar radiation varies daily and annually, and decreases with depth exponentially. The clear sky incoming solar radiation is computed at each time step (1 day) using equations from Iqbal (1983) for each region based on a latitude of 56°N for the Labrador Sea and 54°N for the Labrador Shelf and Hamilton Inlet, (see Appendix 1 for the description of the equations used). To correct for the cloudiness and other losses from transmission through the atmosphere, the equations from Platt *et al.* (1990) are used. The total shortwave radiation at the ground is given by:

$$I_T = H_o(1 - \sum_i A_{ci} F_i)[1 - \hat{m} - A_a(1 - F)]$$

where A_{ci} is the albedo of clouds at level i and the atmosphere above it; F_i is the fractional cloud cover at level i; $\hat{m}$ is the absorption by water vapour; A_a is the albedo of the atmosphere in the clear-sky fraction; H_o is the extraterrestrial radiation on a horizontal surface, and F is the daily cloud cover which is expressed as a fraction. H_o is calculated using the equations from Iqbal (1983) and the units are MJ/day. Cloud cover is in units of octas which can range from 0 to 8 octas. Therefore the partial fraction is computed by dividing the cloud cover values by 8. Since the Labrador Shelf region used for this study is directly outside Hamilton Inlet and they occur at the same latitude, the solar radiation calculated for the Shelf is also used for Hamilton Inlet. Monthly cloud cover data were obtained from the National Centers for Environmental Prediction/ National Center for Atmospheric Research Reanalysis, obtained from the National Oceanic and Atmospheric Administration (NOAA) Climate Diagnostic Center. The cloud data were

obtained for the region from latitude 53°N to 59°N to longitude 49°W to 59°W between the years 1998 and 2001. The data were reviewed to determine the latitude and longitude location with the most complete data set over a 12-month period, which could be used to represent each region. The most complete cloud data sets are from latitude 53°N and longitude 51°W used for the Labrador Sea and from latitude 53°N and longitude 55°W used for Labrador Shelf (Figure 2.7). For the Labrador Sea, the year 2001 is used and for the Labrador Shelf 1998 is used. In 2001 the average octas is 6.46 in the Labrador Sea and 5.3 on the Labrador Shelf. Since the data are monthly, linear interpolation is used to convert to daily values. No data on cloud type was available. There was only cloud cover data. Therefore, a constant cloud albedo is used of 0.5 (Platt *et al.*, 1990) and $\sum_i F_i$ is replaced with F. The value of $\hat{m}$ is set at 0.18 (Platt *et al.*, 1990) and the atmospheric albedo A_a is calculated based on the equation from Platt *et al.*, (1990) assuming a Rayleigh atmosphere;

$$A_a = 0.28/(1 + 6.43(\sin\delta \sin\phi + \cos\delta \cos\phi))$$

where δ is the solar declination, which is the angle of the line joining the centers of the sun and earth to the equatorial plane in units of radians, calculated using the equation from Iqbal (1983) (Appendix 1) and ϕ is the latitude in radians.

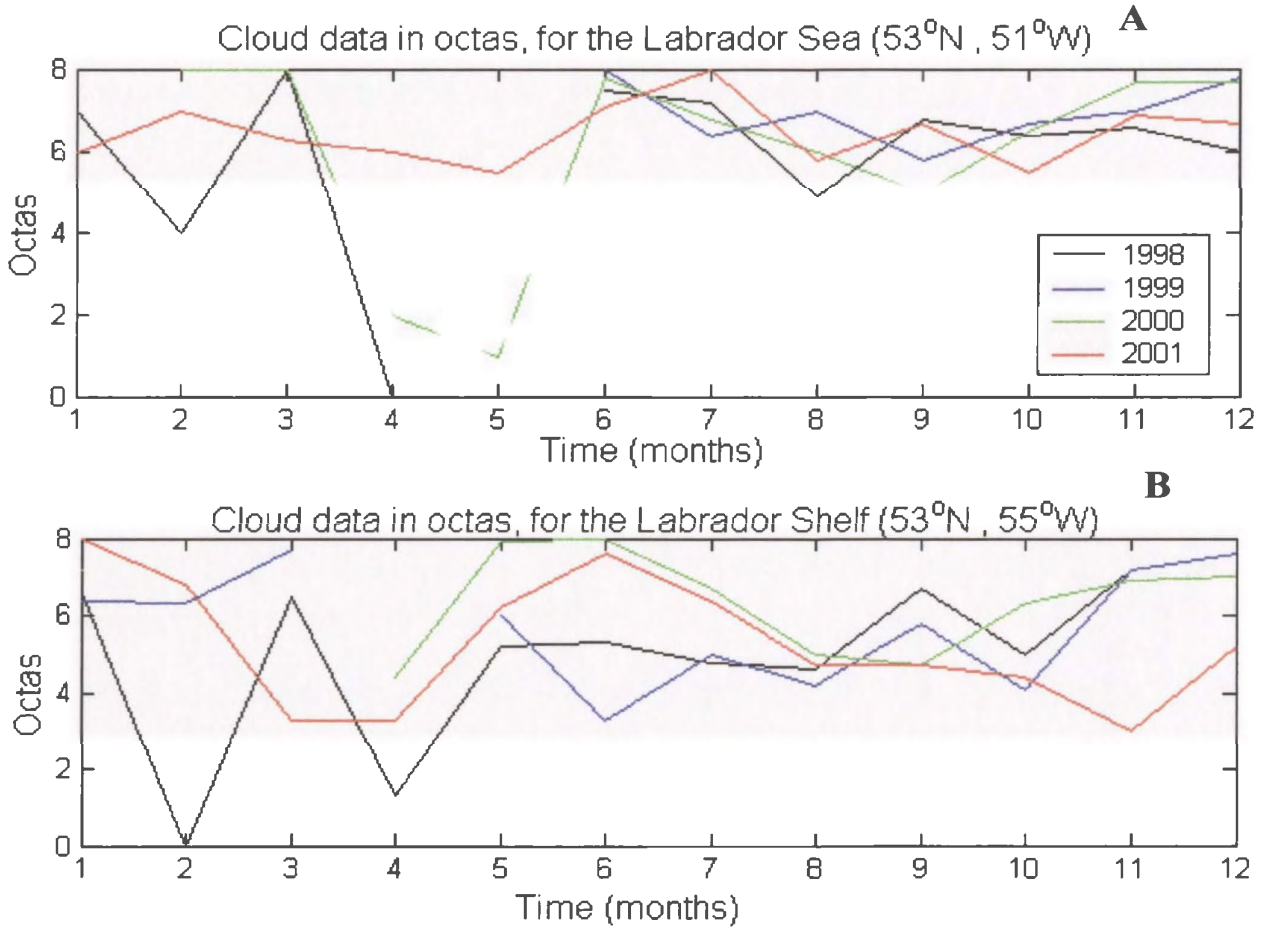

Figure 2.7: Cloud cover data for: A) Labrador Sea (53°N, 51°W) and B) the Labrador Shelf (53°N, 55°W).

In addition to the effect of clouds, Hamilton Inlet also has ice cover, which is another factor that reduces the transmission of radiation. To determine the albedo of the ice cover, a correlation between ice thickness and albedo from Doronin and Kheisin (1977) is used (Figure 2.8). Ice cover data for Lake Melville was obtained from the Lake Melville freeze up study during 1981 to 1982 completed by FENCO Newfoundland Ltd (Figure 2.9). In 1981 the ice formation began December 19 and the Lake was totally ice covered by December 29, at which time the ice thickness was between 20 and 40 cm depending on the location on the Lake. Between January 7 and 9, 1982 the average

thickness at several locations across the Lake was 40 cm. By March the average ice thickness ranged from 80 to 100 cm. The spring thaw commenced in early April and the Lake was free of ice by June 11, 1982.

A Butterworth 5^{th} order filter is used in MATLAB to smooth the annual average incoming solar radiation. The normalized cutoff frequencies used is 4/183 and 8/183 for Hamilton Inlet, where 4 and 8 are the cutoff frequency corresponding to 4 and 8 days since the sample frequency is daily equal to a total of 366 days. The 183 is the Nyquist frequency which is half of the sample frequency and is used to normalize the cutoff frequency. The calculated annual average incoming solar radiation is 99 W/m^2 for Hamilton Inlet, 147 W/m^2 for the Labrador Shelf and 130 W/m^2 for the Sea. This is slightly higher than the annual average for short wave radiation values reported for data collected between 1945 and 1974 at the Bravo station in the Labrador Sea in Ikeda (1987) of 89 W/m^2 and in Smith and Dobson (1984) of 88 W/m^2. This may be due to the different models used to calculate the values.

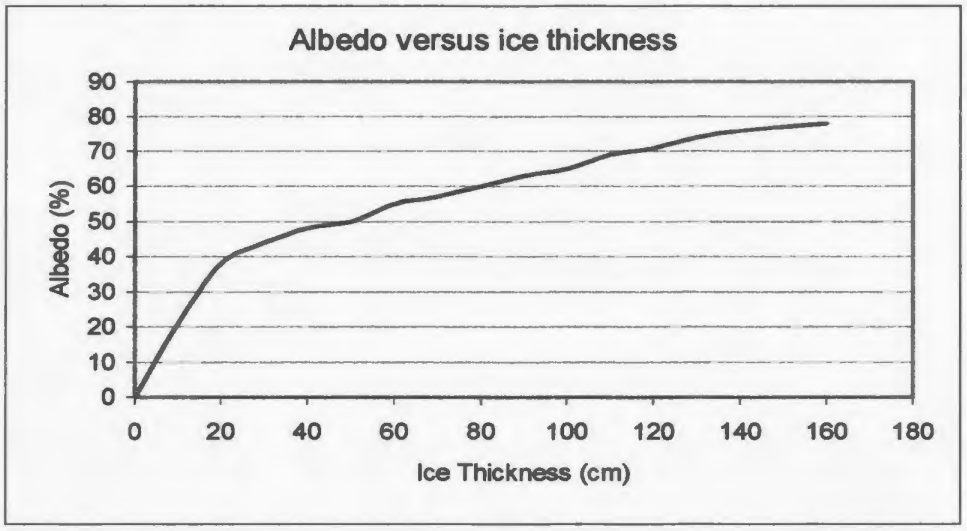

Figure 2.8: Albedo versus ice thickness, obtained from Doronin and Kheisin (1977).

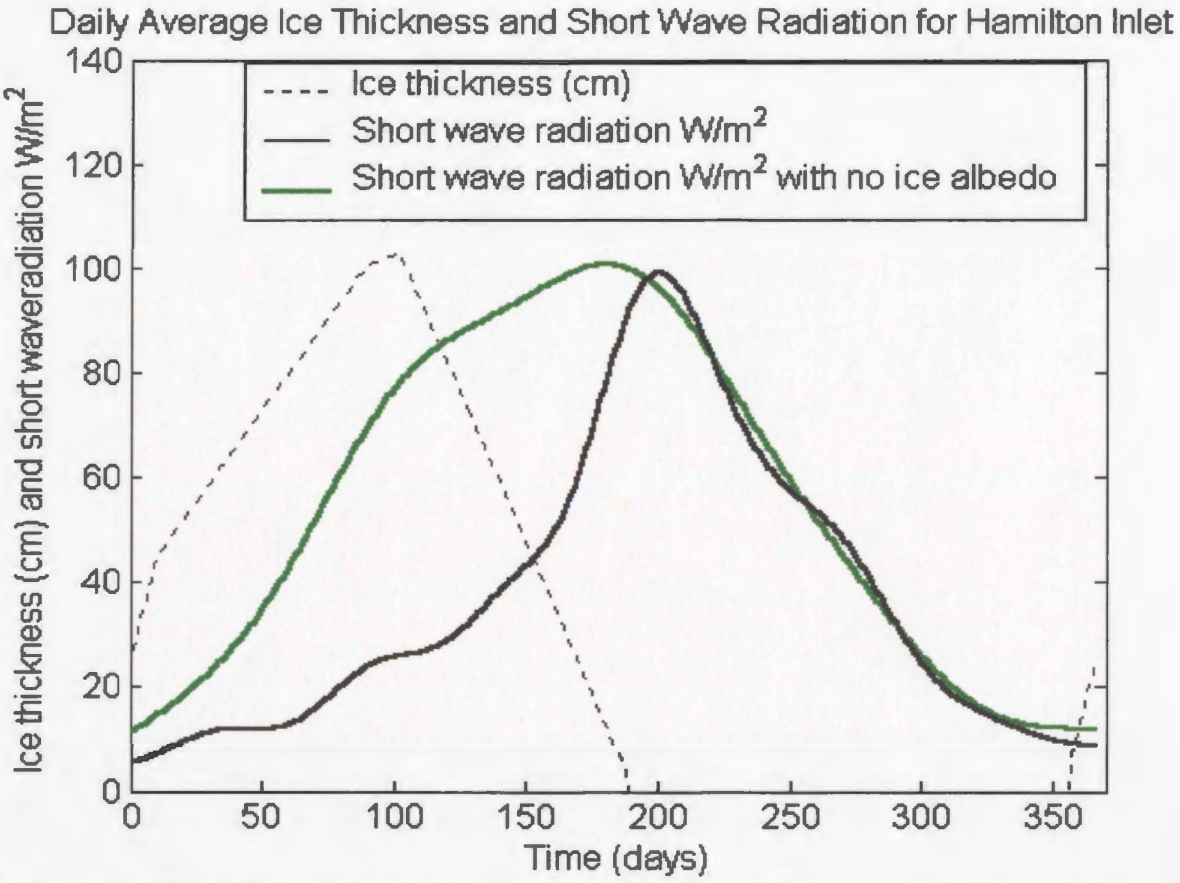

Figure 2.9: Daily ice thickness (dotted line) for Hamilton Inlet estimated from Lake Melville freeze up study during 1981 to 1982 completed by FENCO Newfoundland Ltd. Photosynthetically available radiation, I_{PAR}, for the Labrador Shelf with no ice effects (solid green line) and Hamilton Inlet (54°N) (solid black line). The incoming solar

Part of this incoming solar radiation is reflected back from the sea surface due to the sea surface albedo. A constant sea surface reflectivity of 6% is applied (Denman and Pena, 1999). The remaining solar radiation entering the ocean is divided into a long wave fraction of 60% and a short wave fraction of 40% (Denman and Pena, 1999). The short wave fraction is known as the photosynthetically available radiation (I_{PAR}) which supports primary production in the biological model. The calculated mean annual average I_{PAR} is 37 W/m^2 for Hamilton Inlet, 55 W/m^2 for the Labrador Shelf and 49 W/m^2 for the Sea. Both the incoming solar radiation and I_{PAR} are shown in Figure 2.10 for all regions. The value of I_{PAR} for the Labrador Sea is very similar to that calculated using a similar method by Denman and Pena (1999) of 48 W/m^2 for the ocean station Papa (50°N) using a constant cloudiness of 7 octas.

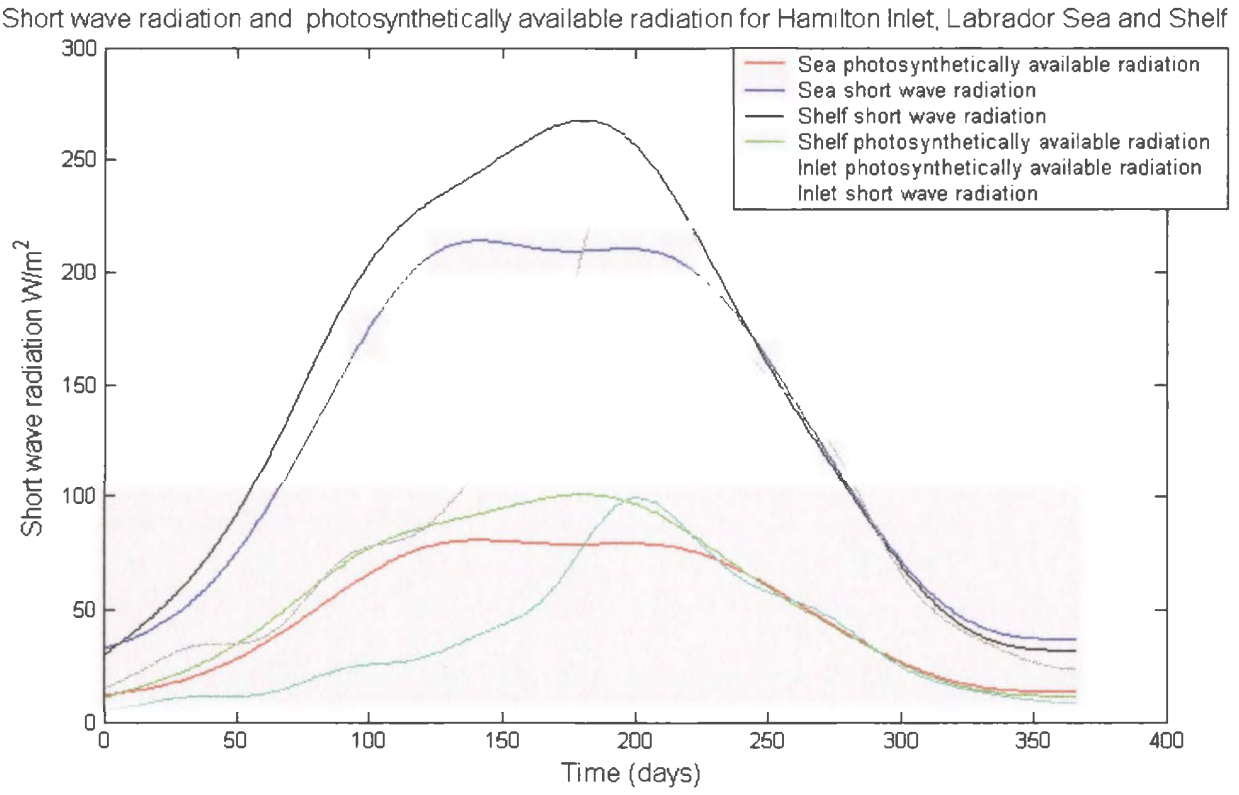

Figure 2.10: Short wave radiation and photosynthetically available radiation, I_{PAR}, for the Labrador Sea (56°N), Labrador Shelf and Hamilton Inlet (54°N). The incoming solar radiation is computed based on equations from Iqbal (1983) and Platt *et al.* (1990). The I_{PAR} is computed as 40% of the total incoming short wave radiation.

2.5. Hydrographic Data

While there has been much analysis of hydrographic data for the Labrador Sea and somewhat less for the Shelf; relatively little work has been published for Groswater Bay and the Hamilton Inlet.

2.5.1. Labrador Sea

The data for the Labrador Sea model simulations and validation were obtained from the literature studies, the BIO database (I.Yashayaev and B. Petrie, personal

communication, BIO and www.mar.dfo-mpo.gc.ca/science/ocean/home.html), and satellite imagery (Figure 2.11).

Historical temperature, salinity and density data from the BIO database were summarized over a period from 1928 to 2000 by I. Yashayaev (personal communication, BIO) to study the long-term changes in the Labrador Sea. The data set was collected from various locations across the Labrador Sea. This already formatted data set is used to determine periods of high and low stratification levels. The model is then run for these time periods to investigate biological changes. The plot using the data from Yashayaev's study reveals large annual and decadal variations in water mass properties. Values of potential temperature, salinity, pressure and potential density are computed as medians of all available measurements per year and plotted in pressure-time coordinates (Figure 2.12). Yashayaev reported that extremely severe winters between 1987 and 1994 led to the formation of Labrador Sea Water (LSW), which reached a depth of 2300 m. This LSW was fresher, cooler and denser than any other water in the entire time period. Following these intense winters, in 1995 the convective mixing only reached 1000 m and by 1996 the LSW was about half its original volume. Therefore, for this study the period between 1992 and 1999 is chosen to represent a period of strong convection and 1968 is chosen to represent a period of weak convection. These periods are also chosen on the basis of availability of continuous data.

The SeaWiFS satellite data used to validate the model are bi-monthly observations between 1997 and 2003 (Figure 2.13). All the original data are plotted and a bi-monthly mean is calculated. It is evident that the value of chlorophyll maximum

does vary from year to year. The maximum concentration of chlorophyll (approximately 15 mmol N/m^3) occurs during 2001 to 2003. The bi-monthly means are significantly lower since they are based on bi-monthly measurements and algal blooms occur in time scales of days. These maxima follow strong winter convection in the winter of 2000 and 2001, but not as strong as in the 1990s (I. Yashayaev, personal communication, BIO).

As well as using biological data collected by satellite imagery to verify the model, data from the literature are also used. Table 2.2 summarizes the reported peak bloom concentrations of chlorophyll from several literature sources and satellite derived data. Values range from 3 mg chl/m^3 from the CZCS (Campbell and Aarup, 1992) and 19 mg chl/m^3 from the BIO primary Productivity experiments (Trela, 1996).

The BIO database contains both nutrient concentrations and physical data. The density data from the BIO database are used to determine the mixed-layer depth and force the model. The nitrate concentration data are used to validate the model and determine the concentration in deep water to initiate the model, and the chlorophyll data are used to validate the model. In 1968, the surface temperature maximum occurs in summer (July, August) reaching about 8°C and the minimum occurs in winter (January to March) (Figure 2.14). Below 100 m the temperature is relatively stable between 3.7 and 3.5°C. A minimum of salinity and density occurs in summer at values below 34.4 psu and 26.6 σ_θ and a maximum occurs in winter of about 34.8 psu and 27.7 σ_θ. Below 200 m the salinity and density is stable at about 34.8 psu and 27.8 σ_θ.

In the 1990s the data are grouped into 7 depth ranges: 0-10 m, 40-50, 90-100 m , 100-150 m, 150-200 m, 400-500, and 800-1000 m and the daily mean and bi-monthly

means for each depth group is calculated (Figure 2.15). The two upper layers (0-10 m and 40–50 m) show a seasonal signal, where as the lower layers have a lesser or no seasonal signal. The temperature maximum occurs between days 210 and 225 (August) and reaches just over 10°C at the surface. The deeper layers have a lower and later temperature peak. The surface minimum temperature occurs at the end of February reaching almost –2°C. The salinity and density are missing data in winter from mid February to mid May and in fall from mid August until the end of September. In January, salinity and density reach a maximum and below 400 m they are stable at a maximum of about 34.8 psu and 27.7 σ_θ. In summer, at the surface they reach a minimum in August, corresponding with the maximum temperature, at 33 psu and 25.5 σ_θ.

The nutrient data consists of chlorophyll, nitrate, and phosphate and the data are quite sparse. For this reason, the nutrient and chlorophyll data are combined over all the years the data are available (1950 to 2001) (Figure 2.16). Chlorophyll data are only available in spring and summer from May to July with a few data points in February and October. The maximum chlorophyll concentration is 13 mg/m^3 at the beginning of June. The data in February and October show a low concentration below 1 mg/m^3. The nitrate data are also sparse in winter and fall. Nitrate is depleted between days 158 and 200 in the surface layers from the maximum levels in winter of around 17 mmol/m^3. The 90-1000 m layers have a more constant concentration between 12 and 17 mmol/m^3. This is consistent with values reported in the literature between 14 and 17.59 mmol/m^3 (Louanchi and Najjar, 2001; Anderson *et al.*, 1985). Phosphate has the most available data but the concentrations are quite variable at all depth layers. The minimum occurs for

the surface layer at day 180, with near depletion. The maximum occurs in February and March, reaching levels of 1.5 mmol/m^3. This is slightly higher than values reported in the literature between 1.07 and 1 mmol/m^3 (Louanchi and Najjar, 2001; Anderson *et al.*, 1985).

Table 2.3: Peak values of chlorophyll from the literature for the Labrador Sea.

Reference	**Data used for model validation**	**Maximum Chlorophyll mg chl/m^3**
Tian *et al.* 2004	W.K.W Li., Late 1990s	10-17
	Irwin, 1986, 1989, 1990	7-12
	Maclaren Atlantic Ltd., 1976, July 23	3.5-4.2
	Myers, 1994	11-18
	Bravo, July 11, 1995	4.7-5.8
Trela 1996	Imperial Oil Cruise, July 1976	4.1
	BIO primary Productivity experiments, 1978-1991	19
Campbell and Head 2000	BIO, May-June, 1997	13-15
Campbell and Aarup 1992	Coastal Zone Color Scanner, 1979-1983	2.99 - >10
Personal communication B. Petrie, THE DFO	SeaWiFS, 1998-2001	8-16

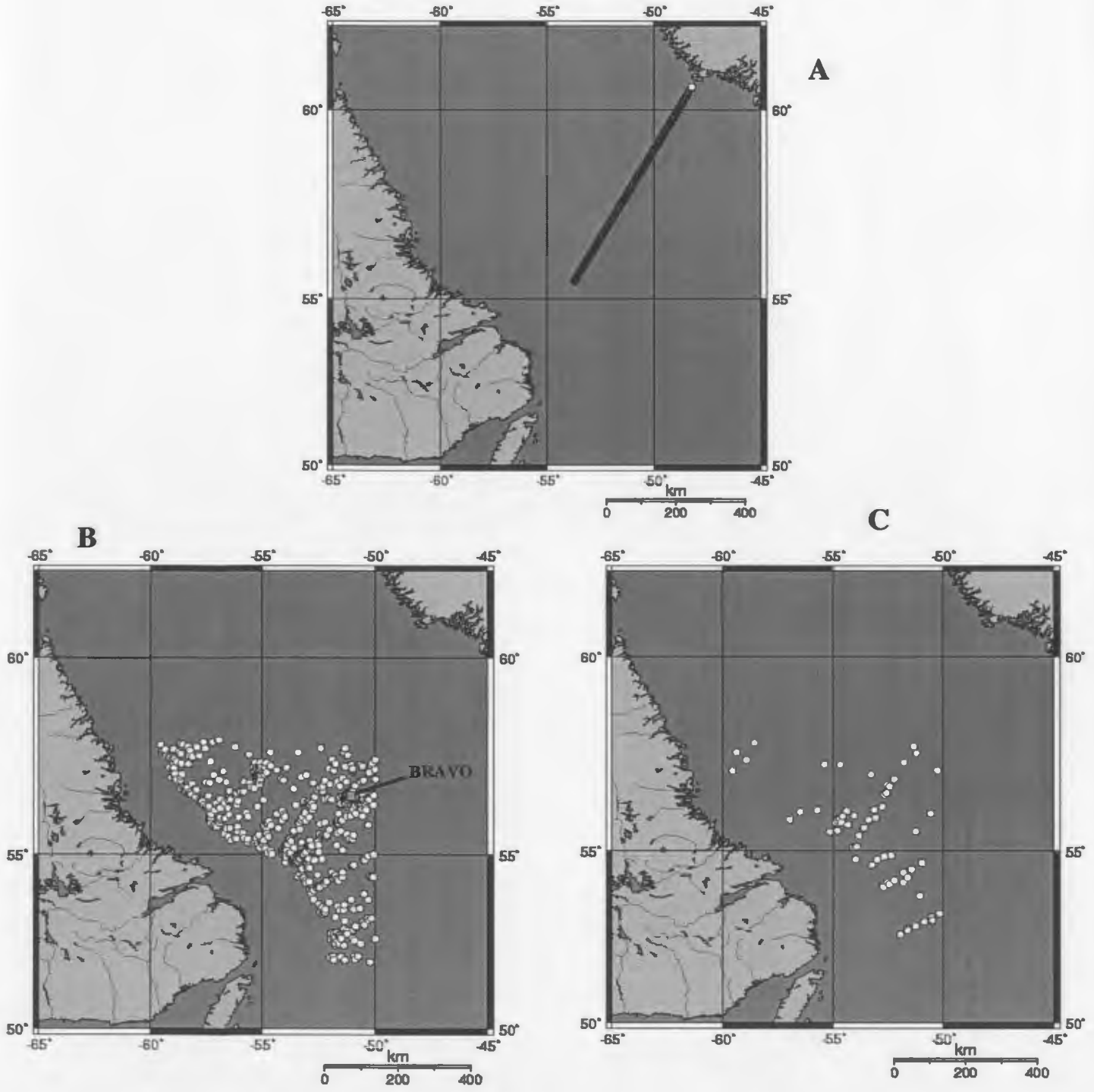

Figure 2.11: Locations of data sampled for the Labrador Sea. A) Temperature and SeaWiFS chlorophyll data from the Labrador Sea transect (B. Petrie, personal communication, BIO), B) temperature, density and salinity data (B. Petrie, personal communication, BIO and www.mar.dfo-mpo.gc.ca/science/ocean/home.html), C) chlorophyll, nitrate, phosphate data (B. Petrie, personal communication, BIO).

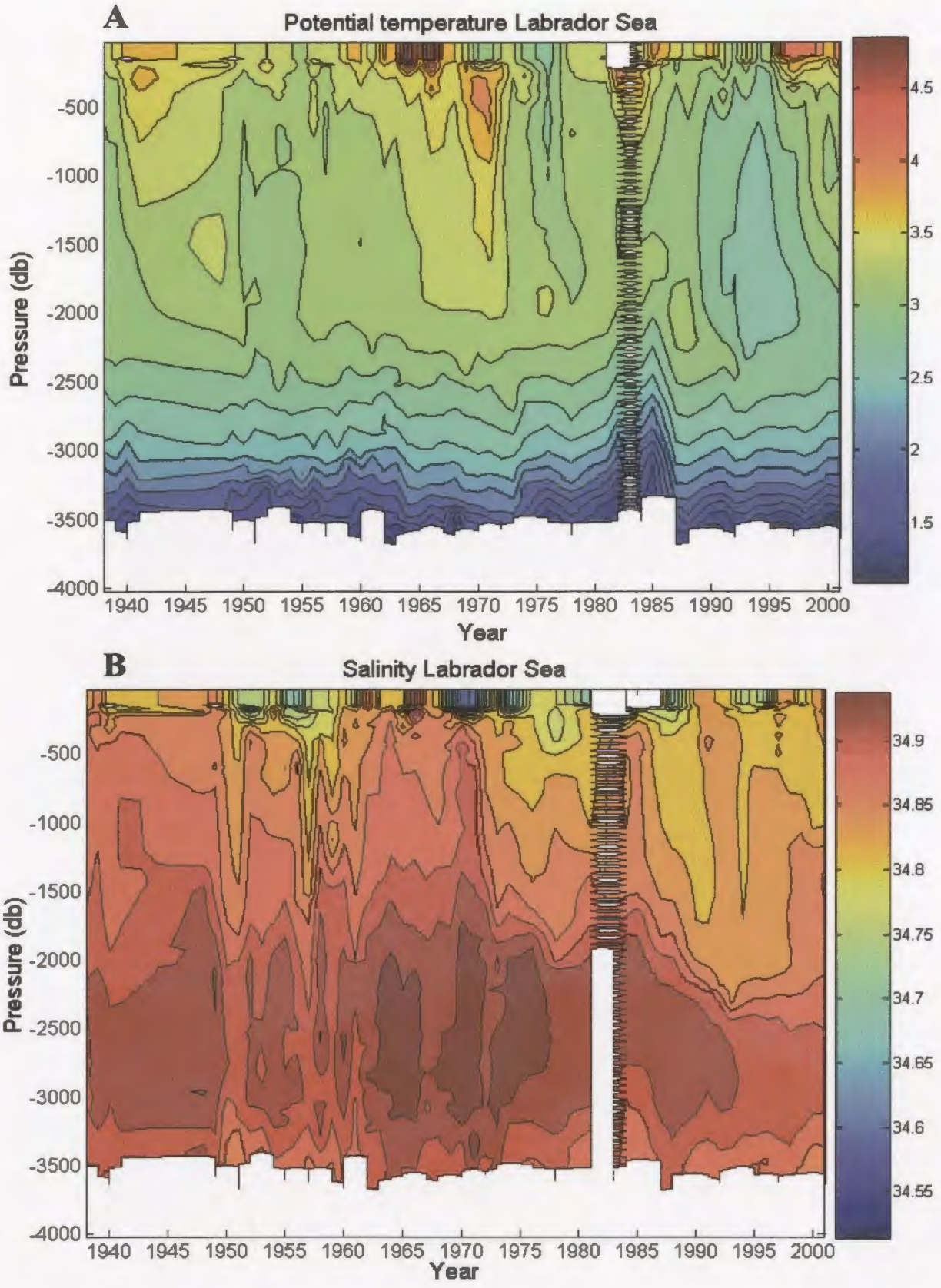
A
Potential temperature Labrador Sea
Pressure (db)
-500
-1000
-1500
-2000
-2500
-3000
-3500
-4000
1940 1945 1950 1955 1960 1965 1970 1975 1980 1985 1990 1995 2000
Year
4.5
4
3.5
3
2.5
2
1.5
B
Salinity Labrador Sea
Pressure (db)
-500
-1000
-1500
-2000
-2500
-3000
-3500
-4000
1940 1945 1950 1955 1960 1965 1970 1975 1980 1985 1990 1995 2000
Year
34.9
34.85
34.8
34.75
34.7
34.65
34.6
34.55

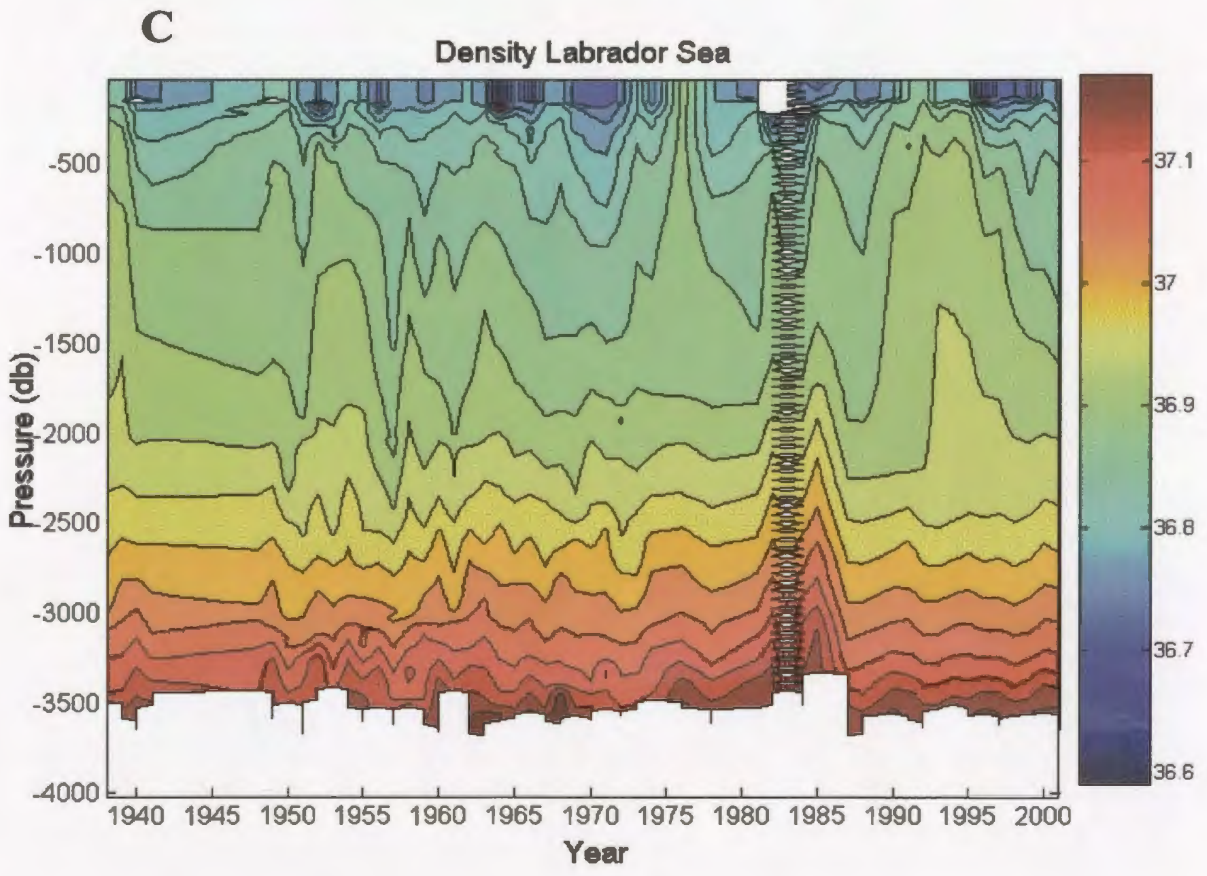

Figure 2.12: Historical data averaged yearly by depth from 1948 to 2001 by I. Yashayaev (personal communication, BIO). A) Potential temperature, B) Salinity and C) Density in *pressure-time* coordinates. The white gaps represent missing data.

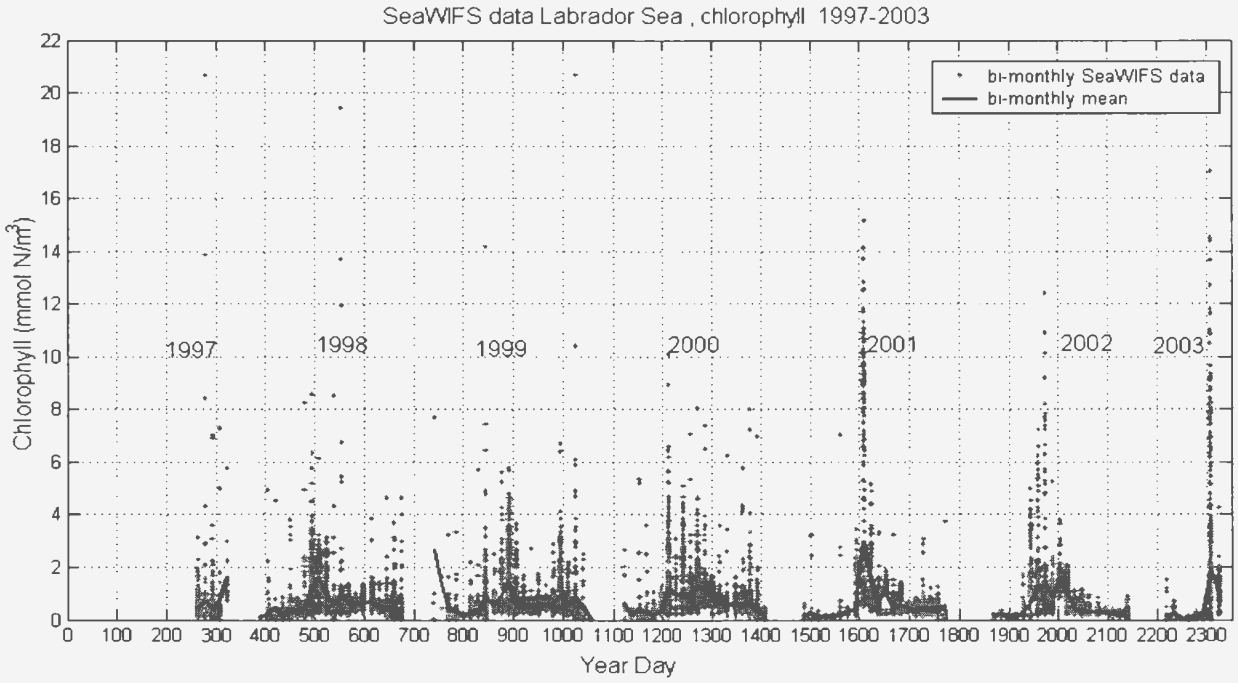

Figure 2.13: SeaWiFS satellite chlorophyll data from 1997 to 2003 for the Labrador Sea transect. The solid line depicts the bi-monthly means over different time periods. (B. Petrie, personal communication, BIO). Chlorophyll data converted from units of mg/m^3 to mmol N/m^3 using Redfield Ratio of carbon to nitrogen of 6.625 and carbon to chlorophyll ratio of 60.

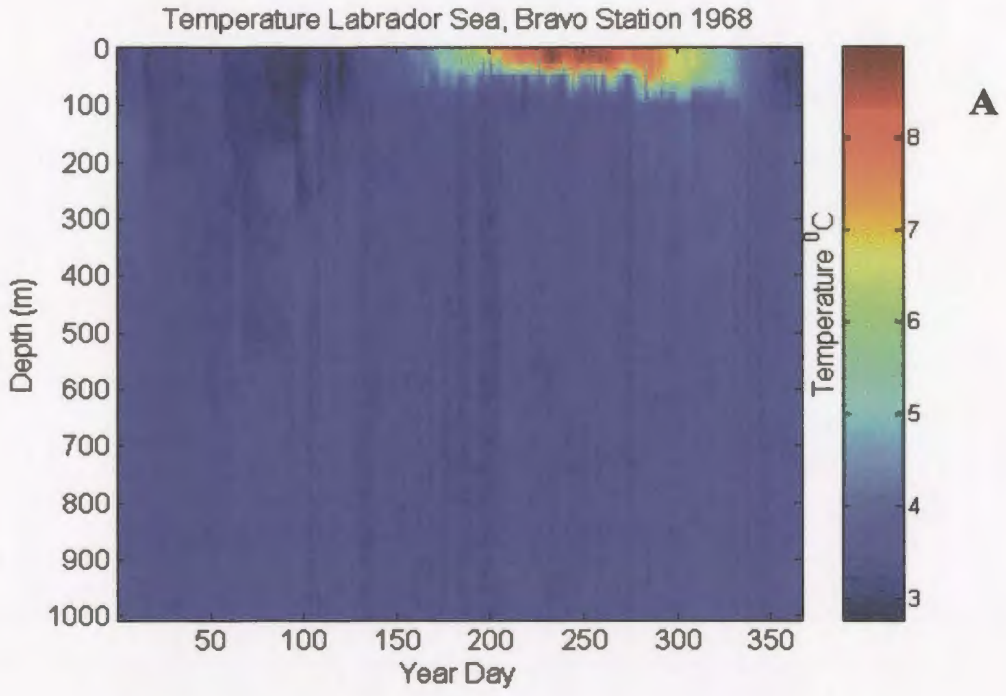
Temperature Labrador Sea, Bravo Station 1968
Depth (m)
0
100
200
300
400
500
600
700
800
900
1000
50
100
150
200
250
300
350
Year Day
Temperature °C
8
7
6
5
4
3

A

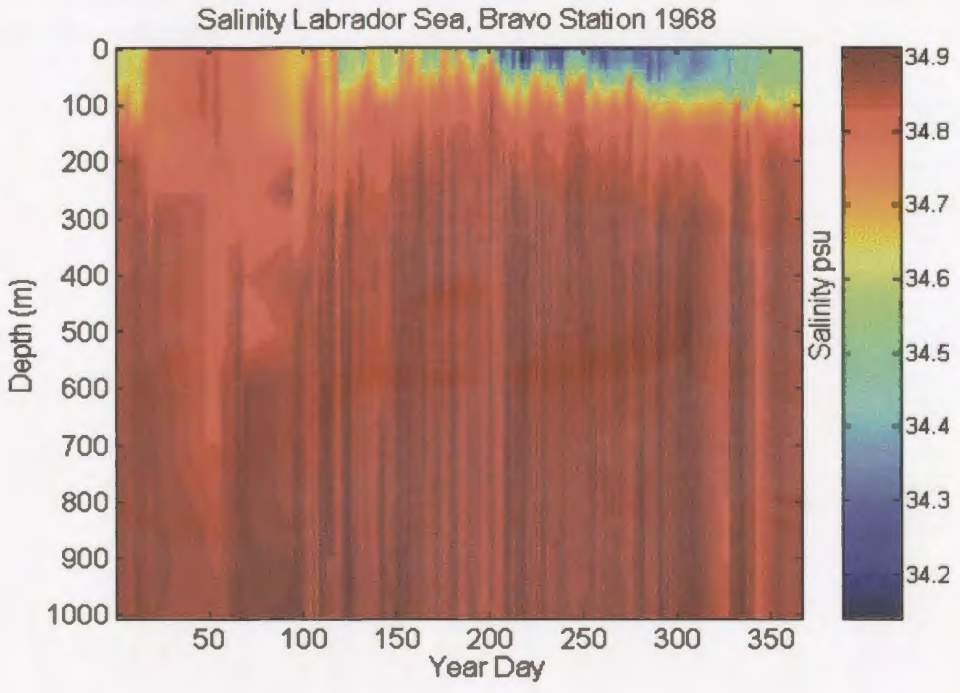
Salinity Labrador Sea, Bravo Station 1968
Depth (m)
0
100
200
300
400
500
600
700
800
900
1000
50
100
150
200
250
300
350
Year Day
Salinity psu
34.9
34.8
34.7
34.6
34.5
34.4
34.3
34.2

B

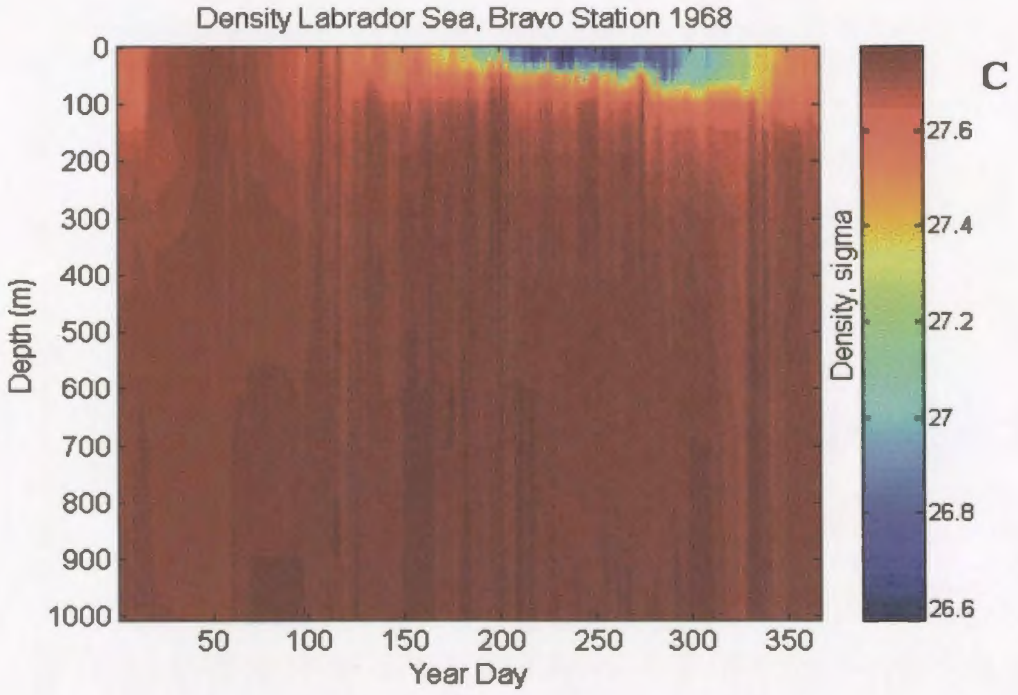

Figure 2.14: Temperature, salinity and density contour plots for the Labrador Sea, Bravo station during 1968. A) Temperature, B) salinity, and C) density. The color scales indicate temperature in °C, salinity as psu and density as σ_θ.

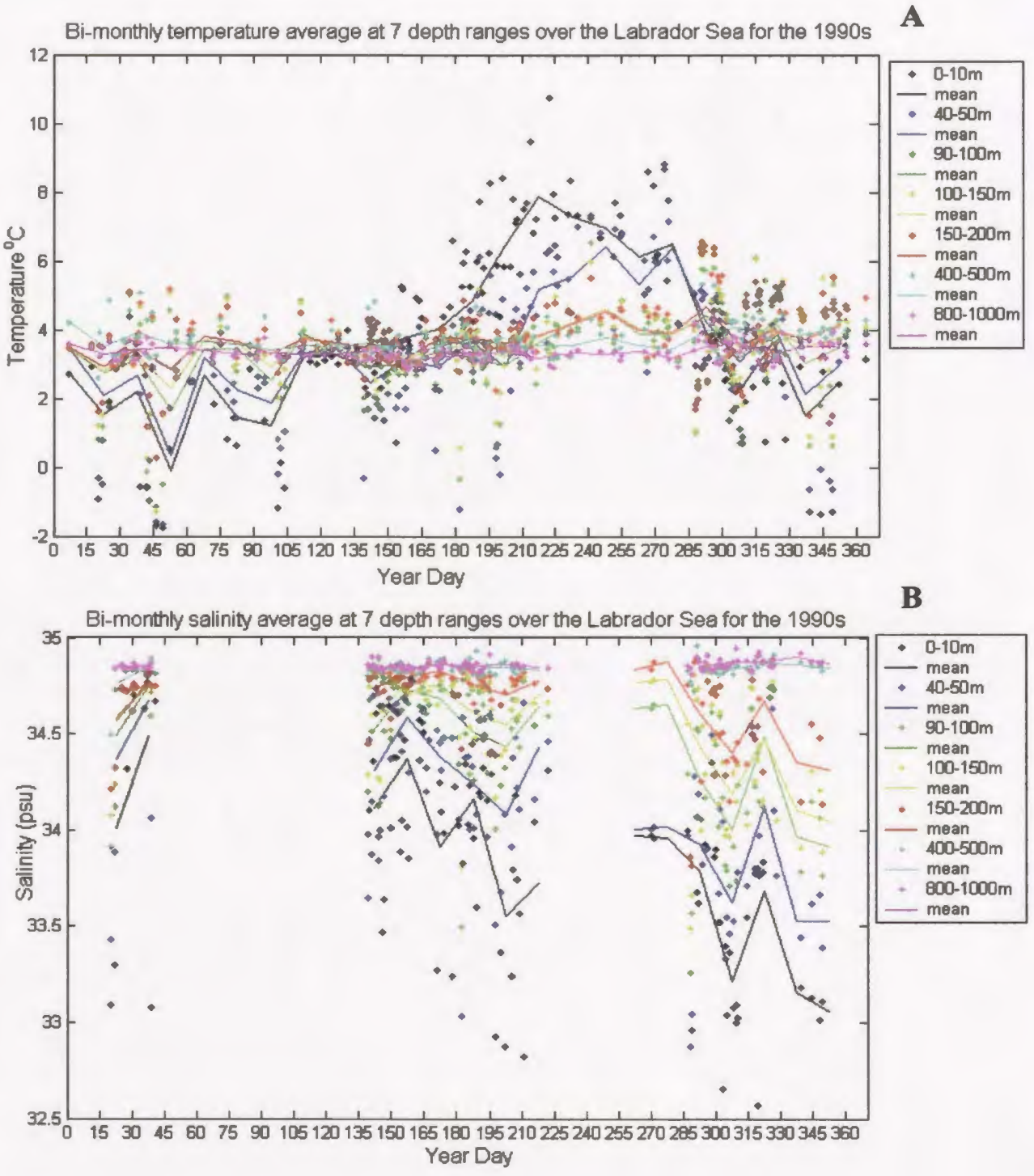
A
Bi-monthly temperature average at 7 depth ranges over the Labrador Sea for the 1990s
Temperature °C
Year Day
0-10m
mean
40-50m
mean
90-100m
mean
100-150m
mean
150-200m
mean
400-500m
mean
800-1000m
mean
B
Bi-monthly salinity average at 7 depth ranges over the Labrador Sea for the 1990s
Salinity (psu)
Year Day
0-10m
mean
40-50m
mean
90-100m
mean
100-150m
mean
150-200m
mean
400-500m
mean
800-1000m
mean

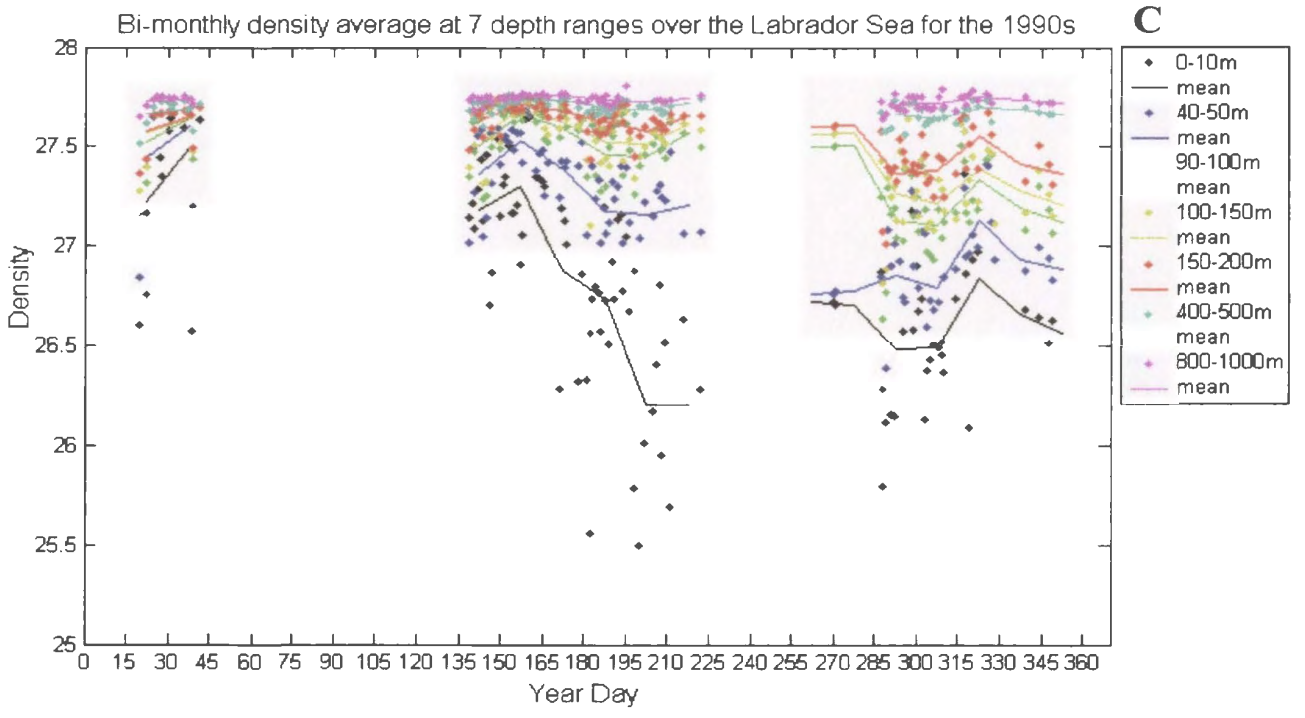

Figure 2.15: Temperature, salinity and density for the Labrador Sea, during the 1990s. A) Temperature °C, B) salinity psu, and C) density σ_t. The data are grouped into 7 depth ranges: 0-10 m (black); 40-50 m (blue); 90-100 m (green); 100-150 m (yellow); 150-200 m (red); 400-500 (cyan); 800-1000 m (magenta). The dots represent the daily mean values and the solid lines are the bi-monthly means.

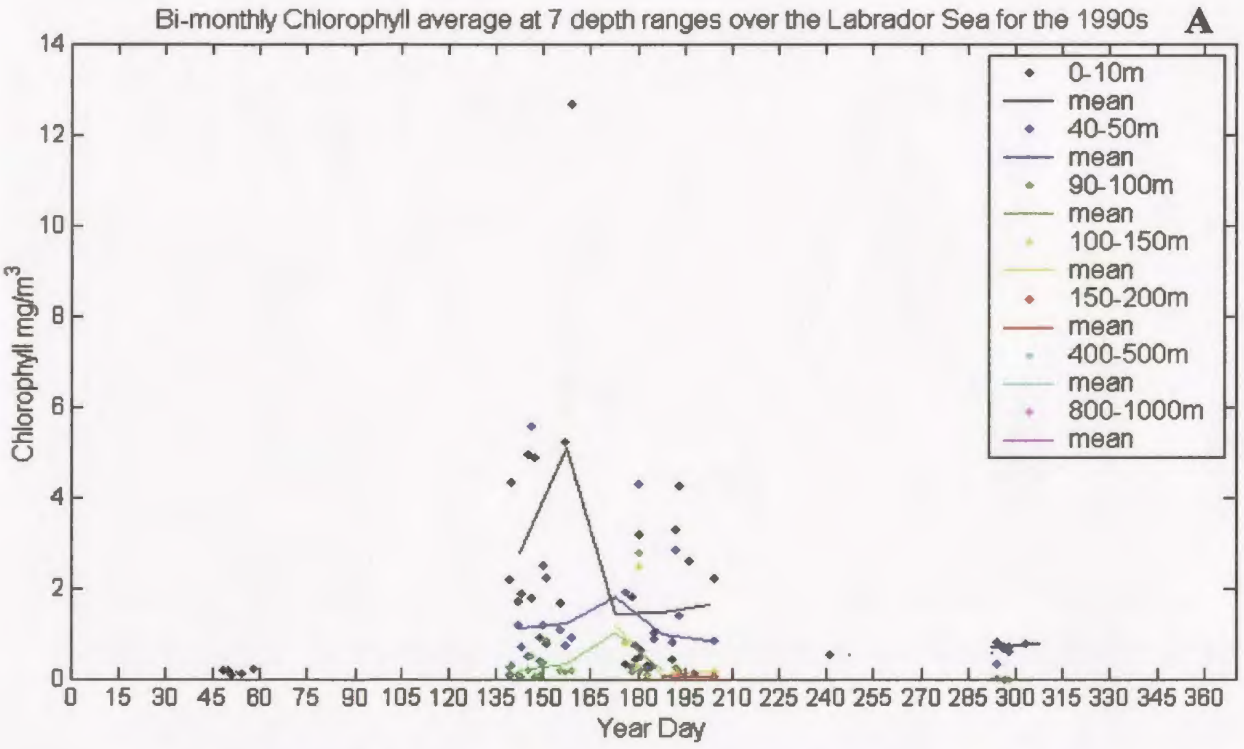
Bi-monthly Chlorophyll average at 7 depth ranges over the Labrador Sea for the 1990s
A
Chlorophyll mg/m3
Year Day
0-10m
mean
40-50m
mean
90-100m
mean
100-150m
mean
150-200m
mean
400-500m
mean
800-1000m
mean

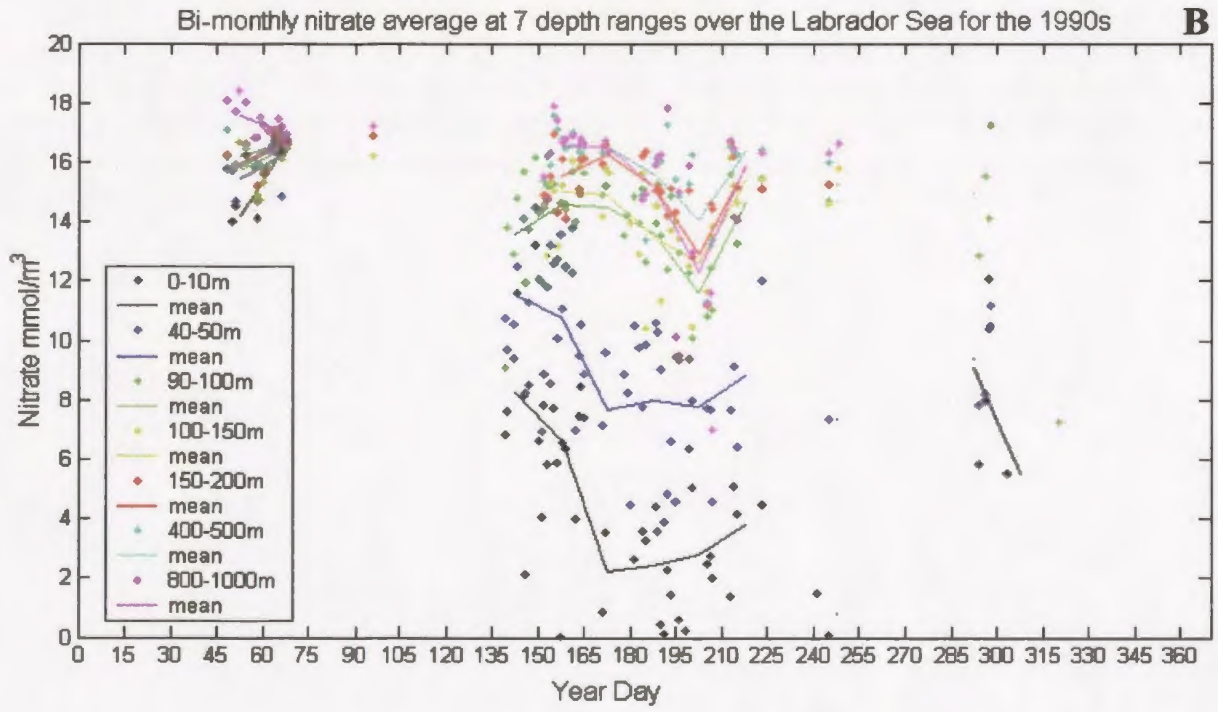
Bi-monthly nitrate average at 7 depth ranges over the Labrador Sea for the 1990s
B
Nitrate mmol/m3
Year Day
0-10m
mean
40-50m
mean
90-100m
mean
100-150m
mean
150-200m
mean
400-500m
mean
800-1000m
mean

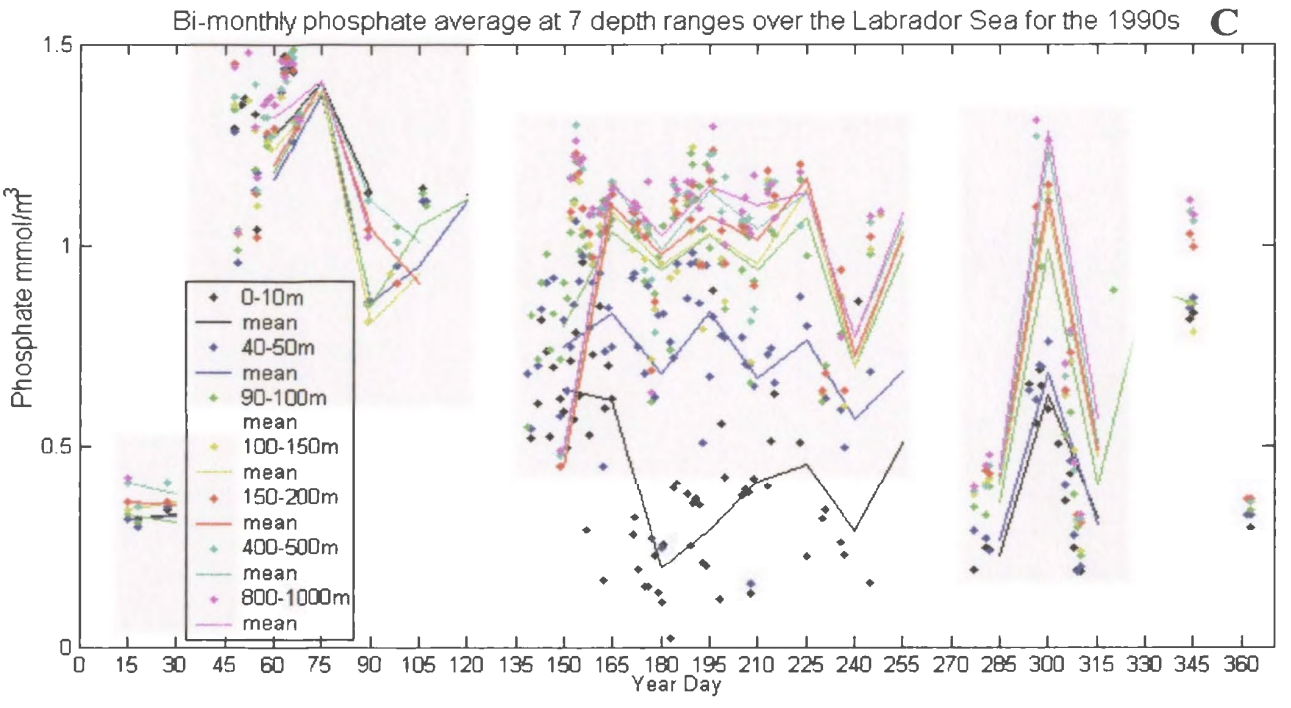

Figure 2.16: Chlorophyll, nitrate and phosphate concentrations for the Labrador Sea, combined over the years 1950 to 2001. A) chlorophyll mg/m^3 , B) nitrate mmol/m^3, C) phosphate mmol/m^3. The data are grouped into 7 depth ranges: 0-10 m (black); 40-50 m (blue); 90-100 m (green); 100-150 m (yellow); 150-200 m (red); 400-500 (cyan); 800-1000 m (magenta). The dots represent the daily mean values and the solid lines are the bi-monthly means.

2.5.2. Labrador Shelf

The data for the Labrador Shelf model simulations and validation were obtained from the BIO database (B. Petrie, personal communication, BIO and www.mar.dfo-mpo.gc.ca/science/ocean/home.html), from the Offshore Labrador Biological Studies Program (OLABS) and from satellite imagery. The data sampling locations for the Shelf were from 55°N to 51.5°N and expand from the shore to about the 500 m isobaths (Figure 2.17).

The data obtained from the Offshore Labrador Biological Studies Program (OLABS) covers the period of July-September 1979 (Buchanan and Foy, 1980). The OLABS study was initiated by the Department of Energy, Mines and Resources. It was a three-year program that collected baseline biological, meteorological and oceanographic data. The data obtained included temperature, salinity, nitrate, silicate, chlorophyll, and phosphorus. The temperature and salinity data are combined with data from the BIO database and are used to calculate the density to determine the mixed-layer depth, which forces the biological model. The chlorophyll and nitrate data are also combined with those from the BIO database and used to validate the model simulations.

The SeaWiFS satellite data used to validate the model are shown in Figure 2.18 between the years of 1997 and 2003 for bi-monthly time periods. All the original data are plotted and a bi-monthly mean is calculated. It is evident that the value of chlorophyll maximum does vary each year, between 8 and 14 mmol N/m^3, and the year 2000 seems to have the highest chlorophyll peak. The bi-monthly means are significantly lower since they are based on bi-monthly measurements, and algae blooms

often occur in time scales of days. There is evidence of a second smaller and later peak in chlorophyll concentrations.

As well as using biological data collected by satellite imagery to verify the model, values reported in the literature are also used. Table 2.3 summarizes the reported peak bloom concentrations of chlorophyll from several literature sources and satellite derived data. Values range from 3 mg chl/m^3 from the CZCS (Campbell and Aarup, 1992) to 20 mg chl/m^3 from the BIO Primary Productivity experiments (Trela, 1996).

The BIO database contains both nutrient concentrations and physical data. The temperature and salinity data from the BIO database is used to determine the mixed-layer depth and force the model. The nitrate concentration data are used to validate the model and determine the concentration in deep water to initiate the model, and the chlorophyll data are used to validate the model. The data are grouped into six depth ranges: 0-10 m, 40-50 m, 90-100 m, 100-150 m, 150-200 m and 350-400 and the daily mean and bi-monthly means for each depth group is calculated. The upper layers (0-10 m) exhibit a pronounced seasonal signal, the lower layers have a lesser or no seasonal signal, as expected (Petrie *et al.*, 1992).

The surface temperature seasonal cycle depicts a temperature minimum in winter increasing to a peak in August and decreasing again to a minimum in January (Figure 2.19). Between 50 m and 400 m the temperature is lowest at 50 m throughout the year and increases gradually as the depth decreases, except in late August and early September where there is a slight peak at 50 m. This seasonal cycle is consistent with that reported by Lazier (1982). The temperature between 350 and 400 m is constant between 3.5 and

just over 4 °C. The surface temperature maximum is about 9°C for all years except for the 1980s when it could not be determined since there is data missing from February to April, in August and in September. The timing of the temperature peak varied slightly from the 1960s to 1990s, increasing from approximately days 225 to 240. The temperature minimum occurred in winter, although winter data were sparse especially in the 1970s and 1980s. The minimum temperature approached –1.8°C.

The surface salinity seasonal cycle depicts a salinity maximum in winter, decreasing to a minimum in August and increasing again to a maximum in January (Figure 2.20). From 50 m to 400 m the salinity is lowest at 50 m throughout the year, increasing gradually with increasing water level to a relatively consistent maximum in the deepest layer between 34.5 and 35 psu. This seasonal cycle is consistent with that reported by Lazier (1982). The winter data are sparse for all years except the 1960s. For the 1960s the surface salinity maximum occurs in March and April. The surface salinity minimum is about 29.5 psu for all years. The timing of the density minimum peak varied slightly from the 1960s to 1990s, increasing from approximately days 215 to 255.

The surface density seasonal cycle is the same as that for salinity (Figure 2.21). The maximum density in the deepest layer is about 27.5 σ_t. The winter data are sparse for all years except the 1960s. For the 1960s, the surface density maximum occurs in March and April. The surface salinity minimum is between 23 and 23.5 σ_t for all years. The timing of the salinity minimum peak varied slightly from the 1960s to 1990s, increasing from approximately days 215 to 240.

The nutrient data consist of nitrate, chlorophyll, and phosphate, and the data are quite sparse. For this reason the nutrient and chlorophyll data are combined over all the years the data are available, from 1950 to 2001 (Figure 2.22). Chlorophyll data are only available in spring and summer from May to July with a few data points in February, March and October. The maximum chlorophyll concentration is 17 mg/m^3 at the beginning of June. The data in February and October show a low concentration below 1 mg/m^3. The nitrate data are also sparse in winter and fall. Nitrate is depleted between days 135 and 210 in the surface layers from the maximum levels in winter in the deep layer of around 17 mmol NO_3^-/m^3. The lower layers have a more constant concentration between 12 and 17 mmol NO_3^-/m^3. Phosphate has the most available data and is quite variable at all depths layers. The minimum occurs for the surface layer at day 190, with near depletion. The maximum occurs in February and March, reaching levels of 1.6 mmol PO_4^{3-}/m^3.

Table 2.4: Peak concentrations of chlorophyll from the literature for the Labrador Shelf.

Reference	**Data used for model validation**	**Maximum Chlorophyll mg chl/m^3**
Drinkwater 2001	Data collected September 1985 Coastal Zone Color Scanner, 1978-1986	>3
Campbell and Aarup 1992 and Sarmiento *et al.* 1993	Coastal Zone Color Scanner, 1979-1983	2.99- >10
Personal communication B. Petrie, BIO	Sea WiFs,1998-2000	8-16
Irwin, *et al.* 1990	Bravo, May 1988	12.47
Stuart *et al.* 2000	BIO, May 1996	18
Pepin and Maillet 2002	BIO, July 2001	16-20

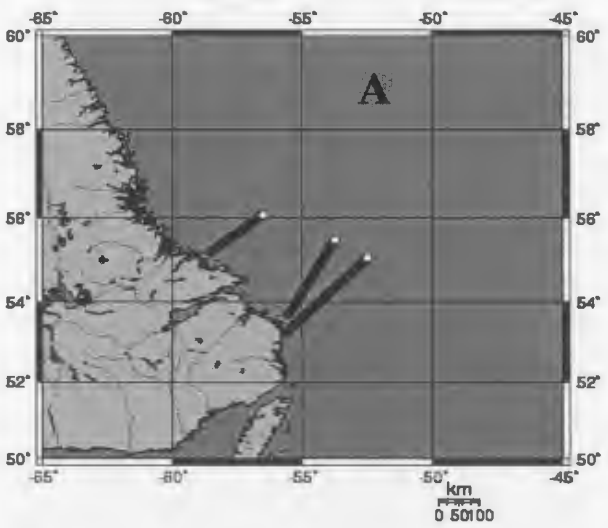
A
-65°
-60°
-55°
-50°
-45°
60°
58°
56°
54°
52°
50°
km
0 50100

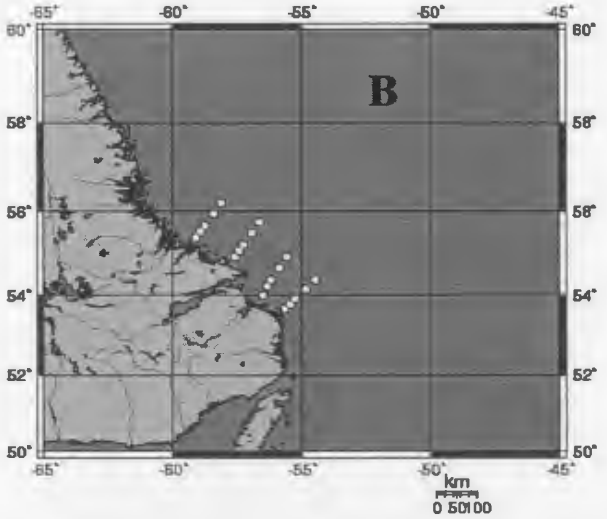
B
-65°
-60°
-55°
-50°
-45°
60°
58°
56°
54°
52°
50°
km
0 50100

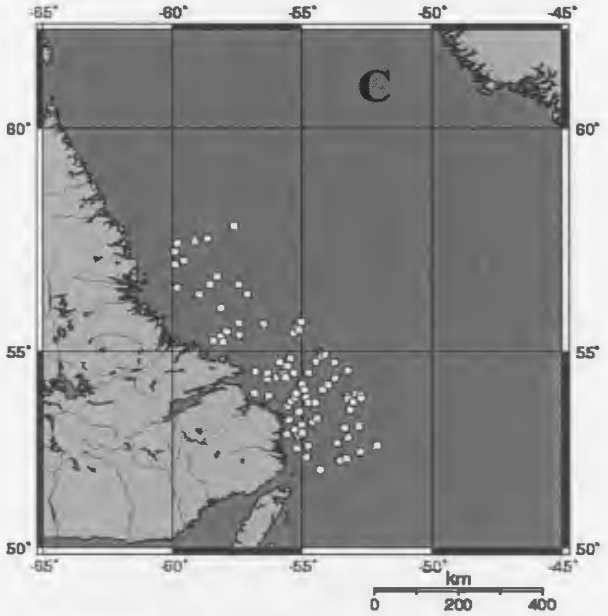
C
-65°
-60°
-55°
-50°
-45°
60°
55°
50°
km
0
200
400

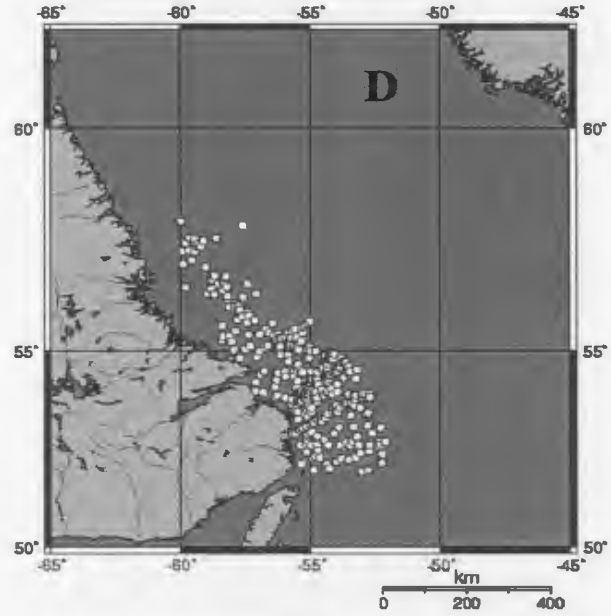
D
-65°
-60°
-55°
-50°
-45°
60°
55°
50°
km
0
200
400

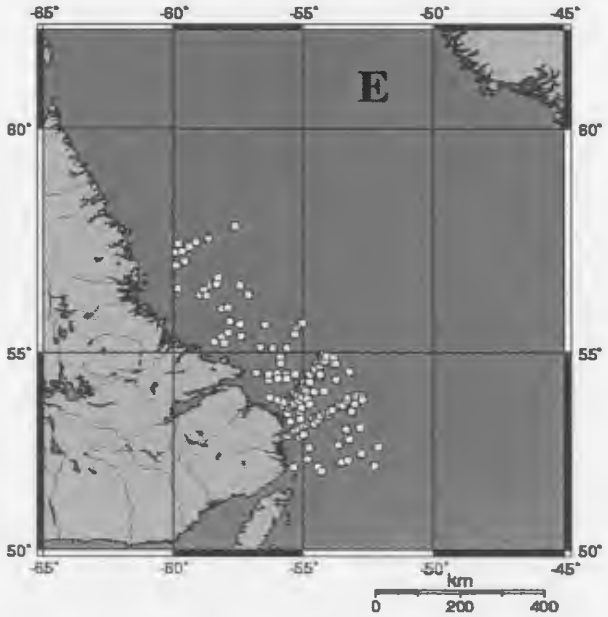
E
-65°
-60°
-55°
-50°
-45°
60°
55°
50°
km
0
200
400

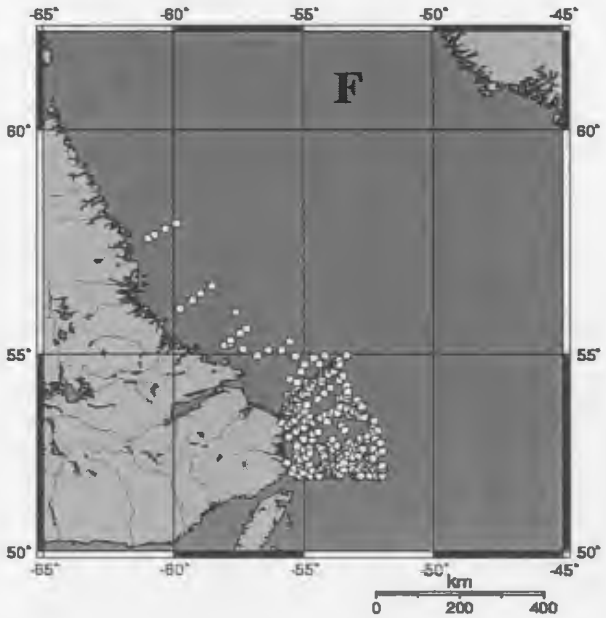
F
-65°
-60°
-55°
-50°
-45°
60°
55°
50°
km
0
200
400

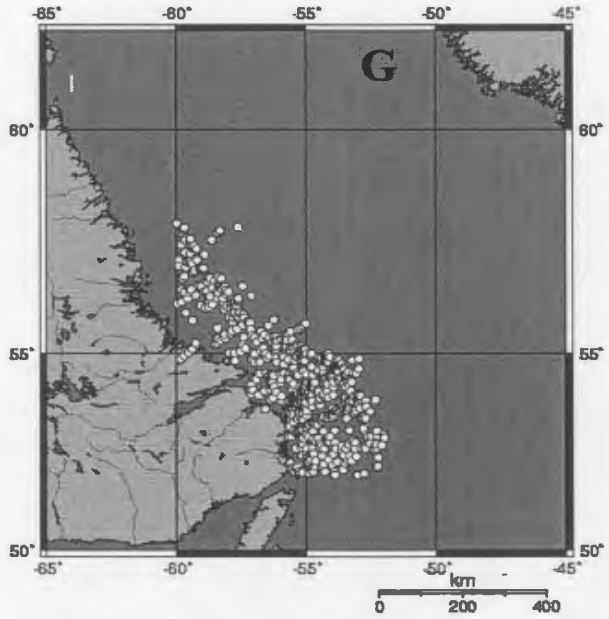

Figure 2.17: Locations of data sampled for the Labrador Shelf. Only data below 55°N was used. A) SeaWiFS temperature and chlorophyll data, B) OLABS temperature, salinity, nitrate, phosphate, silicate and chlorophyll data, C) BIO chlorophyll data, D) BIO phosphate data, E) BIO nitrate data, F) BIO density data and G) BIO temperature and salinity data.

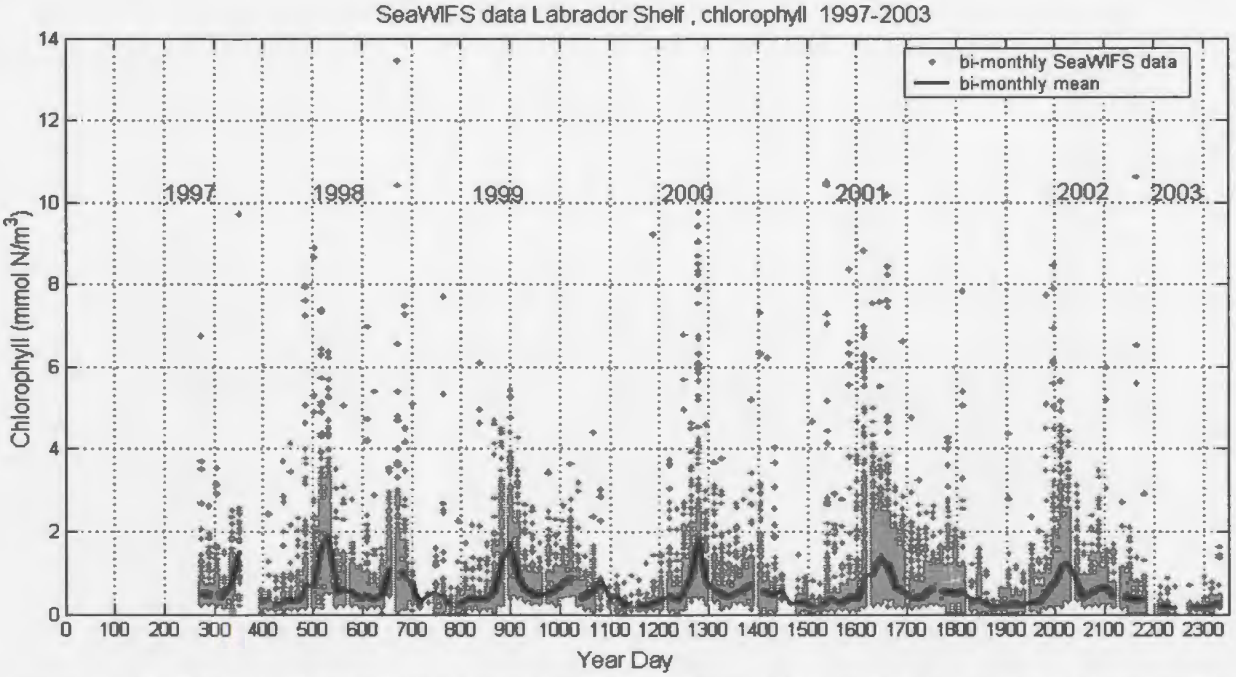

Figure 2.18: SeaWiFS satellite chlorophyll data from 1997 to 2003 for the Labrador Shelf transect. The solid line depicts the bi-monthly means over different time periods. (B. Petrie, personal communication, BIO). Chlorophyll data converted from units of mg/m^3 to mmol N/m^3 using Redfield Ratio of carbon to nitrogen of 6.625 and carbon to chlorophyll ratio of 60.

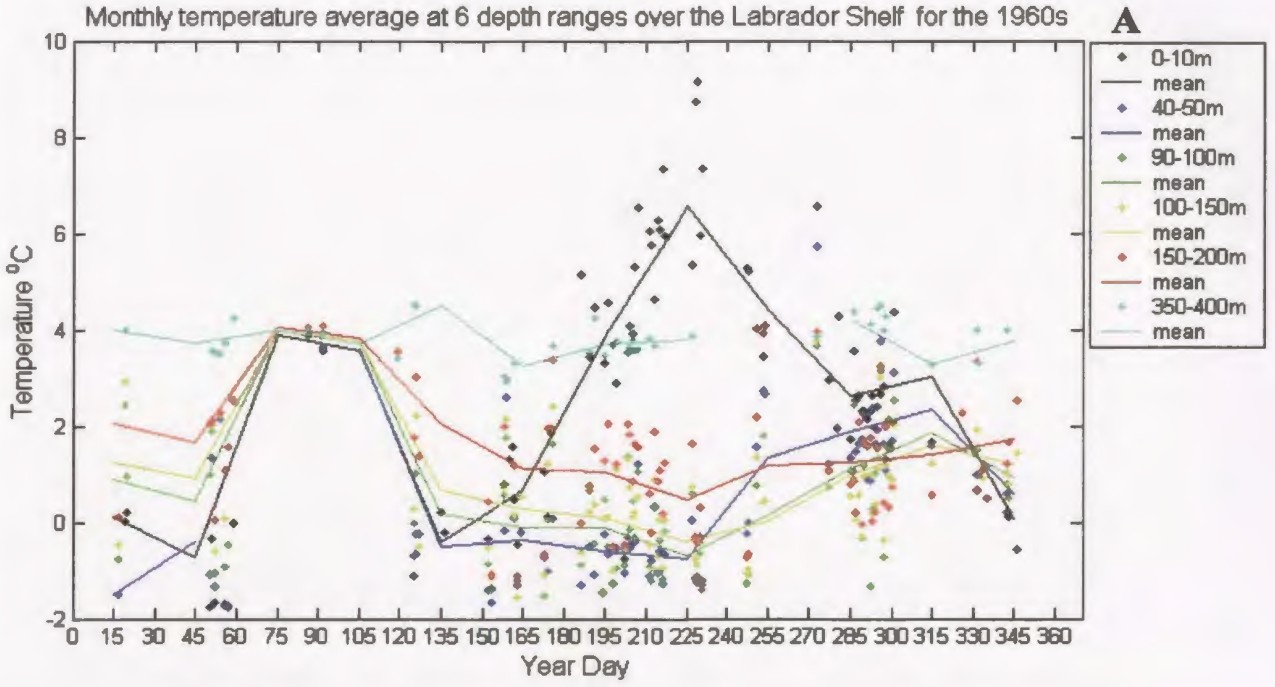
Monthly temperature average at 6 depth ranges over the Labrador Shelf for the 1960s
A
Temperature °C
Year Day
0-10m
mean
40-50m
mean
90-100m
mean
100-150m
mean
150-200m
mean
350-400m
mean

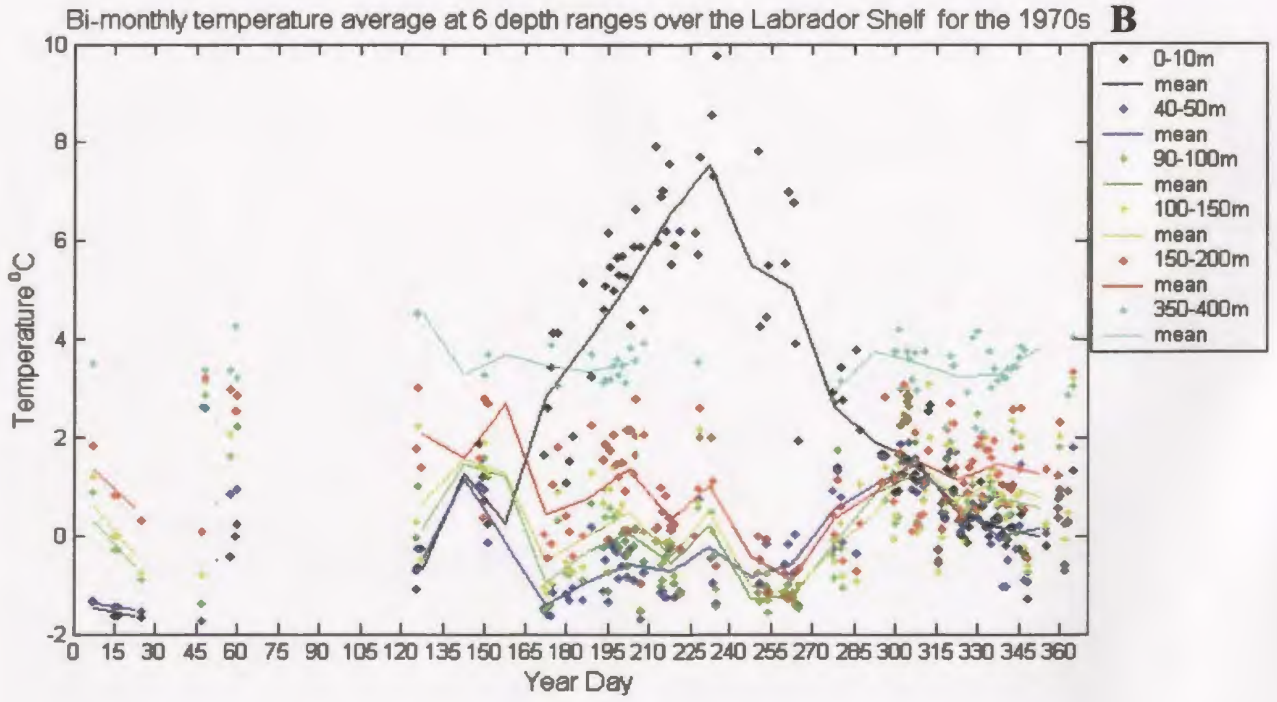
Bi-monthly temperature average at 6 depth ranges over the Labrador Shelf for the 1970s
B
Temperature °C
Year Day
0-10m
mean
40-50m
mean
90-100m
mean
100-150m
mean
150-200m
mean
350-400m
mean

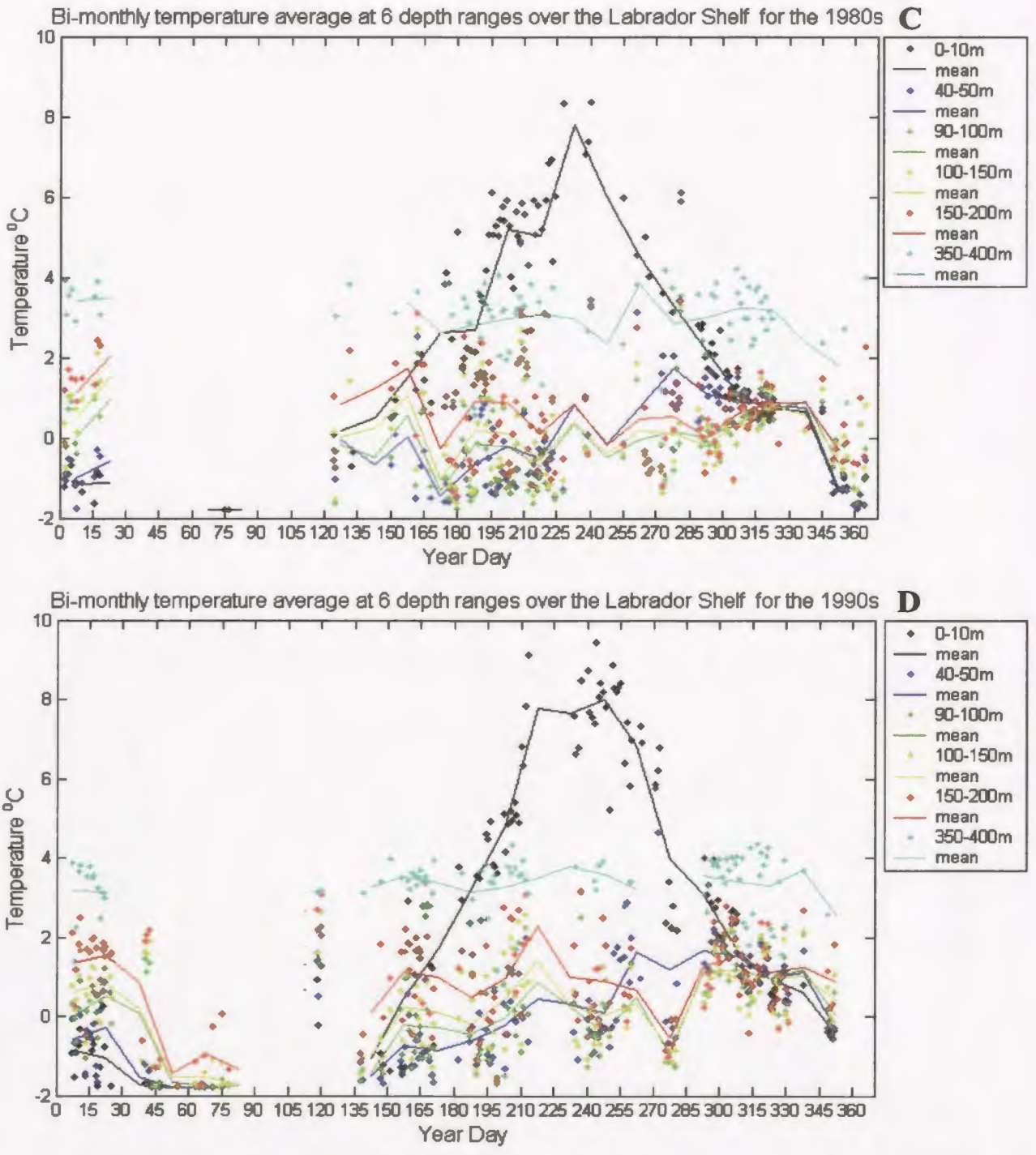

Figure 2.19: Temperature (°C) for the Labrador Shelf, during the; A) 1960s, B) 1970s, C) 1980s, D) 1990s. The data are grouped into 6 depth ranges: 0-10 m (black); 40-50 m (blue); 90-100 m (green); 100-150 m (yellow); 150-200 m (red); 350-400 (cyan). The dots represent the daily mean values and the solid lines are the bi-monthly means.

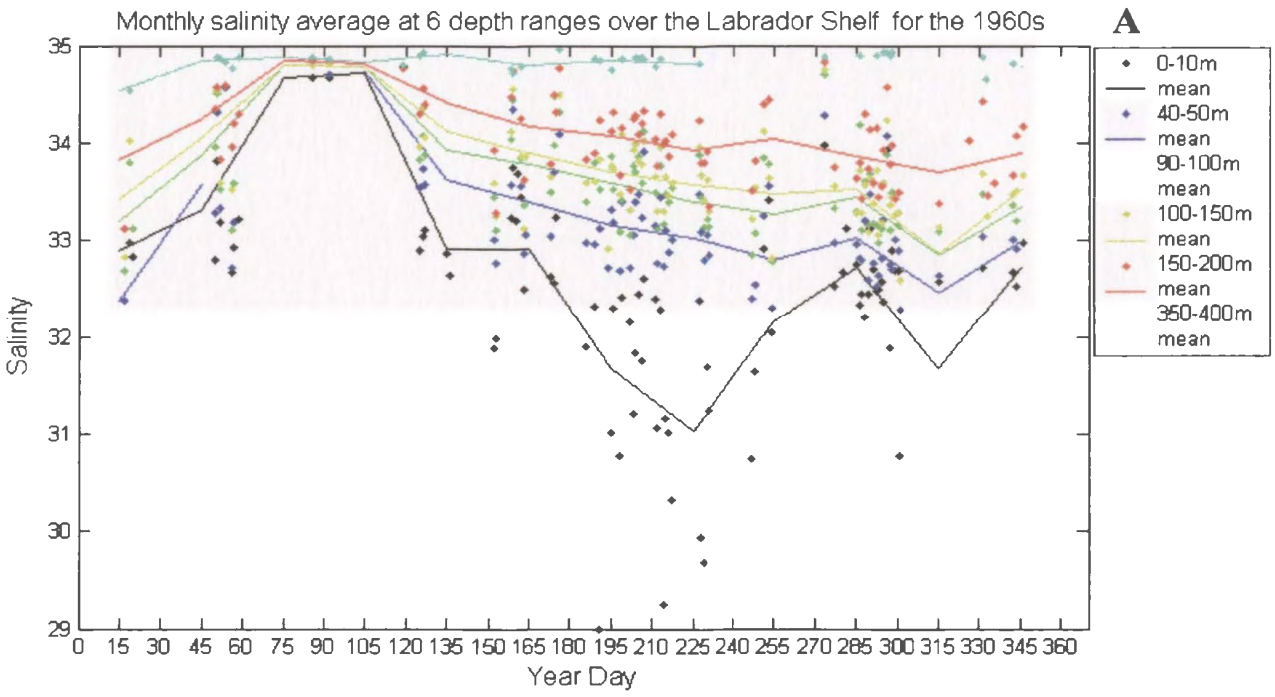
Monthly salinity average at 6 depth ranges over the Labrador Shelf for the 1960s
A
Salinity
Year Day
0-10m
mean
40-50m
mean
90-100m
mean
100-150m
mean
150-200m
mean
350-400m
mean

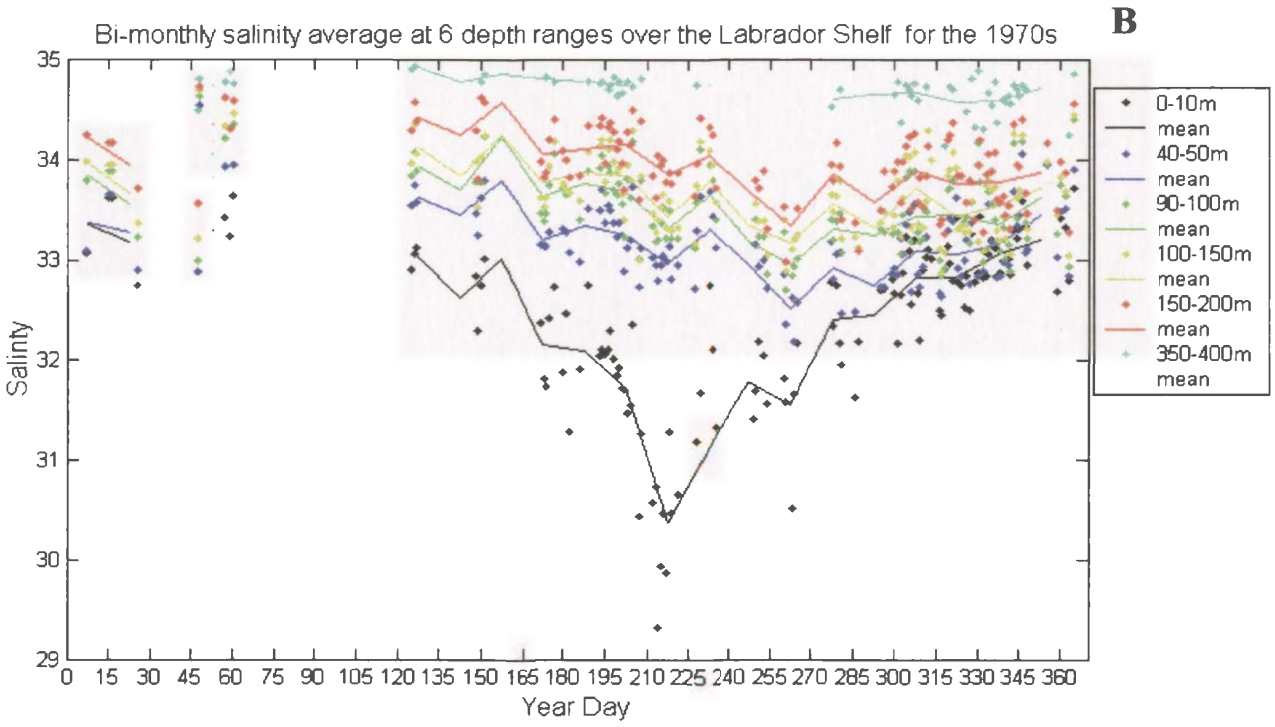
Bi-monthly salinity average at 6 depth ranges over the Labrador Shelf for the 1970s
B
Salinity
Year Day
0-10m
mean
40-50m
mean
90-100m
mean
100-150m
mean
150-200m
mean
350-400m
mean

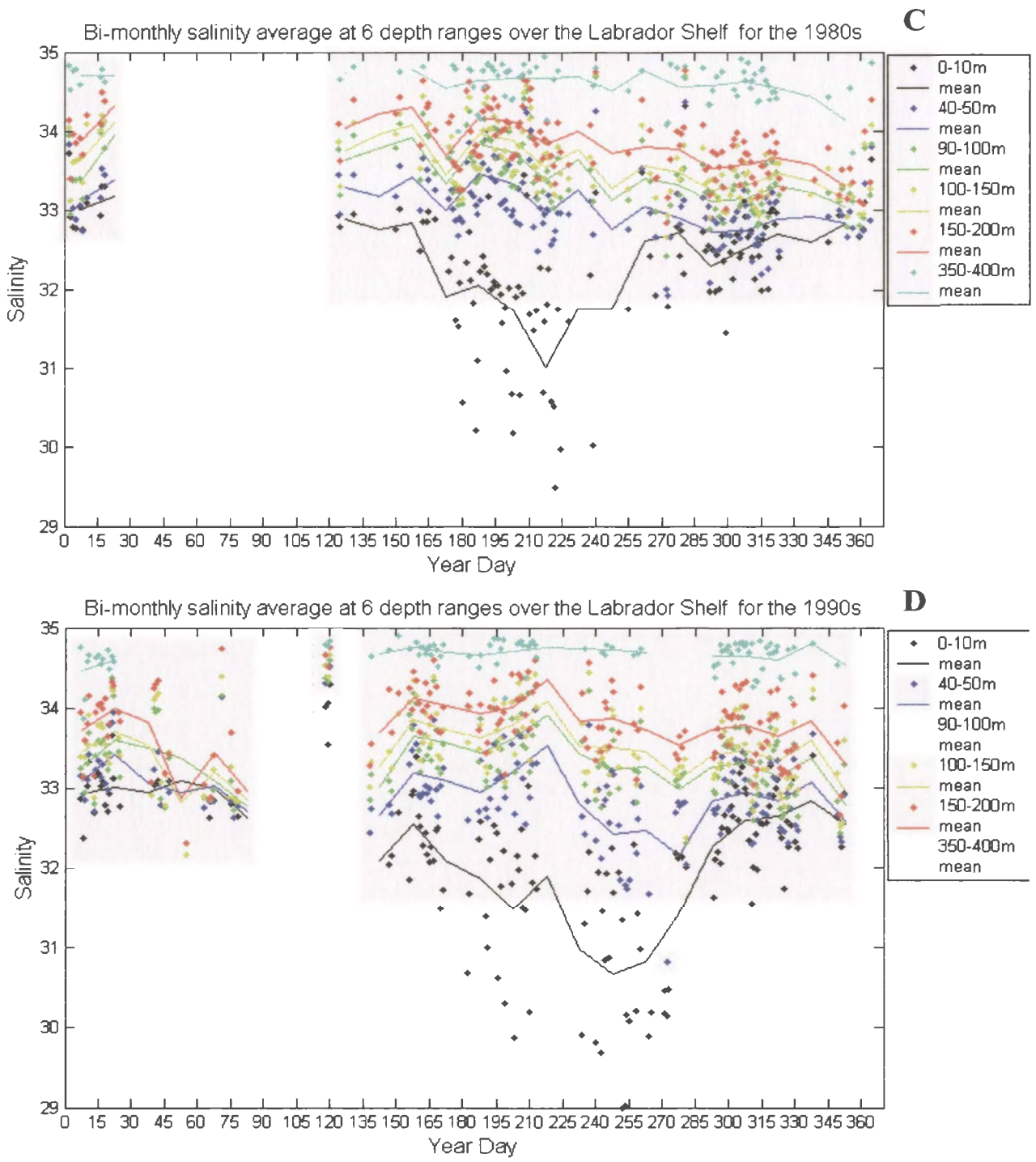

Figure 2.20: Salinity (psu) for the Labrador Shelf, during the; A) 1960s, B) 1970s, C) 1980s, D) 1990s. The data are grouped into 6 depth ranges: 0-10 m (black); 40-50 m (blue); 90-100 m (green); 100-150 m (yellow); 150-200 m (red); 350-400 (cyan). The dots represent the daily mean values and the solid lines are the bi-monthly means.

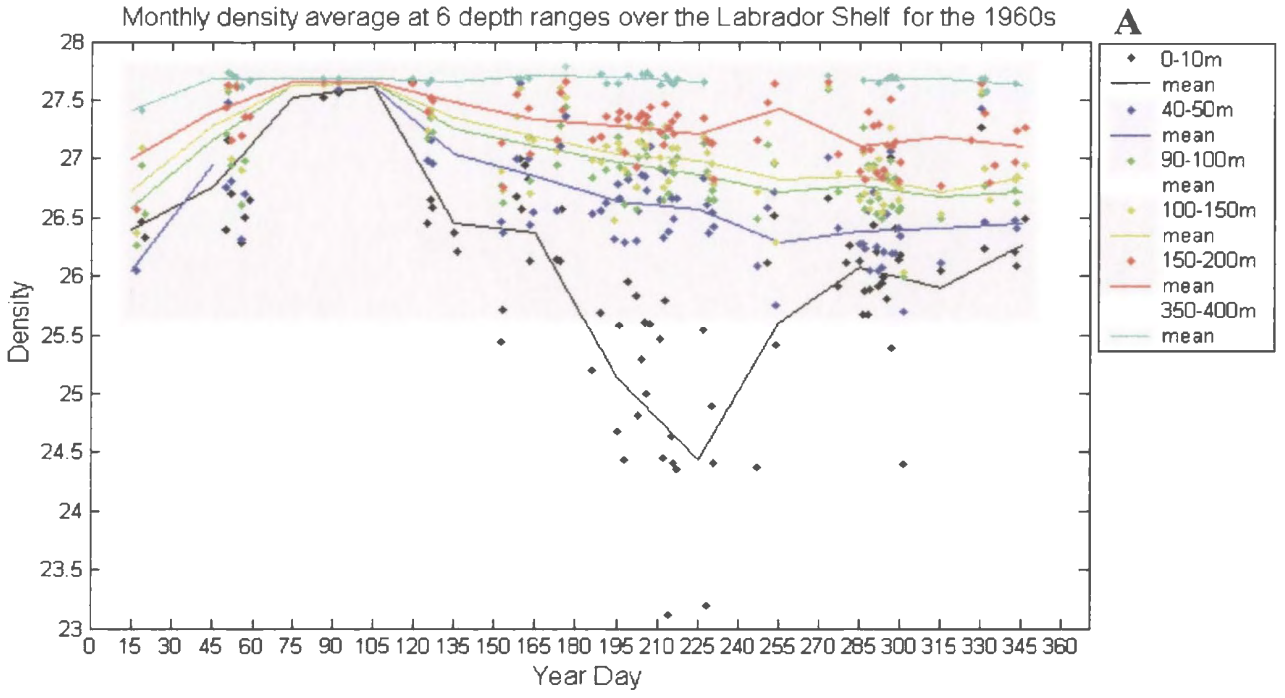
Monthly density average at 6 depth ranges over the Labrador Shelf for the 1960s
A
Density
Year Day
0-10m
mean
40-50m
mean
90-100m
mean
100-150m
mean
150-200m
mean
350-400m
mean

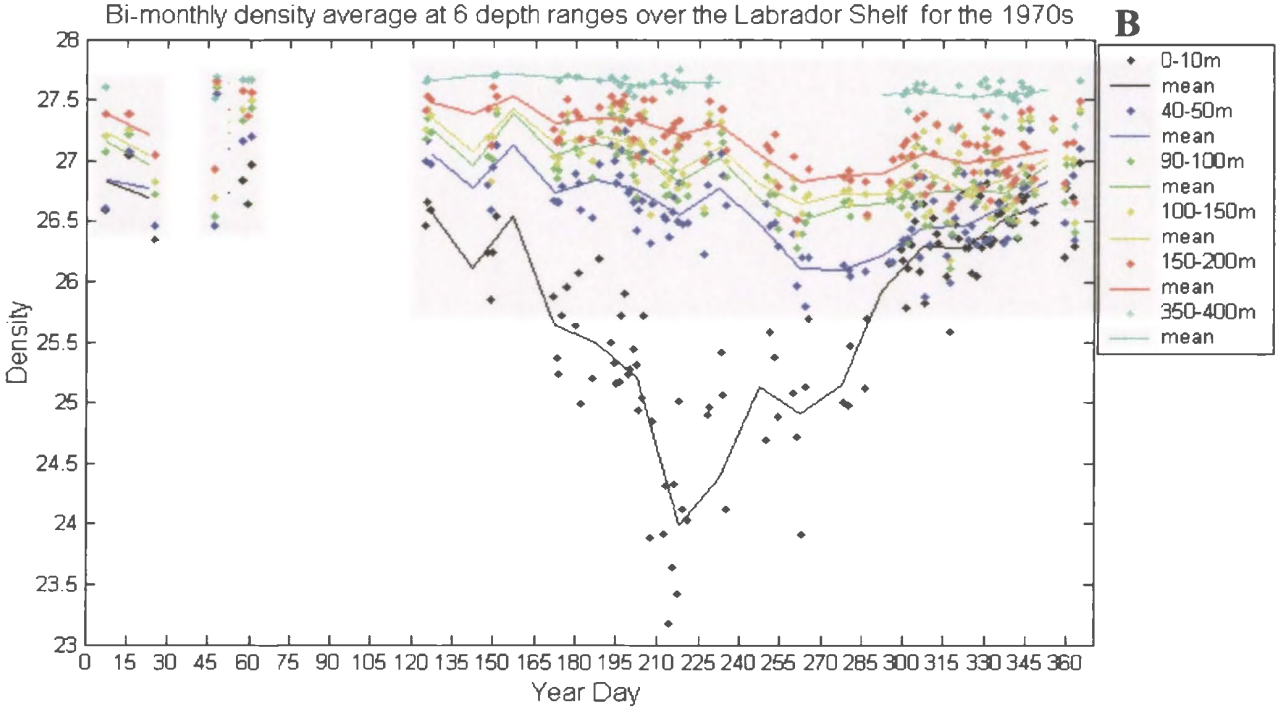
Bi-monthly density average at 6 depth ranges over the Labrador Shelf for the 1970s
B
Density
Year Day
0-10m
mean
40-50m
mean
90-100m
mean
100-150m
mean
150-200m
mean
350-400m
mean

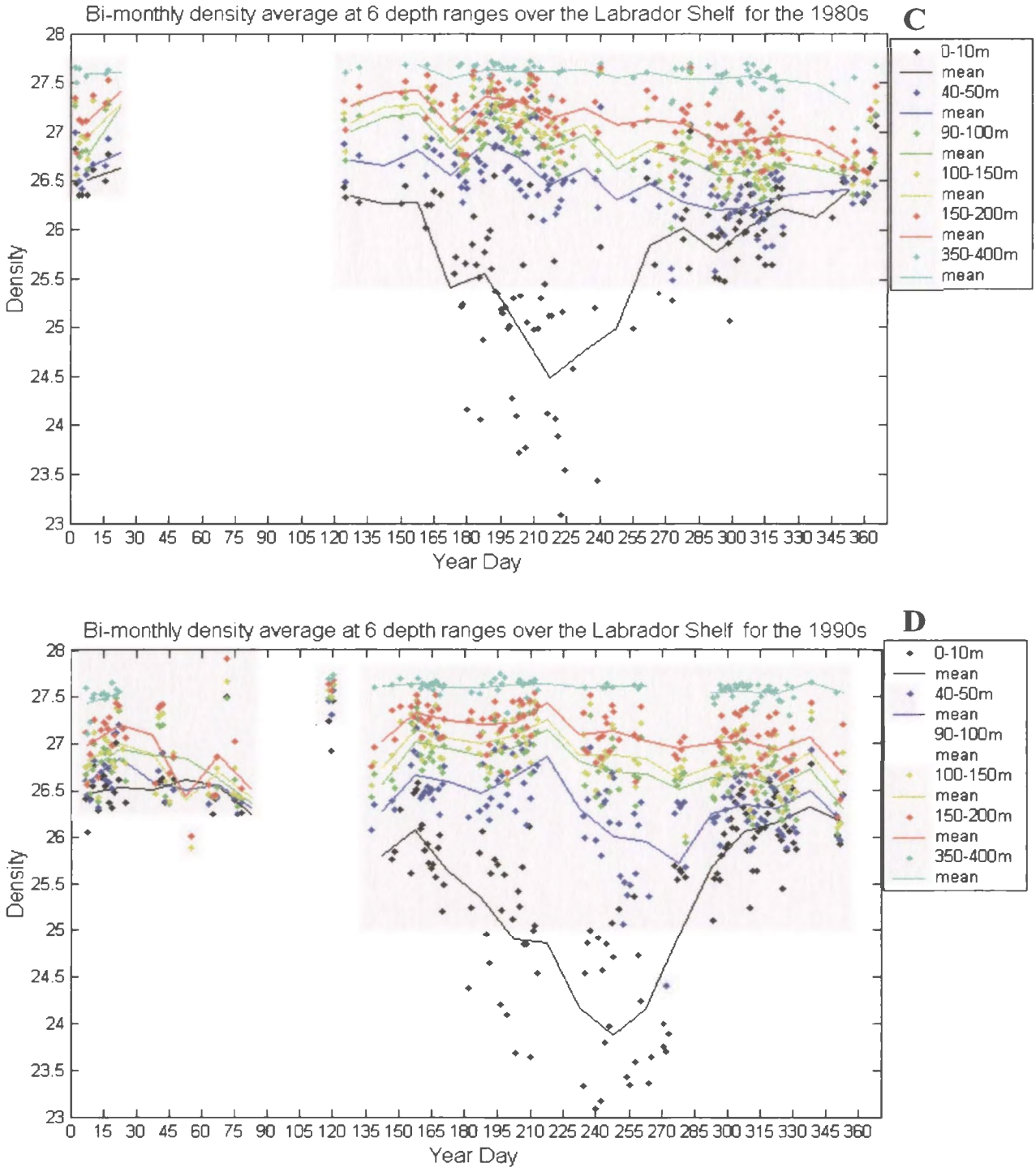

Figure 2.21: Density (σ_t) for the Labrador Shelf, during the; A) 1960s, B) 1970s, C) 1980s, D) 1990s. The data are grouped into 6 depth ranges: 0-10 m (black); 40-50 m (blue); 90-100 m (green); 100-150 m (yellow); 150-200 m (red); 350-400 (cyan). The dots represent the daily mean values and the solid lines are the bi-monthly means.

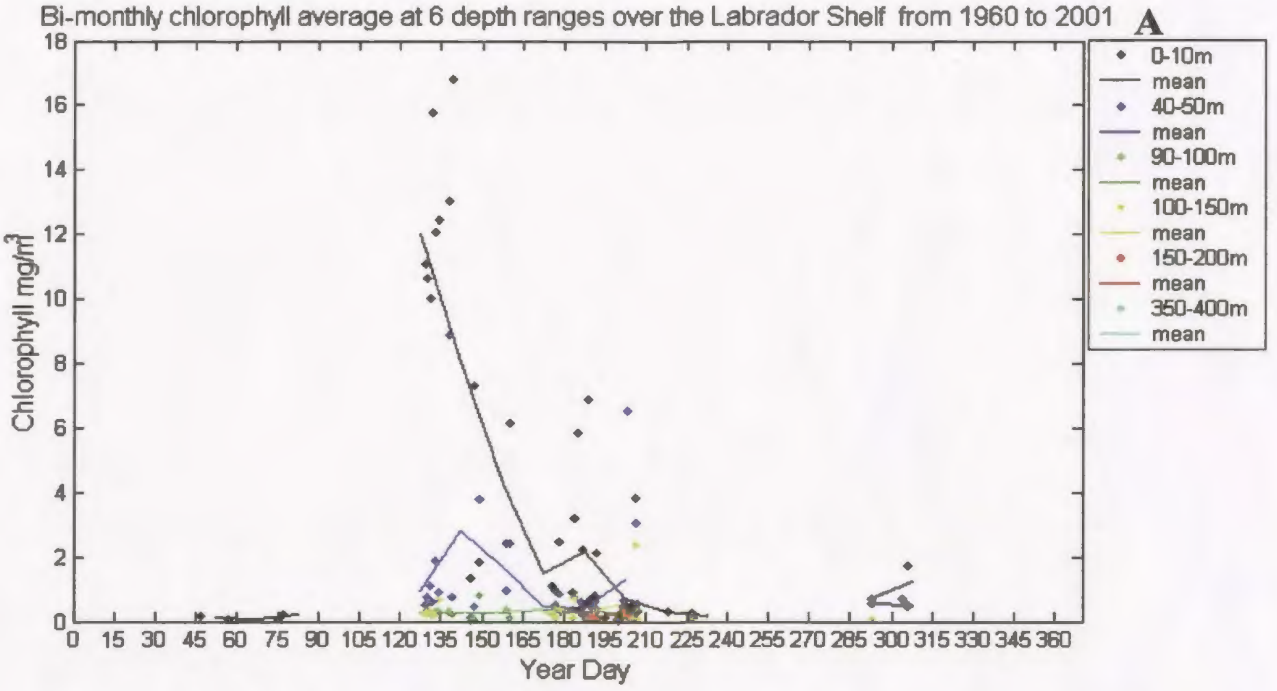
Bi-monthly chlorophyll average at 6 depth ranges over the Labrador Shelf from 1960 to 2001
A
Chlorophyll mg/m3
Year Day
0-10m
mean
40-50m
mean
90-100m
mean
100-150m
mean
150-200m
mean
350-400m
mean

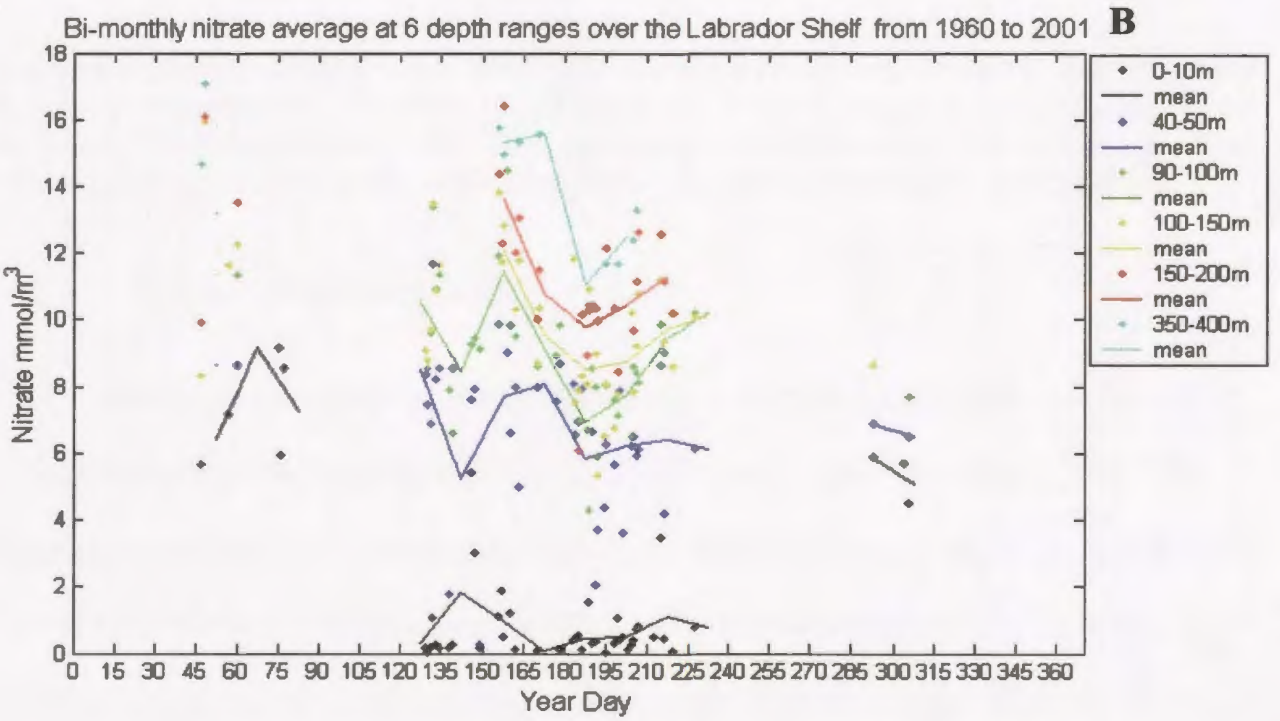
Bi-monthly nitrate average at 6 depth ranges over the Labrador Shelf from 1960 to 2001
B
Nitrate mmol/m3
Year Day
0-10m
mean
40-50m
mean
90-100m
mean
100-150m
mean
150-200m
mean
350-400m
mean

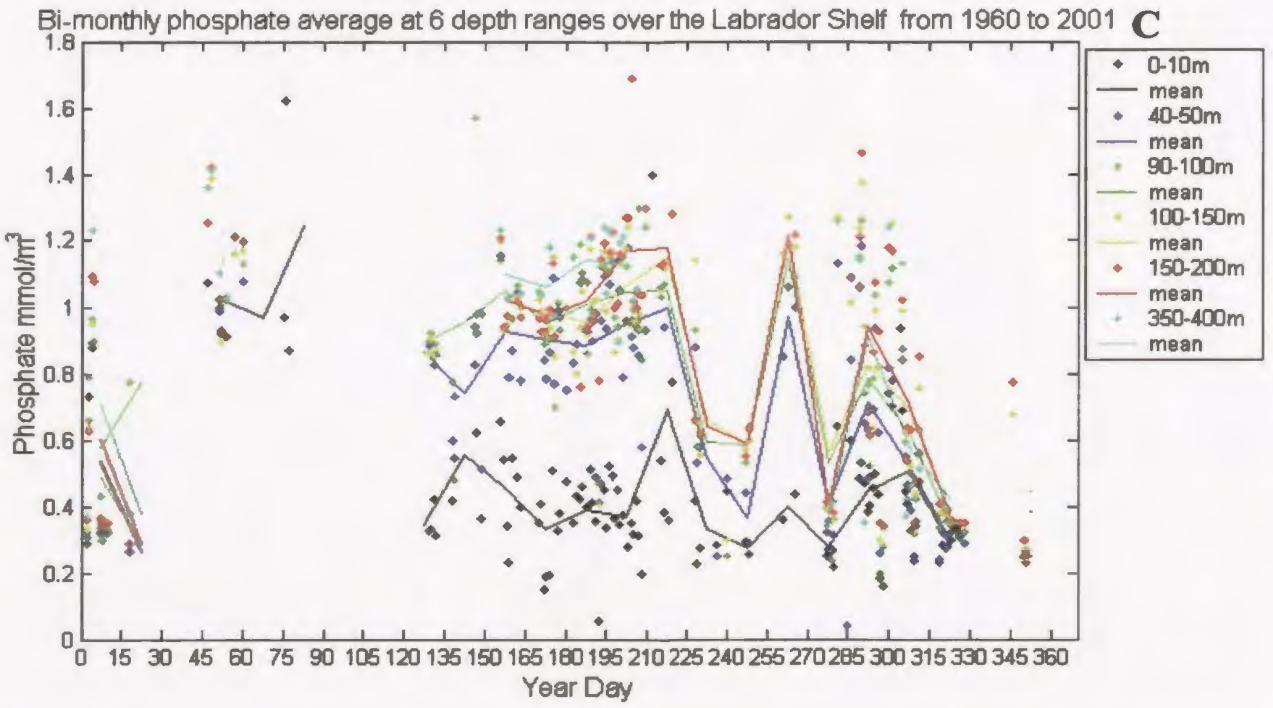

Figure 2.22: Chlorophyll, nitrate and phosphate concentrations for the Labrador Shelf, combined over the years 1950 to 2001. A) Chlorophyll mg/m^3, B) nitrate mmol/m^3, and C) phosphate mmol/m^3. The data are grouped into 6 depth ranges: 0-10 m (black); 40-50 m (blue); 90-100 m (green); 100-150 m (yellow); 150-200 m (red); 350-400 (cyan). The dots represent the daily mean values and the solid lines are the bi-monthly means.

2.5.3. Hamilton Inlet

Historical hydrographic data from Hamilton Inlet were collected from several sources covering the period from 1950 and 1997 (Cardoso and deYoung, 2002). This summary includes nitrate, phosphate, silicate, temperature, oxygen and salinity data and a detailed description of data sources, profiles and locations of sampling. Temperature, salinity oxygen and phosphorus measurements were taken throughout Hamilton Inlet during the periods July and August 1950 and 1951; June, July and August 1952; and March 1953 by the **Blue Dolphin** expeditions. The **Blue Dolphin** expeditions by the Fisheries Research Board of Canada were part of a general biological and physical study

of the coastal waters of Labrador motivated by the oceanographic and economic importance of the area (Nutt, 1950, 1951, 1952, 1953; Coachman, 1953; K. Drinkwater, personal communication, BIO). Other explorations carried out by the Fisheries Research Board of Canada include the **Investigator II** expeditions during October 1952 and September 1953 in which temperature and salinity measurements were made. Other hydrographic data were collected as part of studies to determine the feasibility of winter navigation on Lake Melville. One study was initiated by Memorial University during which temperature and salinity were measured throughout the Lake during January, April, May, and November 1973 and December 1972 aboard the vessels **CCGS Sir J.A. MacDonald, CCGS Sir Humphrey Gilbert** (icebreakers) and **Prima Vista**. Another study was completed by FENCO Ltd. commissioned by the Government of Newfoundland through the Department of Industry and Development. Temperature and salinity measurements were obtained aboard the vessel **CCGS Sir John Franklin** during January and December 1980. Other temperature, salinity, oxygen, nitrate, chlorophyll, silicate and phosphorus data were obtained from OLABS and BIO database (B. Petrie and K. Drinkwater, personal communication, BIO and www.mar.dfo-mpo.gc.ca/science/ocean/home.html). More recent data were collected in response to the hydroelectric project on Churchill River completed in 1971, located at Churchill Falls. A field trip was conducted in August 1981, where temperature and salinity measurements were taken from aboard the vessel **Burin Bay**, by the Department of Fisheries and Oceans (Bobbitt and Akenhead, 1982). Bobbitt and Akenhead investigated changes in water properties in Groswater Bay resulting from the regulation in flow from the

hydroelectric development. Also, Newfoundland and Labrador Hydro contracted various studies in the area, one of which was completed in Goose Bay during 1998 when temperature, salinity, nitrate, chlorophyll, and phosphorus data were measured (L. Ledrew, personal communication, Newfoundland Hydro). Locations of data sampling are shown in Figure 2.23.

The data for Hamilton Inlet are quite sparse, and continuous data over an annual cycle could not be obtained for 10 year periods as was the case for the Labrador Sea and Shelf. The data are combined into two periods before hydroelectric development (1970) and after hydroelectric development (1976). The temperature and salinity data combined from all the sources discussed above is used to determine the mixed-layer depth and force the model. The nitrate concentration data are used to validate the model and determine the concentration in deep water to initiate the model, and the chlorophyll data are used to validate the model. The data are grouped into 5 depth ranges: 0-5 m, 15-20 m, 45-50 m, 90-100 m and 150-300 m and the daily mean and bi-monthly means for each depth group is calculated. The upper layer (0-5 m) has a pronounced seasonal signal, the lower layers have a lesser, or no seasonal signal.

The surface temperature seasonal cycle depicts a temperature minimum in winter, increasing to a peak in August and decreasing again to a minimum in January (Figure 2.24). Throughout the year the temperature is always lowest in the deepest depth layer and increases as the depth layers shallow, except for the upper 5 m in winter, which has a lower temperature than the lower 15-20 m depth range. The surface temperature maximum is about 18°C at day 210 before 1970, however the data after 1976 are missing

from late June to mid August and a maximum therefore could not be determined. The temperature minimum occurs in winter. Winter data are sparse before the 1970s and the minimum that is observed is approximately -1 °C. The minimum temperature after 1976 approached –1°C at the end of December and the beginning of January, below 45 m the temperature remained low until spring. In the upper layers the temperature increases to between 0 and 1 °C and remains there until May, which corresponds to the time of the ice melt.

The surface salinity seasonal cycle depicts a salinity maximum in winter below 15 m and a low salinity in the upper layer decreasing to a minimum in August and increasing again to a maximum in January (Figure 2.25). The same salinity data are missing as for the temperature data, making it difficult to determine the magnitude and timing of the lows and peaks in salinity. The salinity is lowest throughout the year, in the surface layer and the minimum for the data before 1970 was about 3 psu in July and August. The minimum after 1976 is around 2 psu and occurs between days 40 and 165, after which the data are missing. After 1976, salinity in the surface layer is initially at 12 psu, which decreases to a minimum by mid February and remains at this low level until June after which the data are missing. The period of low salinity corresponds to the presence of ice. The maximum salinity is highly variable and reaches 33 psu for both time periods at various periods throughout the annual cycle.

The surface density seasonal cycle is the same as that for salinity (Figure 2.26). The density data are calculated from the temperature and salinity data using the program *swstate* provided by Matlab (The MathWorks Inc.). The maximum density in the deepest

layer is about 27 σ_θ, and the minimum approaches 0 σ_θ occurring at the same times as the salinity minimum for both time periods.

The nitrate and chlorophyll data were only obtained for September 9, 1979 from 0 to 50 m from the OLABS study (Buchanan and Foy, 1980) (Figure 2.27). Total nitrogen values were measured in Goose Bay in 1998 in spring, summer, and fall, obtained from the Newfoundland and Labrador Hydro study (L. Ledrew, personal communication, Newfoundland Hydro) (Figure 2.28). At the surface, the chlorophyll concentration is 0.7 mg/m^3, the maximum concentration occurs at 25 m at 0.9 mg/m^3 and the minimum of under 0.4 mg/m^3 occurs at 50 m. At the surface, the nitrate concentration is at a maximum at 2.65 $mmol/m^3$, and decreases to the minimum at 25 m of about 2 $mmol/m^3$ and increases again to 2.4 $mmol/m^3$ at 50 m. The reported nitrate nitrogen values from the river are low, ranging from 0.04 mg/L to 0.13 mg/L (0.65 to 2.1 mmol NO_3^-/m^3) and therefore the level in Goose Bay is also expected to be low (Hydro Lower Churchill Development Corporation Ltd., Environmental Impact Statement, 1980). Total nitrogen is mostly at the lowest detectable concentrations, 0.25 mg/L (Figure 2.28). From June to August the total nitrogen increases slightly to just over 0.4 mg/L and at depths between 50 and 60 m there is an unusual peak of 1 mg/L. There is slightly more phosphate data over the summer and a daily average is calculated (Figure 2.29). The phosphate concentrations are highly variable and not enough data were present to detect any summer cycle. The maximum concentration measured is 1.6 $mmol/m^3$ between 40 to 50 m and the minimum occurs at 150 to 300 m at 0.2 $mmol/m^3$.

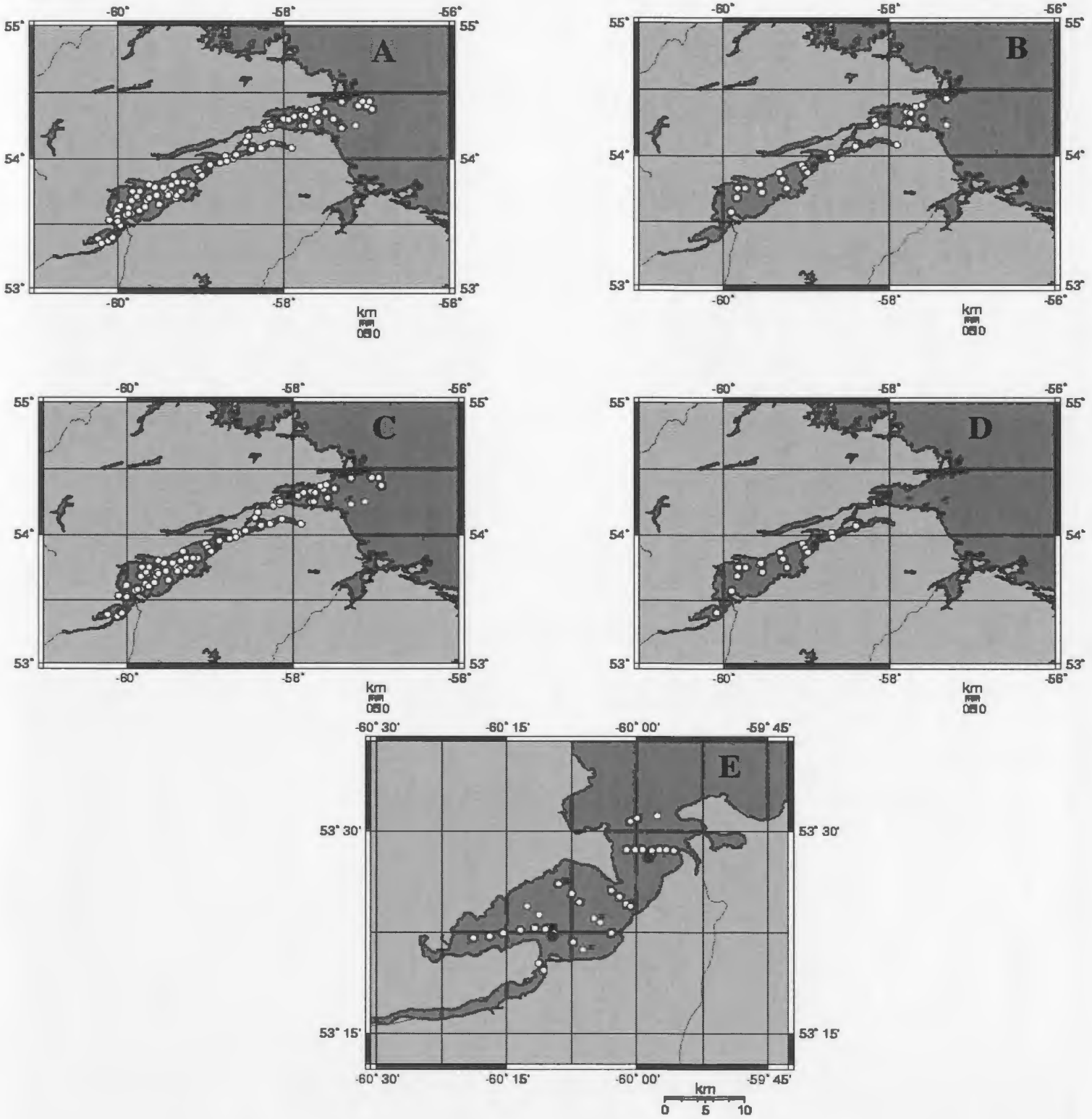

Figure 2.23: Locations of data sampled for Hamilton Inlet. A) Temperature data, B) phosphate data, C) salinity data, D) nitrate data, the solid dot is where chlorophyll and silicate were collected and E) Newfoundland Hydro temperature, salinity, nitrate, phosphate, and chlorophyll data from Goose Bay, x indicates locations where Chl was not measured and solid dotes are locations where T and S were measured.

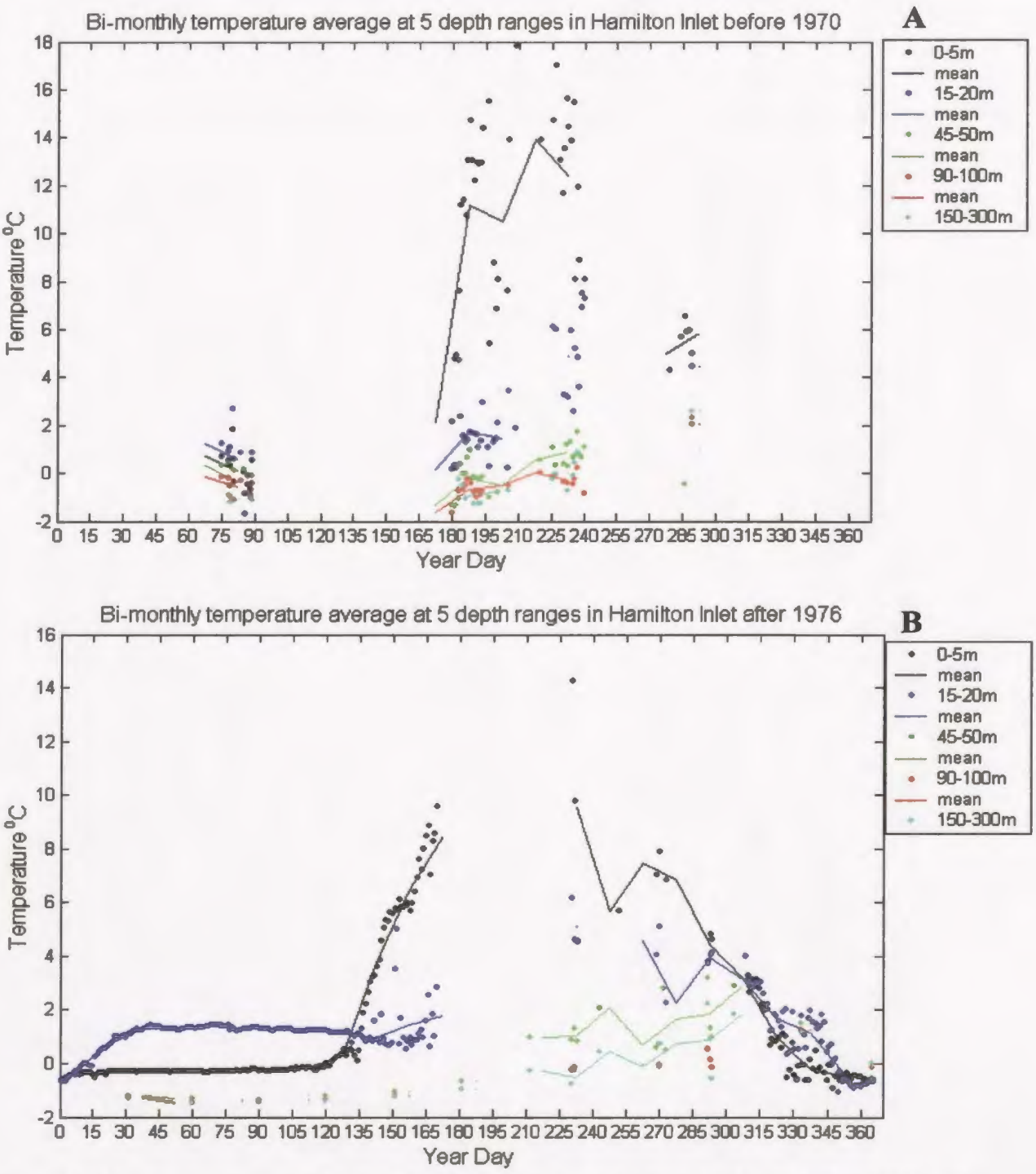

Figure 2.24: Temperature (°C) for Hamilton Inlet; A) before 1970, B) after 1976. The data are grouped into 5 depth ranges: 0-5 m (black); 15-20 m (blue); 45-50 m (green); 90-100 m (red); 150-300 (cyan). The dots represent the daily mean values and the solid lines are the bi-monthly means.

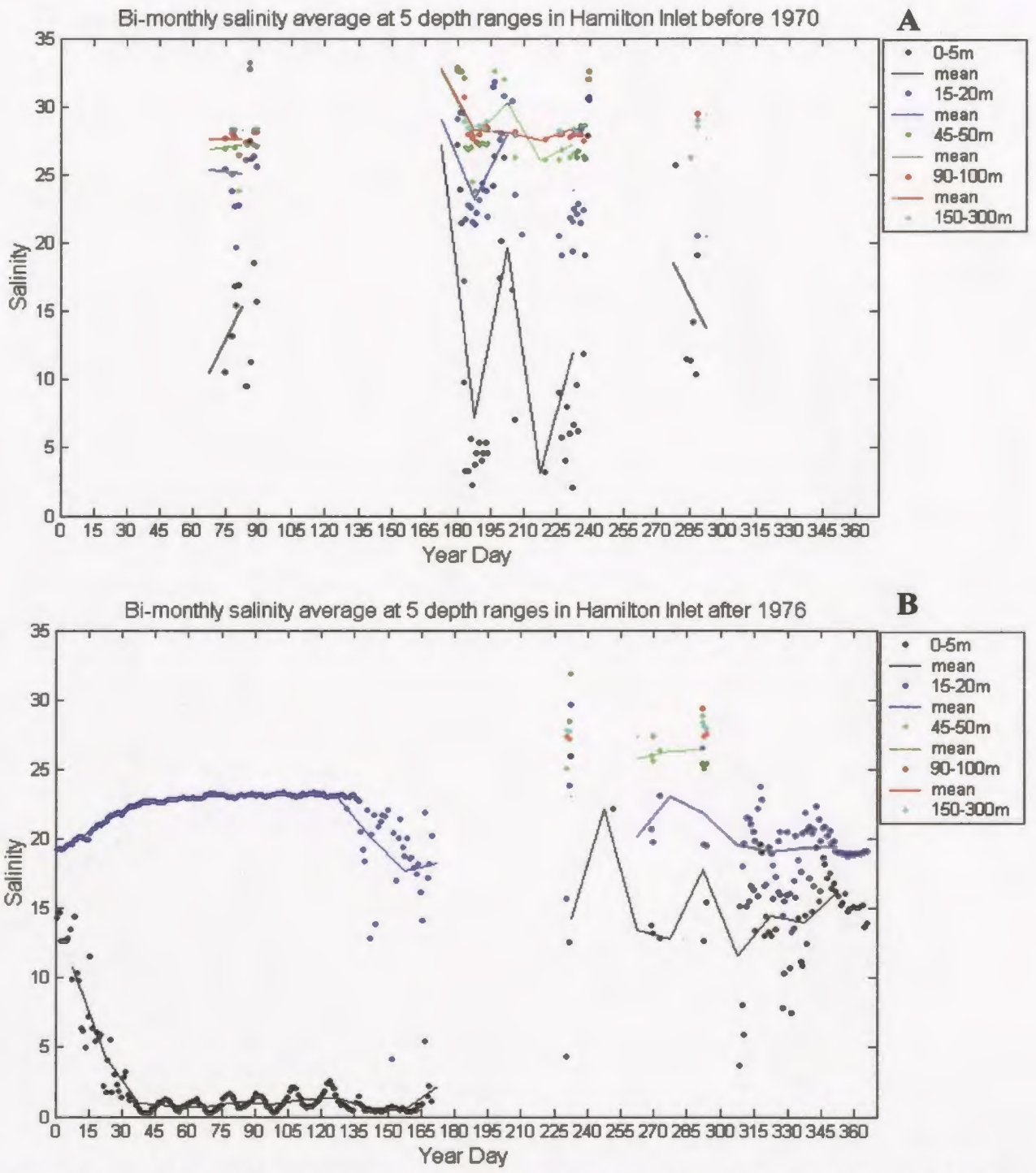

Figure 2.25: Salinity (psu) for Hamilton Inlet; A) before 1970, B) after 1976. The data are grouped into 5 depth ranges: 0-5 m (black); 15-20 m (blue); 45-50 m (green); 90-100 m (red); 150-300 (cyan). The dots represent the daily mean values and the solid lines are the bi-monthly means.

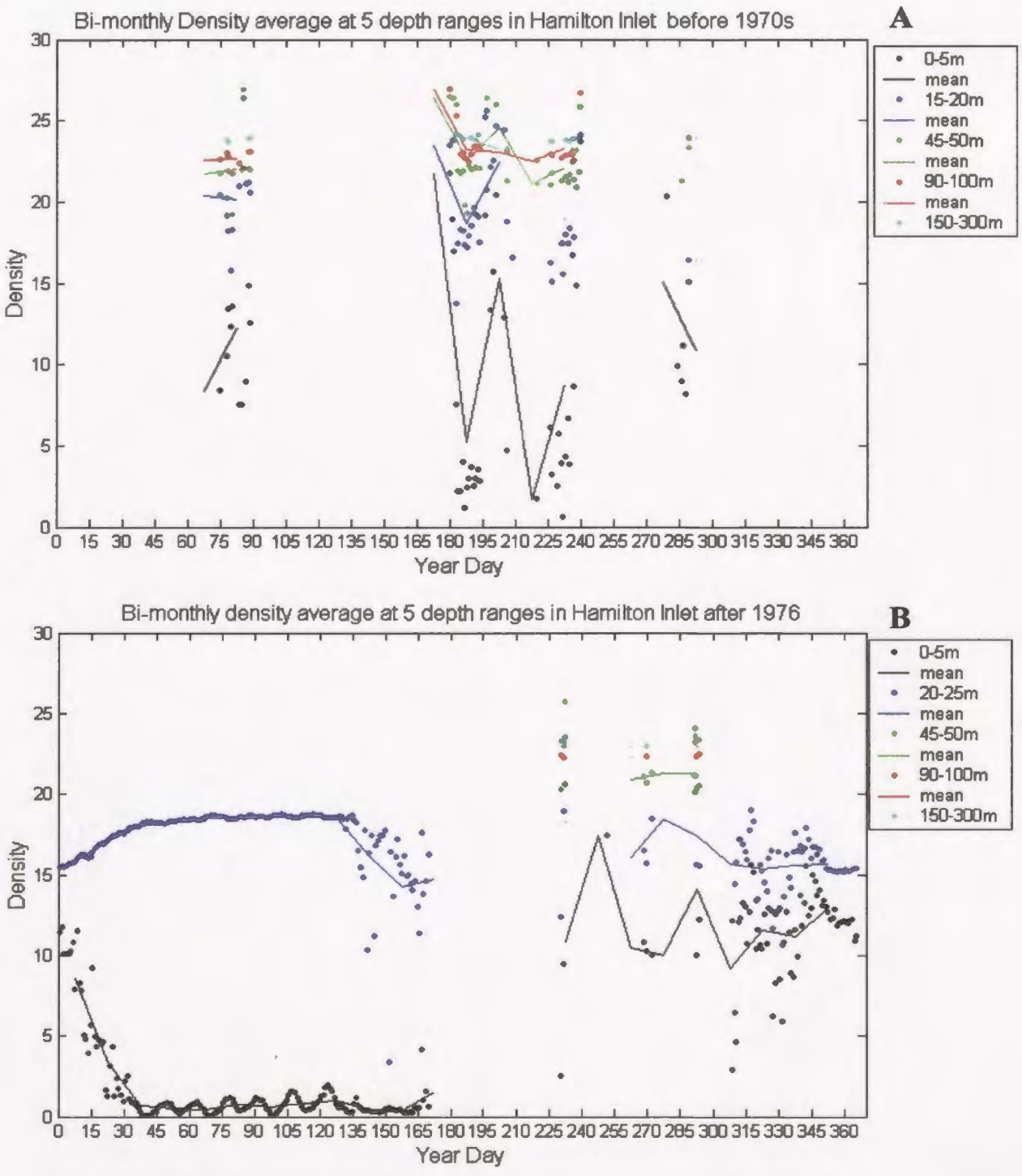

Figure 2.26: Density (σ_θ) calculated from the temperature and salinity data for Hamilton Inlet; A) before 1970, B) after 1976. The data are grouped into 5 depth ranges: 0-5 m (black); 15-20 m (blue); 45-50 m (green); 90-100 m (red); 150-300 (cyan). The dots represent the daily mean values and the solid lines are the bi-monthly means.

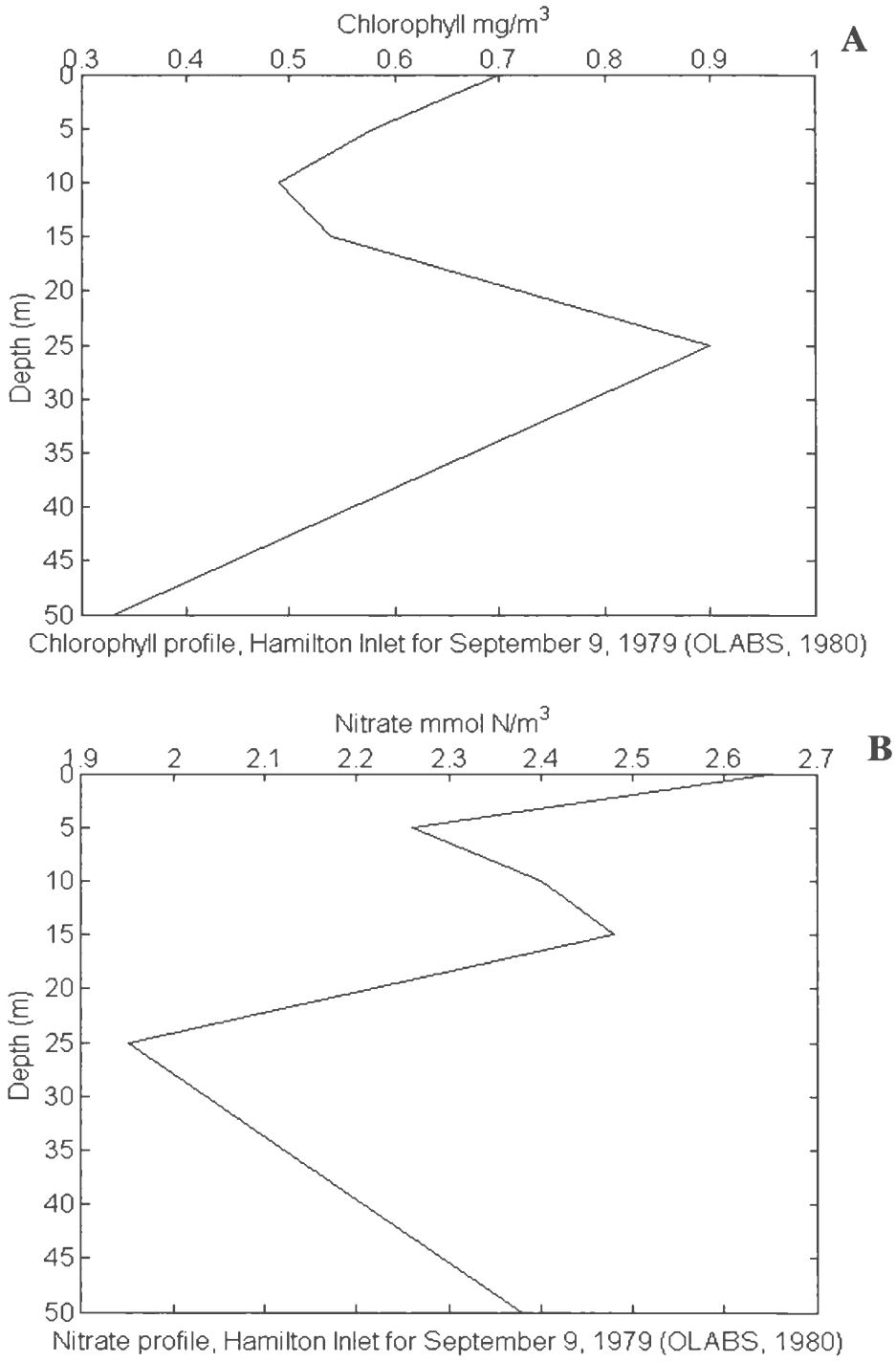

Figure 2.27: Chlorophyll and nitrate profiles for Groswater Bay, September 9, 1979 from the OLABS study (Buchanan and Foy, 1980). A) Chlorophyll mg/m^3 , B) nitrate mmol/m^3.

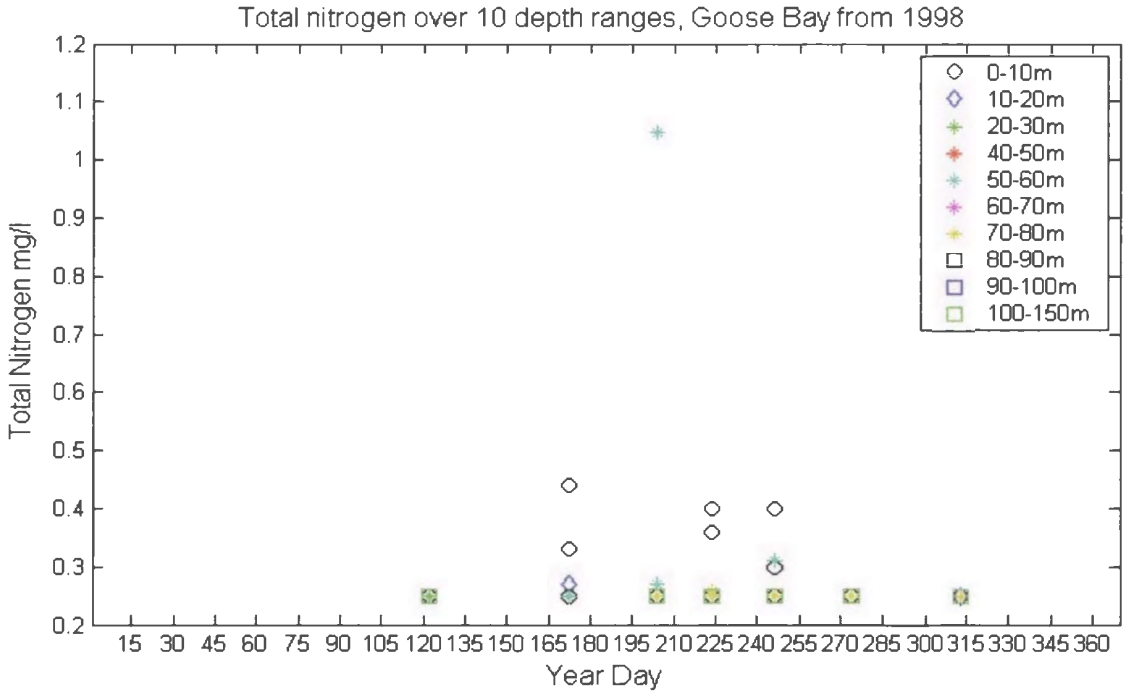

Figure 2.28: Total nitrate concentration (mg/l) over 10 depth ranges for Goose Bay, 1998, from Newfoundland and Labrador Hydro study (L. Ledrew, personal communication, Newfoundland Hydro).

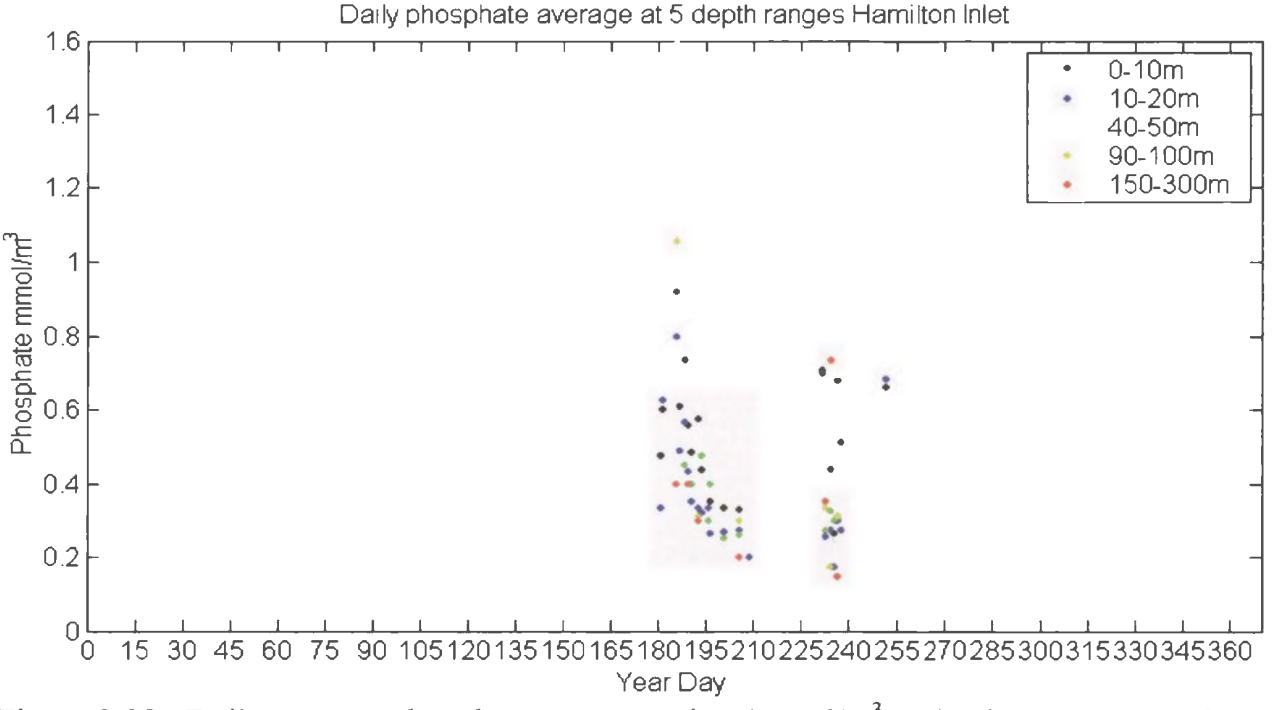

Figure 2.29: Daily average phosphate concentration (mmol/m^3). The data are grouped into 5 depth ranges: 0-10 m (black); 10-20 m (blue); 40-50 m (green); 90-100 m (yellow); 150-300 m (red).

2.5.4. Freshwater Inflow

The freshwater input to Hamilton Inlet is mainly from the four major rivers; Northwest River, Kenamu River, Goose River and the Churchill River. The Churchill River accounts for over 60% of the freshwater inflow and the Goose River contributes the least (Bobbitt and Akenhead, 1982). The Goose and Kenamu rivers have smaller drainage basins and therefore irregular flow. Both rivers usually contribute only 5% of the fresh water, however, after storm conditions in 1952 they contributed 28%. The maximum flow usually occurs in June with a mean value of 5122 m^3/s for years 1954-1966, before the hydroelectric development. The minimum discharge was usually in April with a mean flow of 403 m^3/s (Bobbitt and Akenhead, 1982). Daily flow rates of the Churchill River above Muskrat Falls have been measured by the Inland Water Directorate from 1954 to the present. The monthly mean values before and after the Churchill Falls development are shown in Table 2.5 for the years 1954 to 1966 and 1972 to 1980 (Bobbitt and Akenhead, 1982). It is evident that the monthly flow rates have changed considerably with the greatest difference, up to triple the flow, during the winter months. During June and July the flow rates decreased by 30%. Basically, the flow rates after the development have been evened out over the entire year so that the maximum flow in June is less pronounced. Bobbitt and Akenhead (1982) found that since the fjord is large and the time required for the rivers to replace the fresh water volume lengthy, Lake Melville acts as a buffer between variation in river flow and changes in salinity in Groswater Bay.

Table 2.5: Mean monthly flow above Muskrat Falls on the Churchill River as measured by the Inland Waters Directorate (Bobbitt and Akenhead, 1982).

Month	**Before Hydroelectric Development (m^3/s) (1954-1966)**	**After Hydroelectric Development (m^3/s) (1972-1980)**
January	659	1553
February	527	1586
March	454	1460
April	442	1585
May	1760	2656
June	4188	3232
July	3297	2006
August	2047	1952
September	1799	1746
October	1714	1907
November	1400	1659
December	896	1641

CHAPTER 3

Biological and Physical Model

3.1. Approach Overview

To estimate changes in primary productivity due to long term changes in climate and freshwater inflow, a four compartment NPZD model was used consisting of nutrients N, phytoplankton P, zooplankton Z, and detritus D (Denman and Pena, 1999). This model was coupled with mixed-layer data and driven by solar radiation and nitrogen concentration in deep water. The time step used was 1 day and the model is run for several years to establish a steady annual cycle. The MATLAB (MathWorks Inc.) routine ode 45 was used to numerically integrate the coupled differential equations of the model. Three regions specified to run model simulations were the Labrador Sea, Labrador Shelf and Hamilton Inlet. The model was verified using the historical observations as discussed in Chapter 2 and results from other models from the literature.

The data for Hamilton Inlet were combined across the entire Inlet including Goose Bay, Lake Melville and Groswater Bay. This was due to the lack of data in each region which did not allow a modeling study of each region. Due to this lack of data and the absence of SeaWiFS and CZCS data in the Inlet, it was decided to also run the model just outside Groswater Bay on the Labrador Shelf and Sea to help verify the modeled plankton dynamics for the Inlet and to better study the results of climate change on plankton production. The Labrador Shelf and Sea had more historical data available including satellite data and other model studies. The Labrador Sea, 1968 Bravo station

data were used to determine parameter values and model sensitivity to the parameters. For the Labrador Sea, the model simulations were carried out for 1968 and combing the period from 1990 to 1999. These periods were chosen since they had significant differences in climate due to the severity of the winter. For the Labrador Shelf four periods were investigated between 1960 and 2000, combining the data every 10 years. These periods were chosen to allow comparison between before and after the hydroelectric development on the Churchill River and to compare with the periods used for the Labrador Sea. The following sections describe the NPZD model structure, the forcing, the parameters values and model sensitivity in detail

3.2. NPZ Model Overview

3.2.1. General NPZ Model Structure

NPZ type models typically have three state variables, nutrients, phytoplankton and zooplankton, but they can have more state variables as used in the model by Fasham *et al.* (1990), with 7 state variables requiring 22 parameters. The model by Fasham splits these typical state variables into more specific variables, for example instead of nutrients, nitrate, dissolved organic nitrogen, and ammonium are used. Most models use nitrogen as the common unit throughout the model since nitrogen is often limiting to primary production in the ocean (Franks, 2002). The general NPZ model equations can be written as:

$$\frac{dN}{dt} = -f(I)g(N)P + h(P)Z(1-\gamma) + i(P)P + j(Z)Z$$

$$\frac{dP}{dt} = f(I)g(N)P - h(P)Z - i(P)P$$

$$\frac{dZ}{dt} = \gamma h(P)Z - j(Z)Z$$

There are five functions to consider in this set of equations: f(I) phytoplankton response to light, g(N) phytoplankton nutrient uptake, h(P) zooplankton grazing and i(P) phytoplankton and j(Z) zooplankton loss terms. The zooplankton assimilation efficiency, which is the fraction of the phytoplankton not ingested during feeding, is given by γ. There are several forms that have been used to describe these functions (Franks, 2002). The form of f(I) ranges from simple linear P response to incident light to nonlinear response of P with saturation and photoinhibition. The most common g(N) function is of the Michaelis-Menten form, a saturation response to increasing nutrients. Most h(P) functions also use a form showing saturation response, but can include grazing thresholds and acclimation to changing food conditions.

3.2.2. NPZ Model Application

Biological models have been used for several decades (Franks, 1995). A common biological model that has been proven to be a useful tool in the past and present is the nutrient-phytoplankton-zooplankton (NPZ) model. This model uses simple equations to describe plankton dynamics. However, models are becoming increasingly complex with growing technology and some argue that the NPZ models are too simple to

describe the real world (Franks, 2002). While the typical NPZ model does ignore microbial processes and there is no species distinction, their simplicity allows them to be solved, understood and tested against observations with greater ease (Franks, 2002). There are advantages and disadvantages to complex and simplified NPZ models. Complex models may more accurately represent the system but may be difficult to solve, parameterize, and understand. Often there are inadequate observations to validate and constrain parameter values for complex models. NPZ models are also coupled to physical models to improve accuracy and the forcing factors used include wind stress, temperature, solar input or mixed-layer depth. For example, Doney *et al.* (1996) coupled a NPZ model with a one-dimensional vertical physical model to reproduce chlorophyll dynamics. Wroblewski (1977) modeled phytoplankton blooms forced using coastal upwelling causing winds.

NPZ models have been used for many different applications in the attempt to learn more about plankton dynamics in the ocean. Certain studies have explored the underlying dynamics, such as Evans and Parslow (1985) which used an NPZ model to determine the factors controlling the different plankton cycles in the Atlantic and Pacific. Several studies used the NPZ model to explore the spring phytoplankton bloom (e.g. Wroblewski 1977, 1989; Wroblewski *et al.*, 1988; Marra and Ho, 1993). Others have used the NPZ model to understand nutrient and carbon cycling, and processes such as nitrogen supply and irradiance that limit biological production (Sarmiento *et al.*, 1993). Our understanding of NPZ model behaviour has grown as their application has been extended. NPZ models can produce a range of results depending on the form of the

functions used, the initial conditions chosen or the parameters used. There have been numerous investigations on the behaviour of the model with different functional forms and parameters. For example, Franks *et al.* (1986) compared two forms of the zooplankton grazing function, the Ivlev form and the Mayzaud and Poulet form. They showed there are significant differences in the N, P, and Z dynamics. The Mayzaud and Poulet grazing function quickly reached steady state after initial oscillations while the Ivlev form continued to oscillate. Other examples include the studies by Edwards *et al.* (2000) and Edwards and Brindley (1996, 1999) that explored the stability of the model to different parameters.

In this study, a more general coupled physical-NPZD model is used. It is sensible to start with simple models and move to more complicated models as required. The model used in this study is based upon the Denman and Pena (1999) NPZD model, which is similar to that of Doney *et al.* (1996) and based upon the assumption that phytoplankton do not sink, however detritus (which is composed of dead phytoplankton) does sink. Another assumption is that only one factor limits phytoplankton growth at any one time. The light function is derived from Webb *et al.* (1974). A one-dimensional mixed-layer model is coupled with the NPZD model where biological variables are mixed over the entire mixed-layer. This NPZD model is well characterized, the functional forms have been widely used in the literature, the parameters used are typical and easily found in the literature, and it has proven successful in producing reasonable results. Similar coupled model studies include those of Fasham *et al.* (1990) and Denman and Gargett (1995).

3.2.3. NPZD Model Description

The biological model used is a four-compartment model consisting of nitrogen N, phytoplankton P, zooplankton Z, and detritus D from Denman and Pena (1999) with a few changes. This model does not consider iron limitation of phytoplankton growth and the sinking of detritus is calculated differently. Nitrogen concentration with units of $mmol/m^3$ is used as the common unit for the model. Conversion factors for carbon-to-nitrogen and for carbon-to-chlorophyll were set at 6.625 and 60 respectively. The C:N ratio is the Redfield Ratio (106:16) which has been widely used for studies in the Labrador Sea (e.g., Trela, 1996; Tian *et al.*, 2004). The C:Chl ratio was chosen to be within the range discussed by Trela (1996) (30-75) and matches the value used by Wroblewski *et al.* (1988). Both studies were in the North Atlantic. However, in reality both ratios are not constant and vary depending on several factors including nutrient availability, light history, and species composition (Trela, 1996). For example, the C:N ratio for diatoms can vary from 6 when nitrogen is not limiting to 20 when nitrogen is limiting (Trela, 1996).

The model is represented in Figure 3.1, where the arrows are fluxes between model compartments. Only the nutrients and detritus are removed from the mixed-layer when it shallows and nutrients are added to the mixed-layer when the mixed-layer deepens (Denman and Pena, 1999). The supply of nitrate from below the mixed-layer is necessary to avoid the depletion of nitrogen (Denman and Gargett, 1995). Nitrate is added by taking the deep water concentration of N, the same value used to initiate the

model discussed in Section 3.6, for each region and multiplying it by the increase in the mixed-layer depth at each time step and adding it to the total N in the mixed-layer. D and N is removed from mixed-layer by multiplying the total concentration of each in the mixed-layer at each time step by the fraction the mixed-layer depth decreased. All biological variables are concentrated evenly throughout the mixed-layer.

The biological model is given by;

$$\frac{dN}{dt} = -(growth)P + m_{zn}Z + r_e D$$

$$\frac{dP}{dt} = (growth)P - (grazing)Z - m_{pd}P$$

$$\frac{dZ}{dt} = g_a(grazing)Z - (m_{zn} + m_{zd})Z$$

$$\frac{dD}{dt} = (1 - ga)(grazing)Z + m_{pd}P + m_{zd}Z - r_e D + D_{\text{sinking}}$$

Where

$$\text{Growth} = \nu_m Min\left\{\left(\frac{N}{k_n + N}\right), \left(1 - e^{-\alpha(I_{PAR})/\nu_m}\right)\right\}$$

$$\text{Grazing} = r_m \frac{P^2}{k_p^{\,2} + P^2}$$

The growth refers to the growth rate of phytoplankton concentration and the assumption is that only one factor limits P growth at a time. Therefore the rate of P growth is determined by the minimum value of two functions at each time step. The functions represent limitation by N or I_{PAR}, the photosynthetically available radiation,

and range between 0 and 1. There are many additional possible limiting factors; for example, it has been shown that different taxa of plankton have different roles in the ecosystem and therefore have different limiting factors and parameter values (e.g. Edwards *et al*, 2000). Also Taylor *et al.* (1991) used temperature and Denman and Pena (1999) included iron as a limiting factor for the phytoplankton growth rate. These and other factors are not considered. Therefore, only one set of parameters is used for each region.

The function that represents limitation by N is the nitrogen uptake function given by the common Michaelis-Menten function where ν_m is the maximum uptake rate of nutrients by phytoplankton and k_n is the Michaelis-Menten half saturation constant.

The function that represents limitation by I_{PAR} is the light function from Webb *et al.* (1974) where α is the initial slope of P-I curve. The calculation of I_{PAR} is discussed in Section 2.4 however, it is also necessary to determine the attenuation of I_{PAR} as it passes through the ocean. I_{PAR} is multiplied by the attenuation coefficient $k_t(z)$, calculated using the equation by Denman and Pena (1999):

$$k_t(z) = k_w + k_c(P(z) + D(z))$$

Where k_w is the attenuation coefficient of sea water and k_c is the coefficient providing shading by both phytoplankton P and detritus D. This solution assumes that k_w and k_c do not vary with depth. However, since these parameters depend on wavelength, in reality they do depend on depth (Fasham, 1995).

P does not sink in this model, therefore the only loss terms of phytoplankton are due to mortality, $m_{pd,}$ and grazing by Z. The grazing term is the common quadratic

function known as the Holling type III predator response, where r_m is the zooplankton maximum rate of grazing and k_p is the half saturation constant for Z grazing. This grazing function at low concentrations of P provides a threshold for grazing which provides stability (Steele and Henderson, 1992).

The fraction of the unassimilated material from Z grazing is given by $(1-g_a)$ and this undigested material becomes part of the detritus pool. The growth of Z is due to the assimilated fraction, g_a, that is ingested, and the loss from Z is due to mortality and excretion. The phytoplankton and zooplankton mortalities are linear. The Z losses are divided between regenerated nitrogen, $m_{zn,}$ which becomes part of the N pool and dead body parts, $m_{zd,}$ which becomes part of the D pool.

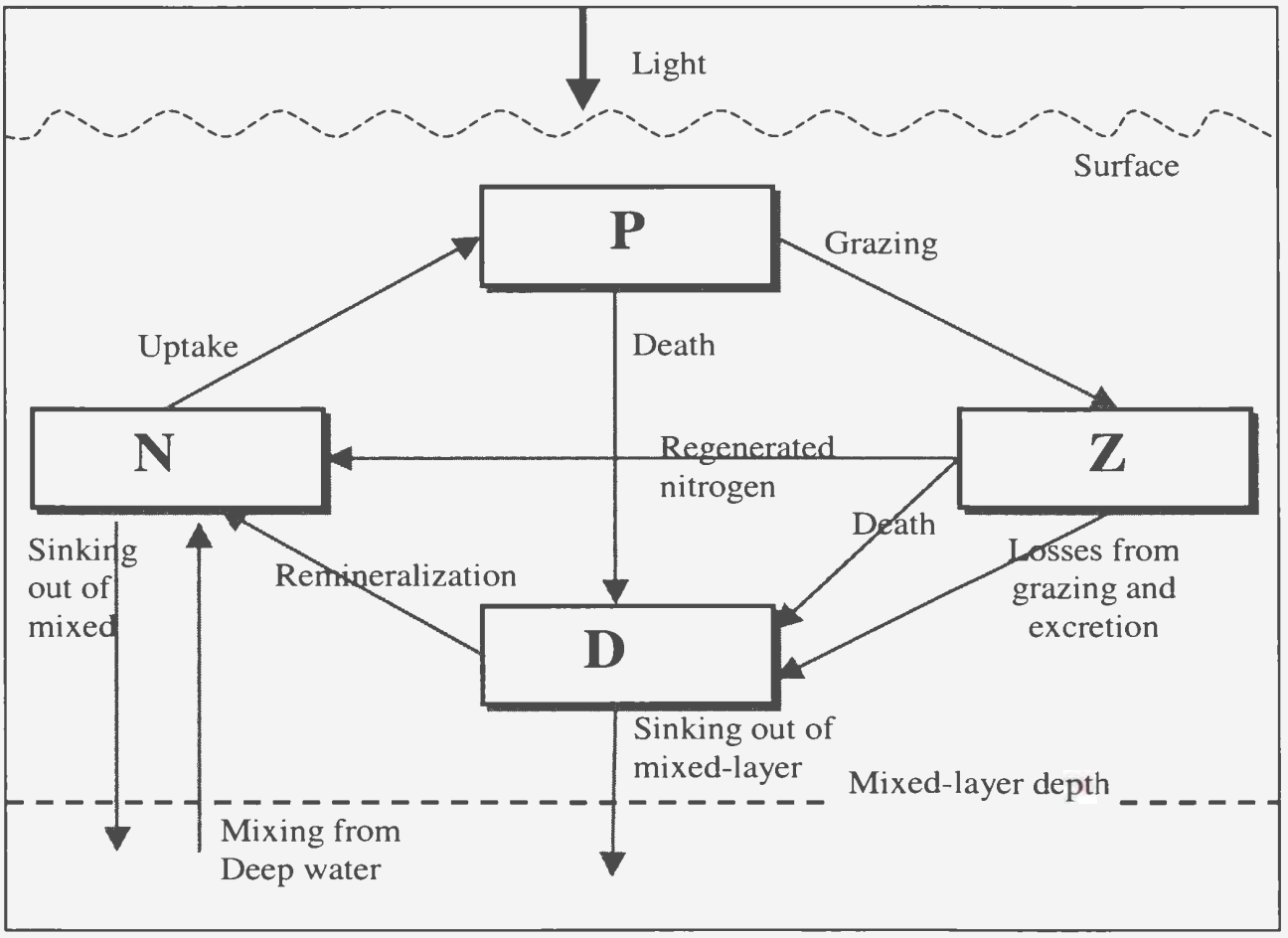

Figure 3.1: The upper ocean ecosystem model. N is nitrogen, P is phytoplankton, Z is zooplankton and D is detritus. The arrows represent fluxes between the compartments.

The D pool consists of sinking, suspended and dissolved organic nitrogen (DON). As well as being removed from the mixed-layer when it shallows, D also sinks out of the mixed-layer at each time step. The sinking rate of D is represented by w_s, the fraction of D that sinks and is determined at each time step and subtracted from the total D in the mixed-layer, using equation:

$$\frac{D_{total}}{day} = \frac{D_{total}}{day} - \frac{D_{total}}{day} \times \min[(w_s / md), 1]$$

Where D_{total} is the total D in the mixed-layer and md is the mixed-layer depth. D is remineralized back to the N pool at a rate of r_e which represents implicitly the role of bacteria.

3.3. Model Initiation

Initializing the model is always a problem. It would be ideal if state variables and parameters were all predetermined from extensive field observations. However, often estimates are based on limited knowledge. With the technical advances in modeling of coupled physics and biological models, it is now the oceanographic field data that is lacking. The deep-layer concentration of N was determined from the historical data collected for each region as well as values reported in the literature. The annual N concentration versus depth for The Labrador Sea and Shelf was calculated by combining all the historical data available (Figure 3.2). Hamilton Inlet nitrate data were only available for September 9, 1979 from the OLABS study (Buchanan and Foy, 1980) and total nitrogen concentration were from the Hydro study (L. Ledrew, personal communication, Newfoundland Hydro) from June to August, 1989 (see Figure 2.27 in Chapter 2). The maximum nitrate concentration at the surface is 2.65 μM and at 50 m (the maximum depth measured) is 2.4 μM. The nitrate values from the river are quite low and range from 0.65 to 2.1 μM (Hydro Lower Churchill Development Corporation Ltd., Environmental Impact Statement, 1980). The Labrador Shelf and Sea data were much more plentiful and available over an entire annual cycle. The Labrador Shelf data shows a maximum nitrate concentration of 14 μM in deeper waters and a minimum at the

surface between approximately 100 and 250 days, which corresponds to the bloom of phytoplankton. The Drinkwater and Harding (2001) study of the Labrador Shelf in September 1985 showed a deep-water maximum of 12 μM, increasing to 20 μM of nitrate on the sloping section of the Shelf. The Labrador Sea data has a similar annual pattern as the Shelf data with a deep-water maximum of 16 μM of nitrate and a minimum occurring slightly later between 150 and 260 days. There are several reported values of deep-water nitrate maxima in the Labrador Sea. Anderson *et al.* (1985) reported 16.55 μM of nitrate for the winter Labrador Sea upper water, 17.59 μM for the Labrador Sea water at about 1000 m and 17.10 μM for the North Atlantic Deep water. Louanchi and Najjar (2001) reported values of 14 μM of nitrate at 300 m depth from the World Ocean Atlas 1998, produced by the Ocean Climate Laboratory at the National Oceanographic Data Center (NODC) (Conkright *et al.*, 1994). Trela (1996) used 16.8 μM as the deep Labrador Sea water concentration of N to force a model. Based on these findings, the deep water nitrate concentration used for Hamilton Inlet is 2.4 μM, for the Labrador Shelf is 14 μM, and for the Labrador Sea 16.5 μM.

Table 3.1: Concentration of N, P, Z and D used to initiate model runs for each region.

State Variable	**Initial Concentration mmol N/m^3**		
	Labrador Sea	**Labrador Shelf**	**Hamilton Inlet**
N	16.78	11.43	2.65
P	0.285	0.1812	0.2705
Z	0.0229	0.001	0.2
D	0.01	0	0

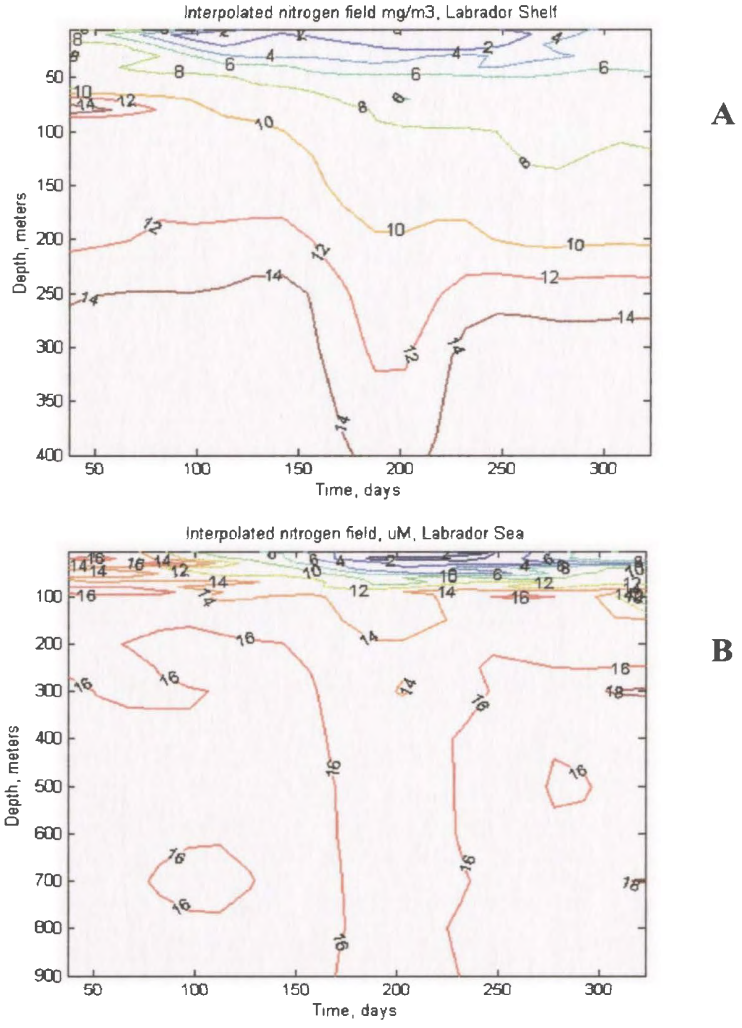

Figure 3.2: Interpolated nitrogen concentration (μM) for data collected between 1928 and 2001 for; a) Labrador Shelf and c) Labrador Sea.

The model is started in winter. The deep-water nitrate concentration is used to initiate the model; the remainder of the state variables are typically low in concentration in the winter and their concentrations are therefore chosen below 1 μM. To determine the state variables initial concentrations the model is run for the Labrador Sea in 1968 and for the Shelf and Hamilton Inlet combining all the data between 1950 and 2000 using

the above initial values until a steady state is reached. The resulting initial concentrations for the Labrador Sea and Shelf are used for the remainder of the simulations for each region (Table 3.1).

3.4. Mixed-Layer Calculation

The depth of the mixed-layer controls the light availability for photosynthesis and the annual cycle of light availability strongly influences the phytoplankton population size and the zooplankton that prey on phytoplankton. The importance of the effects of changing mixed-layer depths on phytoplankton and zooplankton spring blooms (Denman and Gargett, 1995; Franks and Walstad, 1997) demonstrates that the mixed-layer depth has a significant role in the growth and structure of phytoplankton patches. The mixed-layer depth was calculated using the density data. In order to determine the mixed-layer depth, a mean daily density value for each depth over one year is required. If the density data were not available the density was calculated from the temperature and salinity data. The mixed-layer depth for each region was calculated differently according to availability of data. The methods are described below.

3.4.1. Labrador Sea

The depth used in the model is the maximum depth where continuous annual data are available for each region, for the Labrador Sea it is 1000 m. Two trials were completed for the Labrador Sea; one using data from the period of 1968 and the second from 1992 to 1999. The density data from 1968 was from the Bravo station. The depth was divided into 10 m thick layers and density averaged for each day. Linear

interpolation was used for missing data. The mixed-layer is defined as the depth at which the density changes by 0.1 from the surface; this value was determined based on a sensitivity test using a range of values from 0.005 to 0.11 in steps of 0.01. The resulting mixed-layer depths were compared to the density contours over an annual cycle and the mixed-layer depth that best matched the contours of density was chosen. For the Labrador Sea Bravo station data, it is evident that the green circles best match the contours of density, which corresponds to a value of 0.1 (Figure 3.3).

For the second trial, the 1990s, the data were sparser, and included data from both the Bravo station and the surrounding Labrador Sea. The first 100 m is divided into 10 m thick layers; from 100 m to 300 m it is divided into 50 m thick layers and over 300 m it is divided into 100 m thick layers. The density data was combined over all the years from 1992-1999 to determine the annual plankton cycle. A daily mean density at each depth interval was determined, however, the data contained gaps. For the days in which data existed but not for each depth, the missing data were linearly interpolated between the immediately preceding and following depth interval for that day. The mixed-layer was calculated for the days in which density data existed and was linearly interpolated over the days with no data. A few outlier points were removed before interpolating. Due to the lack of data in the winter, the day where the mixed-layer begins to shallow after winter was chosen to be 105 year day following the results of Tian (2004). The mixed-layer was defined as the depth at which the density changed by 0.16 from the surface; this value was determined based on a sensitivity test using a range of values from 0.08 to 0.2 in steps of 0.02. The resulting mixed-layer depths were compared to the daily density

profiles and the results from Tian (2004) to determine the mixed-layer depth that was most reasonable.

3.4.2. Labrador Shelf

The depth used in the model for the Labrador Shelf is 450 m, with the first 100 m divided into 10 m thick layers and from 100 m to 450 m it is divided into 50 m thick layers. Four trials were completed for the Labrador Shelf using data from the 1960s to the 1990s in 10 year periods and only data below 55°N on the southern Shelf were included. For the most part, the same method was used as for the Labrador Sea in the 1990s except density was calculated from temperature and salinity data. Temperature and salinity data were obtained directly from the BIO database (B. Petrie, personal communications, BIO and www.mar.dfo-mpo.gc.ca/science/ocean/home.html). The data were combined from 1960 to 2000 to determine the density gradient from the surface, which best represents the observations. The mixed-layer was defined as the depth at which the density changes by 0.9 from the surface and this value was determined based on a sensitivity test using a range of values from 0.1 to 1 in steps of 0.1. This value was chosen to give a reasonable seasonal mixed-layer depth, which shallows in the spring and summer, deepens in fall and reaches a maximum depth in February or March of approximately 200 m. The temperature and salinity data were then split into each 10 year period and the daily mixed-layer depth calculated were linearly interpolated. However, mixed-layer depth was highly variable, especially in the fall. A Butterworth 5^{th} order filter was used in MATLAB (The MathWorks Inc.) to smooth out the mixed-layer depths and estimate the daily values. In order to make the January and December filtered values

match, the calculated mixed-layer and filter was repeated over 3 years and the 2nd year filter data were chosen to represent the mixed-layer for that given period. The normalized cutoff frequency for each period varied depending on the number of days in which data were available. The number of samples over 3 yrs was used to normalize the cutoff frequency. The normalized cutoff frequency used for each period was; 10/133.5 in the 1960s and 1970s, 10/189 in the 1980s and 12/231 in the 1990s. The first number is the cutoff frequency and corresponds to frequency of sampling. The second number represents the Nyquist frequency, which is half the sample frequency.

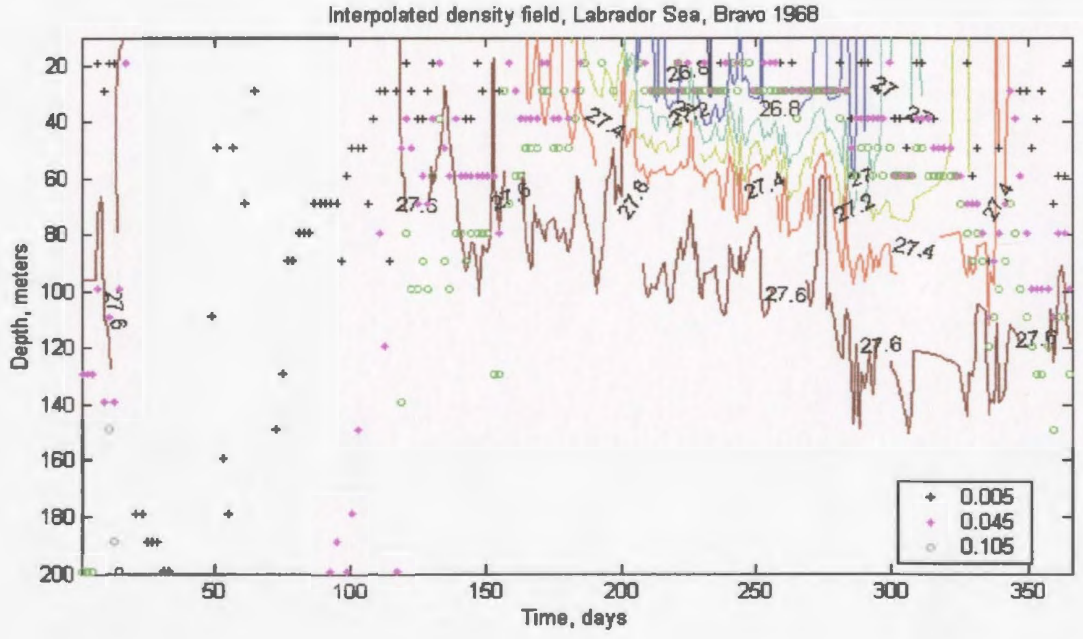

Figure 3.3: Density contours over the upper 200 m based on the Bravo station data in 1968. The different points represent the calculated mixed-layer depth using different values of the maximum allowable difference in density between the surface and deeper layer value. The black + points use a density difference of 0.005, the red solid points use a density difference of 0.045, and the green o points use a density difference of 0.105.

3.4.3. Hamilton Inlet

The depth used in the model for Hamilton Inlet was 300 m, with the first 50 m divided into 5 m thick layers, from 50 m to 100 m it is divided into 10 m thick layers, and the deeper layers are from 100 to 150 m and 150 to 300 m. Two trials were completed for Hamilton Inlet using data collected prior to hydroelectric development (1970) and after hydroelectric development (1976). For the most part, the same method was used as for the Labrador Shelf and density was also calculated from temperature and salinity data. Temperature and salinity data were obtained directly from the BIO database (www.mar.dfo-mpo.gc.ca/science/ocean/home.html and B. Petrie, personal communications, BIO) and industry studies described in Section 2.5.3. All available data were combined initially to determine the density gradient from the surface, which best represents the observations. The mixed-layer was defined as the depth at which the density changes by 5.5 from the surface and this value was determined based on sensitivity test using a range of values from 2 to 8 in steps of 0.5. This value was chosen to give a reasonable seasonal mixed-layer depth which is shallow in fall and winter and deepens in spring and summer following the ice melt to reach a maximum depth in July August of approximately 80 m. The temperature and salinity data were then split into each period and the daily mixed-layer depth was linearly interpolated; again it was highly variable. Before 1970, there were few data in early winter, spring and fall therefore, the mixed-layer was calculated by combing all the data were to fill in the gaps. The density change from the surface values was increased from 5.5 to 6.0. A Butterworth 5^{th} order filter was used in MATLAB (The MathWorks Inc.) to smooth out

the mixed-layer depth and determine the daily values. The January and December filtered values matched so the calculated mixed-layer and filter was only determined for one year period. The normalized cutoff frequency for each period varied depending on the number of days in which data were available. The normalized cutoff frequency used for each period was; 5/100 before 1970s and 5/118.5 after 1976.

3.5. Parameter Selection

The parameters used in the simulations for each region are listed in Table 3.2. The parameters were chosen based on a range of reported values from the literature and the models sensitivity to this range. The literature source of each parameter value and the location for the studies is given in Appendix 2. The parameters were varied within the range listed to attempt to match the modeled seasonal cycle of phytoplankton and nutrients to observations from satellite derived data, the BIO database, and literature values. The sensitivity tests of the model to each parameter were completed using the Bravo station 1968 data set and are described in detail in Section 3.7.

3.5.1. Labrador Sea

The parameters used to calculate the attenuation coefficient for photosynthetically active radiation I_{PAR} were set at 0.04 m^{-1} for k_w, which is commonly used in other models (Fasham *et al.*, 1990; Fasham, 1995; Denman and Pena, 1999; McGillicuddy, 1995; Sarmiento *et al.*, 1993) and at 0.12 m^{-1} mmol N /m^3 for k_c after Evans and Parslow (1985). The initial slope of the photosynthesis-irradiance curve was set at 0.055 d^{-1} $(W/m^2)^{-1}$ which is similar to the value of 0.5 d^{-1} $(W/ m^2)^{-1}$ used by Doney *et al.* (1996) and Tian *et*

al. (2004). The parameters used in the growth rate of phytoplankton expression to limit photosynthesis, other than light, are the maximum growth rate, v_m, and the half-saturation of nutrients, k_n. These parameters are mainly derived from laboratory experiments and therefore may not accurately represent natural phytoplankton communities (Trela, 1996). This may explain the wide range of values for v_m found in the literature however the v_m is not a very sensitive parameter. The value of v_m was set to 0.8 d^{-1}, which is similar to the value used by Trela (1996) and Marra and Ho (1993) of 0.9 d^{-1}, and Tian *et al.* (2004) of 0.96 d^{-1}. The value of k_n was the least sensitive parameter, therefore changing its value meant little change in modeled plankton dynamics. The value was set to 0.1 mmol N/m^3, which was also used by Denman and Pena (1999), Frost (1993) and Edwards *et al.* (2000). The phytoplankton mortality rate, m_{pd}, has been said to be the most important loss term in most marine systems (Walsh, 1983), and Fasham *et al.* (1990) found it to be the most sensitive model parameter and difficult to determine. For this model study the N and Z maximum concentration over one year were found to be sensitive to m_{pd}. The parameter, m_{pd} was set to 0.045 d^{-1}, the same value as used by Fasham *et al.* (1990), and similar to that used by Fasham (1995) and Denman and Pena (1999) of 0.05 d^{-1}. The Z parameters can vary widely due to the fact that this represents an animal compartment that is higher in the food chain, and therefore involves many more considerations. For example, Z comprises herbivores, bacteriovores and detritivores, many of which are capable of migrating out of the mixed-layer. The criteria used to chose Z parameters in most studies is to select within the range of reported values from the literature and ensuring the model results compare reasonably well with observations. The Z maximum grazing rate, r_m,

was found to have the widest range in the literature from 0.01 to 1.5 d^{-1} and was the one of the most sensitive parameters in model simulations to determine. The value of assimilation efficiency, g_a, was also a sensitive model parameter. Therefore, in order to determine both their values a further sensitivity analysis was conducted which looked at bloom timing. Based on a bloom timing of day 170, which is typical in the Labrador Sea, (see Section 2.2) and a maximum P concentration of 12 mg Chl/m^3, the values of r_m and g_a were set at 1.08 d^{-1} and 0.75 respectively. The Z grazing half saturation constant, k_p, was determined to be 0.4 mmol N/m^{-3}, the same as the value of Denman and Pena (1999). The Z losses are difficult to determine since observational data is lacking and again it depends on various processes such as respiration, excretion and mortality (Trela, 1996). The Z losses following the model by Denman and Pena (1999) are divided into losses to the nutrient pool m_{zn} and detritus pool m_{zd}. Both parameters were given the same values as those used by Denman and Pena (1999) and no sensitivity test was done for these parameters. This was due in part to the fact that a range of values for these parameters was not found in the literature but also to simplify the sensitivity testing.

The remineralization rate for the detritus compartment was one of the least sensitive parameters to the model simulations. Therefore, its value did not greatly change the results and its value was set to 0.05 d^{-1}, which is the same as that used by Fasham (1995) and Fasham *et al.* (1990). Changing the sinking rate of D had little effect on the modeled plankton results and therefore was set to 0, however in terms of the biology this is not accurate.

Table 3.2: Parameters used for the model and the range from the literature.

Parameter	Symbol	Units	Range	Labrador Sea	Labrador Shelf	Hamilton Inlet
PAR attenuation coefficient for sea water	k_w	m^{-1}	0.04-0.2	0.04	0.04	0.04
PAR attenuation coefficient for (P+D)	k_c	m^{-1} mmol N $/m^3$	0.02-0.12	0.12	0.14	0.14
Initial slope of P-I curve	α	d^{-1} (W/ m^2) $^{-1}$	0.025-0.15	0.055	0.025	0.025
Maximum P growth rate	v_m	d^{-1}	0.6-3.0	0.87	2.0	2.0
N half saturation constant	k_n	mmol N/m^{-3}	0.1-0.5	0.1	0.1	0.1
P mortality rate	m_{pd}	d^{-1}	0.045-0.15	0.045	0.045	0.045
Z maximum grazing rate	r_m	d^{-1}	0.01-1.5	1.08	1.08	1.08
Z assimilation efficiency	g_a		0.1-0.95	0.75	0.75	0.75
Z grazing half saturation constant	k_p	mmol N/m^{-3}	0.25-1.1	0.25 or 0.45	1.1	1.1
D remineralization rate	r_e	d^{-1}	0.05-0.1	0.05	0	0
Z losses to N	m_{zn}	d^{-1}	0.2	0.2	0.2	0.2
Z losses to D	m_{zd}	d^{-1}	0.05	0.05	0	0
solar constant	Isc	W/ m^2	1367	1367	1367	1367

3.5.2. Labrador Shelf

The choice of parameters for the Shelf was based on the results of the sensitivity analysis for the Labrador Sea, Bravo 1968 model. To determine the parameters, the mixed-layer depth calculated over the entire period from 1960 to 2000 was used to force the model. The model was run initially using the parameters chosen for the Labrador Sea as listed in Table 3.2. As needed, certain parameters were changed to more accurately

represent the plankton annual cycle on the Shelf. The initial run using the parameter values for the Labrador Sea is shown in Figure 3.4. It is evident that the singular peak in the late winter and oscillatory behaviour is not consistent with plankton dynamics in the Labrador region away from the coastal waters. To change the plankton dynamics it was decided to first change the two parameters that proved to have the highest sensitivity to phytoplankton and zooplankton dynamics and are associated with Z grazing: the g_a, k_p and r_m terms. By changing g_a and r_m, the P oscillatory behaviour was either increased or the annual signal was completely eliminated. By increasing k_p oscillatory behaviour was somewhat reduced and two peaks in P concentration were beginning to appear but insufficiently. It was decided to eliminate the detritus state variable and use a higher value of k_p and this resulted in more realistic results when compared to the Continuous Plankton Recorder data and satellite imagery. However, the timing of the P blooms was still not accurate. Therefore, the sensitivity to light was changed by altering the alpha and k_c parameters. As expected, by increasing alpha the spring bloom timing was earlier and by increasing k_c, thereby increasing shading by P and reducing the light availability, the timing was later. The resulting parameters used for the Labrador Shelf are listed in Table 3.2.

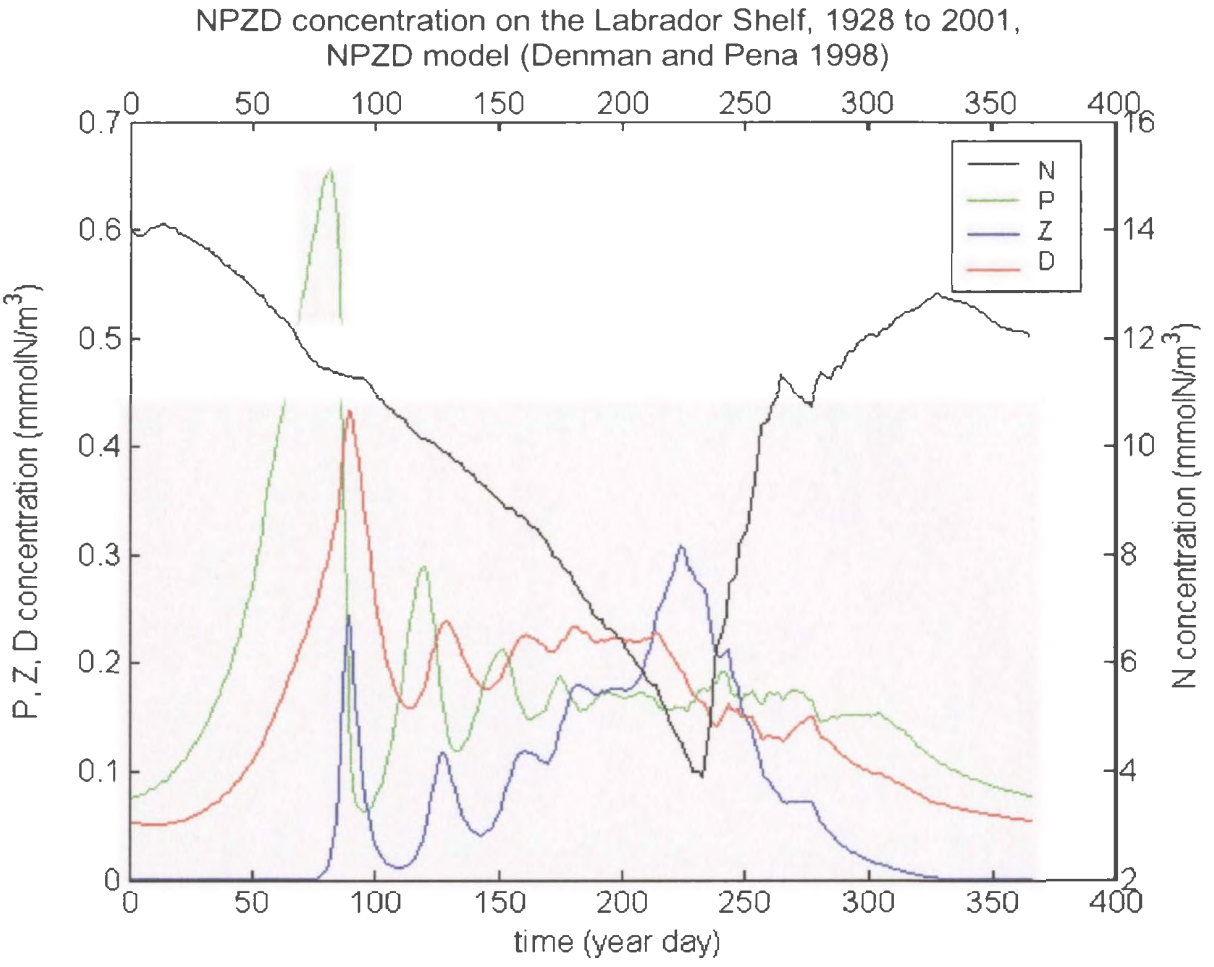

Figure 3.4: Model run showing nutrient, phytoplankton, zooplankton and detritus concentration over one year in the mixed-layer for the Labrador Shelf combining all years from 1928 to 2001. Parameters used are those for the Labrador Sea.

3.5.3. The Hamilton Inlet

The choice of parameters for Hamilton Inlet was based on the results of the sensitivity analysis for the Labrador Shelf. To determine the parameters, the mixed-layer depth calculated over the entire period from 1950 to 2000 was used to force the model. The model was run initially using the parameters chosen for the Labrador Shelf as listed in Table 3.2. The results were reasonable and since there was no seasonal cycle of phytoplankton and nutrients with which to verify the results, it was decided to not change the parameters. The same parameters were therefore used as for the Shelf.

3.6. Model Sensitivity

A parameter sensitivity analysis of the model of an annual cycle was completed for all the parameters listed in Table 3.2 excluding Z losses to N and D and the solar constant. The model was tuned using the range found in the literature for each of the parameters (Table 3.2 and Appendix 2) and the 1968 data set for the Bravo station. The Bravo station was chosen since it is in the Labrador Sea and there is a comparatively large amount of biological data for the Labrador Sea.

The ranges in Table 3.2 were divided into equal steps between the maximum and minimum to ensure anywhere from 5 to 10 values for each parameter with which to run the model (Table 3.3). A standard set of parameters was chosen, which was kept constant for all runs while testing each parameter (Table 3.3). This presents the problem of numerous plots of the simulated annual cycles of N, P, Z and D for the various parameter values making it difficult to review and present. Therefore two features were chosen to focus on; the maximum concentrations and the total production over an annual cycle of each state variable. These features of the annual cycle were chosen since they also can be used to compare with observations. The maximum concentration of N and P were compared to SeaWiFS and CZCS satellite data as well as the literature (Table 2.3). The satellite and literature data reports P concentration as chlorophyll concentration, the maximum chlorophyll concentration over an annual cycle based on the literature review in Table 2.3 was approximately 12 mg chl/m^3 or 8 mmolN/ m^3, using the conversion of C:chl of 60 and C:N of 6.625. Also, it is important to consider the timing of the P peak concentration and not only its magnitude. Due to the number of parameters, it was

decided to test only those with the greatest influence on the timing of the bloom and that proved to be sensitive. These parameters were assumed to be g_a, r_m, v_m and m_{pd} and were varied using the same range while investigating the day of the P maximum concentration. According to the literature review, the day of maximum chlorophyll concentration varies from days 158 to 180 (see Section 2.2). A value of day 170 was chosen to represent the day for maximum P concentration which is the middle of the month of June for the Labrador Sea.

Shown below are only the results for the maximum concentrations of each state variable (Figure 3.5), and the bloom timing (Figure 3.6), since these were used to compare with observations. The remainder of the results are presented in Appendix 3. The range of each parameter was normalized based on the maximum value to obtain a range from 0 to 1 to allow an easier comparison. The model sensitivity to each parameter was rated on a scale of 1 to 5, 1 being the highest sensitivity. To determine the sensitivity of each parameter, the plots were reviewed and the standard deviation of each parameter for the maximum concentrations and total annual concentrations of each state variable was calculated. The standard deviation over the range of results for each parameter for the maximum concentrations and total annual concentrations was plotted for each state variable. The plots for each state variable were divided equally into five levels based on the maximum standard deviation over all the parameters (Table 3.3). Parameter g_a proved to be the most sensitive parameter over all, followed closely by r_m. Below a certain value of g_a and r_m 0.5 and 0.81 d^{-1} respectively, the values of the maximum and total concentrations of each state variable reached a plateau at a much higher or lower

value compared with the remainder of the parameter results. For example, the maximum P concentration for g_a and r_m values below these values reached a plateau at almost 60 mmol N/m^3 while for the remainder of the parameter ranges the peak P concentration was below about 45 mmol N/m^3 unless the parameter was close to the limits of its range in which case some did reach 60 mmolN/m^3. Model simulations of P and Z maximum concentrations also showed a high sensitivity to the value of k_p and k_w, and N and D maximum concentrations showed a high sensitivity to the value of k_c. Fahsam *et al.*(1990) also found that the their plankton model was sensitive to the choice of k_w. The sensitivity to the parameter k_w and k_c may be due to the inaccuracy of assuming these values are constant with depth. In reality k_w and k_c vary with depth since they are wavelength dependent (Fahsam, 1995). A solution to this used by Anderson (1993) was to divide the mixed-layer into depth zones and assign different values of k_w and k_c to each zone. However, such a solution would increase the complexity of the model dynamics and has not been included. The least sensitive parameters of the maximum and total annual concentrations of all the state variables were r_e and k_n, which resembles an almost straight line across all the plots.

Comparing the maximum concentration of N to that from the literature review of 17.59 mmol N/m^3 in the Labrador Sea (Anderson, 1993), (see Section 3.5) most parameter values reveal a greater concentration. This is also true for the maximum concentration of P which from the results from Table 2.3 is 8 mmol N/m^3; most model simulations show a peak value above 10 mmolN/ m^3. However, these model simulations do not take into account the cloud effects, which would reduce the phytoplankton

productivity. In model runs using the same parameters but including cloud effects, the peak of P changed by approximately 3 to 4 mmolN/m^3 and the peak N concentration remained unchanged (Figure 3.7). Taking this into consideration, the P maximum would be reduced to a more desirable range, but most results still show much higher peak concentrations. The plot of P (Figure 3.5) reveals that to obtain a peak of approximately 8 mmolN/m^3, one must choose most parameter values towards the upper or lower limits of the ranges. The parameter ranges chosen (Table 3.4) were used for model simulations of the seasonal cycle of NPZD with and without the clouds (Figure 3.7). The model simulation did predict the pattern of the phytoplankton cycle in the Labrador Sea as discussed in Chapter 2 and shown in Figure 2.2. Also, the maximum N concentration between 16 and 18 mmolN/m^3 did match the value from the literature review. It is evident from Figure 3.7 that the P peak concentration decreases with the effect of clouds, however, the bloom timing does not change. The P peak with effect of clouds is 4.93 mmolN/m^3, which is too low. Also, the timing of the bloom climax occurs at day 133, which is too early in the year compared to day 170. Due to this discrepancy it was also decided to investigate the sensitivity to the timing of the bloom climax using four parameters, g_a, r_m, v_m and m_{pd} as discussed above. The results in Figure 3.6 reveal that at a certain range of the parameters the bloom timing remains at day 188. As g_a increases over 0.7 and r_m increases over 0.8 $d^{-1}$and v_m increases over 0.6 d^{-1}, the day of maximum bloom of P decreases until at the upper range of these parameters values, when the bloom timing remains at day 156. The opposite is true of m_{pd}. The bloom timing remains at day 188 for the upper range of the parameter and decreases as m_{pd} decreases. However,

within the range used for m_{pd} the bloom timing of day 156 is not reached. Based on obtaining a value of the bloom peak timing of day 170 the values of the four parameters in question were chosen (Table 3.5), along with the corresponding peak concentrations of P. A model simulation was run using the parameters from Table 3.4 and replacing g_a, r_m, v_m and m_{pd} with the values from Table 3.5. The results show that the P and N maximum concentration and day of the P peak are similar to the reported values from the literature (Figure 3.8). The maximum P concentration was 7.67 mmol N/m^3 that occurred at day 168, and the maximum N concentration was between 17 mmol N/m^3 and 19 mmol N/m^{-3}.

Figure 3.5: Normalized range of each parameter and the corresponding maximum N, P, Z and D concentrations from NPZD model simulations using Bravo station 1968 data. Legend: k_p is the half saturation constant for Z grazing, k_w is the attenuation coefficient of sea water, k_n is the Michaelis-Menten half saturation constant, alpha is the initial slope of P-I curve, g_a is the assimilated fraction that is ingested by Z, ν_m is the maximum uptake rate of nutrients by phytoplankton, r_m is the zooplankton maximum rate of grazing, r_e is D is remineralization rate, m_{pd} phytoplankton mortality and k_c is the coefficient providing shading.

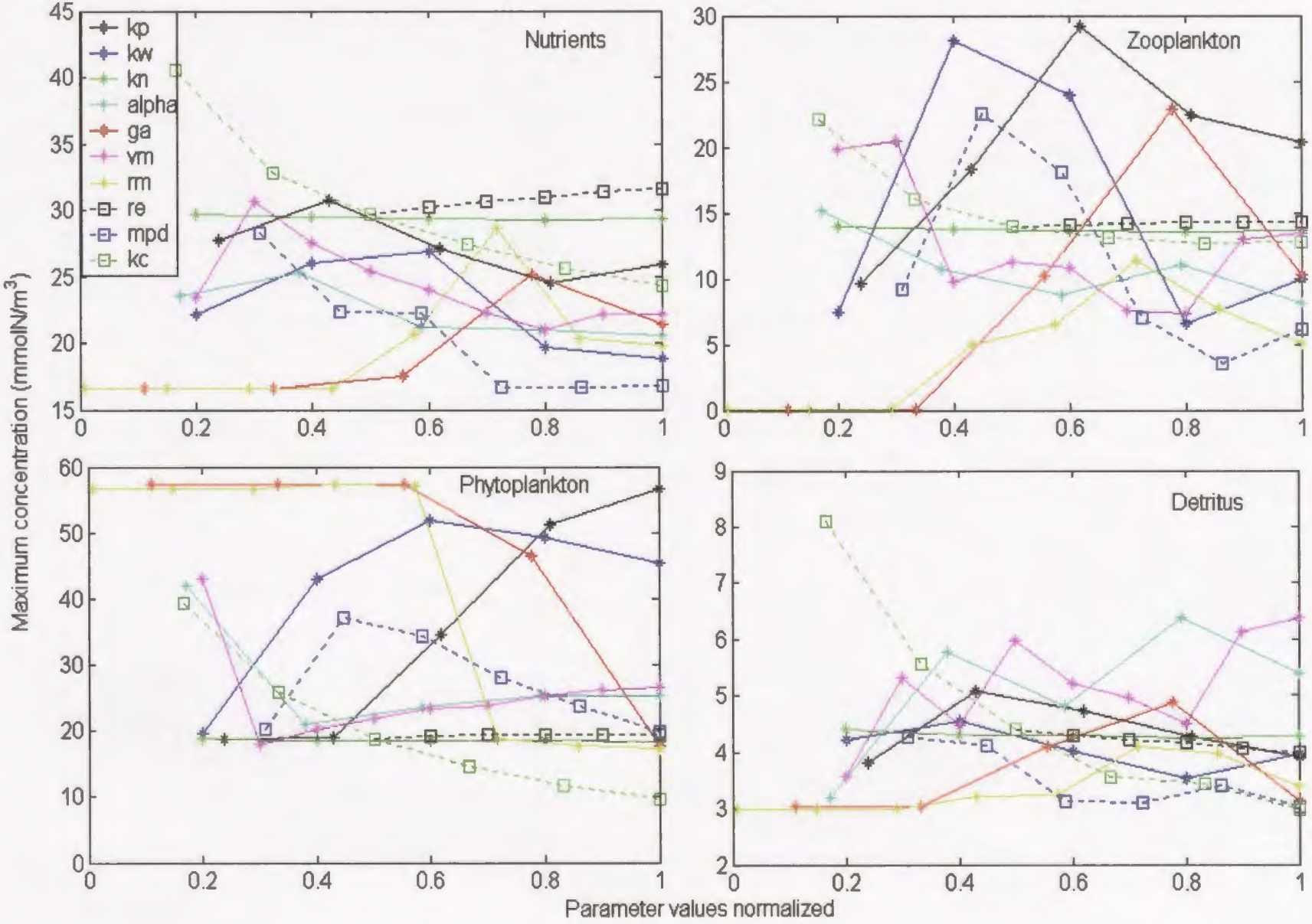
Nutrients
Zooplankton
Phytoplankton
Detritus
kp
kw
kn
alpha
ga
vm
rm
re
mpd
kc
Maximum concentration (mmolN/m3)
Parameter values normalized

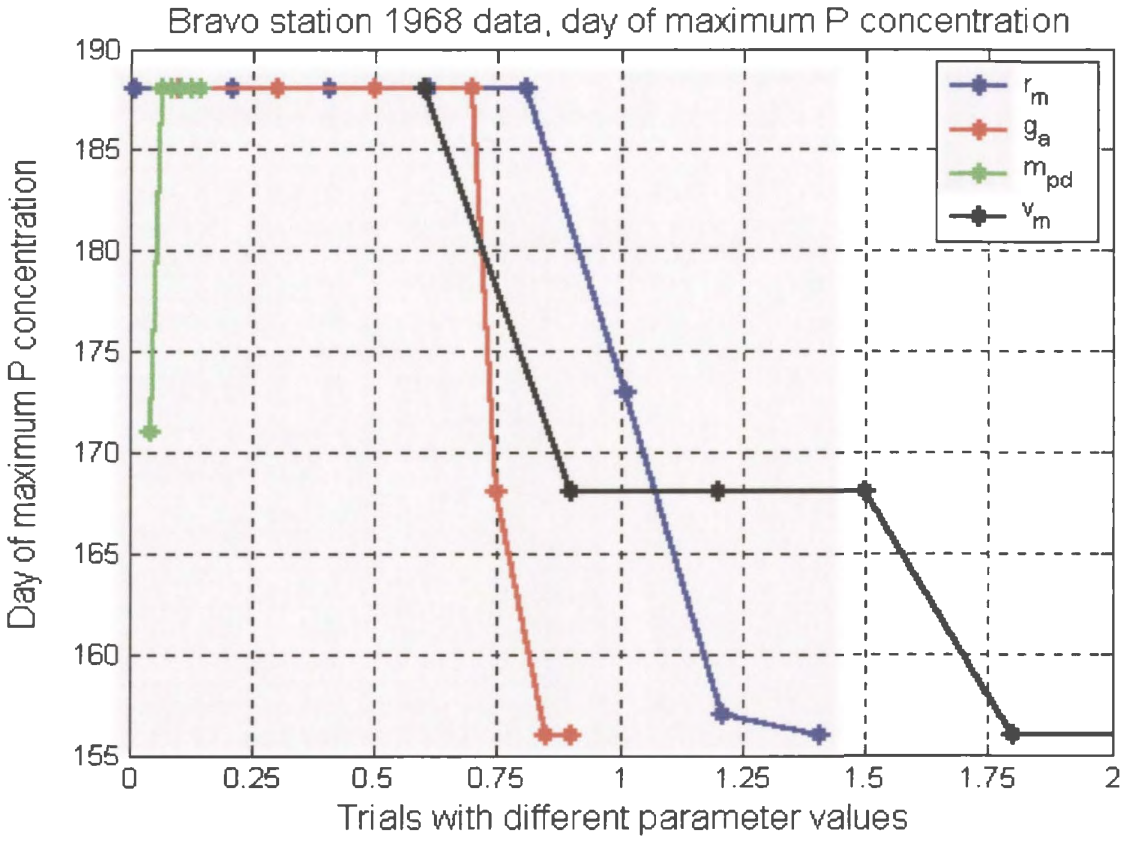

Figure 3.6: Range of r_m (blue), g_a(red), m_{pd} (green) and v_m(black) and the corresponding Julian day of maximum P concentration from NPZD model simulations using Bravo station 1968 data.

Table 3.3: Sensitivity of each parameter to the maximum and total concentration over an annual cycle for each state variable. Model simulations were done using Bravo station 1968 data. The scale used is 1 to 5, 1 is highest sensitivity and 5 is the lowest. Each colour represents a scaling value; 1(blue), 2 (green), 3 (yellow), 4 (orange), and 5 (red).

Parameter	Common value	Range used	Sensitivity 1 (high) to 5 (low)							
			Nutrients		Phytoplankton		Zooplankton		Detritus	
			Max	Area	Max	Area	Max	Area	Max	Area
k_w	0.06	0.04-0.2 steps 0.04	3	5	2	4	1	2	5	5
k_c	0.06	0.02-0.12 steps 0.02	1	4	3	4	4	2	1	3
α	0.04	0.025-0.15 steps 0.03	4	5	3	5	4	4	2	4
v_m	1.0	0.6-3.0 steps 0.3	3	5	4	5	3	4	3	4
k_n	0.1	0.1-0.5 steps 0.1	5	5	5	5	5	5	5	5
m_{pd}	0.05	0.045-0.15 steps 0.02	2	4	4	5	2	2	4	5
r_m	1.0	0.01-1.5 steps 0.2	2	1	1	1	3	2	4	1
g_a	0.75	0.1-0.95 steps 0.2	2	1	1	1	1	1	3	1
k_p	0.4	0.25-1.1 steps 0.2	4	4	1	5	2	3	4	3
r_e	0.05	0.05-0.1 steps 0.01	5	5	5	5	5	5	5	5

Table 3.4: Values of parameters chosen from the sensitivity model simulations in an attempt to match the value the maximum P concentration from the literature.

Parameter	Units	Value chosen
k_w	m^{-1}	0.04
k_c	m^{-1} mmol N /m^3	0.12
α	d^{-1} (W/ m^2) $^{-1}$	0.055
v_m	d^{-1}	1.2
k_n	mmol N/m^{-3}	0.1
m_{pd}	d^{-1}	0.045
r_m	d^{-1}	1.41
g_a		0.85
k_p	mmol N/m^{-3}	0.25
r_e	d^{-1}	0.05
m_{zn}	d^{-1}	0.2
m_{zd}	d^{-1}	0.05

Table 3.5: Tests using 4 parameters to determine the day of maximum concentration of P over an annual cycle. Model simulations were done using Bravo station 1968 data.

Parameters	Range used	Value when Julian day is 170	Corresponding maximum P (mmol N/m^{-3})
r_m	0.01-1.5 steps 0.2	1.08	17-18
g_a	0.1, 0.3, 0.5, 0.7, 0.75, 0.85, 0.90	0.75	35-40
m_{pd}	0.045-0.15 steps 0.02	0.045	17-20
v_m	0.6-3.0 steps 0.3	0.87	20-22

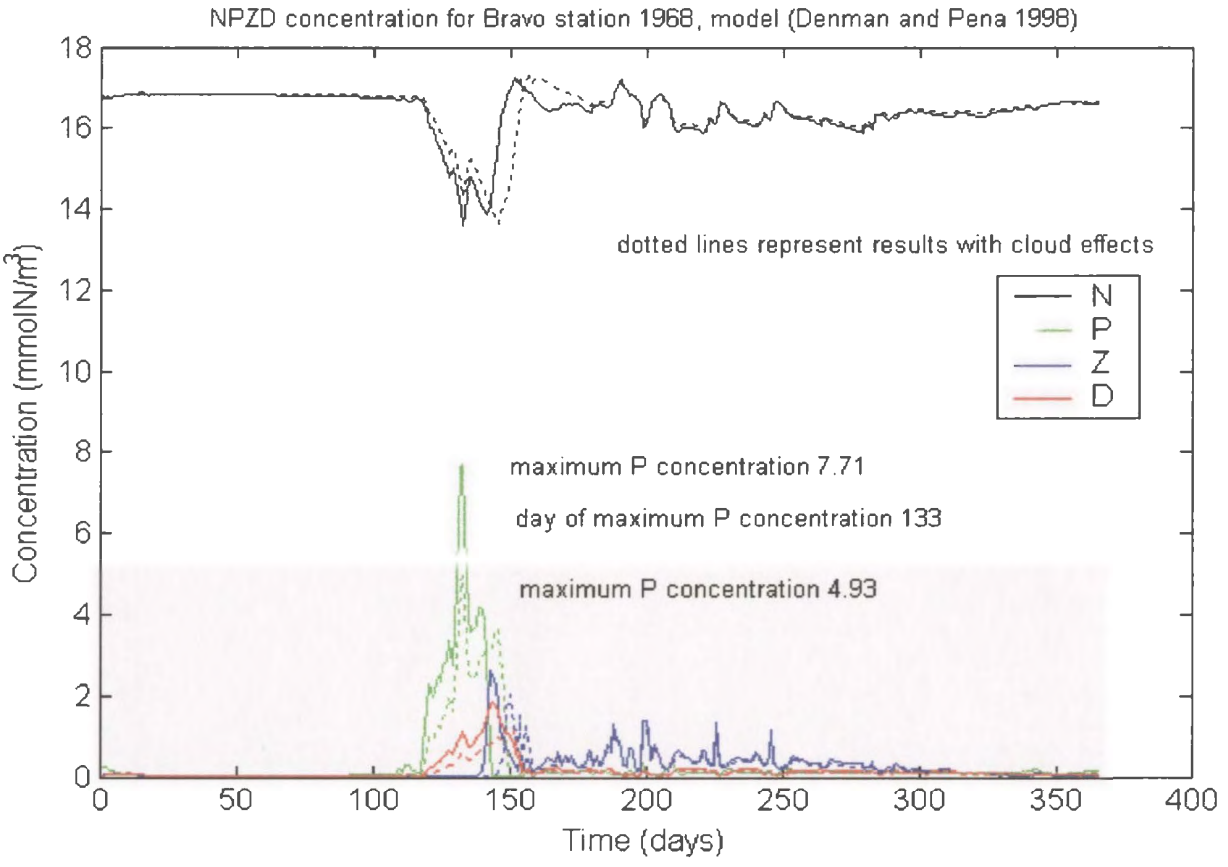

Figure 3.7: Model simulation using parameter choices to minimize P peak concentration with (dotted) and without cloud effects (solid). Model simulation using Bravo station 1968 data. Parameter values used are included in Table 3.5.

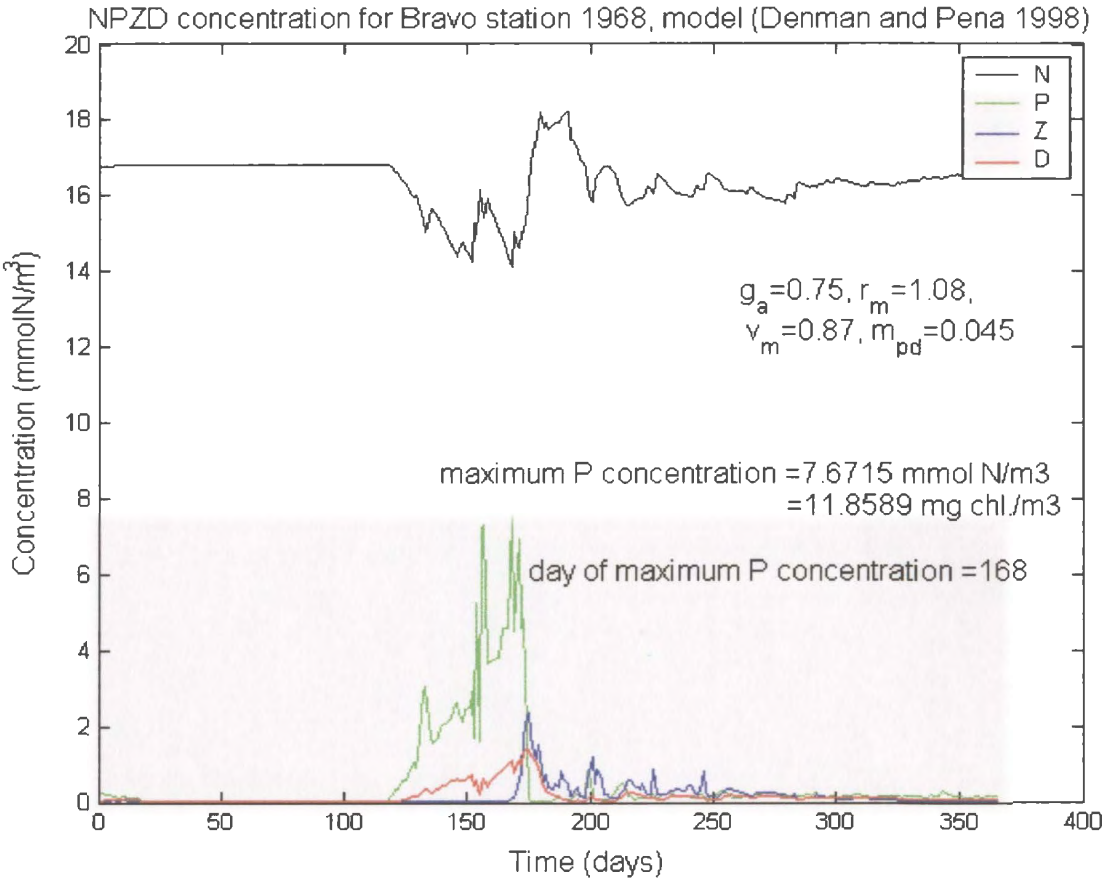

Figure 3.8: Model simulation using parameter choices from Tables 3.4 and 3.5. Model simulation using Bravo station 1968 data.

CHAPTER 4

Results

The annual cycles of the four state variables, nitrate, phytoplankton, zooplankton and detritus were modeled for three regions; the Labrador Sea and Shelf and Hamilton Inlet. In this section the resulting dynamics of these variables over an annual cycle are discussed and compared with observations, *in-situ* data, shipboard measurements, remote sensing data, and the results of other models. The analysis is focused on answering three main questions. The first is whether climate change during the 1990s affected the abundance and seasonal dynamics of the planktonic ecosystem in the Labrador Sea and Shelf. The second is whether the Churchill River flow and changing stratification associated with freshwater input significantly contribute to the circulation and entrainment of nutrients in Hamilton Inlet and, therefore, influence the abundance and seasonal dynamics of the planktonic ecosystem in Hamilton Inlet and Labrador Shelf. The third is whether the Churchill River significantly contributes to the nutrient budget of Hamilton Inlet and therefore influences seasonal dynamics of the planktonic ecosystem in the Hamilton Inlet and Labrador Shelf.

4.1. Labrador Sea

The model for the Labrador Sea was run during two periods, 1968 and the 1990s. The model was initialized January 1 and run for one complete year. The initial concentrations of each state variable are listed in Table 3.1 and the parameters used are listed in Table 3.2. In the following sections the results of the calculated annual mixed-

layer depth and results of the model simulations are discussed and compared with observations, *in-situ* data, shipboard measurements, remote sensing data, and the results of other models.

4.1.1. Annual Mixed-layer

The mixed-layer depth was calculated from density measurements during the two periods 1968 and from 1992 to 1999 as discussed in Section 3.4.1 (Figure 4.1). The annual cycle of the mixed-layer depth for the Labrador Sea starting in the beginning of January is shallow above 300 m, then deepens to a maximum depth by the end of January and remains deep until late March. The mixed-layer depth shallows by the beginning of April and by the end of April the depth in most open water regions in the Labrador Sea is reduced to 50 m or less and remains shallow until December and January when increasing winds deepen the mixed-layer and the cycle begins again (Tang *et al.*, 1999). This annual cycle is consistent with the annual mixed-layer depth from Tian *et al.* (2004) (Figure 4.2). The mixed-layer depth in the study by Tian *et al.* (2004) was determined by finding the point of zero gradient for temperature and salinity. For 1968, at the Bravo station, the mixed-layer deepens to 1000 m, the maximum depth used in the model, from mid January until March. This deep convection, down to 1000 m, is deeper than the published value of 800 m in 1968 (Lazier, 1980; Tian *et al.*, 2004). Therefore, the model was run with the mixed-layer depth of 1000 m, and 800 m. The mixed-layer begins to shallow at approximately day 118 and continues to shallow until it reaches a minimum between days 180 and 280, after which it gradually deepens to 100 to 200 m by the end of the year. In comparison, the 1968 density data for the Labrador Sea shows a minimum

between days 225 and 300 and is uniform throughout the water column between days 15 and 90, corresponding with the deep convection. In the 1990s there was insufficient data for any one year and therefore data for the years between 1992 and 1999 were combined. Unlike the 1968 data, which was all obtained from one location, the data in the 1990s was distributed among many sites throughout the area. Tian *et al.* (2004) had the same problems when trying to determine the depth of the mixed-layer in the 1990s, they combined data between 1990 and 1998 to determine a mixed-layer annual cycle. Between 1992 and 1999 the density data (Section 2.5.1) are sparse in the winter and the data from the period when the mixed-layer begins to shallow after the winter deep convection is absent. For this reason, the results of Tian *et al.* (2004) in the 1990s are used to determine the day that the mixed-layer begins to shallow, day 105, and the depth of winter convection, 2300 m (Figure 4.2). The 1990s mixed-layer depth continues to shallow after day 105 until it reaches a minimum between days 135 and 210, after which the data are sparse again. This makes it difficult to determine when the mixed-layer begins to deepen again in autumn. Figure 4.1 shows the points in blue where data were available to calculate the mixed-layer and the points circled in red were outliers that were subsequently removed. Other studies have shown that the depth of the mixed-layer in winter and the time of the maximum mixed-layer depth vary throughout the Sea (Tang *et al.*, 1999; Lavender and Davis, 2002). For example, in the central Labrador Sea (58°N, 55°W) the maximum mixed-layer depth occurs at the end of March, whereas farther north (62°N, 53°W) the maximum occurs at the end of February (Tang *et al.*, 1999). The mixed-layer depth for that study was determined using a Niiler-Kraus type model coupled

to sea-ice. Lavender and Davis (2002) plotted the mixed-layer depths across the Labrador Sea between November 1996 and June 1997 and showed they varied between less than 200 m to 1350 m. They also showed when combining all the data that overall, the mixed-layer deepened to 1200 m in March and was shallow by the end of April and remained shallow until November when it began to deepen again. The mixed-layer for that study was calculated from measured temperature and salinity by determining the break between the least squares fit of a straight line to the upper layer and a second order polynomial plus exponential fit to the lower layer of each temperature profile. These results are consistent with this studies calculated mixed-layer except in the 1990s in December and early January, when the mixed-layer remained quite shallow. The 1990s, data are spread across the Sea and the deep winter convection depths can vary annually and by location. Therefore, the model was run in the 1990s using two winter convection depths, 1000 and 2000 m. Otherwise the annual mixed-layer depth remained unchanged.

During 1968, relative to the 1990s, as discussed previously, winter convection was shallower. Compared with the data obtained from I. Yashayaev (personal communication, BIO) (Section 2.5.1) for the Labrador Sea, the lowest salinity and highest temperature recorded between 1938 and 2001 occurred during 1968 to 1971. Lazier (1980) reported similar findings and the low salinity period was also combined with a milder winter between 1967 and 1971. The lower salinity combined with the milder winter changed the stratification of the upper layers. Therefore, even though there was weaker stratification in the intermediate layers, the strong upper layer stratification limited deep convection.

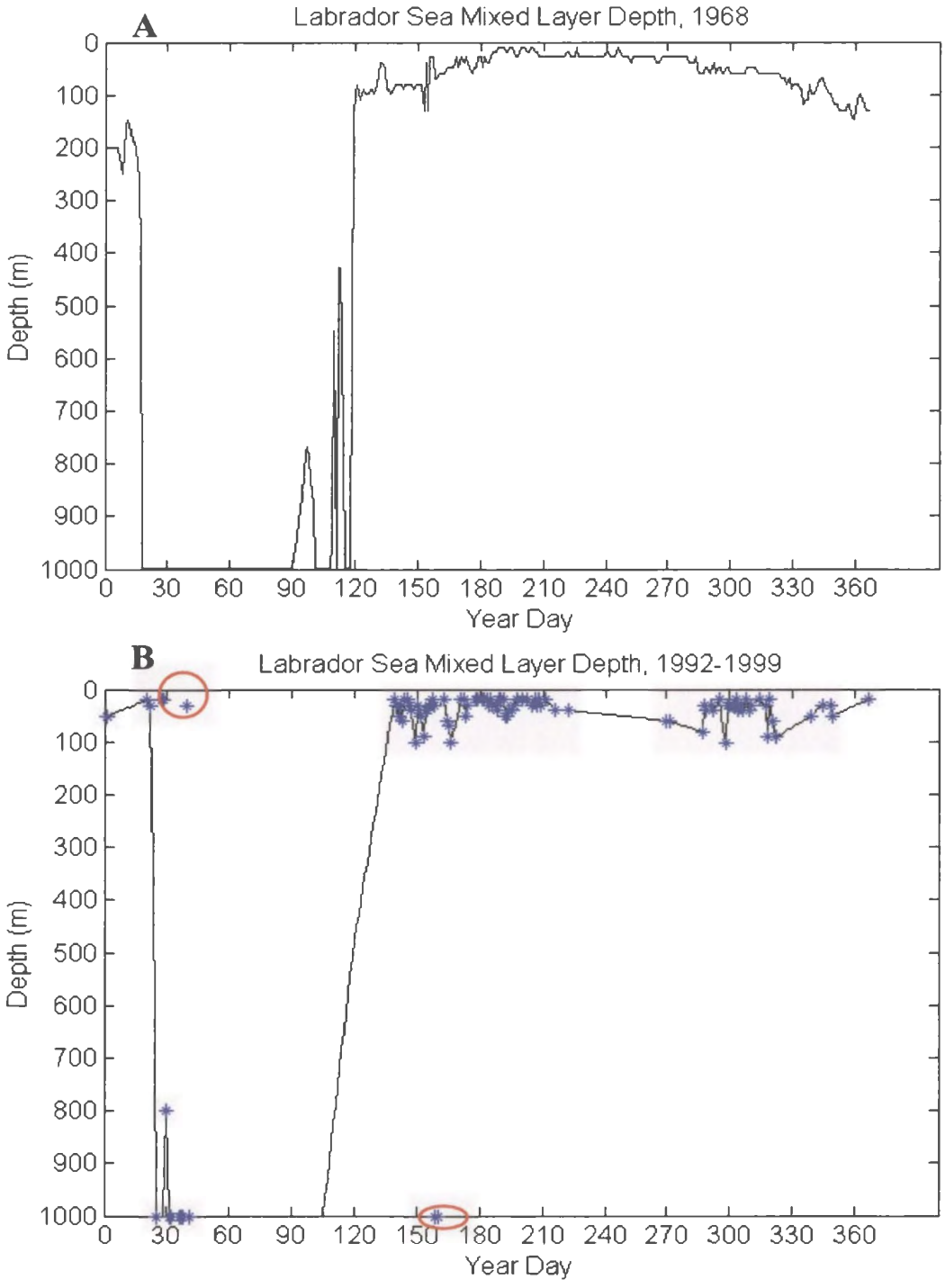

Figure 4.1: The mixed-layer depth for the Labrador Sea calculated from measured density data. (A) Weather ship station BRAVO, 1968; (B) various locations in the Labrador Sea, 1992 to 1999. In B) the line is the linear interpolated mixed-layer depth, the blue dots indicate the days in which density data are available to calculate the mixed-layer depth and the circled points are the outliners that were removed.

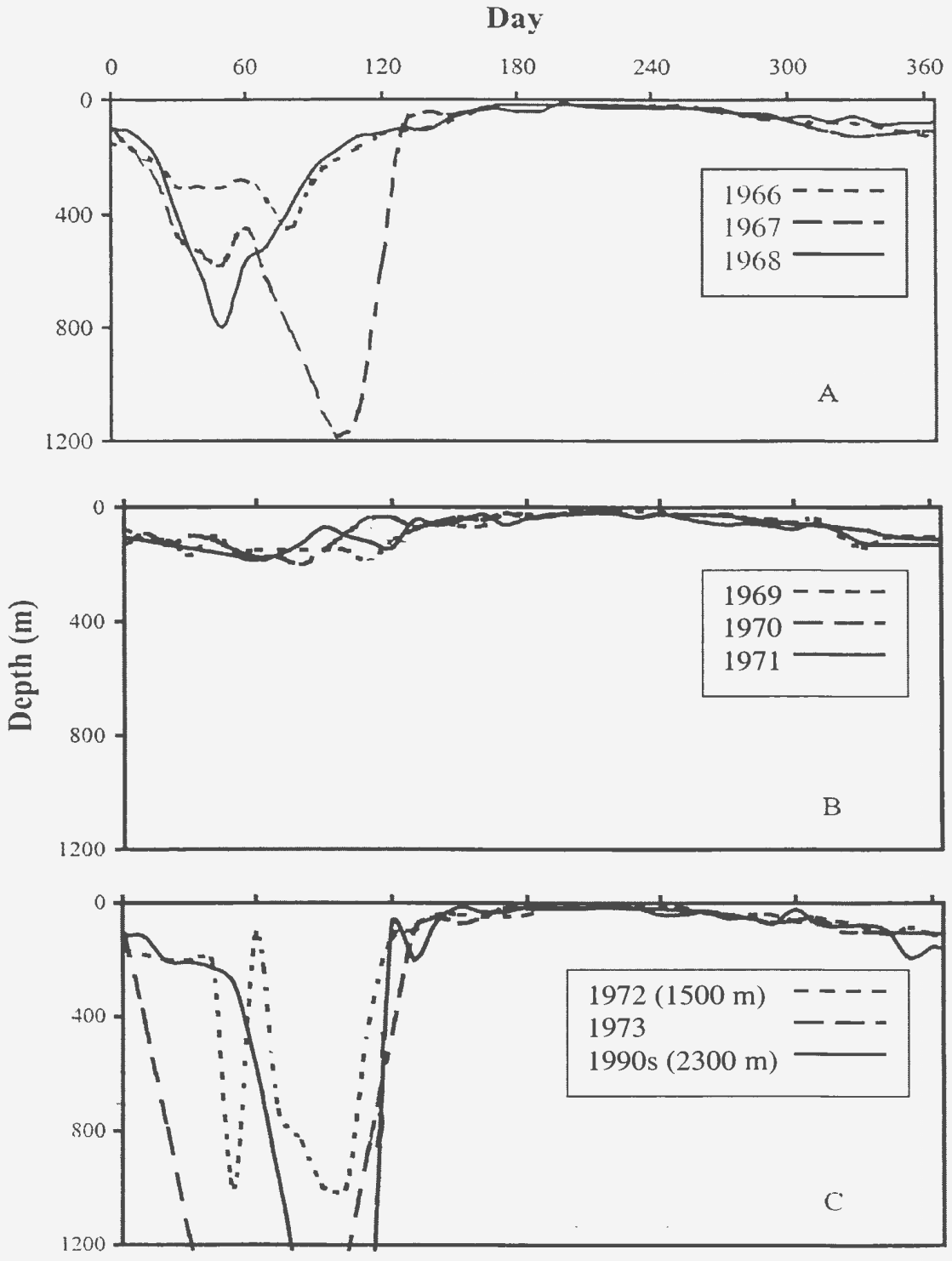

Figure 4.2: Mixed-layer depth for the Labrador Sea from CTD profiles: A) 1966 to 1968, B) 1969 to 1971 and C) 1972 to 1973 and the early 1990s (Adapted from Tian *et al.*, 2004).

4.1.2. Annual Cycles of Biological Variables

All the biological variables, nitrate, N, phytoplankton, P, zooplankton, Z and detritus, D, show a distinct annual cycle typical for the Northwest Atlantic with a pronounced spring bloom in P and Z and depletion of N concentration in the surface layer in the summer (Siegel *et al.*, 2002) (Figure 4.3 and Table 4.1). The model for the 1990s was run over several annual periods using the output from the previous run to obtain stable N dynamics.

Starting in January the concentration of N is high and reaches levels found in the deep ocean of around 16 mmol/m^3 and remains unchanged until early May. At the same time, deep convection is occurring that supplies the upper layer with nutrients and maintains the high level of nutrients, since the primary production is light limited and remains at a minimum. Z and D are also at a minimum during the winter deep convection. In the spring, when the mixed-layer begins to shallow in May the irradiance increases in the surface layer, the photosynthetically available radiation (PAR) increases, and the high concentration of N becomes trapped in the mixed-layer causing a P bloom. The initiation of the P bloom is determined as the day at which the P concentration reaches over 0.1 mmol N/m^3 (Table 4.1). The model simulations for 1968 reveal an earlier start to the P bloom at day 119 compared with day 130 for the 1990s. P continued to increase until reaching a maximum concentration. There is some variability in P concentration, therefore, a 5-day mean was used to smooth the data and determine the timing of the bloom (Figure 4.3). In 1968 the P peak concentration shows little change in response to decreasing the winter convection depth (Figure 4.4 b). However, the

decrease in deep convection depth causes the P bloom to occur 10 to 15 days earlier. In the1990s there is very little difference between the timing or magnitude of the P bloom by changing the winter convection. There is a considerable difference between the 1990s and 1968 P bloom timing and maximum. The P peak concentration is lower in the 1968 simulations than in the 1990s simulations. The 5-day mean P concentration in 1968 (5.36 and 5.48 mmol N/m^3) is almost doubled in the 1990s (10.1 and 9.98 mmol N/m^3). The timing of the maximum concentration for the 5-day mean of P is approximately 10 days later in the 1990s compared to the 1968 simulation using 1000 m winter convection and 20 days later compared to the 1968 simulation using 800 m winter convection.

The increase in P concentration reduces the nutrient concentrations and a minimum N concentration occurs during the P bloom. Nutrients are never completely depleted, and are reduced by less than 25% relative to deep-water concentrations. In 1968 the N is reduced from just over 16 to 14 mmol N/m^3 for both runs, however the timing of the N minimum occurs 16 days later when deep convection increases to 1000 m (Figure 4.4 a). In the 1990s the increase in winter convection had little effect on the magnitude and timing of the N minimum. In the 1990s the N minimum during the bloom is lower than the 1968 simulations, reduced from just over 16 to 11 mmol N/m^3. The timing of the N minimum is later in the 1990s by 15 days when compared to 1000 m winter convection in 1968, and 31 days later compared to 800 m winter convection.

The P bloom period causes an increase in Z biomass and a peak in concentration of Z occurs as the peak in P concentration quickly declines (Figure 4.4 c). Changing the winter convection depth made little difference to the timing of the Z bloom. Decreasing

the winter convection depth increases the maximum Z concentration by approximately 1 mmol N/m^3 for 1968 and by 3.3 mmol N/m^3 for the 1990s (over double). As for N, the 1990 modeled timing of the Z peak concentration is also approximately 15 days later than in 1968. The Z peak concentration of approximately 2.3 mmol N/m^3 is similar to the 1968 model with 1000 m convection and the 1990s model with 2000 m convection. A similar result occurs with D, with a similar timing of peak concentration for the runs during each period and an increase in concentration associated with a decrease in convection in the 1990s and 1968.

During summer, from mid July to September, the stratification increases and vertical mixing is reduced. The P concentration declines to below 0.1 mmol N/m^3 and remains at low levels until the following spring when the bloom cycle starts again. The Z and D concentrations also decline to very low levels until the following spring as the food supply diminishes in the surface waters. The N temporal minimum is followed by a sharp maximum to about 18 mmol N/m^3 of nitrate. This may be caused by remineralization within the mixed-layer and the trapping of nutrients in the mixed-layer due to the strong stratification. The nitrate maximum gradually declines and in the case of 1968 it returns back to the level found in the deep waters as the mixed-layer deepens in autumn and remains at this level until the spring. In the 1990s, in October the nitrate levels drop, approaching the minimum levels during the bloom. This may be caused by the stratification breaking down, allowing nutrients to escape the mixed-layer, however, the mixed-layer does not deepen enough and vertical mixing does not increase sufficiently to regenerate surface nutrients. Unfortunately, this is a period in which data

were lacking and interpolation was used to determine daily values, possibly leading to errors in nutrient dynamics. As the mixed-layer continues to deepen and vertical mixing increases in November and December the nutrient levels return back to a high level of over 16 mmol N/m^3. In the 1990s, from the end of December until mid January, there is a slight decrease in nutrients, which may again be caused by the lack of data during this period. After mid January, the nutrient levels return to the level in the deep ocean until spring.

The biomass over an annual cycle was calculated by determining the total area under the curve over one year. The area was calculated using different time intervals until the time interval was small enough that the total area under the curve for each variable did not change over the year. The time interval chosen was one-half day. There are small changes in N, Z and D between simulations with the highest N and Z content in 1968 and the highest D content in the 1990s (Table 4.2). However, the P content almost doubles from 186.9 and 190.8 mmol N/m^3yr for 800 m and 1000 m respectively in 1968 to 349.9 and 358.0 mmol N/m^3yr for 1000 m and 2000 m respectively in the 1990s.

Overall the most evident differences between the 1968 and 1990s runs are during the spring bloom period and the P biomass over an annual cycle. In the 1990s the P maximum concentration is higher and occurs approximately 10 to 20 days later than in 1968 while the N concentration is lower and occurs 15 to 31 days later. The Z and D maximum concentration occurs approximately 16 to 19 days later in the 1990s. The P biomass almost doubles from 1968 modeled values to the 1990s modeled values. The major differences in 1968 from decreasing the winter convection to 800 m from 1000 m

is that the P bloom and N minimum occur approximately 15 days earlier. When the convection decreases to 800 m there is a general decrease in the yearly biomass of P, an increase in yearly biomass of Z and D and no change in N. In the 1990s the major change is the increase in Z peak when the winter convection decreases to 1000 m from 2000 m. When the convection decreases to 1000 m there is a general decrease in the yearly biomass of P, an increase in yearly biomass of Z and almost no change in N and D.

Table 4.1: Summary of minimum N concentration, maximum P, Z, and D concentrations, timing of the maximum, and start time of P and Z bloom for model simulations.

Peak concentrations and bloom initiation	**Model simulation 1968, 800 m winter convection**		**Model simulation 1968, 1000 m winter convection**		**Model simulation 1990-1996, 1000 m winter convection**		**Model simulation 1990-1996, 2000 m winter convection**	
	Year Day	**Concentration** (mmol N/m^3)	**Year Day**	**Concentration** (mmol N/m^3)	**Year Day**	**Concentration** (mmol N/m^3)	**Year Day**	**Concentration** (mmol N/m^3)
N minimum during bloom	152	14.2	168	14.1	183	11.2	183	11.1
Start of P bloom (when P reaches 0.1 mmol N/m^3)	119	0.288	119	0.117	132	0.127	135	0.153
P maximum	157	7.83	168	7.67	171	11.0	171	10.8
P maximum, 5 day mean	155-160	5.48	165-170	5.36	175-180	10.1	175-180	9.98
Start of Z bloom (when Z reaches 0.1 mmol N/m^3)	166	0.117	168	0.108	183	0.118	187	0.138
Z maximum	173	3.28	175	2.35	190	5.73	194	2.40
D maximum	171	1.74	174	1.41	190	2.21	191	1.49

Table 4.2: Total yearly biomass of N, P, Z, and D for model simulations.

State Variable	Model simulation 1968		Model simulation 1990-1996	
	Total yearly biomass (mmol N/m^{3}yr)		Total yearly biomass (mmol N/m^{3}yr)	
	800 m winter convection	1000 m winter convection	1000 m winter convection	2000 m winter convection
N	5990	5990	5425	5421
P	186.9	190.8	349.9	358.0
Z	60.55	55.69	54.03	50.62
D	59.69	57.69	65.95	66.00

Figure 4.3: Modeled daily concentration and the 5 day mean of N (black), P (green), Z (blue) and D (red) in mmol N/m^3 over one year for four model simulations: A) 1968 with 800 m winter mixed-layer; B) 1968 with 1000 m winter mixed-layer; C) 1990s with 1000 m winter mixed-layer; and D) 1990s with 2000 m winter mixed-layer.

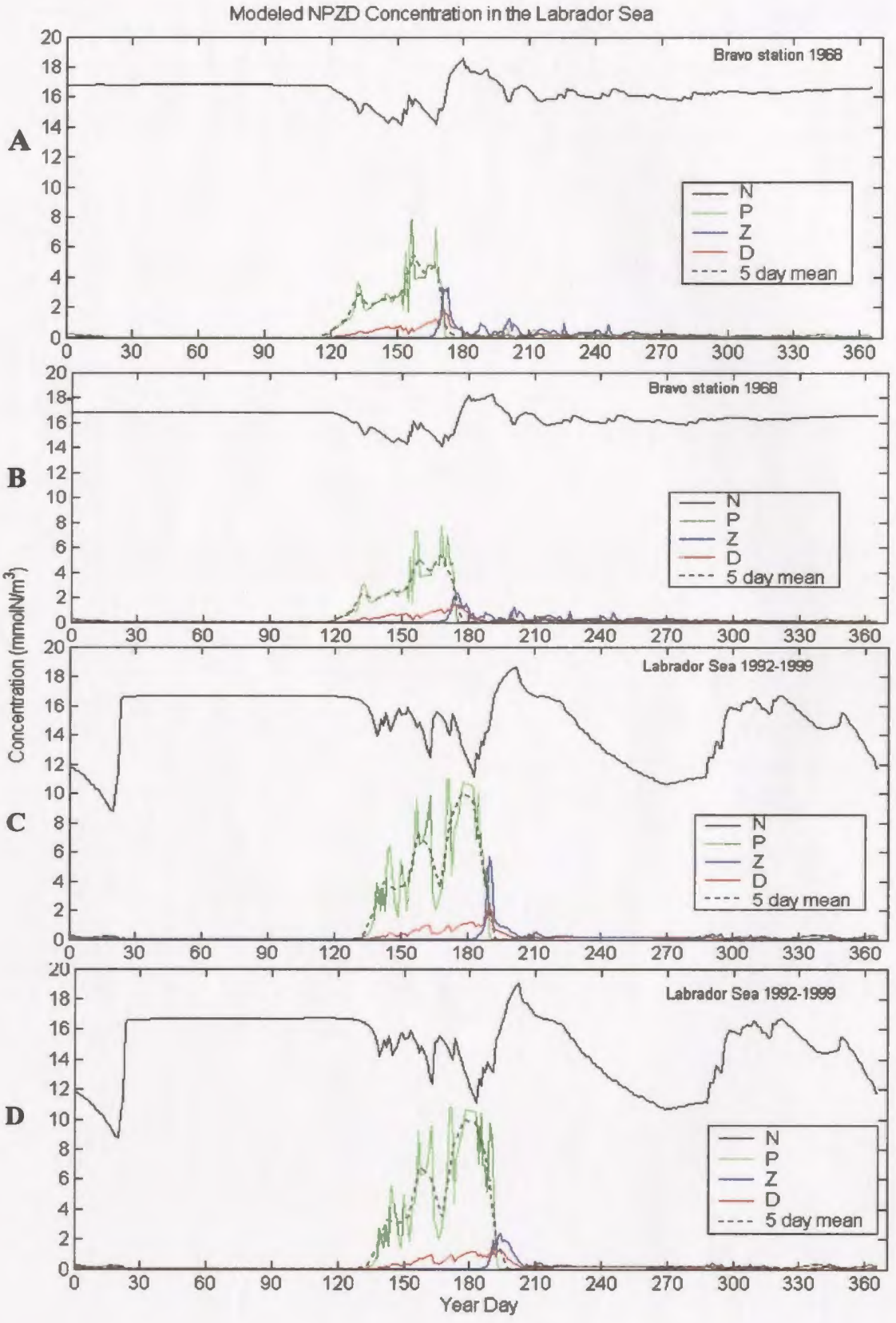
Modeled NPZD Concentration in the Labrador Sea
A
Bravo station 1968
B
Bravo station 1968
C
Labrador Sea 1992-1999
D
Labrador Sea 1992-1999
N
P
Z
D
5 day mean
Concentration (mmolN/m3)
Year Day

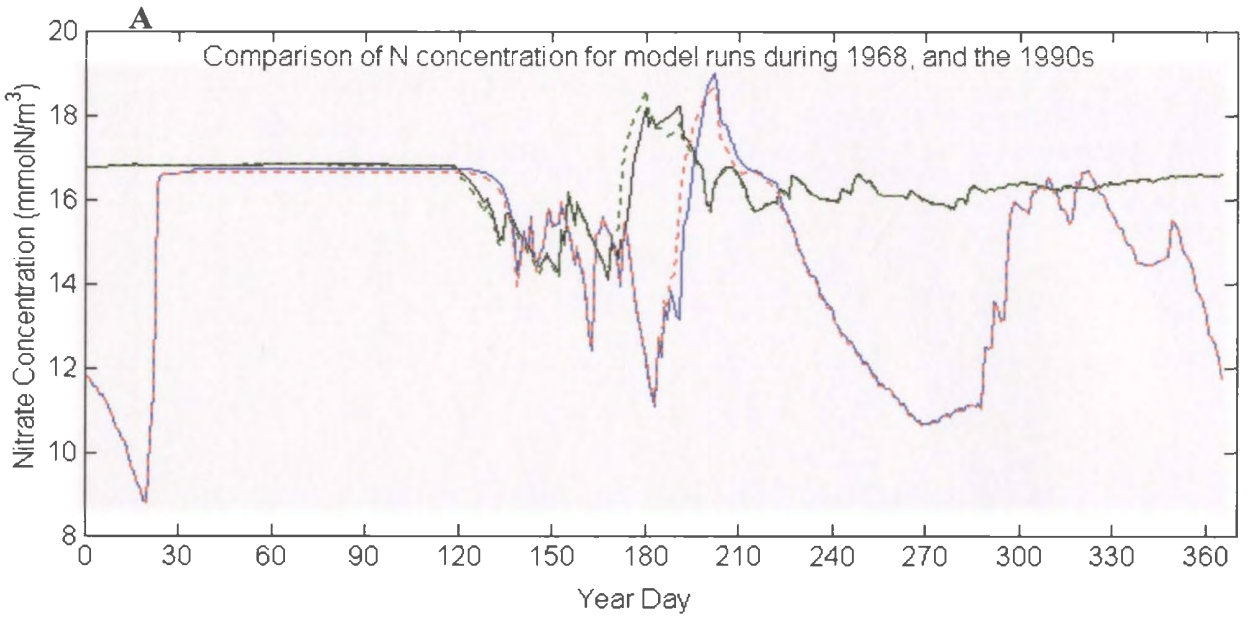
A
Comparison of N concentration for model runs during 1968, and the 1990s
Nitrate Concentration (mmolN/m3)
Year Day

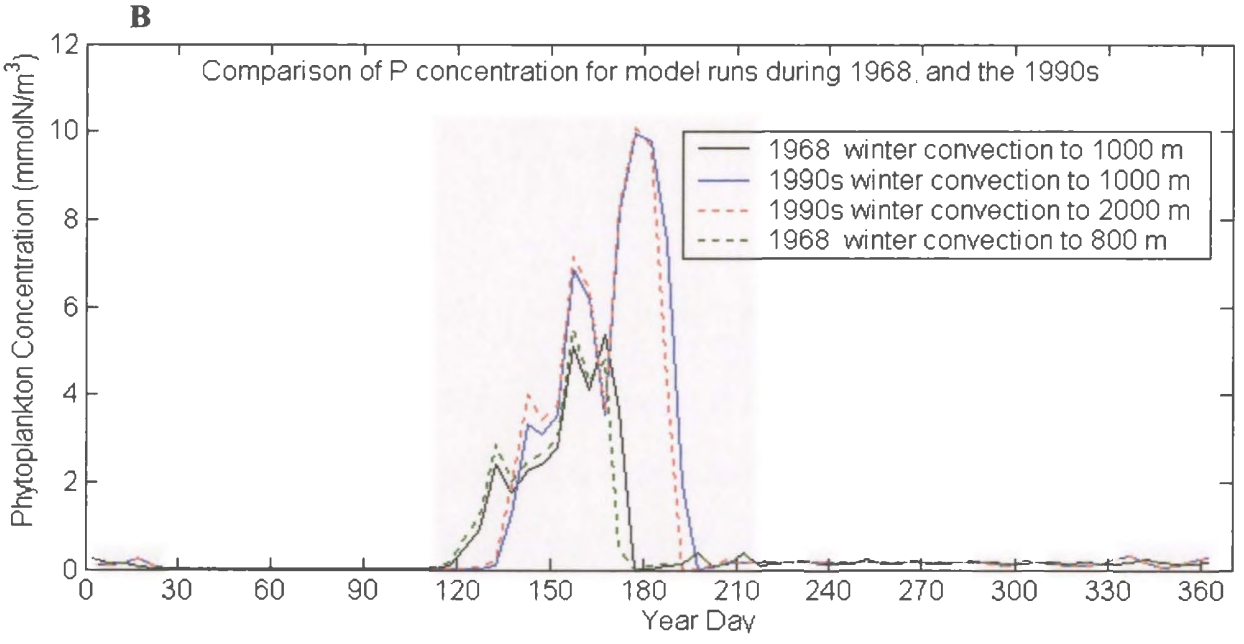
B
Comparison of P concentration for model runs during 1968, and the 1990s
1968 winter convection to 1000 m
1990s winter convection to 1000 m
1990s winter convection to 2000 m
1968 winter convection to 800 m
Phytoplankton Concentration (mmolN/m3)
Year Day

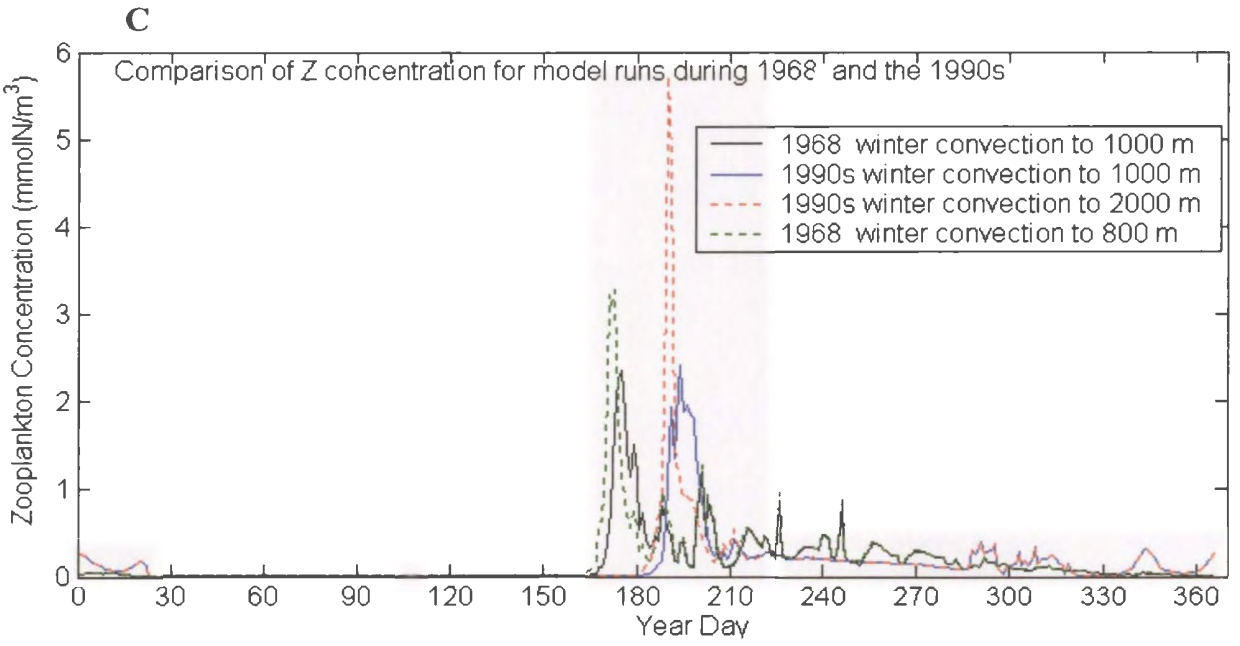

Figure 4.4: Comparison of modeled nitrate, phytoplankton and zooplankton for four model runs: 1968 with 800 m winter mixed-layer (green solid line); 1968 with 1000 m winter mixed-layer (black solid line); the 1990s with 1000 m winter mixed-layer (red dotted line); and the 1990s with 2000 m winter mixed-layer (blue solid line). A) Nitrate; B) Phytoplankton; and C) Zooplankton in mmol N/m^3.

4.1.3. Comparison with Other Models

The modeled nutrients, phytoplankton, and zooplankton in the mixed-layer over an annual cycle are compared with the output of two other ecosystem models of the Labrador Sea, that of Trela (1996) and Tian *et al.* (2004).

The model of Trela (1996) simulated the annual cycles of N, P and Z in the surface layer (0 to 30-200 m) and the intermediate layer (30-200 m to 230 m) in the Labrador Sea (Figure 4.5). In that model, the surface layer annual cycle of variables showed a similar pattern of a distinct spring bloom. The nutrient levels in the surface layer became depleted in July following the spring bloom, which is not consistent with

this model results in which the nutrients fall about 25 % below the winter value. In the intermediate layer the N concentration decreases slightly in spring, which is more consistent with this models results. Another notable difference in the N annual cycle in the model by Trela (1996) is the nutrients gradually return to the winter level and do not peak in concentration following the low levels as in this model. The P bloom in the Trela model (1996) occurred at the end of June (days 170 to 180), which is within the range from all model runs with the exception of the run in 1968 with the winter convection to 800 m. In the Trela model (1996) there was a second small increase in P biomass in summer caused by the shift in P composition towards a higher C:N ratio, allowing the uptake of additional nutrients from the surface waters. This shift did not occur in these model runs. The maximum P concentration in the Trela model (1996) was over 80 mmolC/m^3 (10.35 mmol N/m^3), which is close to the values from the 1990s model runs. The Z peak in the Trela model (1996) occurred at the beginning of June (days 180 to 190), which is also close in timing to the 1990s runs. The peak concentration of Z was much lower than this models results at 0.9 mmolC/m^3 (0.12 mmol N/m^3).

The model by Tian *et al.* (2004) simulated the annual cycles of N, P and Z in the surface layer in the Labrador Sea. The model was run from 1966 to 1973 and in the early 1990s, and the simulated P annual cycle was plotted yearly with one line representing the 1990s (Figure 4.6). Similar to the model by Trela (1996), there is a distinctive spring bloom in P with a second smaller increase in biomass in the summer and fall. The latest and highest P bloom was initiated at the end of April (~ day 120) and occurred at the end of June in the 1990s, which had the deepest winter convection. The earliest and lowest P

bloom occurred from 1969 to 1971 during the period of virtually no winter deep convection (Figure 4.2). The period from 1966 to 1968 was somewhere in-between. The peak P concentration in the 1990s was ~18 gC/m^2 (9.7 mmol N/m^3, assuming a mixed-layer depth of 20 m) and in 1968 it was ~14 gC/m^2 (7.55 mmol N/m^3, assuming a mixed-layer depth of 20 m) which is within the values found for this model study. The P peak was approximately 20 days later in the 1990s as compared to the periods with shallow winter convection, which is slightly more than this model. The general pattern found by Tian *et al.* (2004) was that during periods of strong winter convection (1972 and 1990s) the P bloom is later and greater in concentration than during periods of weak winter convection (1969-1971).

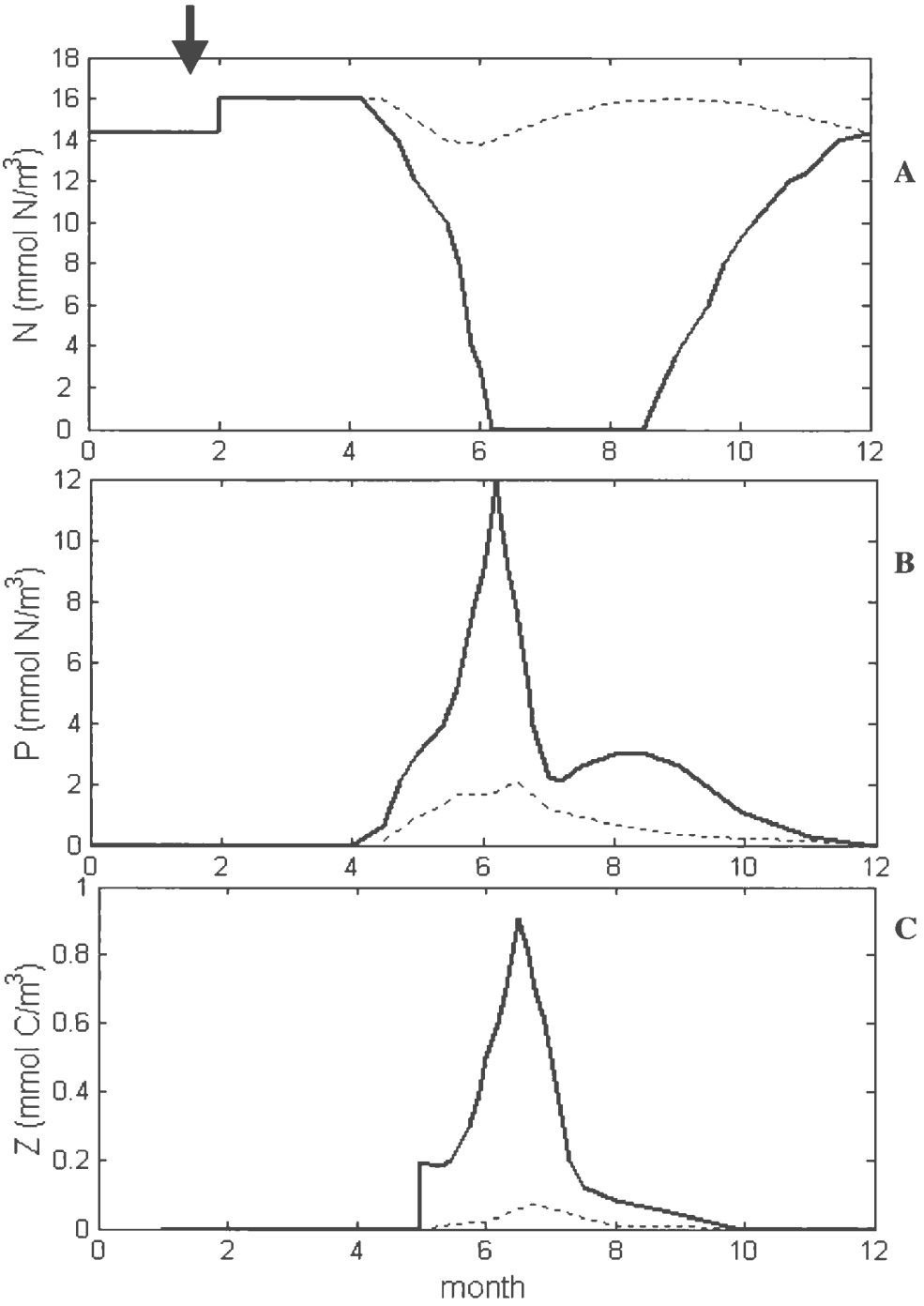

Figure 4.5: Annual cycles of modeled A) nutrients, N in mmolN/m^3; B) phytoplankton, P in mmolN/m^3; and C) zooplankton, Z in mmolC/m^3 from the model by Trela (1996). The solid line represents the annual cycle in the surface layer which is 0 to 30- 200 m deep varying seasonally. The dotted line represents the annual cycle in the intermediate layer which is 30- 200 to 230 m deep. The arrow indicates the time of the simulated deep winter convection.

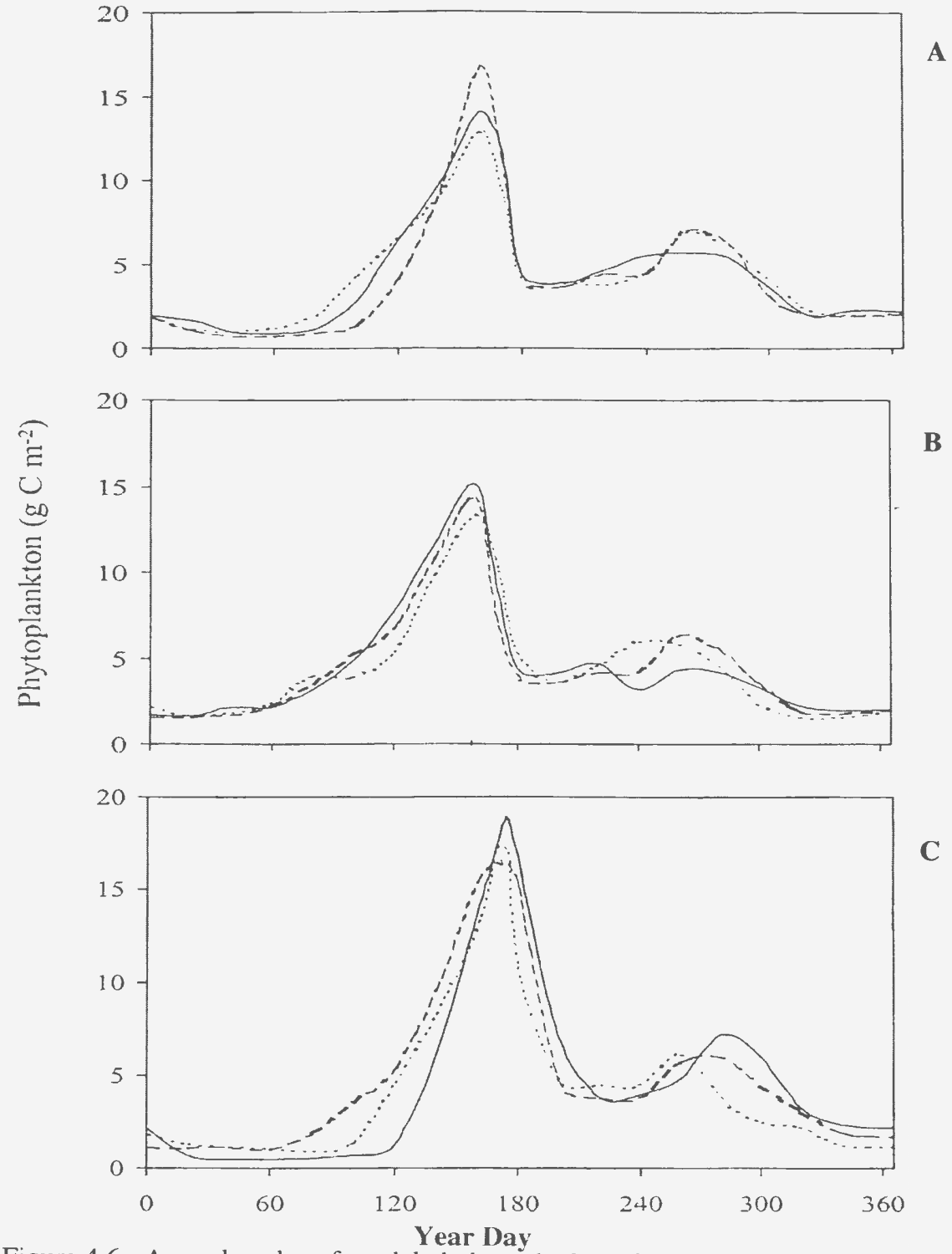

Figure 4.6: Annual cycles of modeled phytoplankton from 1966 to 1973 and in the early 1990s in g C/m^2 (Modified from Tian *et al.*, 2004). A) 1966 (dotted line), 1967 (dashed line), 1968 (solid line); B) 1969 (dotted line), 1970 (dashed line), 1971 (solid line); and C) 1972 (dotted line), 1973 (dashed line), 1990s (solid line).

4.1.4. Comparison with Observations, *In-situ* Data, and Shipboard Measurements

Nutrients and phytoplankton in the mixed-layer are chosen for comparison with observations since there are data from the Labrador Sea. The data obtained over a year are sufficient to determine whether modeled annual cycles have realistic magnitude, timing and overall seasonal dynamics. However, there is a lack of data for the specific periods investigated, 1968 and the 1990s. Therefore, the data are combined over all years for which data were available. The sources of data used are the BIO database (B. Petrie, personal communication, BIO and www.mar.dfo-mpo.gc.ca/science/ocean/home.html), the Continuous Plankton Recorder Program and a study by Louanchi and Najjar (2001). For further details on the sources of data see Chapter 2.

a) Nitrate

The modeled N for two runs in 1968 and the 1990s for 1000 m winter convection is compared with the data from the BIO database between the years of 1962 and 1999 (Figure 4.7). The BIO data are averaged daily by depth and the bi-monthly mean is determined from these points. Three depth intervals are used: 0 – 10 m, 40 – 50 m and 90 – 100 m. The model cycle of N does not compare well with the N concentration in spring, summer and fall seasons in the two shallow depth levels. The N levels sink much lower in the spring and summer during the bloom than the modeled N concentrations. In the surface layer, the N levels are almost depleted similarly to the model by Trela (1996) discussed above. In the spring, summer and fall the modeled N levels are more comparable to N in the deeper layer from 90 to 100 m. It is difficult to determine the

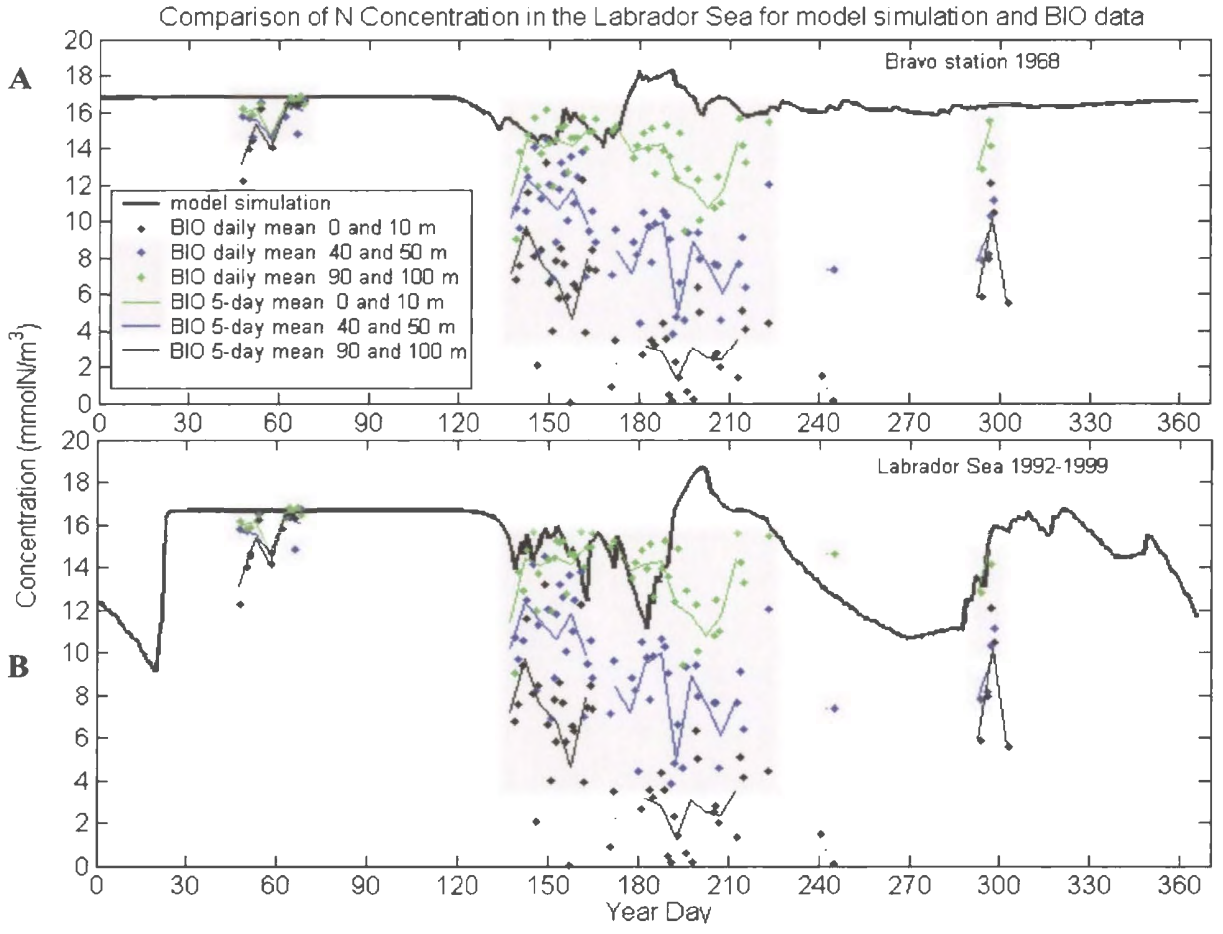

Figure 4.7: Comparison of modeled nitrate concentration (black solid thick line) and measurements from the BIO database between the years of 1962 and 1999. The BIO data are averaged daily by depth (dots) and the bi-monthly mean is determined from these points (solid thin lines). The depths are divided into 3 levels: 0 – 10 m (black); 40 – 50 m (blue); and 90 – 100 m (green). Comparison using two model runs: A) 1968; and B) the 1990s with 1000 m winter mixed-layer.

timing of the N minimum from the observations due to the high variability in the data. In the winter the modeled N seems to fit well to the measured N concentrations.

Another study by Louanchi and Najjar (2001) investigated the nutrients in the upper Atlantic Ocean in the late 1990s using data from World Ocean Atlas 1998 (Conkright *et al.*, 1994) (Figure 4.8). The units are μM N which is equivalent to mmol

N/m^3. The levels in the winter are slightly lower (~14 μmol N/l) than the modeled nitrate (~16 mmol N/m^3). In the summer the N concentration also sinks to much lower levels than the modeled nitrate, but is not totally depleted. The timing of the N minimum is at the same time as the model, but the N remains at the low level for longer, and gradually increases to the level found in deep waters.

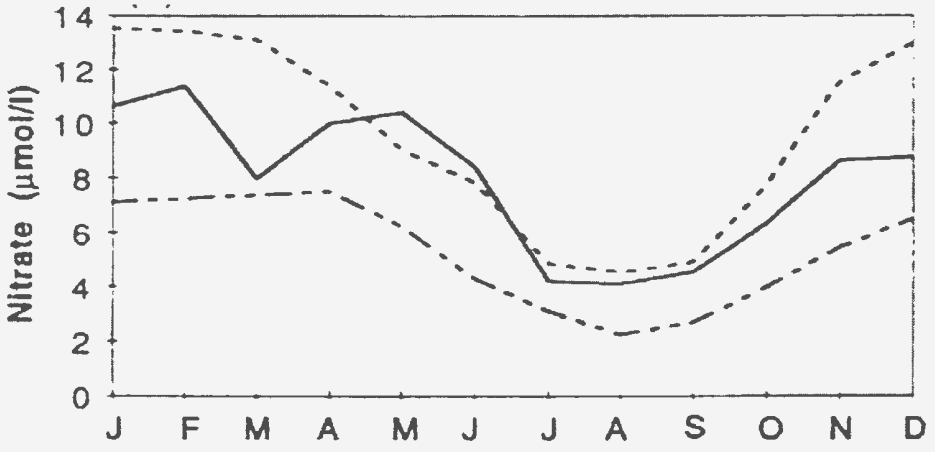

Figure 4.8: Annual cycle of nitrate averaged between 0 and 20 m in mmol N/m^3, using data obtained from the World Ocean Atlas 1998 for the Arctic (solid line), Labrador (dotted line), and sub Arctic (dash-dotted line). (Modified from Conkright *et al.*, 1994; Louanchi and Najjar, 2001).

b) Phytoplankton

The modeled phytoplankton for two runs in 1968 and the 1990s for 1000 m winter convection is compared with the data from the BIO database between the years of 1977 and 2001 (Figure 4.9). The BIO data are averaged daily by depth and the bi-monthly mean is determined from these points. The depth interval used is 0 – 10 m. The modeled annual cycle of P broadly compares with the observations. The maximum P concentration measured is just over 12 mmol N/m^3, and the daily mean maximum is 8

mmol N/m^3 which is higher than the modeled 1968 values but falls in the range of modeled values from the 1990s. The timing and start of the bloom is not clear due to the lack of data. The measured levels of P in winter and autumn are quite low and consistent with modeled results.

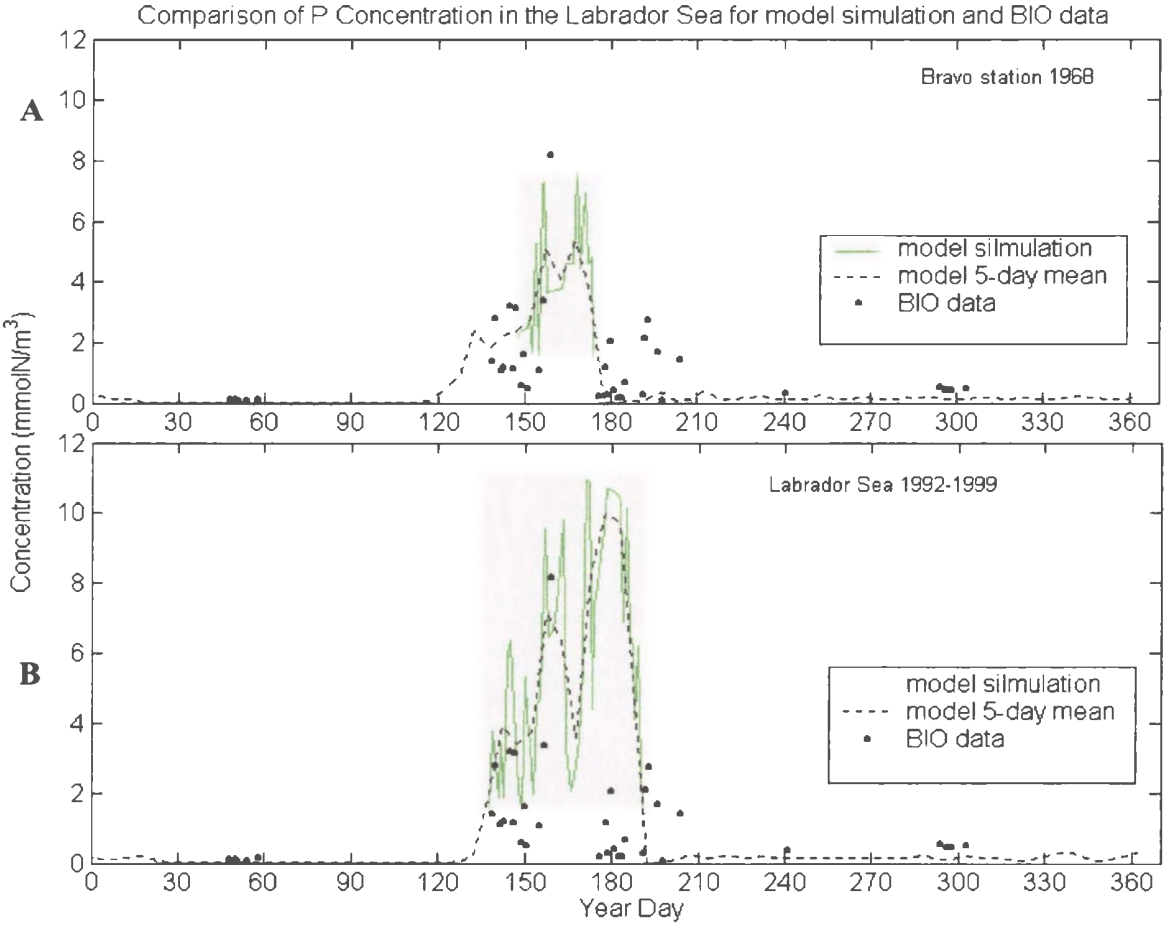

Figure 4.9: Comparison of daily (green solid line) and 5-day mean (black dotted line) of modeled phytoplankton concentration with the daily average from the BIO database for the upper 10 m between the years of 1977 and 2001, with the majority of the data collected from 1982-1984 (black dots). Units in mmol N/m^3. Comparison using two model runs: A) 1968; and B) the 1990s with 1000 m winter mixed-layer.

Other studies have reported various values for the P bloom, which are summarized in Table 2-3. The Continuous Plankton Recorder Program (CPR) (see

Section 2.1) revealed a bloom timing at the end of June (~173 day year) with a magnitude that ranged from 11-18 mg chl/m^3 (7.12-11.64 mmol N/m^3). This is consistent with the modeled data. The CPR also showed a small second peak in phytoplankton consistent with the model by Tian *et al.* (2004) and Trela (1996).

4.1.5. Comparison with Remote Sensing Data

The P annual cycle can be further verified by comparing with remote sensing satellite images. Satellite imagery has a greater number of measurements and is continuous over an annual cycle therefore allowing for greater accuracy for comparison. The modeled P for two runs in 1968 and the 1990s for 1000 m winter convection is compared with the data from the CZCS between the years of 1979 and 1983 and the SeaWiFS between the years 1998 and 2002 (see Section 2.2) (Table 4.3 and Figure 4.11).

The CZCS images from the Labrador Sea region indicate a maximum P concentration beginning in June and lasting until late August. The maximum concentration ranges from 3 to over 10 mg chl/m^3 (1.94 to > 6.47 mmol N/m^3). This corresponds roughly to the modeled P bloom timing and maximum concentration.

The SeaWiFS data are measured bi-monthly. Therefore the data and modeled daily P concentrations were averaged bi-monthly. The SeaWiFS bi-monthly means per year shows a lower maximum P concentration than the modeled P. However, when taking into account the standard deviation of the mean of the modeled P, represented by the error bars in Figure 4.10, the modeled values are within the range of the observed P peak. The SeaWiFS low P peak may be due to the fact that the SeaWiFs may miss the bloom unless it happens to occur on the day when the measurement is obtained. In 2000

for example, there are two small blooms, one too early in the season and the other in spring (Figure 4.10). The individual bi-monthly measurements reveal a much higher concentration of up to 15 mmol N/m^3 (Figure 2-12 and Figure 2-5). The timing of the bloom varies and is highly dependent on how much of the bloom the images were able to capture bi-monthly. In 1998, 1999 and 2001 there is a more distinct bloom and the timing was between days 150 and 165, which is consistent with the 1968 model runs but slightly earlier than in the 1990s. Deep convection did not occur later in the 1990s. Therefore one might expect the data to be more consistent with the 1968 period. The years 2001 and 1998 show a second small peak in P concentration in summer, similar again to the models by Trela (1996) and Tian *et al.* (2004), and to the CPR program.

Table 4.3: Summary of maximum P concentrations and timing for model simulations and SeaWiFS data.

Data Source	**Phytoplankton maximum concentration, bi-monthly mean**		**Phytoplankton maximum concentration**	
	Year Day	**Concentration** (mmol N/m^3)	**Year Day**	**Concentration** (mmol N/m^3)
Model simulation 1968	150-165	4.01	168	7.67
Model simulation 1990-1996, winter convection 1000 m	165-180	7.33	171	10.9
Model simulation 1990-1996, winter convection 1000 m	165-180	9.98	171	10.8
SeaWiFS 1998	135-150	2.42	195	13.7
SeaWiFS 1999	150-165	2.25	120	14.2
SeaWiFS 2000	165-180	1.95	120	10.1
SeaWiFS 2001	135-150	4.63	150	15.2
SeaWiFS 2002	165-180	2.50	150	12.4

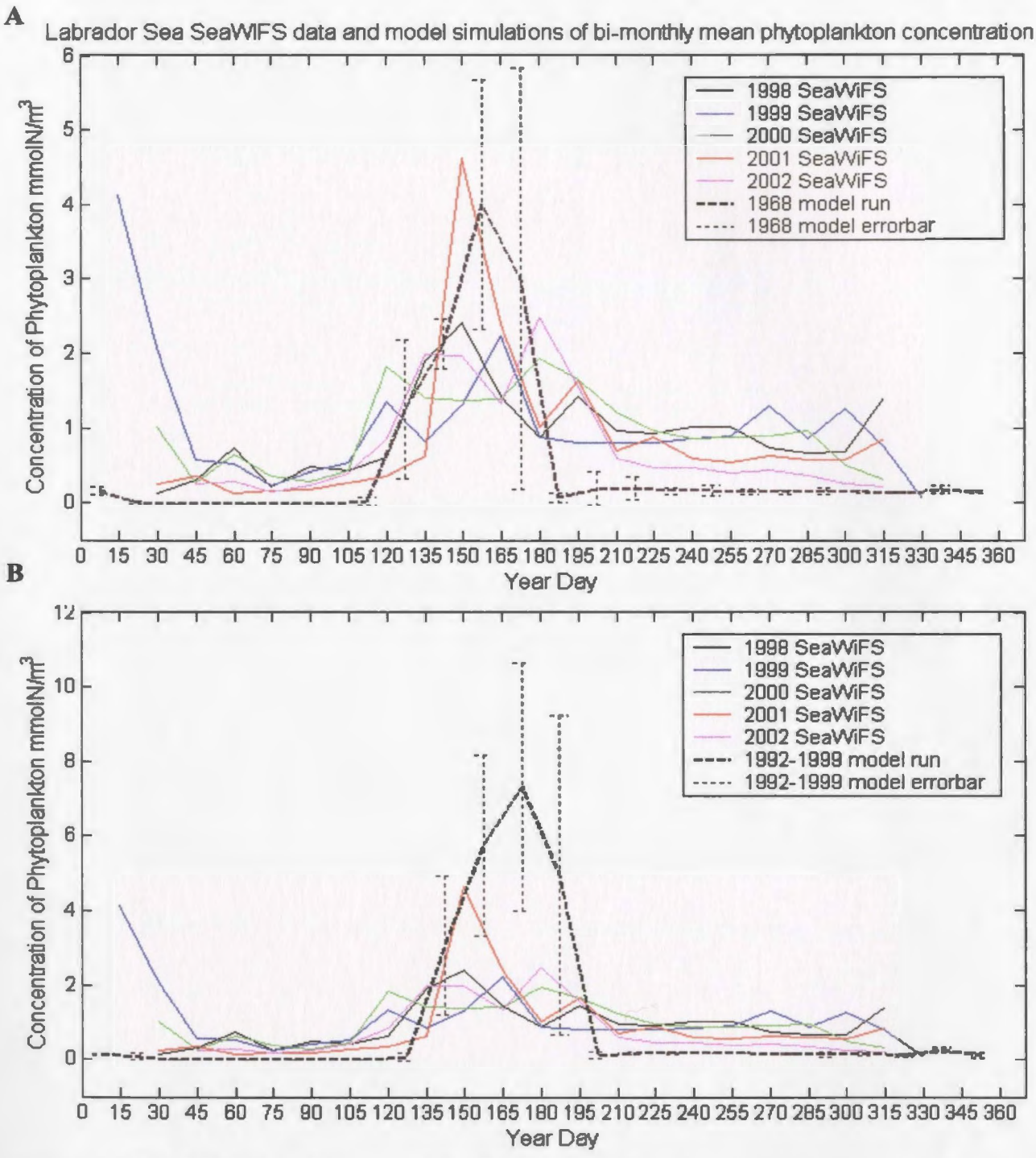

Figure 4.10: Modeled and measured SeaWiFS phytoplankton concentration over an annual cycle. Units in mmol N/m^3. SeaWiFS is measured bi-monthly and averaged bi-monthly (solid coloured lines). The modeled results are also averaged bi-monthly (dashed black lines) and error bars show the standard deviation. A) Model simulation 1968, and B) model simulation the 1990s. SeaWiFS data from B. Petrie (personal communication, BIO).

4.2. Labrador Shelf

The model for the Labrador Shelf was run during four periods, the 1960s, 1970s, 1980s and the 1990s. As described in Section 3.5.2, only 3 state variables are used for this model since detritus was removed. The model was initialized on January 1 and run for one complete year. The temperature and salinity data during each 10 year period were combined. The initial concentrations of each state variable are listed in Table 3.1 and the parameters used are provided in Table 3.2. In the following sections the results of the calculated annual mixed-layer depth and results of the model simulations are discussed and compared with observations, *in-situ* data, shipboard measurements, and remote sensing data. The results are not compared with the results of other models as was done for the Labrador Sea since no models have previously been applied to this region.

4.2.1. Annual Mixed-layer

The mixed-layer depth was calculated from measured temperature and salinity data during four periods the 1960s, 1970s, 1980s and 1990s as described in Section 3.4.2 (Figure 4.11 and 4.12). All available data for each 10 year period were combined. The annual cycle of the mixed-layer depth for the Labrador Shelf starting in January is between 186 and 137 m, deepening to a maximum in February and March (1960s and 1990s) between 160 and 170 m or shallowing to between 130 and 140 m (1970s and 1980s) and remains there until early May. After May the mixed-layer depth shallows to mid June, reaching a minimum across all periods of roughly 40 m where it remains until

late August. In early September, increasing winds deepen the mixed-layer, reinitiating the cycle. There are few studies of the annual cycle of mixed-layer depth for the Labrador Shelf. Tang and DeTracey (1998) studied the mixed-layer properties in the Newfoundland marginal ice zone during March 1992. They found that ice arrived on the Shelf between day 2 and 24 and caused the mixed-layer to shallow. In March, the mixed-layer was at 100 m defined by the depth at which the density changed by 0.002 from the surface. This is shallower than all the calculated mixed-layer depths but also the value used for the density change from the surface to calculate the mixed-layer is greater. They also found the mixed-layer to varied across the Shelf from east to west at a given time with different ice conditions.

For the 1960s the mixed-layer deepens from 137 m at the beginning of January to the maximum depth of 163 m at the end of February. The mixed-layer reaches a minimum (above 40 m) between days 190 and 230, after which it begins to deepen gradually back to 137 m by the end of the year. In comparison, the 1960s surface density data (0-10 m) for the Labrador Shelf shows a minimum at day 225 and is uniform throughout the water column between days 70 and 105 corresponding with the deep mixed-layer depth.

For the 1970s, in contrast to the 1960s, the mixed-layer shallows from 186 m at the beginning of January to 130 m by the end of February. The mixed-layer remains between 130 and 120 m until just over day 120 when it begins to rapidly shallow. It reaches a minimum (above 40 m) between days 180 and 253 after which it begins to deepen gradually back to 186 m by the end of the year. In comparison the 1970s surface

density data (0-10 m) for the Labrador Shelf shows a minimum just at about day 210 and the winter data are sparse, making it difficult to determine when there is a small density gradient in winter.

The 1980s annual mixed-layer cycle is very similar to the 1970s. The mixed-layer shallows from 182 m in the beginning of January to 140 m by mid January. The mixed-layer remains between 134 and 140 m until, as in the 1970s, post day 120 when it begins to rapidly shallow. It reaches a minimum (above 40 m) between days 187 and 222 after which it deepens gradually back to 182 m by the end of the year. In comparison the 1980s surface density data (0-10 m) (Figure 2.21) shows a minimum between days 210 and 225; the winter data are sparse as for the 1970s.

The 1990s annual mixed-layer cycle follows a similar pattern to the 1960s. The mixed-layer deepens from 150 m in the beginning of January, reaching a maximum depth of almost 170 m by mid February, the deepest mixed-layer depth relative to the other periods. The mixed-layer remains below 140 m until day 120 when the mixed-layer begins to shallow. At approximately day 170 it reaches a minimum (above 40 m) and remains shallow until day 260, after which it begins to deepen gradually back to 150 m by the end of the year. In comparison the 1990s surface density data (0-10 m) (Figure 2.21) has a minimum at between days 240 and 255, which is later than the other years and is uniform throughout the water column starting about day 70 (after the data are sparse) corresponding with the deep mixed-layer depth.

The major differences in mixed-layer depths between the years investigated summarized by season are; in winter the 1990s mixed-layer deepenes in the beginning of

the year to the deepest depth of 170 m. The 1960s also deepens in the beginning of the year but to a shallower depth of 162 m. The 1970s and 1980s mixed-layer shallows in January reaching a plateau at around 140 and 130 m. In spring all years shows a rapid shallowing of the mixed-layer but the timing is slightly later in the 1980s and 1990s. In summer all periods reach a similar minimum depth but the timing and duration of the minimum depth varies. The 1990s mixed-layer reaches a minimum (above 40 m) the earliest followed by the 1970s and 1980s, which are very similar, and the latest is the 1960s. However, the 1960s mixed-layer reaches a plateau just below 40 m before day 165, earlier than any other years. In comparison the daily surface (0-10 m) density mean data has a similar pattern, the earliest density minimum is in the 1960s, becoming increasingly later towards the 1990s and the minimum value is similar for all periods, approximately 23 σ_t. In autumn, the 1980s mixed-layer deepens earliest, followed by the 1960s and 1970s. The latest deepening occurs in the 1990s.

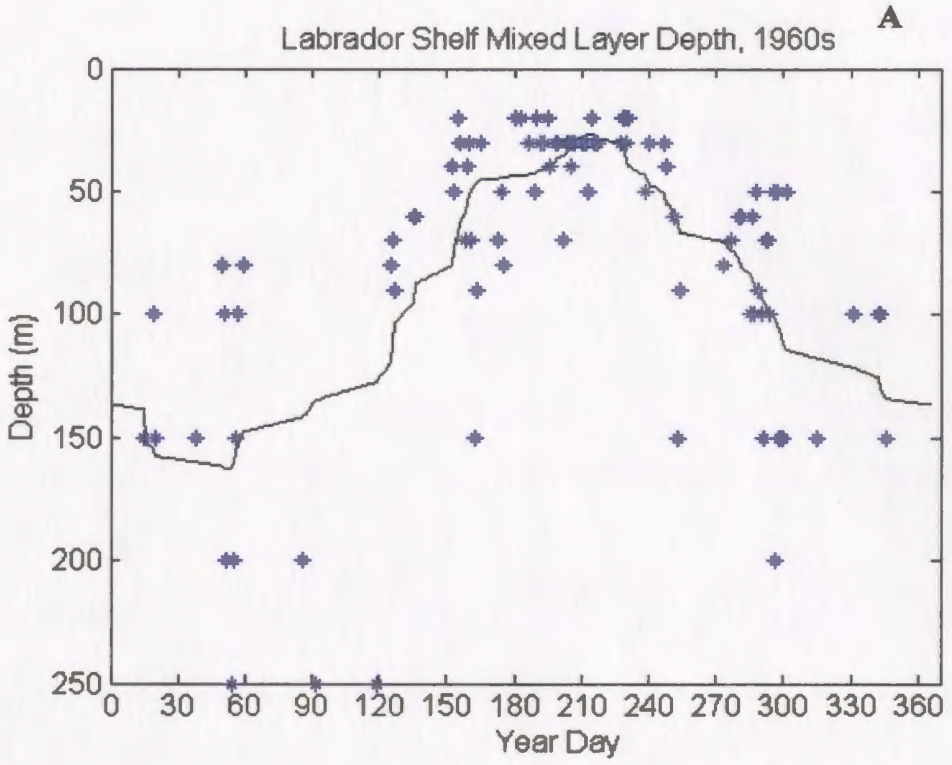
A
Labrador Shelf Mixed Layer Depth, 1960s
Depth (m)
0
50
100
150
200
250
0 30 60 90 120 150 180 210 240 270 300 330 360
Year Day

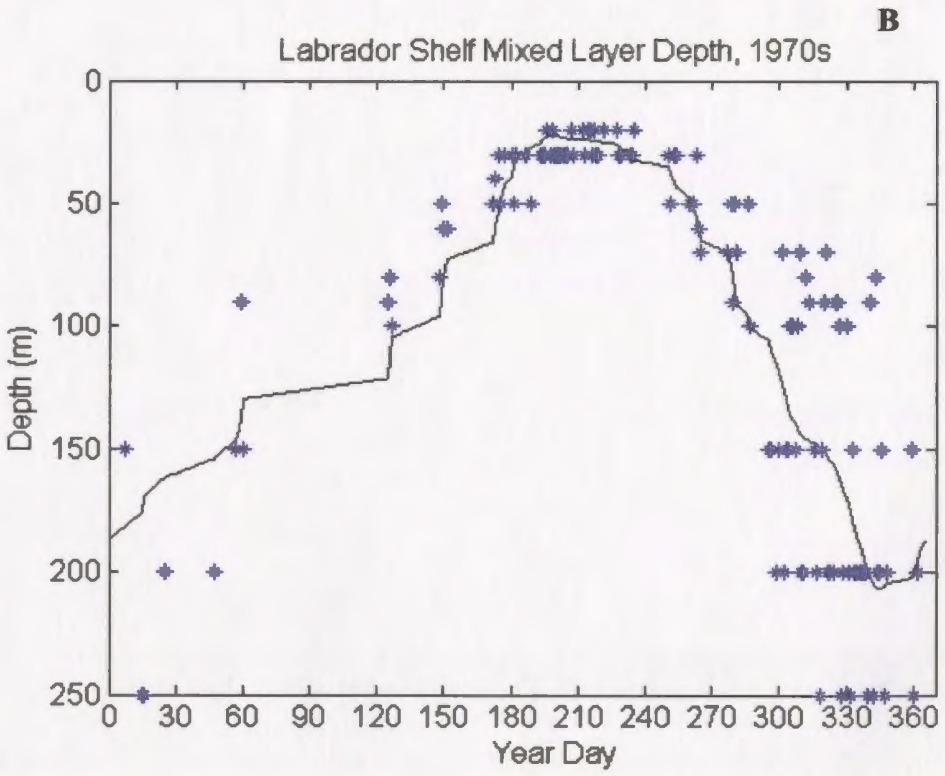
B
Labrador Shelf Mixed Layer Depth, 1970s
Depth (m)
0
50
100
150
200
250
0 30 60 90 120 150 180 210 240 270 300 330 360
Year Day

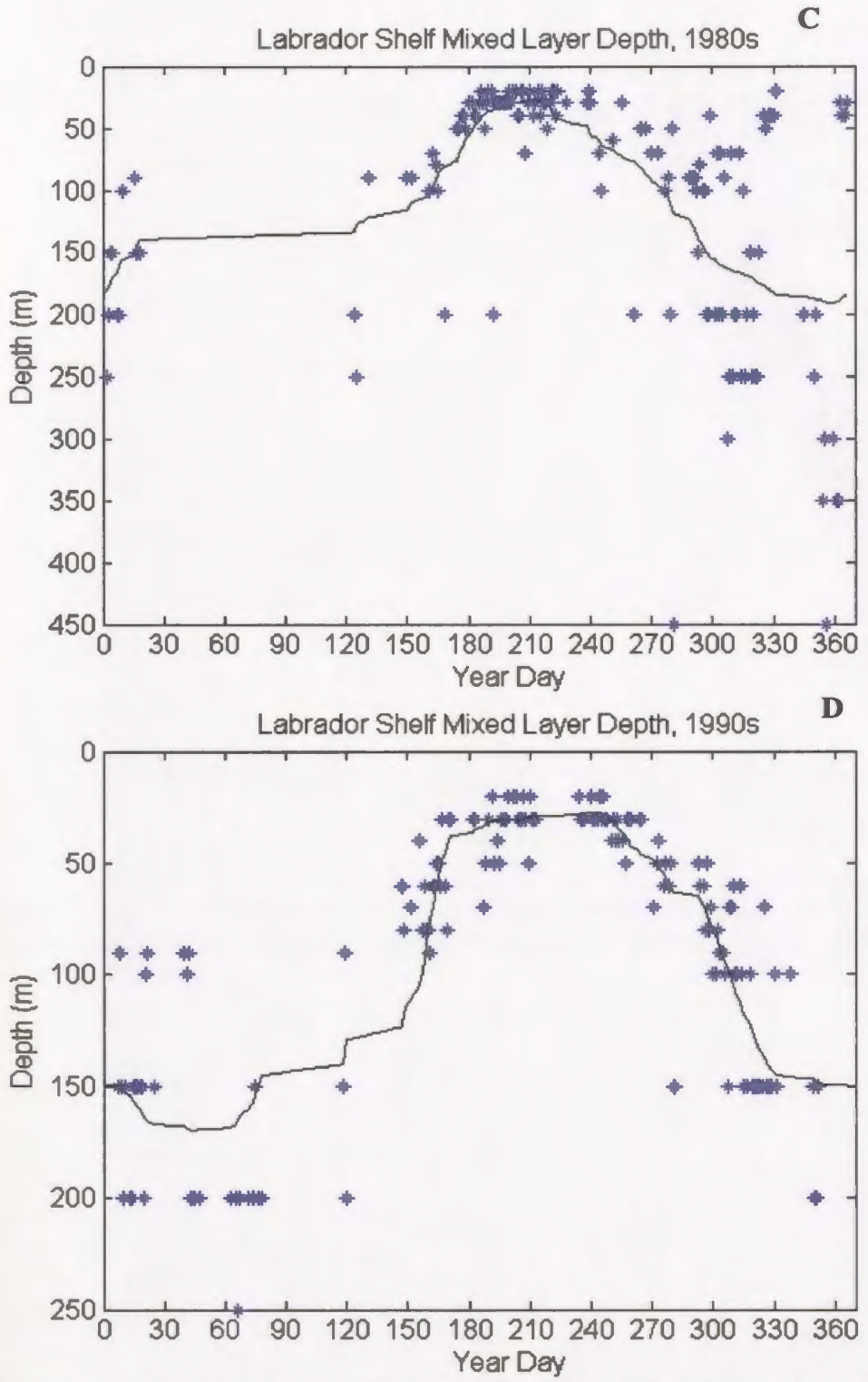

Figure 4.11: The mixed-layer depth for the Labrador Shelf calculated from measured temperature and salinity data. (A) 1960s; (B) 1970s; (C) 1980s; and (D) 1990s. The line is the linear interpolated mixed-layer depth, the blue dots indicate the days in which data are available to calculate the mixed-layer depth.

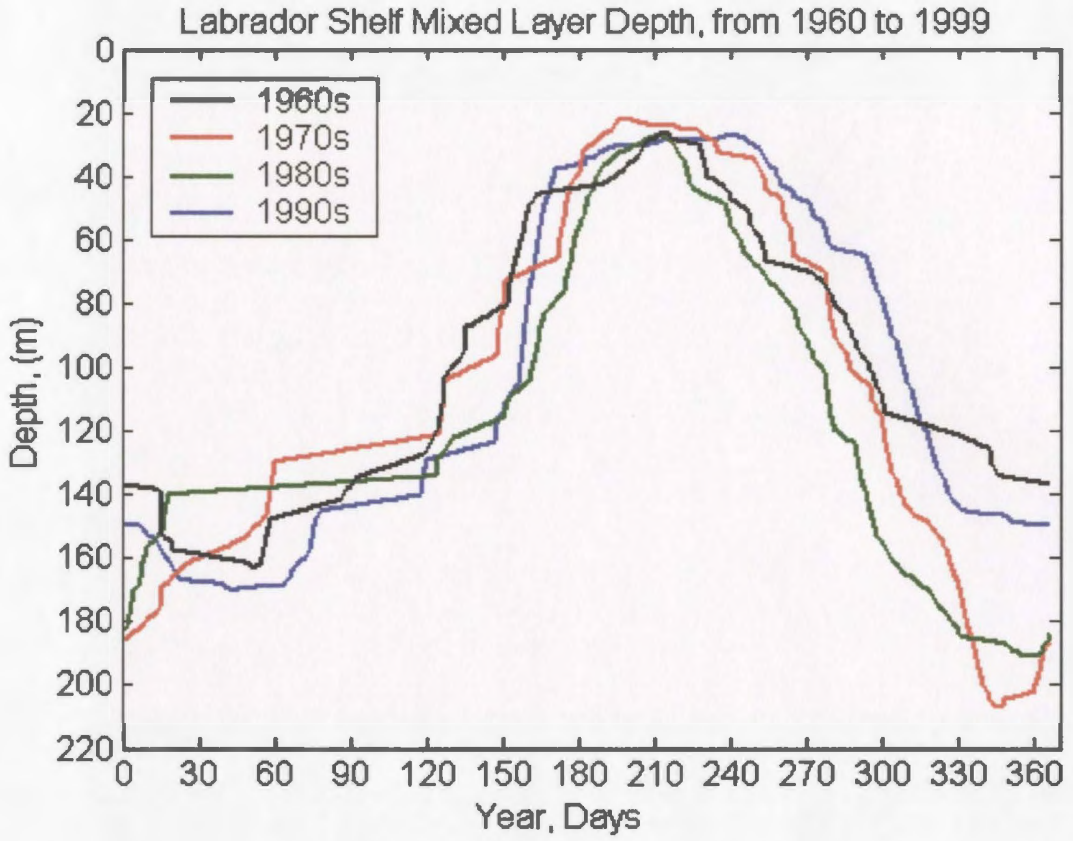

Figure 4.12: The mixed-layer depths for the Labrador Shelf calculated from measured density, temperature and salinity data during the 1960s (black), 1970s (red), 1980s (green) and 1990s (blue).

4.2.2. Annual Cycles of Biological Variables

All the biological variables, N, P, and Z on the Labrador Shelf, have the same annual cycle with one difference compared to the Labrador Sea. There is a pronounced spring bloom in P and Z and a depletion of N concentration in the surface layer in the summer but there is also a second bloom in P and Z between August and October that is not seen in the Labrador Sea (Figure 4.13 and Table 4.4).

Starting in January the concentration of N is high for all years and reaches levels found in the deep waters of the Shelf, around 11 mmol/m^3. This is the same time as the deepest mixed-layer, supplying the upper layer with nutrients and maintaining the high level of nutrients since the primary production is light limited and remains at a minimum. The concentration of N gradually decreases throughout the winter from the maximum. In the spring, the mixed-layer begins to shallow in April and the irradiance increases in the surface layer, the photosynthetic available radiation (PAR) increases, and the high concentration of N becomes trapped in the mixed-layer causing a P bloom.

The initiation of the P bloom is difficult to determine since the P gradually increases starting in winter and in some cases increases in steps. Therefore unlike the Labrador Sea, only the magnitude of the P bloom is discussed and not the timing. In the 1960s, the first P peak concentration is relatively high between 2.01 and 2.32 mmol N/m^3, the 1970s and 1980s has a lower peak between 1.71 and 1.98 mmol N/m^3, and the 1990s has the greater peak concentration at 2.58 mmol N/m^3 (Figure 4.14 b). In terms of mixed-layer depths, the 1990s has the greatest mixed-layer depth in winter and the 1960s, though there is not such a deep mixed-layer in winter, there is the earliest shallowing of

the mixed-layer which remained shallow for the longest duration. The second P peak is lower than the first peak except for the 1980s. The 1960s and 1980s has the highest second peak at 2.03 mmol N/m^3, where as the 1970s and 1990s peak is lower between 1.66 and 1.77 mmol N/m^3. Between the 1960s, 1970s and 1980s there is very little difference between the first P bloom timing, which occurs between days 127 and 156. This timing is consistent with the results of Pavshtiks (1968) who found the spring bloom to occur from days 120 to 150. The 1990s first peak timing is later, on day 165. The second peak timing is also latest in the 1990s (day 271) followed by the 1960s (242-246 days), and the earliest timing is during the 1970s and 1980s (232-239 days). Comparing to the mixed-layer in the 1990s, the mixed-layer in the fall shallows the latest.

The increased P concentration causes a reduction in the N concentration and a minimum N concentration occurs during the P bloom. Nutrients are nearly depleted, reducing to less than 0.001 mmol N/m^3 from deep-water concentrations for all years. Following the P bloom timing, the N minimum also occurs at about the same time for the 1960s to 1980s and occurs later in the 1990s (Figure 4.14 a). The N concentration at the end of the year does not return to the value observed in the deep-water and instead returns to a lower value between 4 and 7 mmol N/m^3. This pattern may be due to the removal of detritus from the model, resulting in no remineralized detritus to be added to the nutrient pool.

The P bloom period also causes an increase in Z biomass, creating a peak in concentration of Z as the peak P concentration declines. The timing of the first Z bloom is between day 157 in the 1970s and day 171 in the 1990s (Figure 4.14 c). The

magnitude of the first Z bloom increases from 0.40 in the 1980s to 1.27 in the 1990s. In the 1990s, there was only one Z bloom, which may be the reason it is the largest and latest bloom. The second Z peak timing decreases from days 261 to 243 from the 1960s to 1980s, with little variation in the magnitude.

The yearly biomass is calculated as for the Labrador Sea, and the results are shown in Table 4.5. The N increases slightly from the 1960s to 1970s by approximately 160 mmol N/m^3yr to 1689 mmol N/m^3yr and from there decreases in the 1990s to 1569 mmol N/m^3yr. The P decreases from the 1960s to 1980s by approximately 20 mmol N/m^3yr to 249 mmol N/m^3yr and increases in the 1990s to 266 mmol N/m^3yr. In contrast the Z biomass decreases from the 1960s to 1990s from 19.75 mmol N/m^3yr to 16.79 mmol N/m^3yr.

Overall in the 1990s, the first P maximum concentration is higher and occurs approximately 10 to 30 days later than during other periods while the N minimum concentration occurs at about the same time but lasts 14 to 28 days later than other periods. Since the N remains low later than other years, the second P peak in the 1990s was 6 to 14 days later and relatively low. The first Z maximum concentration is also higher and occurs later in the 1990s by about 4 to 14 days. There is no second peak of Z in the 1990s. The P biomass is lowest in the 1970s and 1980s, while the N biomass is highest. By contrast, the Z biomass on the other hand is lowest in the 1990s and highest in the 1960s.

Figure 4.13: Modeled daily concentration of N (black), P (green), and Z (blue) in mmol N/m^3 over one year for four model simulations: (A) 1960s; (B) 1970s; (C) 1980s; and (D) 1990s.

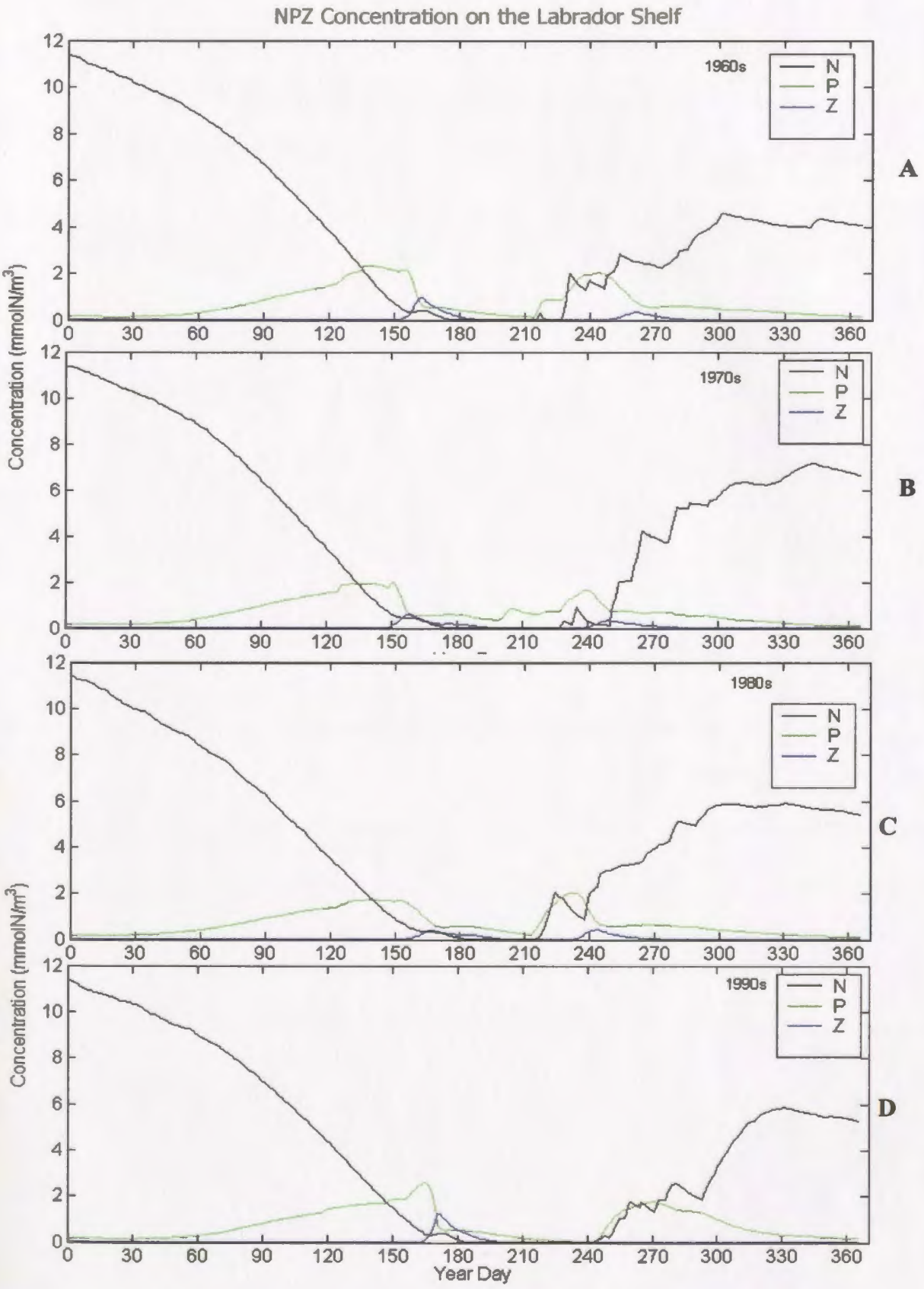
NPZ Concentration on the Labrador Shelf
1960s
1970s
1980s
1990s
N
P
Z
A
B
C
D
Concentration (mmolN/m3)
Year Day

Figure 4.14: Comparison of modeled nitrate, phytoplankton and zooplankton for four model runs during the 1960s (black solid line), 1970s (blue solid line), 1980s (red dotted line) and 1990s (green dotted line). A) Nitrate, B) phytoplankton, and C) zooplankton in mmol N/m^3

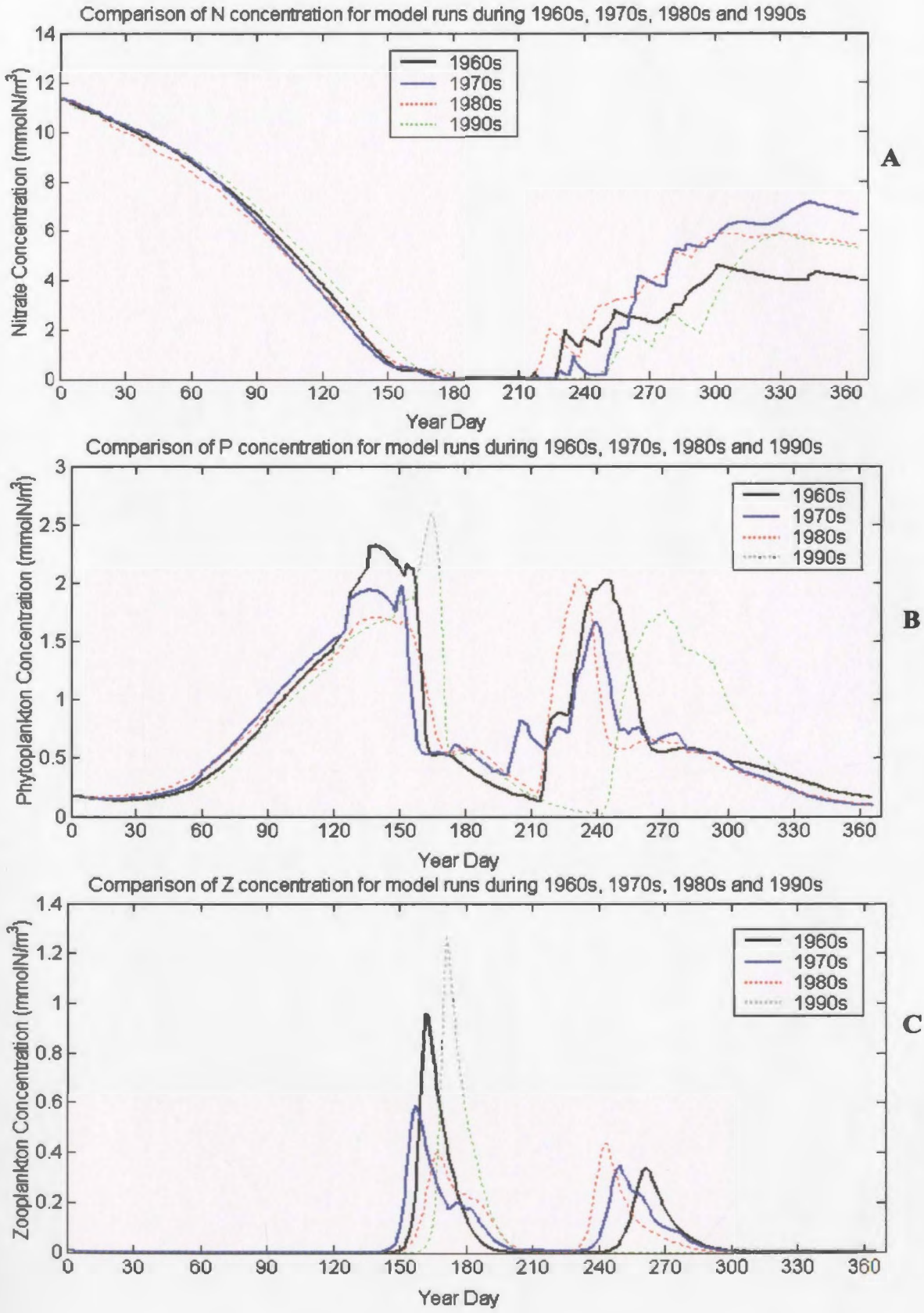
Comparison of N concentration for model runs during 1960s, 1970s, 1980s and 1990s
Nitrate Concentration (mmolN/m3)
Year Day
1960s
1970s
1980s
1990s
A
Comparison of P concentration for model runs during 1960s, 1970s, 1980s and 1990s
Phytoplankton Concentration (mmolN/m3)
Year Day
1960s
1970s
1980s
1990s
B
Comparison of Z concentration for model runs during 1960s, 1970s, 1980s and 1990s
Zooplankton Concentration (mmolN/m3)
Year Day
1960s
1970s
1980s
1990s
C

Table 4.4: Summary of minimum N concentration, maximum P, and Z concentrations, timing of the maximum, and start time of P and Z bloom for model simulations.

Peak concentrations and bloom initiation	Model simulation 1960s		Model simulation 1970s		Model simulation 1980s		Model simulation 1990s	
	Year Day	Concentration (mmol N/m^3)	Year Day	Concentration (mmol N/m^3)	Year Day	Concentration (mmol N/m^3)	Year Day	Concentration (mmol N/m^3)
N minimum during bloom	189-214	>0.001	196-227	>0.001	201-213	>0.001	201-241	>0.001
P maximum	131-156	2.01-2.32	127-152	1.75-1.98	129-155	1.69-1.71	165	2.58
	242-246	2.00-2.03	239	1.66	232	2.03	271	1.76
Start of Z bloom (when Z reaches 0.1 mmol N/m^3)	156	0.160	151	0.152	159	0.117	165	0.118
	253	0.109	242	0.112	236	0.130		
Z maximum	162	0.958	157	0.587	167	0.401	171	1.27
	261	0.337	250	0.349	243	0.435		

Table 4.5: Total yearly biomass of N, P and Z for model simulations.

State Variable	Total yearly biomass (mmol N/m^{3}yr)			
	1960s	1970s	1980s	1990s
N	1531	1698	1688	1569
P	268.7	250.7	249.1	266.1
Z	19.75	19.69	17.63	16.79

4.2.3. Primary Production Rate

The primary production rate was determined for each period using the differential P equation (Section 3.2.1), however all the loss terms in the equation were neglected. The daily primary production increases gradually to a peak at about day 200 and gradually decreases again (Figure 4.15). The daily maximum is lowest in the 1960s at about 1.6 gC/m^2 day and highest in the 1970s at about 2.3 gC/m^2 day. The yearly primary production varies little (less than 10 %) between the periods investigated (Figure 4.16). The greatest value is in the 1970s at 212.4 gC/m^2 yr and the lowest is in the 1990s at 199.3 gC/m^2 yr. The reported values of productivity in the region are: in the mid Atlantic, 306 ± 4 gC/m^2 yr; at a latitude of 55°N in the North Atlantic, approximately 190 gC/m^2 yr; and in the Northwest Atlantic continental Shelf, 540 gC/m^2 yr, which is higher than the values calculated for the Shelf (Longhurst *et al.*, 1995; Harrison and Parsons, 2000). Primary production rate can be compared to sustainable fish catch and based on the published correlation (Harrison and Parsons, 2000), 200 gC/m^2 yr corresponds to a sustainable fish production of roughly 3.6 to 4.7 t /km^2 yr (Figure 4.17). The actual total fish catch from NAFO area 2J (www.nafo.ca/activities/FRAMES/AcFrFish.html) was combined with the total crab catch in 2J from 1989 to 2003 (DFO, 2003) and compared to the yearly primary production (Figure 4.18). The fish catch, which includes ground fish and shrimp, was averaged over 10 year periods starting from 1960 until 1999. The average total fish catch in the 1990s is 3.8 tons/km^2yr, which is in the range of the correlation from Harrison and Parsons (2000) for the primary productivity value of 200 gC/m^2 yr in the 1990s. The fish catch for the remainder of the periods are quite high

compared to the primary production, which has little change, and do not fit the correlation from Harrison and Parsons (2000). The fish catch and primary productivity is lowest in the 1990s and both gradually increase to 20 tons/m^2yr and 212 gC/m^2 yr respectively in the 1970s. In the 1960s the fish catch reaches a maximum of 35 tons/m^2yr, and the primary productivity is slightly lower than the value in the 1970s at 207.4 gC/m^2 yr. Fish catches in the 1960s, 1970s and 1980s were clearly not sustainable.

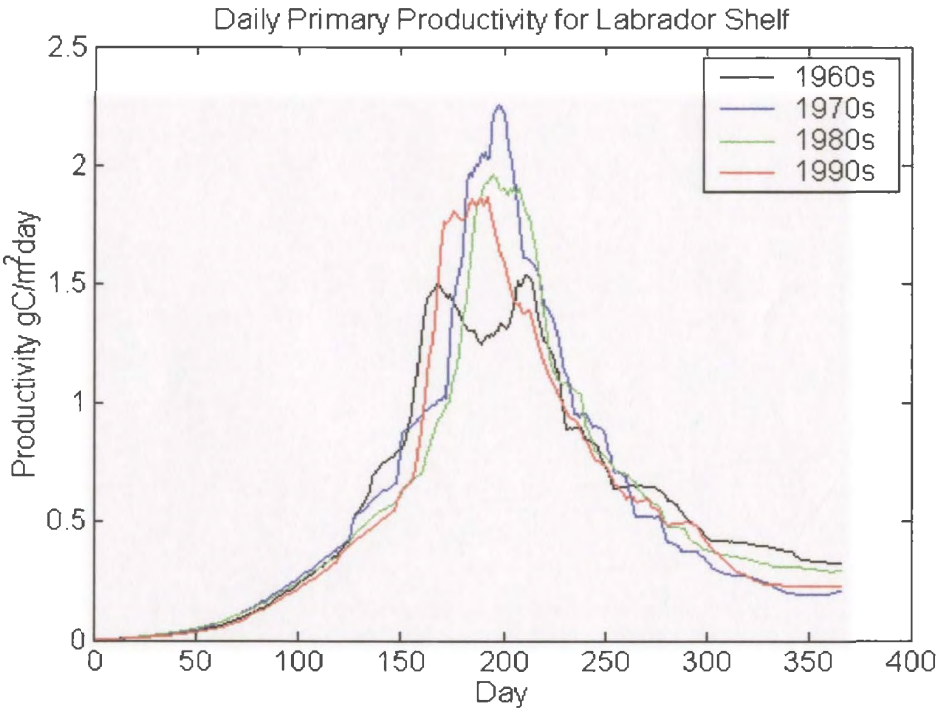

Figure 4.15: Daily primary productivity in mgC/m^2 day for the each period the model was run, 1960s (black), 1970s (blue), 1980s (green), and 1990s (red).

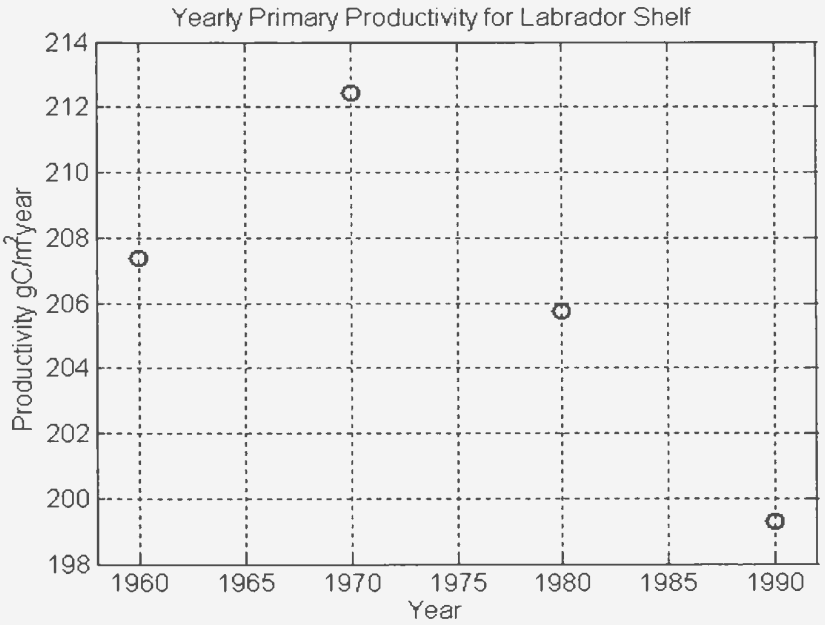

Figure 4.16: Yearly primary productivity in gC/m^2 year for each 10-year period the model was run from 1960 to 1999. The yearly primary production varies less than 10 %.

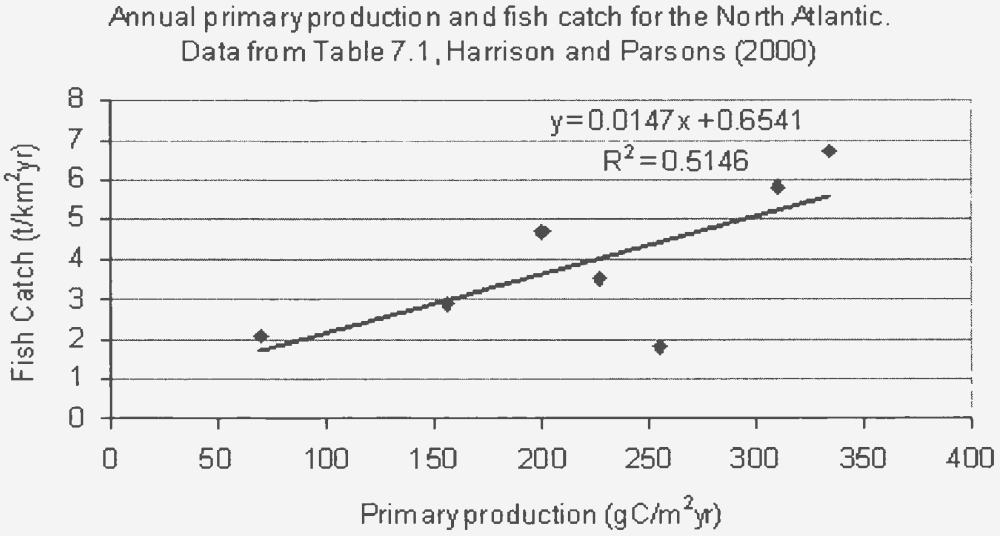

Figure 4.17: Correlation between annual primary production and sustainable fish catch in the North Atlantic. Data are taken from Table 7.1 of Harrison and Parsons (2000).

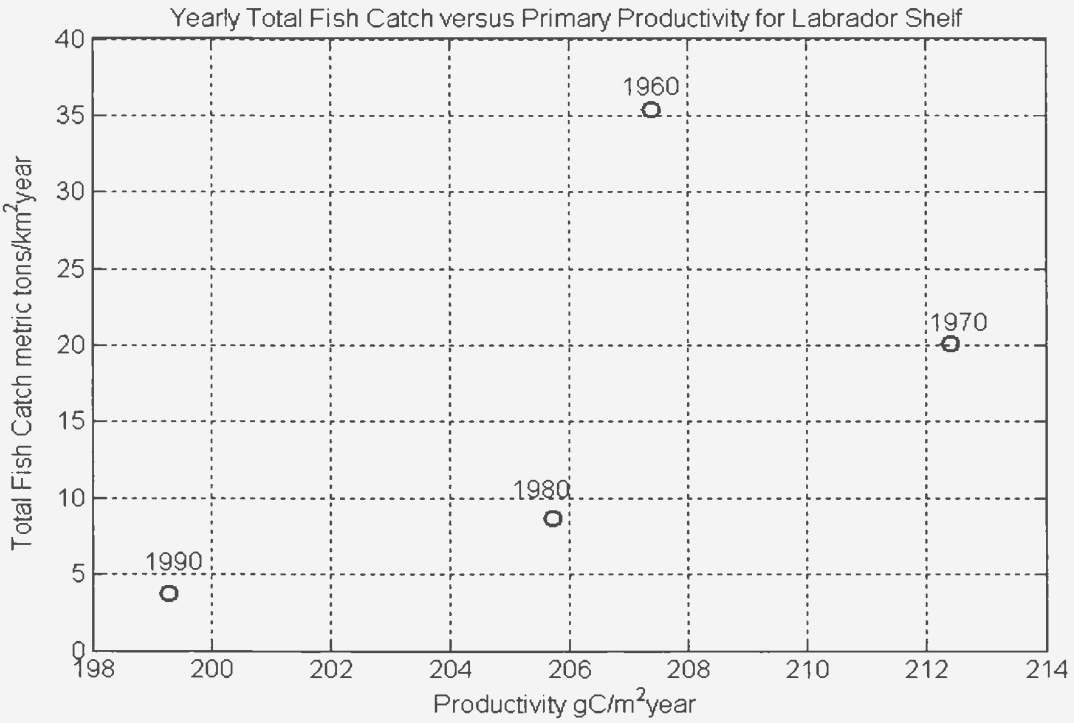

Figure 4.18: Yearly primary productivity in gC/m^2 year versus total fish catch in $tons/km^2yr$ in NAFO region 2J averaged over 10 year periods for the period the model was run 1960 to 1999.

4.2.4. Comparison with Observations, *In-situ* Data and Shipboard Measurements

Nutrients and phytoplankton in the mixed-layer are selected for comparison with observations. For the Labrador Sea, data are sparse for the specific periods investigated. Therefore, the N and chlorophyll data are combined over all years for which data were available. The sources of data used are the BIO database (B. Petrie, personal communication, BIO and www.mar.dfo-mpo.gc.ca/science/ocean/home.html), the Continuous Plankton Recorder Program and the study by Drinkwater and Harding (2001). See Chapter 2 for further details on the sources of data.

a) Nitrate

The modeled N for all four runs are compared with the data from the BIO database between the years of 1962 and 1999 (Figure 4.19). The BIO data are averaged daily by depth over three depth intervals: 0 – 10 m, 40 – 50 m and 90 – 100 m. The modeled cycle of N compares reasonably well with the observed surface N concentration in the winter, spring, and summer. In the fall, the 1960s and 1990s modeled N concentration is lower than observed values. In winter, there are few data, however, for the data that do exist in February and March, the modeled N level is within the range of measured values from the surface to 100 m depths. In the spring and summer there is more data available and this data indicates that the surface N sinks to very low levels, which is consistent with the modeled N. The deeper layer of water shows a higher N concentration in spring and summer than the surface concentrations. The approximate timing of the N minimum at the surface from the observations is between days 130 and 215, which begins earlier than any model run. The modeled N minimum is within this range except for the 1990s, during which the N minimum remains until day 240.

Drinkwater and Harding (2001) investigated the biology on the Shelf and found that from 0-50 m, below 55°N on the Shelf, the average nitrate concentration varied from 2 to 4 mmol N/m^3 which is within modeled values. Also, for a transect across the Hamilton Bank they found the nitrate concentration to vary from 1 mmol N/m^3 at the surface to around 10 mmol N/m^3 at 100 m depth.

Figure 4.19: Comparison of modeled nitrate concentration (solid black line) and measurements from the BIO database between 1962 and 1999. The BIO data are averaged daily by depth (dots) and the bi-monthly mean is determined from these points (solid thin lines). The depths are divided into 3 levels: 0 – 10 m (black); 40 – 50 m (blue); and 90 – 100 m (green). Comparison with four model runs: (A) 1960s; (B) 1970s; (C) 1980s; and (D) 1990s.

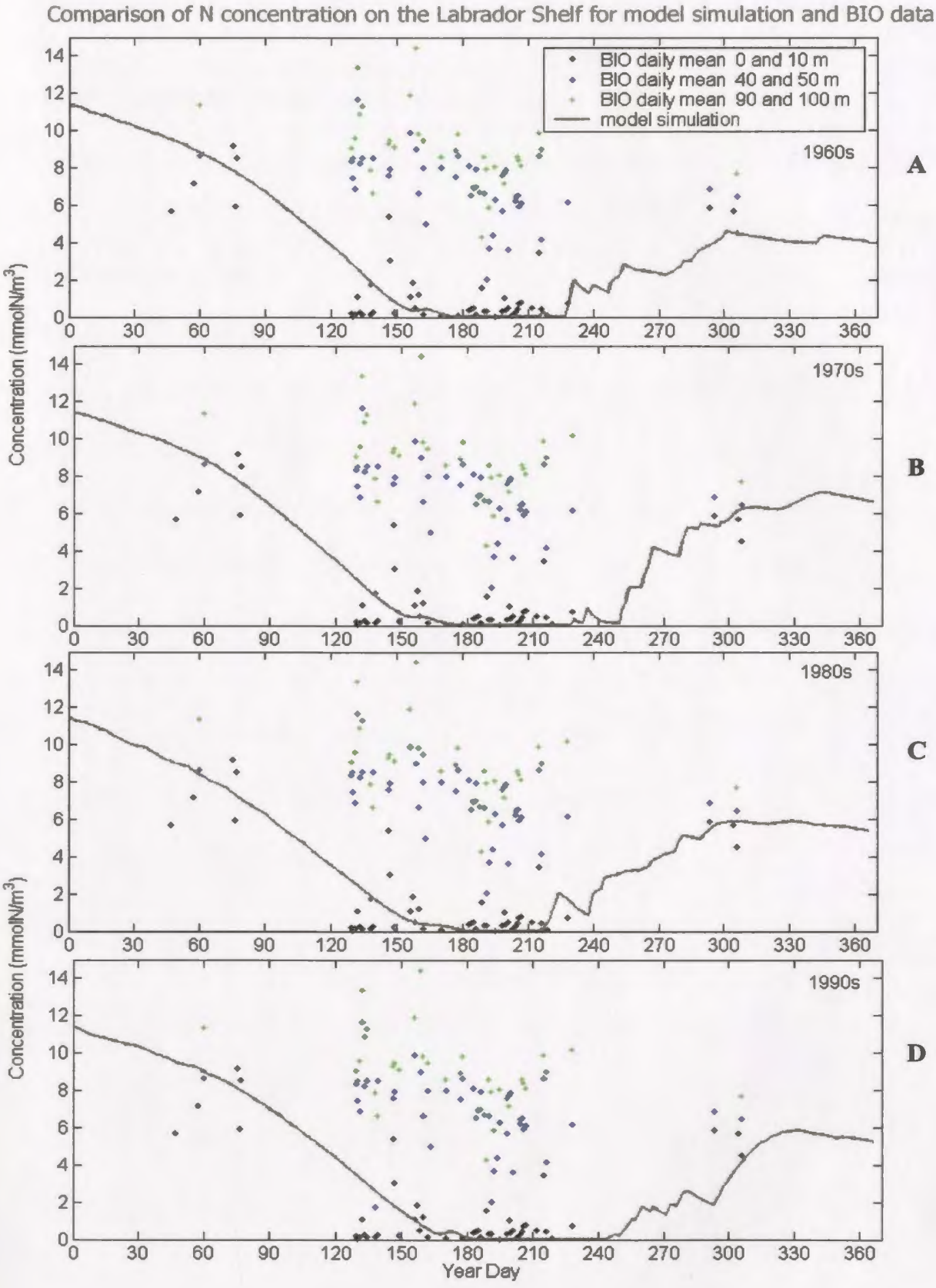
Comparison of N concentration on the Labrador Shelf for model simulation and BIO data
BIO daily mean 0 and 10 m
BIO daily mean 40 and 50 m
BIO daily mean 90 and 100 m
model simulation
1960s
1970s
1980s
1990s
A
B
C
D
Concentration (mmolN/m3)
Year Day

b) Phytoplankton

The modeled P for all four runs is compared with data from the BIO database for the years 1977 and 2001 (Figure 4.20). The BIO data are averaged daily by depth over two depth intervals: 0 – 10 m, and 0 – 30 m. The maximum P concentration measured is over 12 mmol N/m^3 and the daily mean maximum is about 11 mmol N/m^3 that is higher than the modeled P. The timing and start of the bloom is not clear due to the lack of data, but the highest concentrations were measured in May, which is during the first P peak of the modeled simulations. In winter and autumn the measured levels of P are quite low, which is consistent with modeled results.

Other studies have reported various magnitudes for the P bloom (Table 2-3). Drinkwater and Harding (2001), in September 1985, found from 0-50 m, below 55°N on the Shelf, the average P concentration was 1 mmol N/m^3 or lower, which is consistent with modeled values except in the 1990s, which has a higher modeled value. The CPR (see Section 2.1) revealed a similar seasonal cycle as the model, with two blooms. The first bloom occurred at the beginning of June (~ day 160) and the second larger bloom occurred at the end of September (~ day 270). This is consistent with the modeled 1990s P concentration. From the 1960s to 1980s the modeled second P peak occurred around day 240, which was earlier than the CPR data.

Figure 4.20: Comparison of modeled daily phytoplankton concentration (black solid line) with the daily average from the BIO database for the upper 10 m (black dots) and upper 30 m (blue dots) between the years of 1977 and 2001, with the majority of the data collected from 1982-1984. Units in mmol N/m^3. Comparison with four model runs: (A) 1960s; (B) 1970s; (C) 1980s; and (D) 1990s.

Comparison of P concentration on the Labrador Shelf for model simulation and BIO data

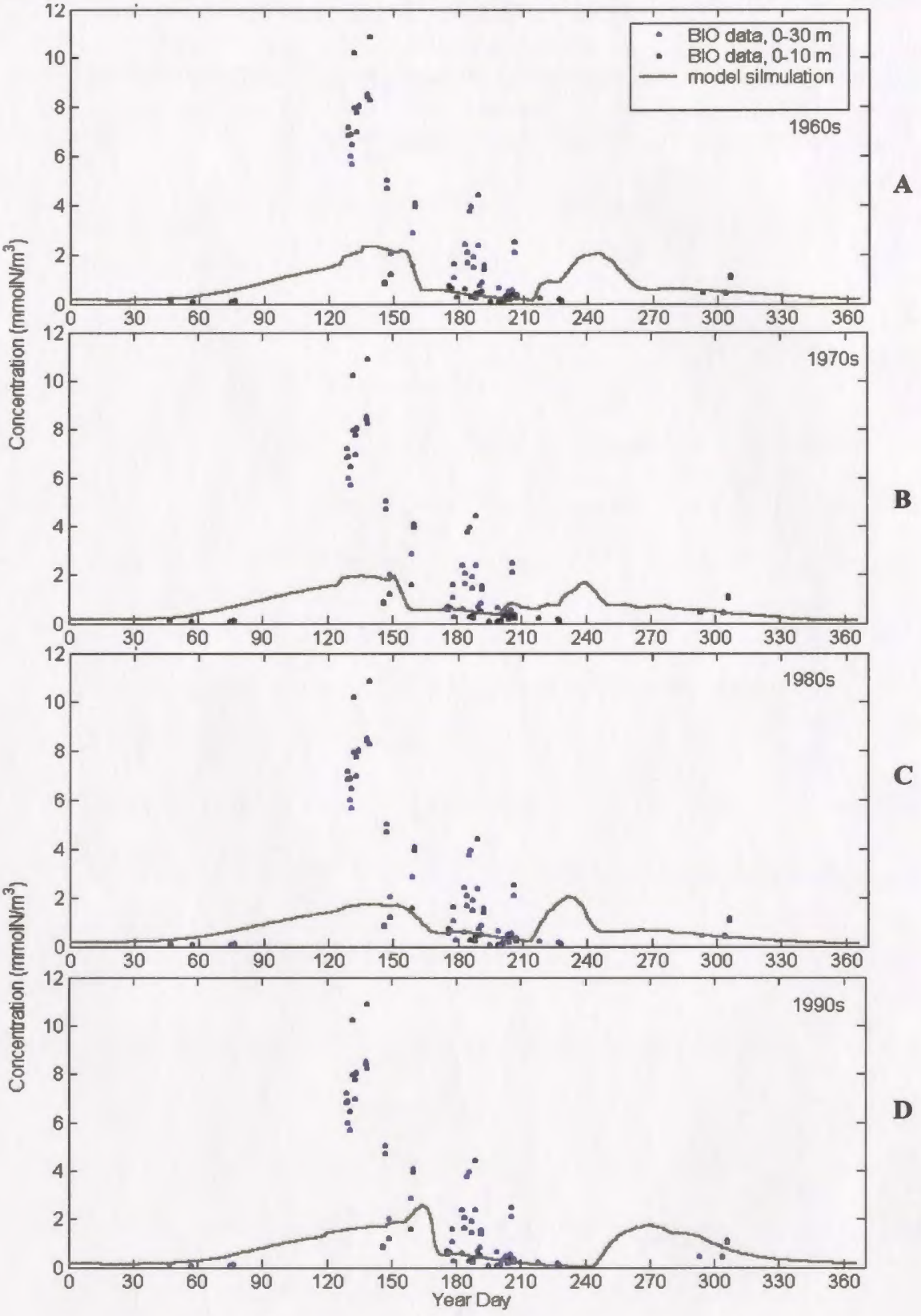

4.2.5. Comparison with Remote Sensing Data

The model of the P annual cycle can be further verified by comparing with remote sensing satellite images. Much more satellite data are available for this region than *in-situ* measurements, allowing description of the annual cycle. The modeled P for all four runs is compared with the data from the CZCS for the years of 1979 to1983 and the SeaWiFS for the years 1998 to 2002 (see Section 2.2) (Table 4.6 and Figure 4.21).

The CZCS images from the Labrador Shelf region indicate a maximum P concentration beginning in June and lasting until late August. The maximum concentration ranges from 3 to over 10 mg chl/m^3 (1.94 to over 6.47 mmol N/m^3). This roughly corresponds to the modeled P bloom timing, but the modeled P maximum concentrations were lower in some cases.

The SeaWiFS data and modeled daily P concentrations were averaged bi-monthly. The SeaWiFS bi-monthly means per year shows a similar maximum P concentration to the modeled P between 1.2 and 1.9 mmol N/m^3. The individual bi-monthly measurements reveal a much higher concentration up to 10 mmol N/m^3 during the bloom as shown in Figure 4.21 by the gray dots. The estimate of the bloom timing from satellite images varied and was highly dependent on how much of the bloom the images were able to capture bi-monthly, the bloom peak ranged from about day 150 to day 195. This is slightly later timing than for the modeled concentration from the 1960s to 1980s. The modeled 1990s first bloom concentration does match reasonably well with the SeaWiFS bloom during 1998 and 1999 when measurements coincided. The SeaWiFS averaged data did not show a second larger P bloom in autumn as the CPR data did. But

the SeaWiFS original data, not averaged, did show a slight increase in P concentration in October.

Table 4.6: Summary of maximum P concentrations and timing for model simulations and SeaWiFS data.

Data Source	**Phytoplankton maximum concentration, bi-monthly mean**		**Phytoplankton maximum concentration**	
	Year Day	**Concentration** (mmol N/m^3)	**Year Day**	**Concentration** (mmol N/m^3)
Model simulation 1960s	135-150	2.26	131-156	2.01-2.32
	240-255	1.81	242-246	2.00-2.03
Model simulation 1970s	135-150	1.89	127-152	1.75-1.98
	225-240	1.26	239	1.66
Model simulation 1980s	135-150	1.69	129-155	1.69-1.71
	225-240	1.81	232	2.03
Model simulation 1990s	150-165	2.13	165	2.58
	255-270	1.59	271	1.77
SeaWiFS 1998	150-165	1.89	135	~9
SeaWiFS 1999	150-165	1.70	165	~5
SeaWiFS 2000	165-180	1.84	180	~14
SeaWiFS 2001	165-180	1.33	180	~7.5
SeaWiFS 2002	180-195	1.23	165	~9

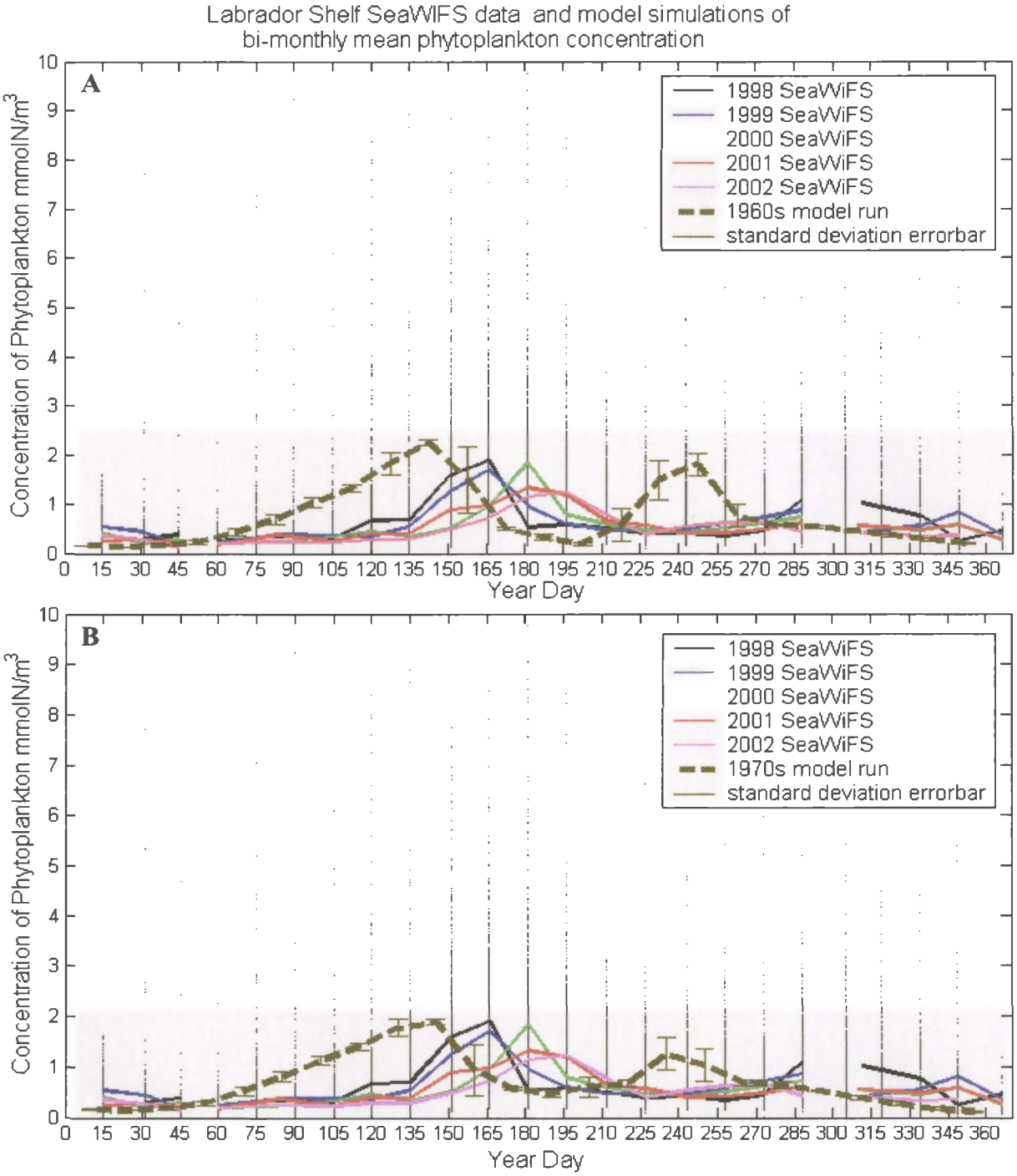
Labrador Shelf SeaWIFS data and model simulations of
bi-monthly mean phytoplankton concentration
A
1998 SeaWiFS
1999 SeaWiFS
2000 SeaWiFS
2001 SeaWiFS
2002 SeaWiFS
1960s model run
standard deviation errorbar
Concentration of Phytoplankton mmolN/m3
Year Day
B
1998 SeaWiFS
1999 SeaWiFS
2000 SeaWiFS
2001 SeaWiFS
2002 SeaWiFS
1970s model run
standard deviation errorbar
Concentration of Phytoplankton mmolN/m3
Year Day

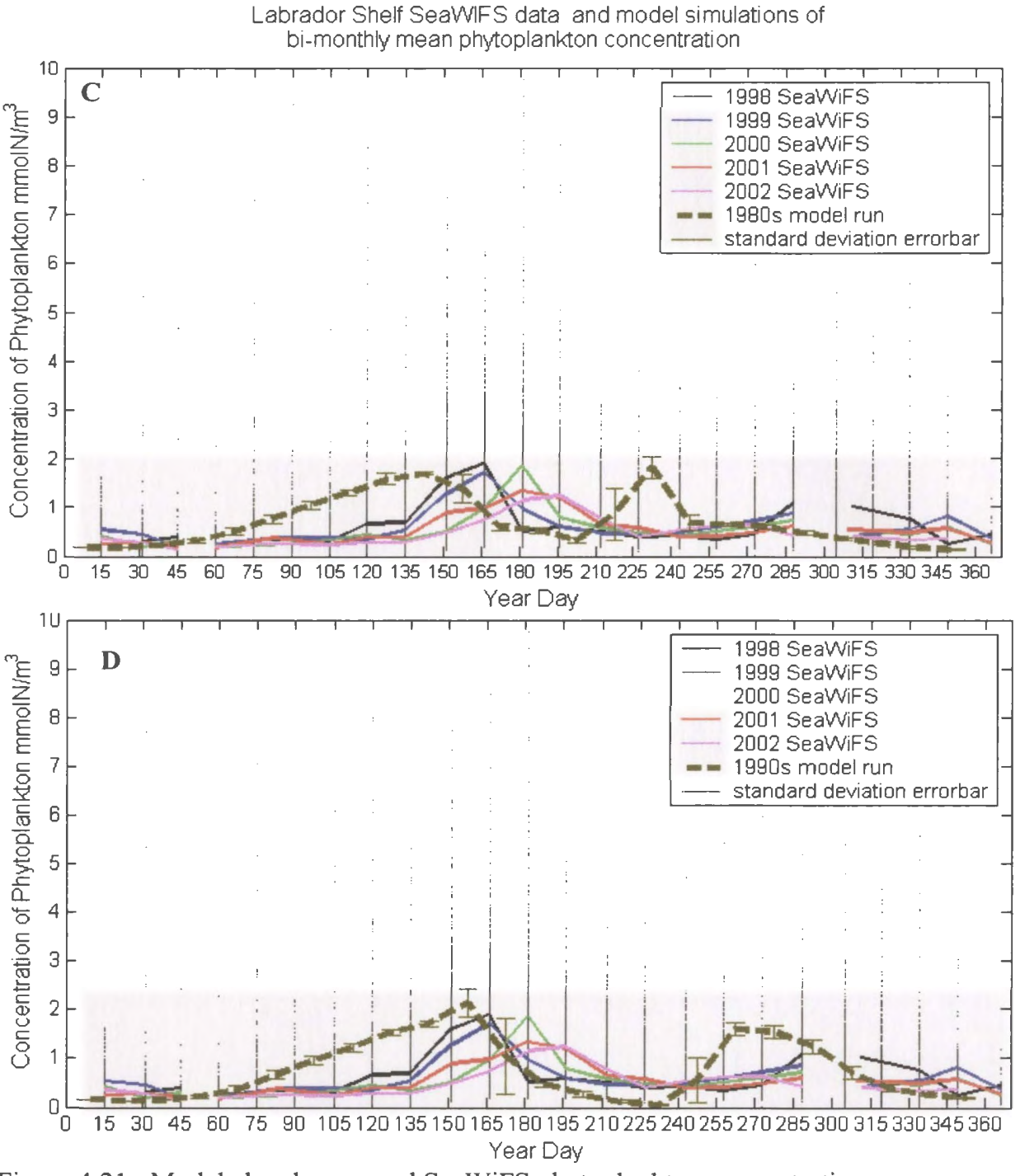

Figure 4.21: Modeled and measured SeaWiFS phytoplankton concentration over an annual cycle. Units in mmol N/m^3. SeaWiFS is measured bi-monthly (grey dots) and averaged bi-monthly (solid coloured lines). The modeled results are also averaged bi-monthly (dashed line) and error bars show the standard deviation during the; A) 1960s model results; B) 1970s model results; C) 1980s model results; and D) 1990s model results. SeaWiFS data from B. Petrie (personal communication, BIO).

4.3. Comparison Between Labrador Shelf and Sea

The results from the model runs for the Labrador Sea for 1968 with a winter convection to 800 m and for the 1990s with a winter convection to 2000 m are compared to results from the Shelf for the 1960s and 1990s (Figure 4.22 and 4.23).

As expected, the nutrient concentrations are higher in the Labrador Sea throughout the entire year. The N concentration on the Shelf is depleted in spring while in the Sea there is only a slight decrease in N. The N minimum on the Shelf occurs later and remains longer than in the adjacent Sea. Comparing the timing of the N minimum in the Sea to the start of the N minimum on the Shelf in the 1960s, the minimum occurs 37 days later on the Shelf. In the 1990s, the N minimum occurs 18 days later on the Shelf. On the Shelf there are two P blooms while in the Sea there is only one. The first P peak on the Shelf occurs slightly earlier than the peak in the Sea. On the Shelf, the first P bloom is also initiated earlier and is much broader compared to the Sea, which has a sharp peak. In the 1960s, the P bloom in the Inlet slightly overlaps the bloom in 1968 in the Sea. In the 1990s, the peak occurs earlier on the Shelf than in the Sea by about 5 days. This is consistent with Pavshtiks (1968) who found the spring bloom to occur earlier on the Shelf except in the southern Labrador Sea. The maximum P concentration for the Shelf is less than half the value from the Sea. However, when comparing the total biomass over the year the values are not so drastically different since there is a second P peak on the Shelf. In 1968 there is actually more P biomass per year on the Shelf than in the Sea. In the 1990s the opposite is true and there is more P biomass per year in the Sea (Figure 2.1). The Z peak concentration and yearly biomass over doubled that in the Sea.

On the Shelf there are two Z blooms in the 1960s and one bloom in the 1990s. The Sea has only one Z bloom. The Z timing of the first peak in the Z bloom is about 10 to 20 days earlier on the Shelf in the 1960s and 1990s.

Figure 4.22: Comparison of modeled nitrate, phytoplankton and zooplankton for the Labrador Shelf and Sea during the1960s (blue and green), and the 1990s (black and red). A) Nitrate; B) Phytoplankton; and C) Zooplankton in mmol N/m^3

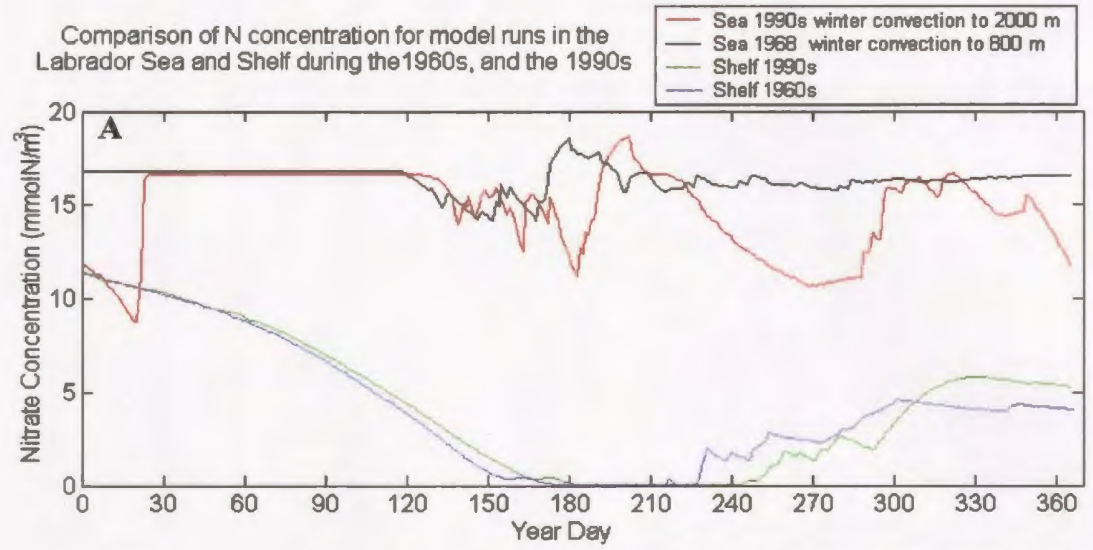
Comparison of N concentration for model runs in the Labrador Sea and Shelf during the1960s, and the 1990s
Sea 1990s winter convection to 2000 m
Sea 1968 winter convection to 800 m
Shelf 1990s
Shelf 1960s
A
Nitrate Concentration (mmolN/m3)
Year Day

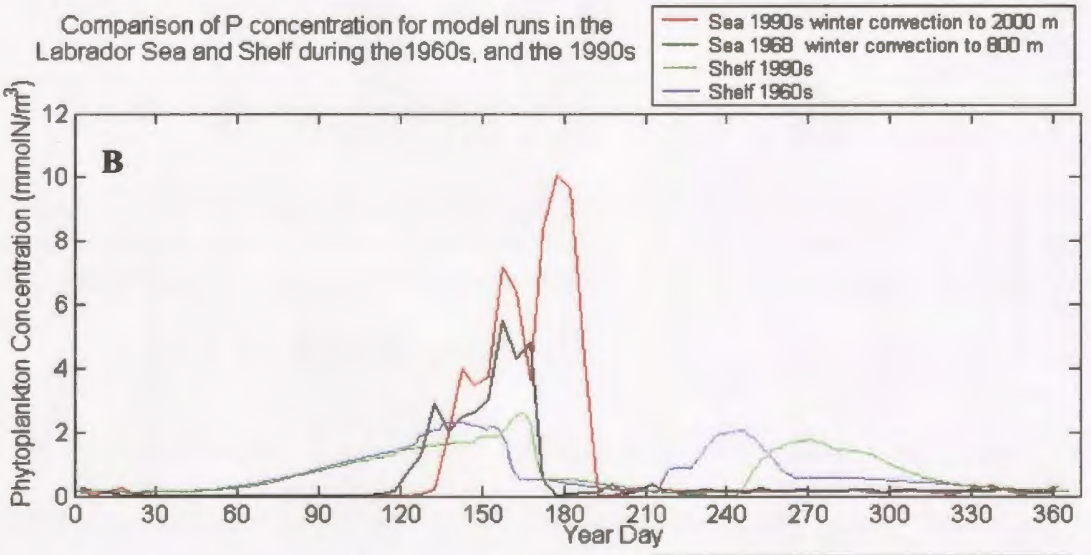
Comparison of P concentration for model runs in the Labrador Sea and Shelf during the1960s, and the 1990s
Sea 1990s winter convection to 2000 m
Sea 1968 winter convection to 800 m
Shelf 1990s
Shelf 1960s
B
Phytoplankton Concentration (mmolN/m3)
Year Day

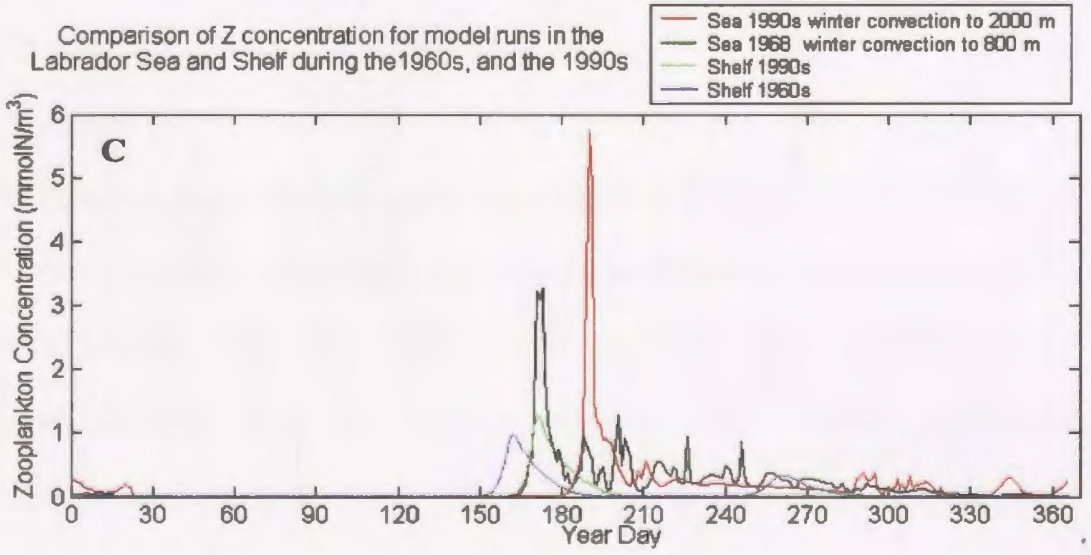
Comparison of Z concentration for model runs in the Labrador Sea and Shelf during the1960s, and the 1990s
Sea 1990s winter convection to 2000 m
Sea 1968 winter convection to 800 m
Shelf 1990s
Shelf 1960s
C
Zooplankton Concentration (mmolN/m3)
Year Day

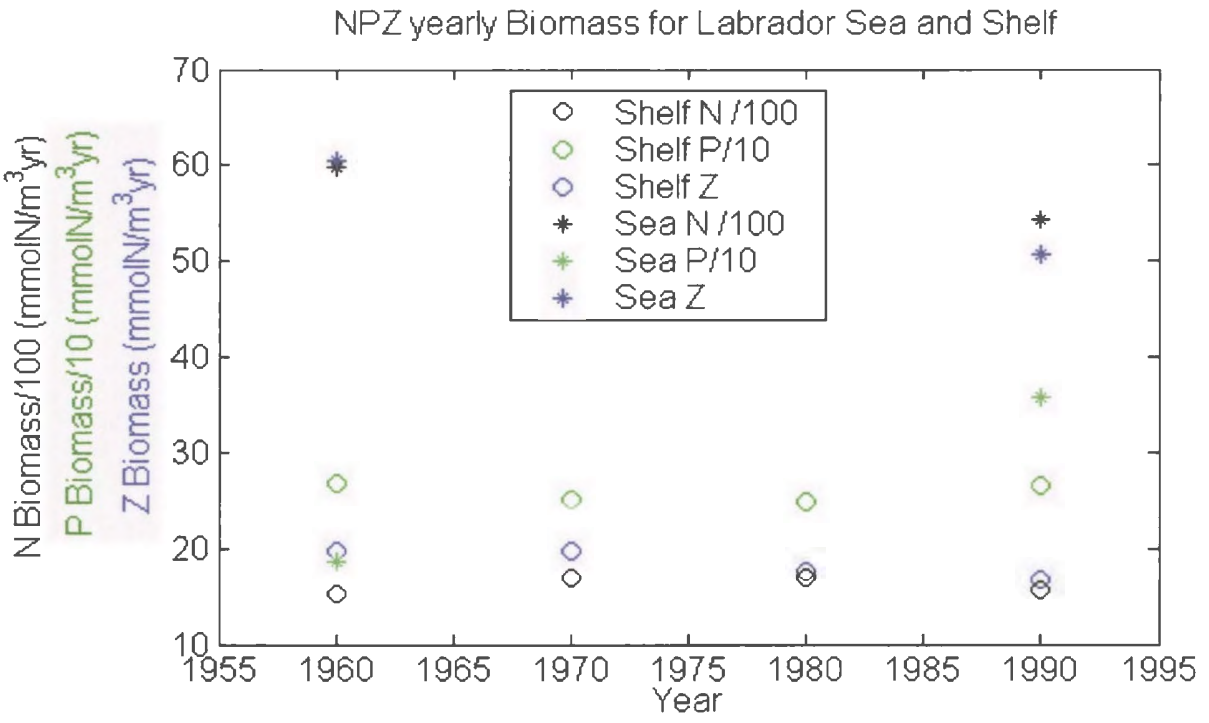

Figure 4.23: N (black), P (green) and Z (blue) yearly biomass for Labrador Sea (asterisk) and Shelf (circles). The N values are divided by 100 and the P values are divided by 10. The Labrador Sea results are from the 800 m and 2000 m deep winter convection runs.

4.4. Hamilton Inlet

The model for the Hamilton Inlet was run for two periods, before 1970 and after 1976, representing before and after the hydroelectric development of Churchill River. As described in Section 3.5.3, only three state variables are used for this model since detritus was removed. The model was initialized January 1 and run for one complete year. The temperature and salinity data during each period were combined. The initial concentrations of each state variable are listed in Table 3.1 and the parameters used are listed in Table 3.2. In the following sections, the results of the calculated annual mixed-layer depth and results of the model simulations are discussed and compared with observations, *in-situ* data and shipboard measurements. The results are not compared

with remote sensing data or with the results of other models since there was no reliable satellite imagery and no models found that describe the annual cycle of plankton in the Inlet.

4.4.1. Annual Mixed-layer

The resulting calculated mixed-layer depths for Hamilton Inlet vary considerably between the two periods (Figure 4.24 and 4.25). The mixed-layer depth was calculated from measured temperature and salinity before and after the hydroelectric development as described in Section 3.4.3. All available data for each period were combined. The annual cycle of the mixed-layer depth for the Hamilton Inlet is opposite to that of the Sea and Shelf. The mixed-layer in the Inlet shallows over winter and does not deepen. This may be due to ice cover. The mixed-layer deepens after June when there is no longer ice cover (Figure 4.26). As the ice thickens during winter the mixed-layer shallows, and when ice thickness reaches 30 cm the mixed-layer is above 30 m. As the ice melts during spring the mixed-layer deepens, but it is not until the ice leaves that the mixed-layer reaches a maximum depth. The mixed-layer is also compared to the Churchill River mean monthly river flow (Figure 4.26). The river flow is greatest during the ice melt when the mixed-layer shallows in spring.

Before the 1970s the mixed-layer shallows from 35 m in the beginning of January to the minimum depth of 10 m at the end of February. The mixed-layer deepens slightly from February to April and shallows back to 10 m before deepening again to the maximum depth of 70 m by day 240. The mixed-layer gradually begins to shallow by day 280 following the maximum depth. It deepens back to 43 m by the end of the year.

After 1976, similarly to the 1960s, the mixed-layer shallows from 35 m in the beginning of January to 10 m at the end of February. The mixed-layer remains between 10 and 8 m until just over day 150 when it begins to rapidly deepen. It reaches a maximum depth between days 170 and 315, after which it begins to shallow gradually back to 45 m by the end of the year.

There are only minor differences in mixed-layer depths between the years investigated. This maybe caused by the lack of data before 1970 and the filling of gaps in the data using the entire data set. In winter after 1976 the mixed-layer does not deepen slightly as it does prior to the1970s. After 1976 the mixed-layer deepens more rapidly and does not reach as deep as before 1970. The data set after 1976 contains many observations from Goose Bay that is shallower than Lake Melville and Groswater Bay, and this may be the cause of the shallower mixed-layer in summer after 1976. In November the mixed-layer shallows earlier in 1976 than before the1970s.

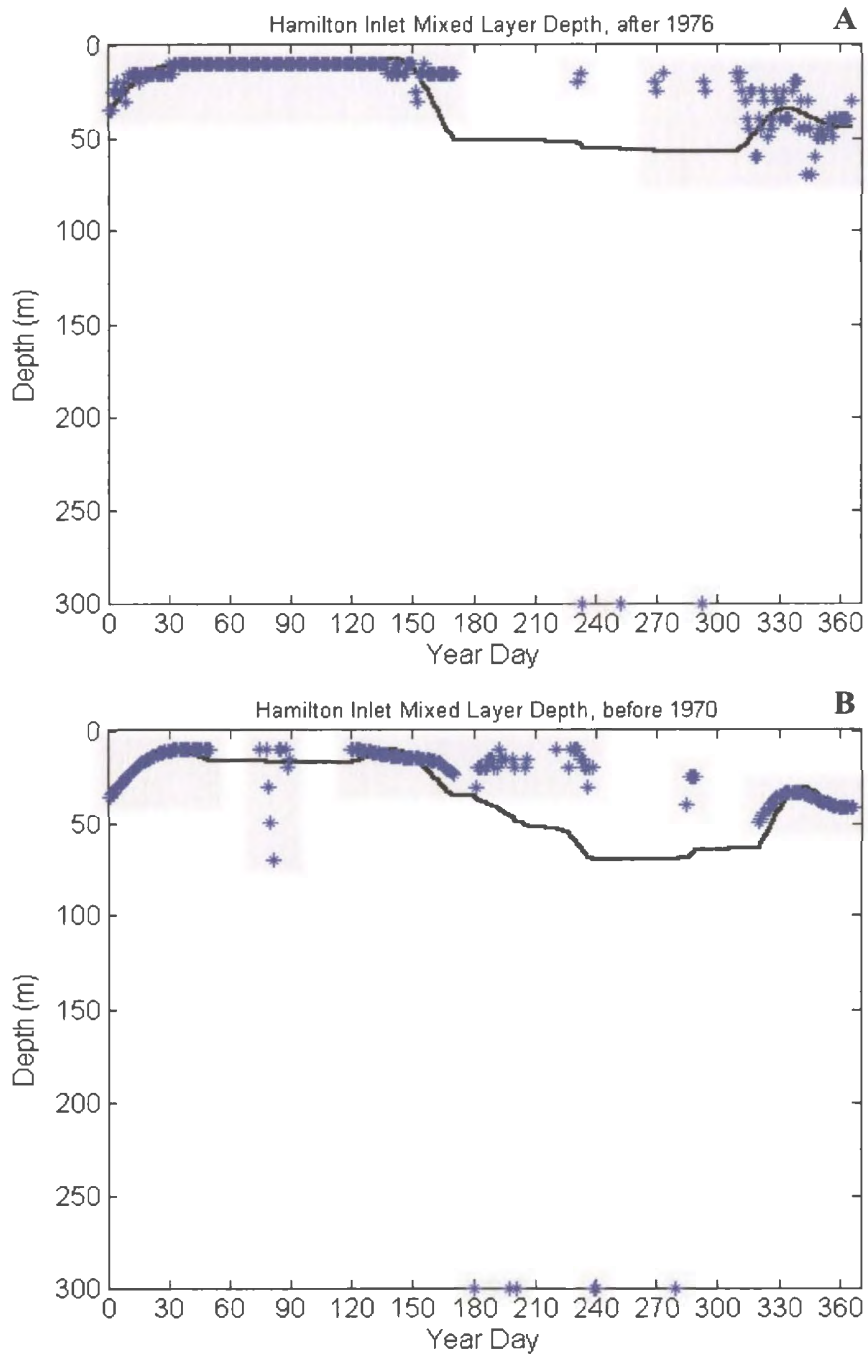

Figure 4.24: The mixed-layer depth for Hamilton Inlet calculated from measured temperature and salinity data. (A) After 1976 and (B) before 1970. The line is the daily linear interpolated mixed-layer depth, and the blue dots indicate the days in which density data are available to calculate the mixed-layer depth.

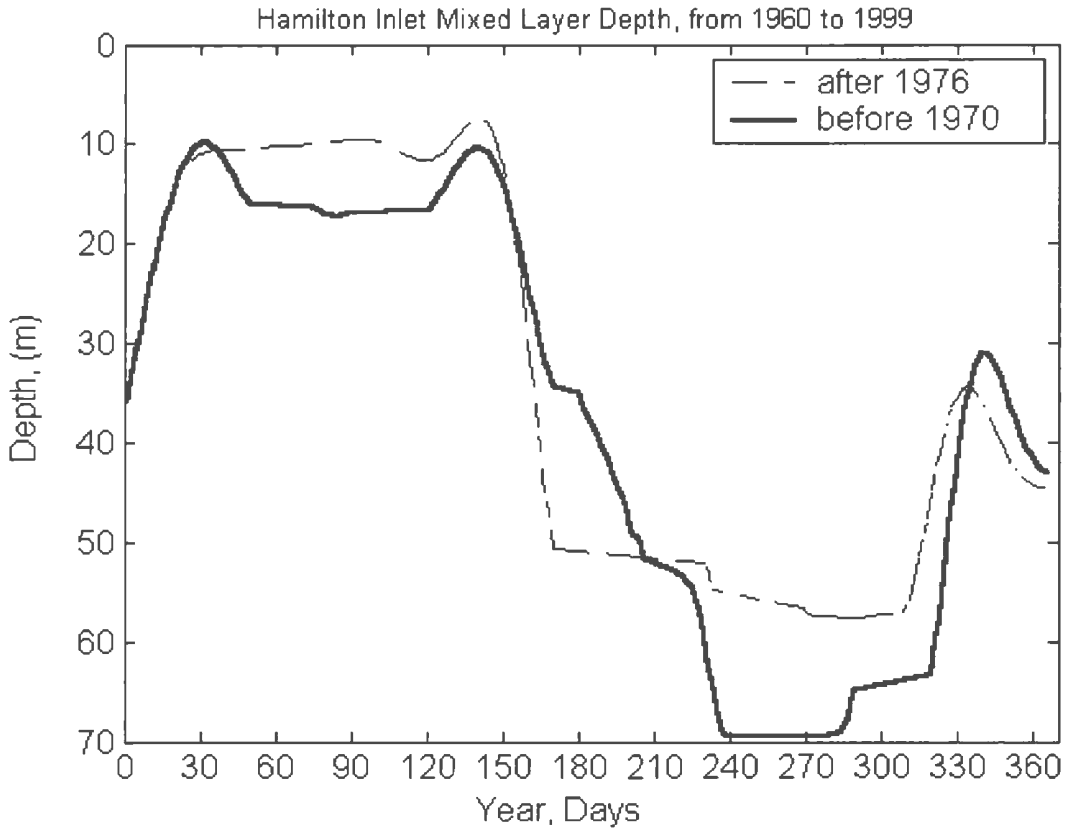

Figure 4.25: The mixed-layer depths for Hamilton Inlet calculated from measured temperature and salinity data before 1970 (solid line) and after 1976 (dashed line).

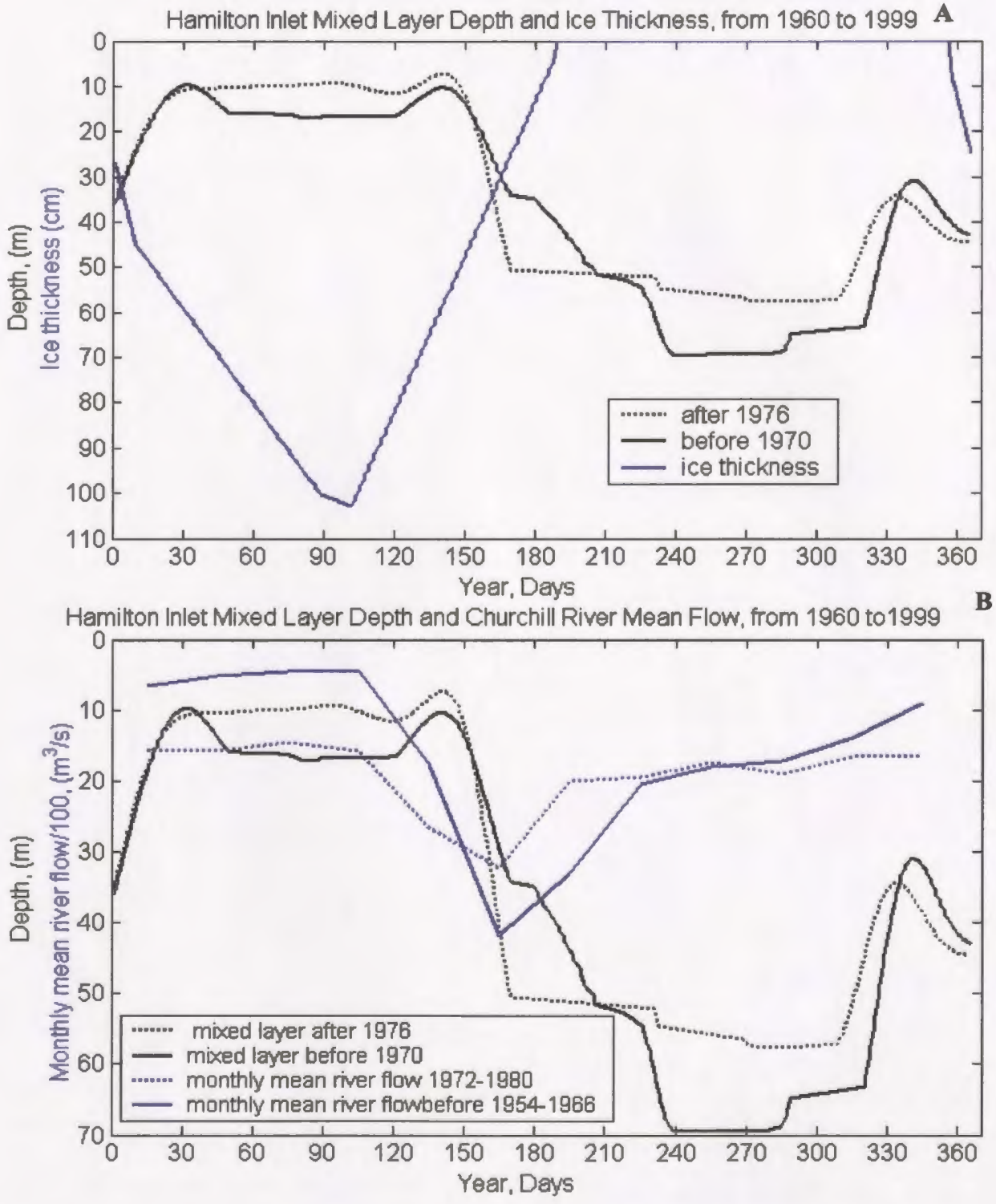

Figure 4.26: The mixed-layer depths (black) for Hamilton Inlet compared to A) ice thickness (cm) (blue) and B) monthly mean Churchill River flow (m^3/s) (blue) for before (solid line) and after (dotted line) the hydroelectric development.

4.4.2. Annual Cycles of Biological Variables

The biological variables, N, P, and Z, in Hamilton Inlet have an annual cycle distinct from that of the Labrador Sea and Shelf. There is a pronounced spring bloom in P but not in Z and an increase of N concentration in the surface layer in the summer and decrease in the winter and fall (Table 4.7 and Figure 4.27 and 4.28).

The concentration of N is high in January for all years. This is the same time that the mixed-layer is deeper, supplying the upper layer with nutrients and causing an increase in P concentration. The N concentration gradually decreases until the end of January. In February, before 1970, there is a second increase in N to 1 mmol N/m^3 followed by an increase in P to 1.1 mmol N/m^3 by day 62. The increase in P concentration reduced the N concentration to a minimum until the following spring. In February, after 1976, the N concentration remains low until day 108, which had a slight peak of N followed by an increase in P concentration. The mixed-layer begins to deepen in June and the irradiance increases in the surface layer, due to the disappearance of ice. The concentration of N also increases in the mixed-layer, beginning about day 140 and subsequently causing a P bloom. N concentration reaches a maximum between 150 and 163 at around 0.72 mmol N/m^3 before 1970 and day 168 with a higher maximum of 1.9 mmol N/m^3 after 1976. The P reaches a peak at the same time as the N peak with a value of approximately 1.9 mmol N/m^3 for both periods. The N and P concentration decline following the bloom and there is another slight increase in N and P concentration in late August before values return to a minimum. At the end of the year, the mixed-layer

deepens and the nutrients increase again, however, there is no further increase in P concentration.

The Z is very low in both model runs. Before 1970 there is a slight Z peak of 0.05 mmol N/m^3 at day 250, however after 1976 Z disappears.

The yearly biomass was calculated just as for the Labrador Sea and the results are shown in Table 4.8. The N is slightly lower before 1970 by approximately 6 mmol N/m^3yr. The P is 45 mmol N/m^3yr higher before 1970 at 184.7 mmol N/m^3yr. The Z is very low at 1.96 mmol N/m^3yr before 1970s and 0.72 mmol N/m^3yr after 1976.

Overall, before 1970 there are two main P maxima one of which was in March and the other larger peak, which is in June. There are also two main N maxima, the larger of which is in February and the other is in June. After 1976 there are also early winter blooms of N and P but they are minor compared to the peak in June.

Table 4.7: Summary of maximum N, P, and Z concentrations and timing of the maximum for model simulations

Peak concentrations and bloom initiation	**Model simulation before 1970**		**Model simulation after 1976**	
	Year Day	**Concentration** (mmol N/m^3)	**Year Day**	**Concentration** (mmol N/m^3)
N maximum during blooms	50	1.0375	108	0.355
	150-163	0.713-0.731	168	1.90
	235	0.389	233	0.127
P maximum	62	1.08	25	0.677
	172	1.90	115	0.599
	---	---	177	1.88
Z maximum	250	0.049	---	---

Table 4.8: Total yearly biomass of N, P, and Z for model simulations.

State Variable	Total yearly biomass (mmol N/m^3yr)	
	Before 1970	**After 1976**
N	79.491	85.478
P	184.74	140.95
Z	1.9559	0.7159

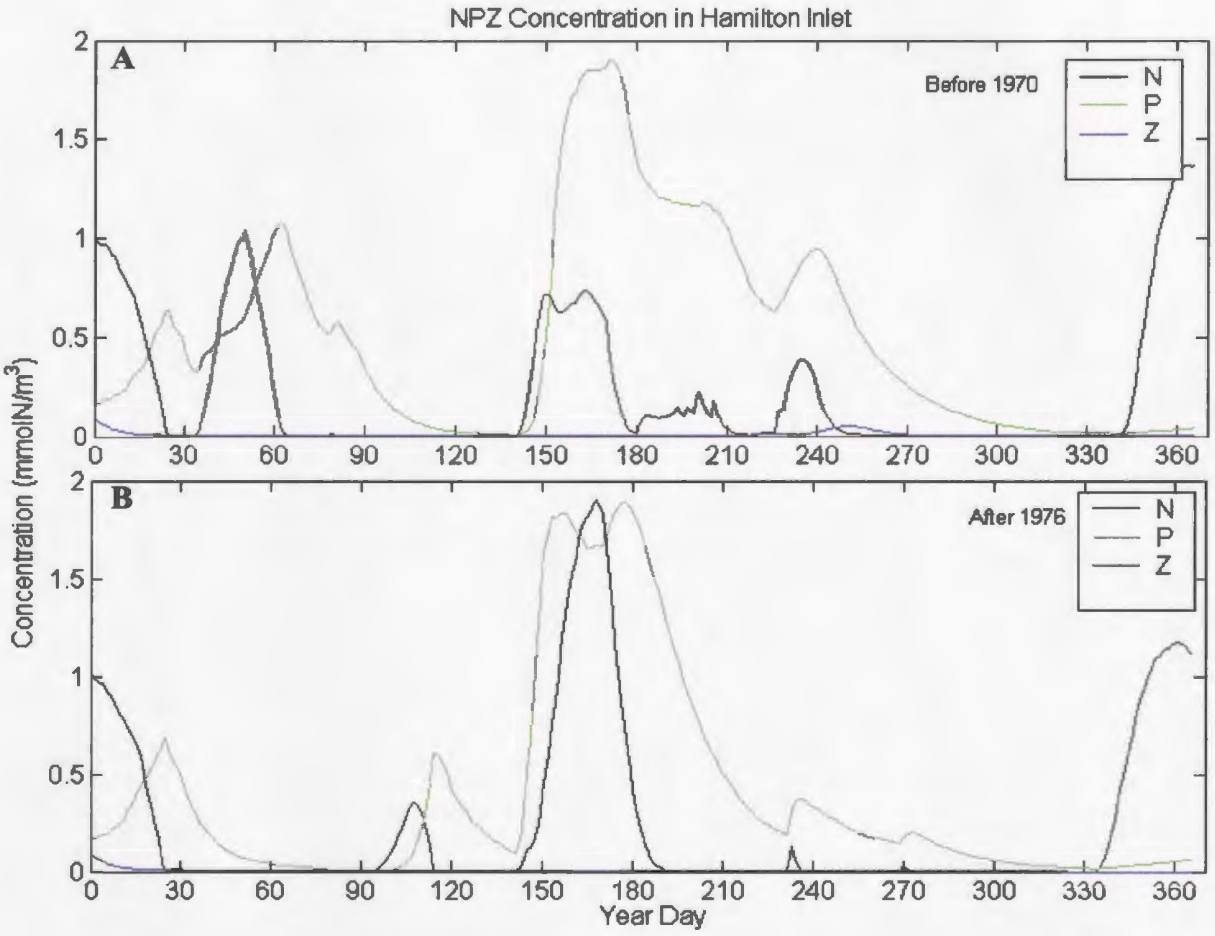

Figure 4.27: Modeled daily concentration of N (black), P (green), and Z (blue) in mmol N/m^3 over one year for four model simulations: (A) before 1970 and (B) after 1976.

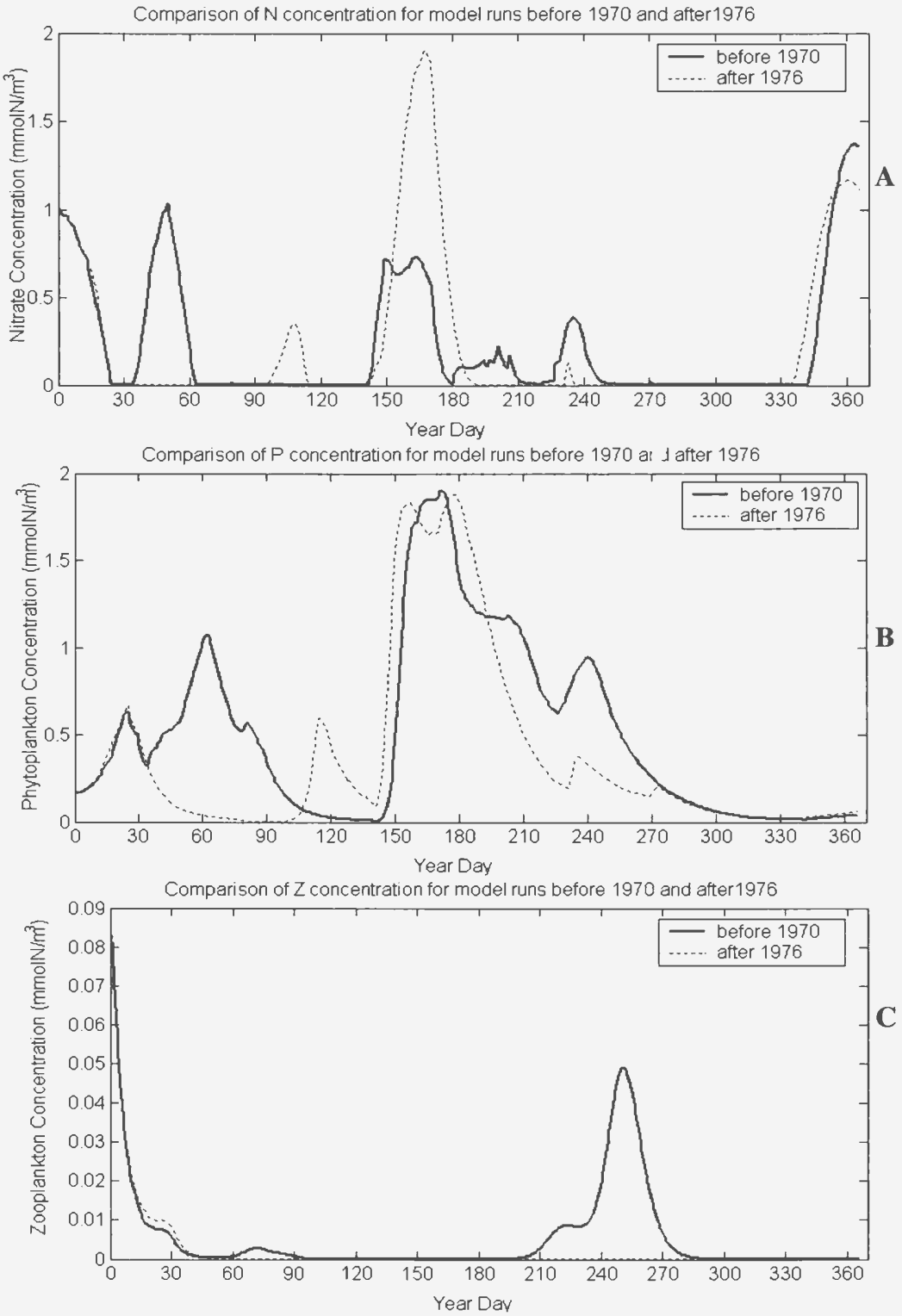

Figure 4.28: Comparison of modeled nitrate, phytoplankton and zooplankton for four model runs before 1970 (black solid line) and after 1976 (dotted line). A) Nitrate; B) Phytoplankton; and C) Zooplankton in mmol N/m^3

4.4.3. Comparison with Observations, *In-situ* Data and Shipboard Measurements

There are very few observations for Hamilton Inlet, as noted in Section 2.5.3. As a result, the model simulations of N and P can only be compared to the September 9, 1979 OLABS study (Buchanan and Foy, 1980) (Figure 2.29). In the beginning of September the model P values are 0.35 and 0.94 mmol N/m^3. These are within the values measured from 0 to 50 m in the OLABS study. The model N values in the beginning of September are much lower (>0.35 mmol N/m^3) than those reported by OLABS (2.65-1.8 mmol N/m^3)

The model simulations are also compared to ice cover over Lake Melville and the river flow (Figure 2.29 and 2.30). The spring P bloom began during ice melt and reaches a peak when the ice was quite thin or totally gone. During the freeze up there are also increases in N and P concentrations. When the ice is at a maximum thickness there is virtually no P and very few nutrients. The river flow is greatest in spring before 1970 and reduces after 1976 as discussed in Section 2.5.4. The maximum P bloom occurs at the same time as the peak in river flow. During the increased river flow in spring, before 1970, there is actually less N. However, this has little effect on the P peak concentration and only reduces the total yearly biomass by 6 mmol N/m^3yr.

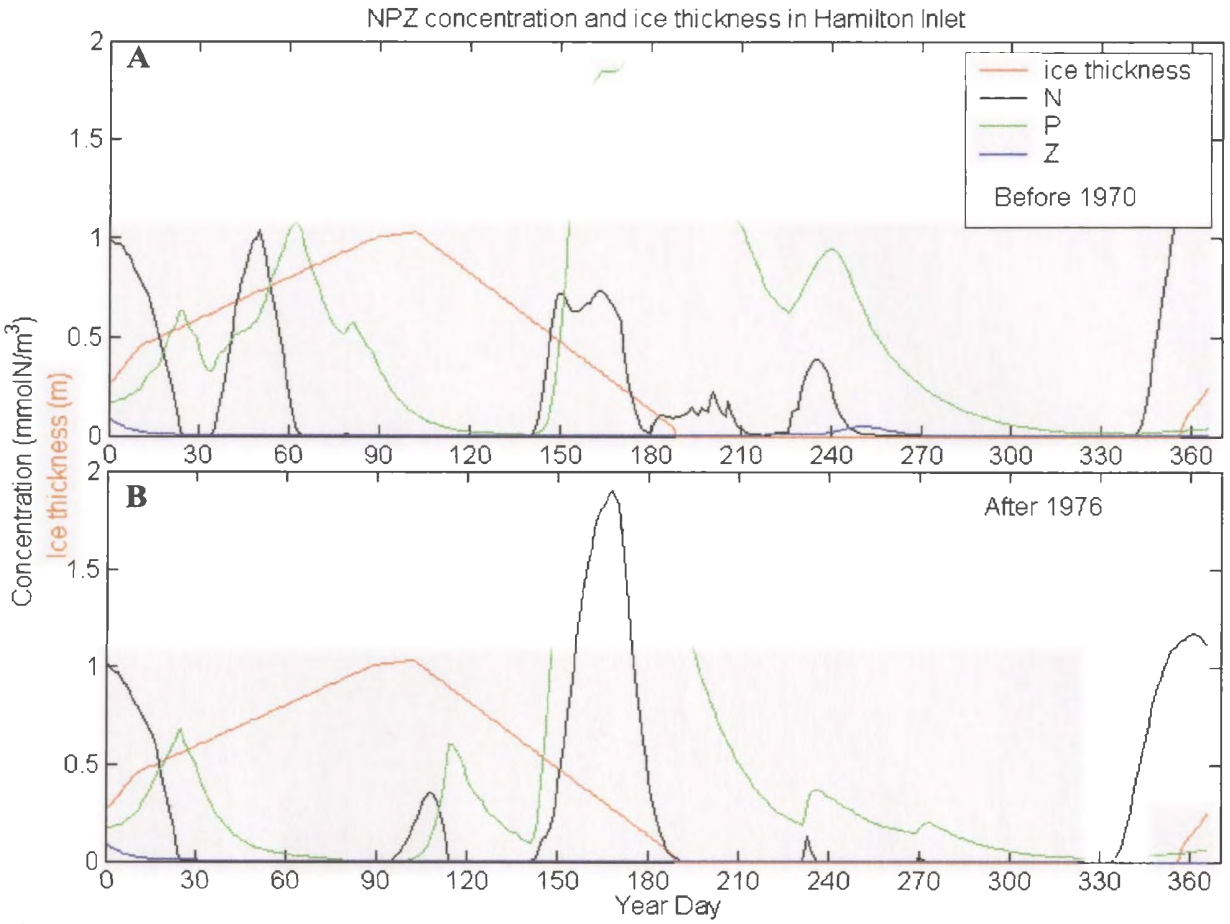

Figure 4.29: Modeled daily concentration of N (black), P (green), and Z (blue) in mmol N/m^3 compared to ice thickness in m (orange) over one year for two model simulations: (A) before 1970 and (B) after 1976.

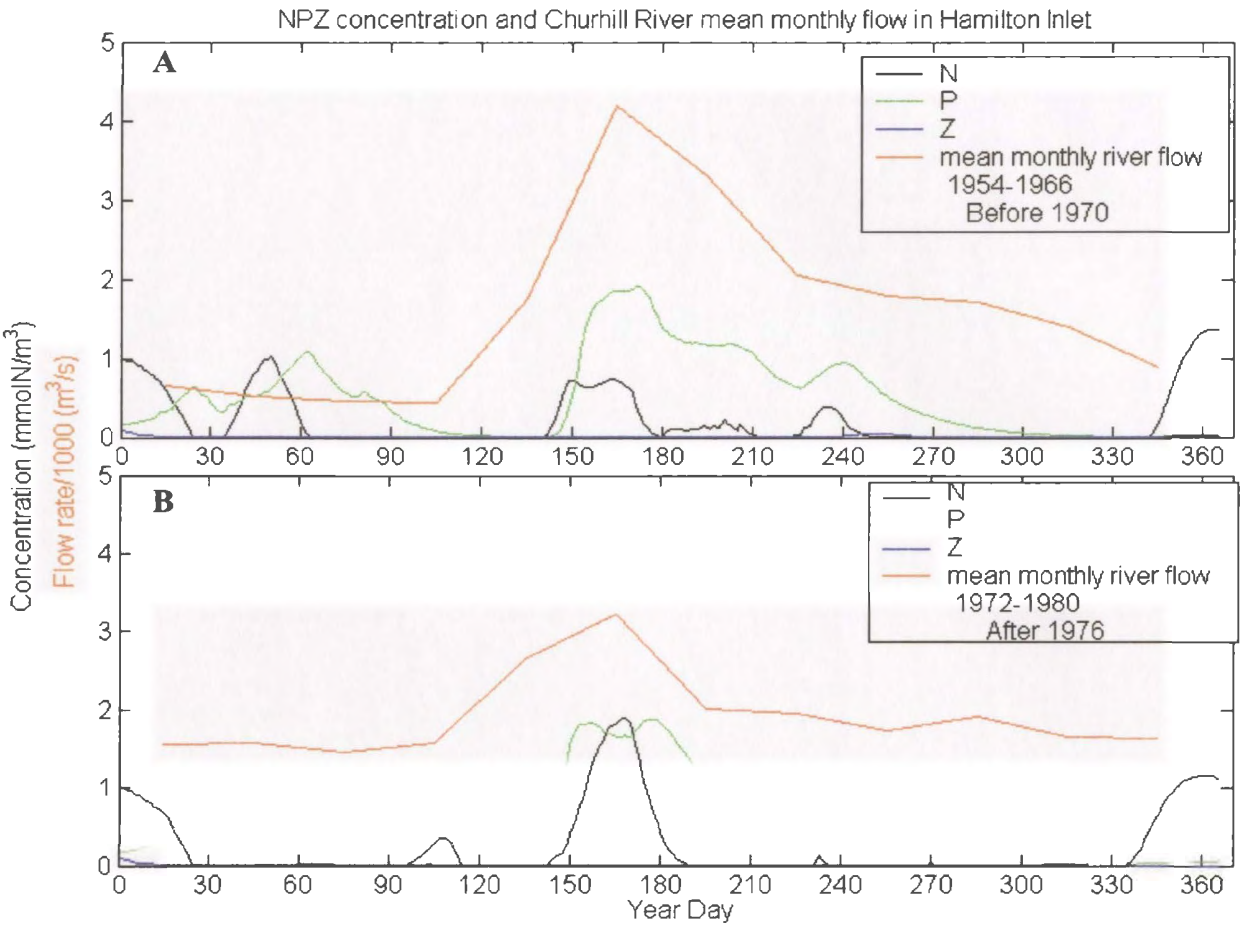

Figure 4.30: Modeled daily concentration of N (black), P (green), and Z (blue) in mmol N/m^3 compared to mean monthly Churchill River flow in m^3/s (orange) over one year for two model simulations: (A) before 1970 and (B) after 1976.

4.4.4. Primary Production Rate

The primary production rate was determined for each period using the differential P equation (Section 3.2.1), however all the loss terms in the equation were neglected. The daily primary production after 1976 increases gradually to a major peak at about day 200 and then gradually decreases again with another slight peak at day 330 (Figure 4.31). The primary production peaks at 0.32 gC/m^2day after 1976. Before 1970 the daily productivity is more variable and has 3 peaks: day 62, between days 165 and 260 and day 340. The three maximum primary production peaks are approximately; 0.17, 0.30 and 0.32 gC/m^2 day respectively. The yearly primary production is found to be 64.072 gC/m^2 yr before 1970 and 48.033 gC/m^2 yr after 1976. Therefore the primary production decreased by 16 gC/m^2 yr after 1976. Primary production rate can be compared to fish catch and based on the published correlation (Harrison and Parsons, 2000) (Figure 4.17), according to this correlation 64 gC/m^2 yr corresponds to roughly 1.6 t /km^2 yr and 48 gC/m^2 yr corresponds to 1.4 t/km^2. yr.

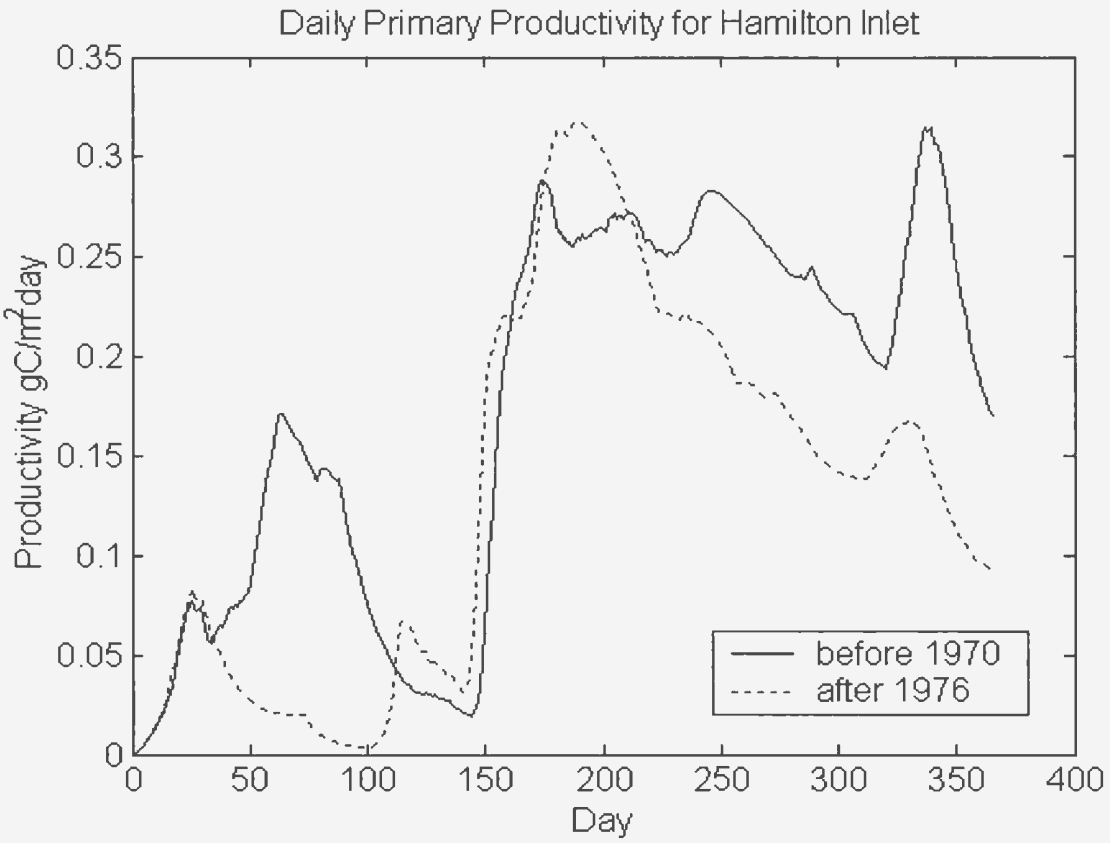

Figure 4.31: Daily primary productivity in mgC/m^2·day for the each period the model was run, before1970 (solid line) and after 1976 (dotted line).

4.5. Comparison Between Labrador Shelf and Hamilton Inlet

The results from the model runs for the Labrador Shelf are compared to results for Hamilton Inlet (Figure 4.32 and 4.33). As expected, the nutrient concentrations are higher on the Shelf throughout the entire year. The N concentration on the Shelf is depleted in spring while in the Inlet there is an increase in N concentration. There are several N minimums in the Inlet compared to the Shelf. In winter in the Inlet the N concentration is at a minimum with a few slight increases. On the Shelf, in winter the N

concentration is at a maximum and gradually decreases until spring. On the Shelf there are two P blooms while in the Inlet there are some initial P blooms and one major bloom in spring. The first P peak on the Shelf occurs slightly earlier than the spring peak in the Inlet. For example, in the Inlet the P bloom before 1970 occurs around day 172 while on the Shelf it is between days 131 and 156. This is expected due to the duration of the ice cover in the Inlet. On the Shelf the first P bloom is initiated earlier compared to the Inlet, which had a sharp initial peak that gradually declines. The maximum P concentration for the Inlet is similar to that of the Shelf for the 1970s and 1980s. However, when comparing the total biomass over the year the Shelf has higher values by about 100 $mmolN/m^3yr$. In the 1960s there is a greater P biomass per year on the Shelf and the Inlet, when compared to later years (Figure 4.33). The Z peak concentration and yearly biomass in the 1960s is greater on the Shelf by about a factor of 10. On the Shelf there are two Z blooms while in the Inlet there is only one bloom, at the same time as the second bloom on the Shelf. After 1976 in the Inlet the Z concentration is very low and no bloom occurs; on the Shelf the Z population is similar in size to that before 1980 and bloom does occur.

The yearly primary production for the Labrador Shelf and Hamilton Inlet shows that in the 1960s the yearly productivity on the Shelf is greater by a factor of about 3 (Table 4.9). After 1976, yearly productivity on the Shelf is greater by a factor of 4.

Figure 4.32: Comparison of modeled nitrate, phytoplankton and zooplankton for the Labrador Shelf and Hamilton Inlet during the1960s (black and grey), 1970s (blue), 1980s (red) and 1990s (green and grey). A) Nitrate; B) Phytoplankton; and C) Zooplankton in mmol N/m^3

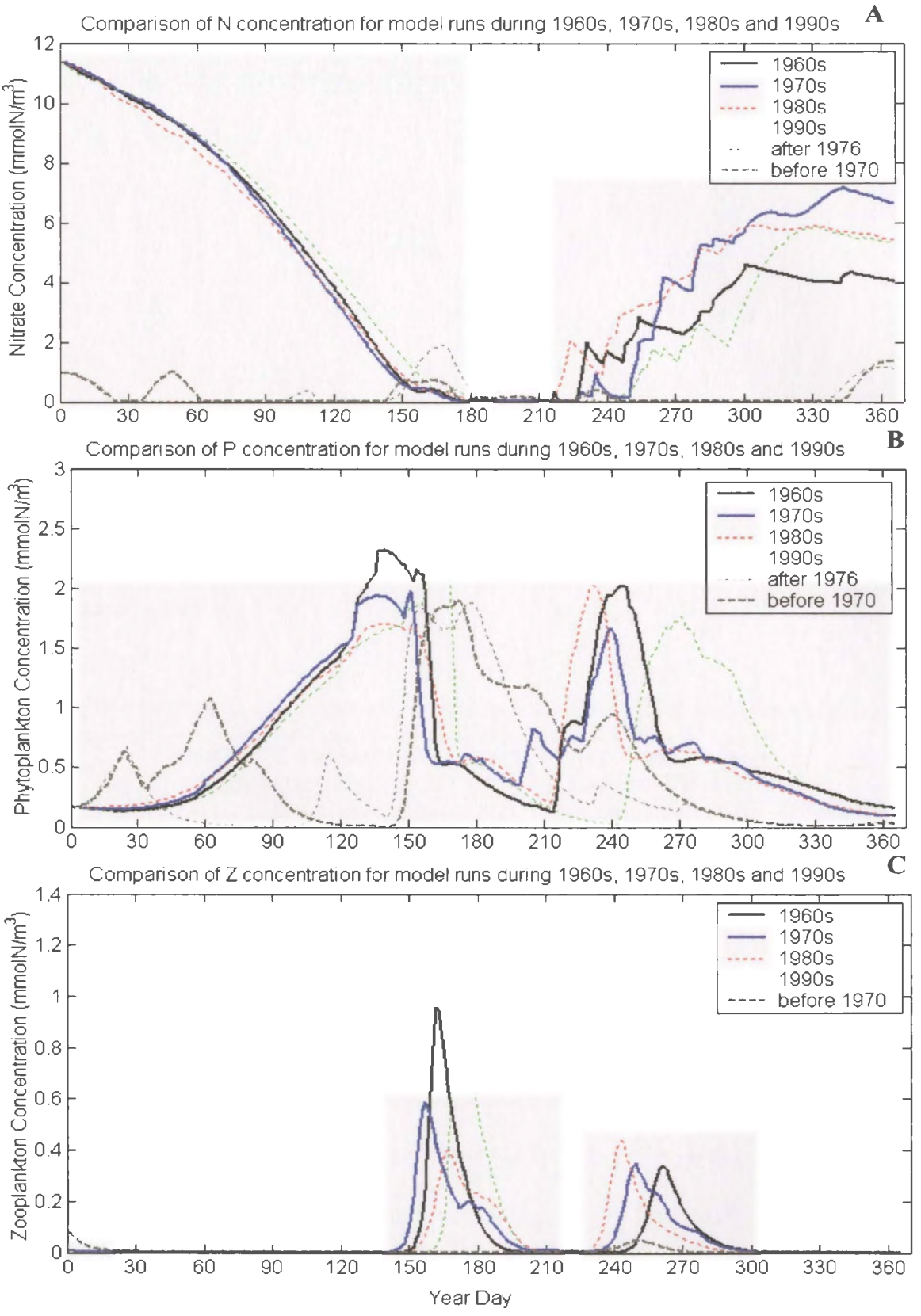
A
Comparison of N concentration for model runs during 1960s, 1970s, 1980s and 1990s
Nitrate Concentration (mmolN/m3)
1960s
1970s
1980s
1990s
after 1976
before 1970
B
Comparison of P concentration for model runs during 1960s, 1970s, 1980s and 1990s
Phytoplankton Concentration (mmolN/m3)
C
Comparison of Z concentration for model runs during 1960s, 1970s, 1980s and 1990s
Zooplankton Concentration (mmolN/m3)
Year Day

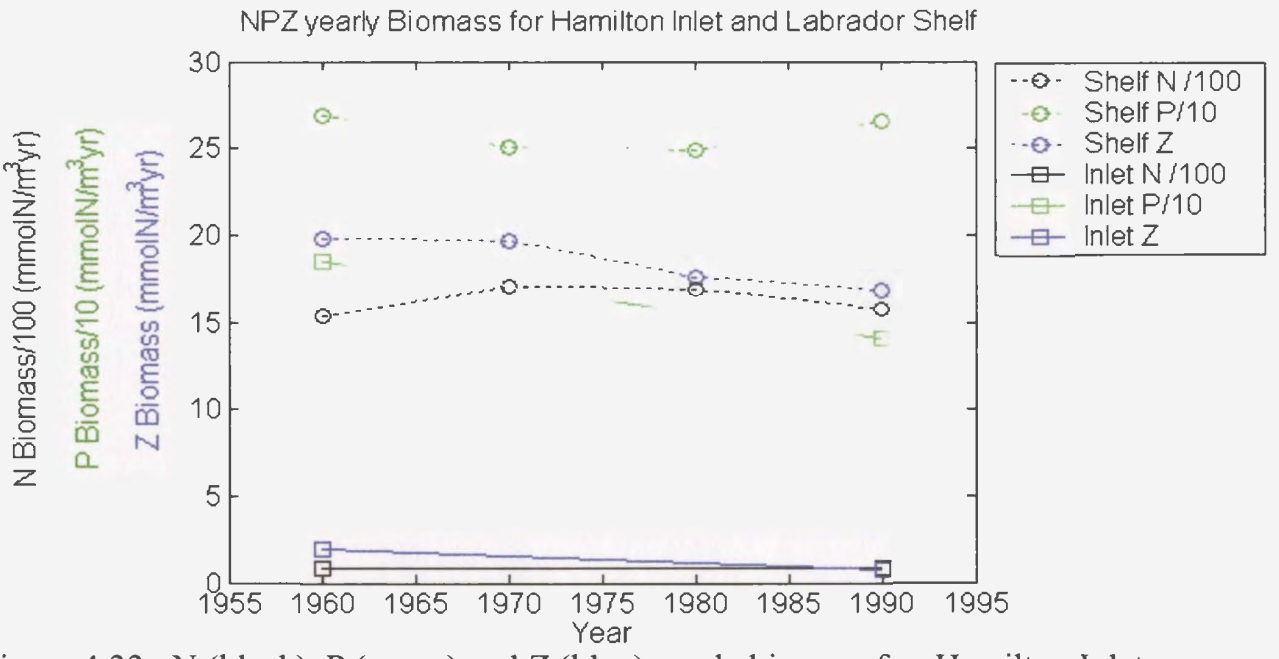

Figure 4.33: N (black), P (green) and Z (blue) yearly biomass for, Hamilton Inlet (squares) and Labrador Shelf (circles). The N values are divided by 100 and the P values are divided by 10

Table 4.9: Yearly primary production for the Labrador Shelf and Hamilton Inlet.

Year	Primary Production Labrador Shelf (gC/m^2 year)	Primary Production Hamilton Inlet (gC/m^2 year)
1960	207.37	64.072
1970	212.38	48.033
1980	205.70	
1990	199.26	

4.6. Comparison with NAO Index

During the 1960s the NAO index is highly negative, whereas in the 1970s the index is slightly negative (Figure 4.34 and Table 4.10). From the 1980s to the 1990s the index is positive and increases. The greatest contrast in the NAO index is between the negative values in the 1960s and the high positive index in the 1990s. Comparing the

1960s to the 1990s (Figure 4.35), on the Shelf there is little change in N and P annual biomass, and Z annual biomass slightly decreases. The Labrador Sea P biomass increases significantly in the 1990s however, the N and Z biomass decrease slightly. Hamilton Inlet results combines all the data after 1976 so there is no specific data for the 1990s. Comparing the results from before 1970 and after 1976 the P and Z biomass decreases while the N biomass has little change.

On the Shelf as the primary productivity decreases the NAO index increases (Figure 4.36 and Table 4.10). In the Inlet before 1970 the NAO index was negative and the productivity was higher.

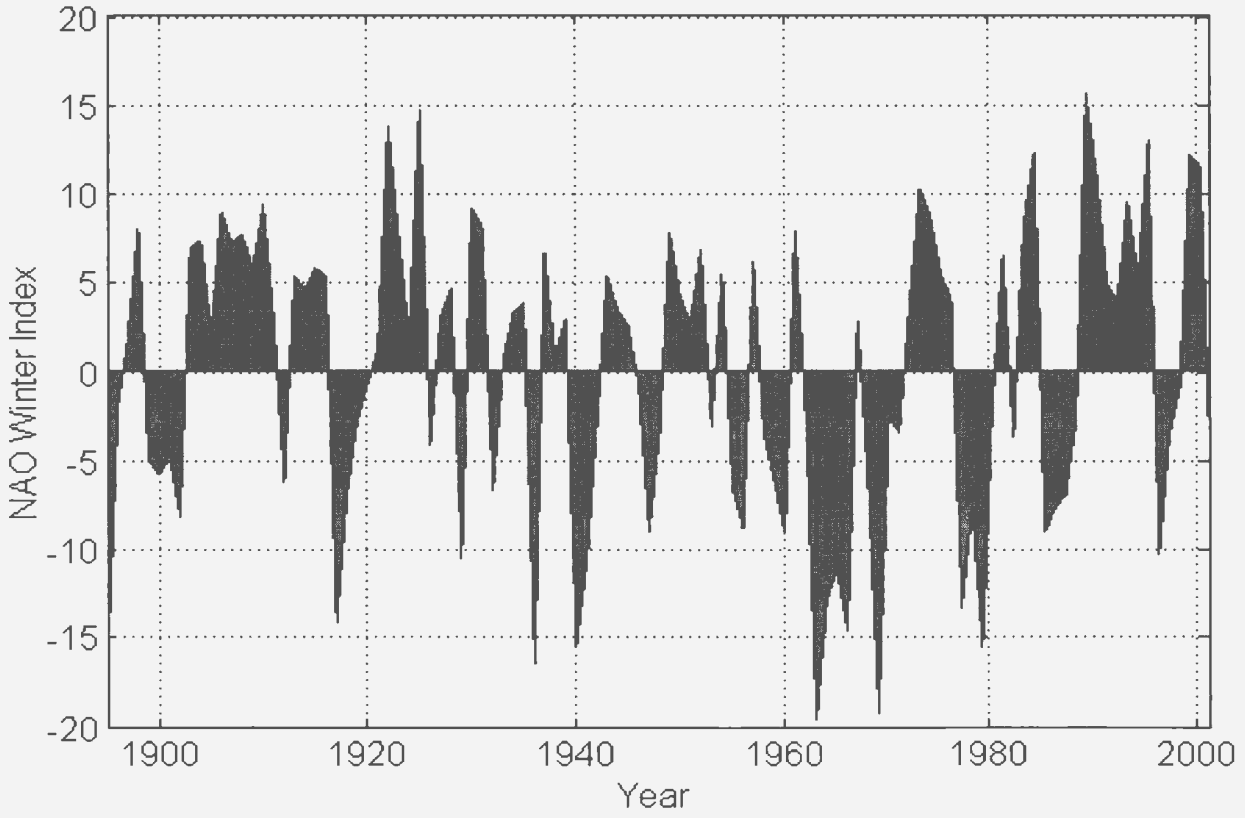

Figure 4.34: Time series of the NAO index, winter mean.

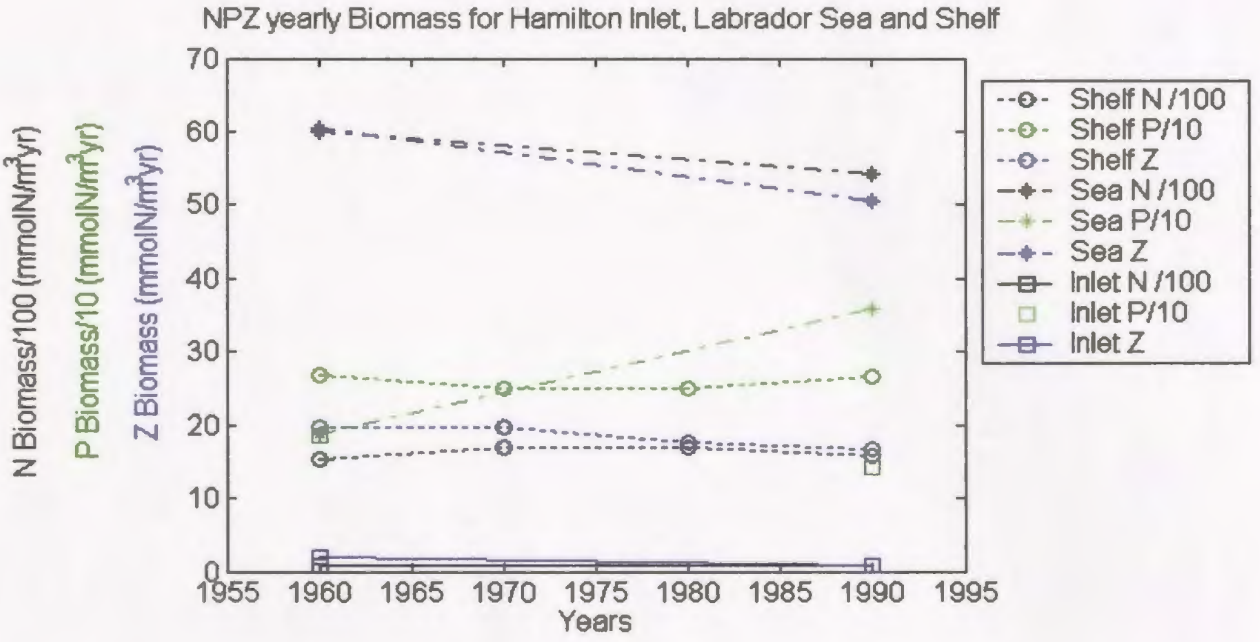

Figure 4.35: N (black), P (green) and Z (blue) yearly biomass for Hamilton Inlet (squares and solid lines), Labrador Sea (asterisk and dashed lines) and Shelf (circles and dotted line). The N values are divided by 100 and the P values are divided by 10.

Table 4.10: Yearly primary production for the Labrador Shelf and Hamilton Inlet compared to the NAO index.

Year	Primary Production Labrador Shelf (gC/m^2 year)	Primary Production Hamilton Inlet (gC/m^2 year)	NAO Index Average
1960s	207.4	64.07	-8.40
1970s	212.4	48.03	-1.02
1980s	205.7		1.08
1990s	199.3		4.49

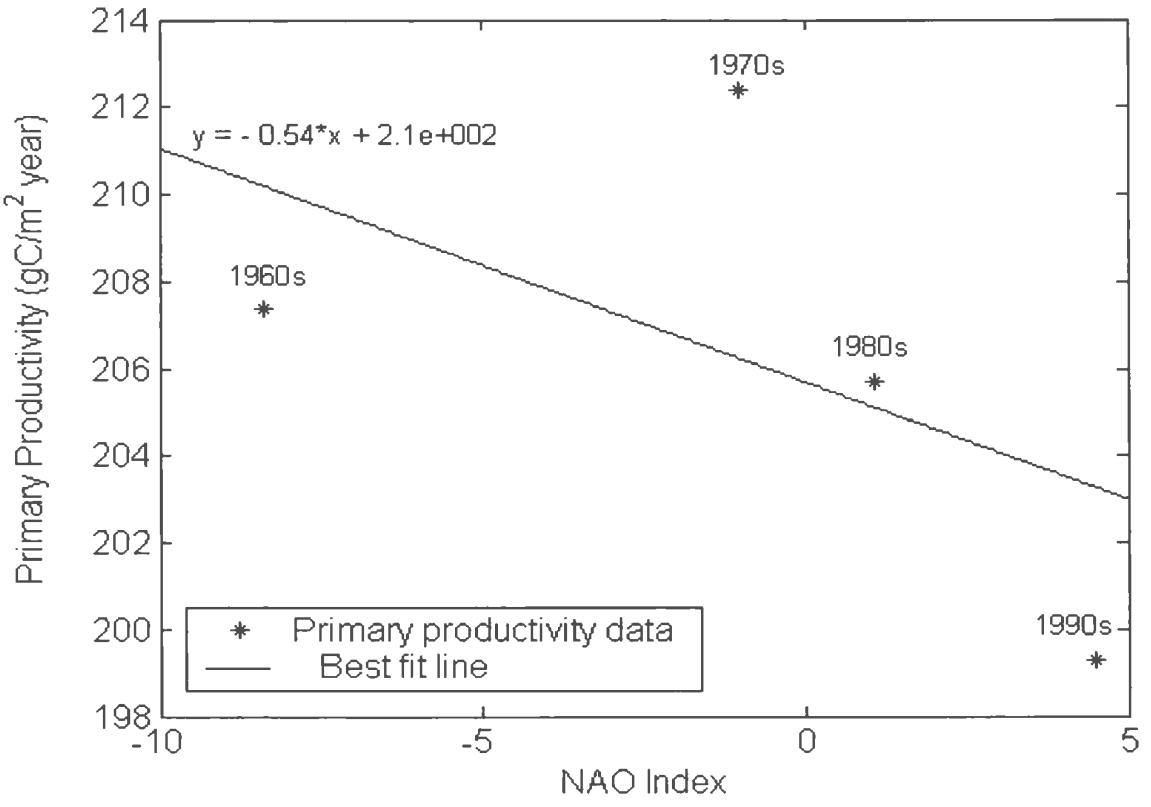

Figure 4.36: Comparison of annual primary production on the Labrador Shelf with the NAO Index during the 1960s, 1970s, 1980s, and 1990s.

CHAPTER 5

Summary and Conclusions

Determining the impacts on plankton dynamics of climate change and anthropogenic factors in the Labrador region requires continuous long-term observations of climate and biological and physical properties. Unfortunately, existing observations throughout the Labrador Sea and coast are inadequate to determine the influence of climate variability on the marine ecosystem. The goal of this research was to integrate the available data with simplified ecosystem models to enhance our understanding. The ecosystem model used was the four compartment nutrient-phytoplankton-zooplankton-detritus, NPZD, model of Denman and Pena (1999) forced with historical salinity, temperature and density used to determine mixed-layer depth, solar radiation and initial nitrate concentration. The model was used to determine the plankton ecosystem response to variability in freshwater flow into Hamilton Inlet and the climate changes over the Labrador Sea and Shelf that significantly altered the stratification of these regions (Lazier *et al.*, 2000; Yashayaev, 2002). The model was run for the Labrador Sea and Shelf for periods with different environmental conditions, resulting from climate variability. The model was also run for Hamilton Inlet for the period before and after the hydroelectric development to determine the possible effects of changing freshwater discharge.

Each region in the model exhibited distinct seasonal plankton cycles. The Labrador Sea had a pronounced spring bloom with a slight decrease in N from its winter

maximum concentration. The Shelf had a spring bloom, which depleted the N from its maximum in winter as well as one later in the fall. Hamilton Inlet had an early P bloom in winter, a major bloom in spring, and a smaller bloom in summer. The nutrients in the mixed-layer were completely depleted several times throughout the year, and not just during the blooms.

The mixed-layer in the Labrador Sea and on the Shelf deepened in winter and gradually shallowed in spring. On the Shelf, the mixed-layer remained shallow during spring and part of the summer before deepening again to a maximum by the end of the year. The mixed-layer of the Sea remained shallow from spring straight through to the fall and only deepened slightly by the end of the year. Hamilton Inlet mixed-layer seasonal cycle was opposite. It shallowed in winter during the ice cover and deepened in June with the disappearance of the ice.

It was found that in the Sea and Shelf, the P and Z spring bloom timing was later in the 1990s when the NAO index was positive as compared to the 1960s which exhibited a negative NAO index (Figure 5.1). Also, the total annual P biomass in the Sea increased and Z decreased from the 1960s to the 1990s. However, on the Shelf the total annual biomass of P remained unchanged while the Z decreased slightly from the 1960s to the 1990s. In the 1990s the Shelf also had only one spring bloom of Z while other years showed two blooms of Z following the P blooms. On the Shelf, the P biomass decreased slightly during the 1970s, when there was a slightly negative phase in the NAO index, and the 1980s, when there was a positive phase of the NAO index. The primary productivity on the Shelf generally decreased as the NAO index increased. The NAO

index has been shown to influence the mixed-layer depth, thereby affecting the onset of the spring bloom and the biomass (Mann and Lazier, 1996). Tian *et al.* (2004) also found that the P bloom in the Labrador Sea occurred later in the 1990s than in previous years. Dickson *et al.* (1988a) found that along the coasts of northern Europe and the United Kingdom when the NAO index was positive the bloom was earlier and the biomass was greater. Increased northerly winds during negative phases of the NAO deepens the mixed-layer and delays the P bloom and decreases the annual biomass. The mixed-layer of the model for the Labrador Sea was changed from 800 to 1000 m in 1968 and from 1000 to 2000 m in the 1990s to explore the effects of changes in mixed-layer depth. The deepening of the mixed-layer depth during both periods proved to make little difference in the seasonal plankton dynamics. The Z and P annual biomass decreases when the maximum mixed-layer depth deepened. The annual P biomass increased slightly while the Z biomass decreased slightly.

On the shelf the primary productivity was calculated and compared to fish catch. The primary production changed by less than 10% between the time periods the model was run. The lowest primary productivity was in the 1990s (199 gC/m^2 yr) corresponding to a total sustainable annual fish catch of 3.6 to 4.7 t/km^2 yr based upon the correlation analysis of Harrison and Parsons (2000). This was within the range of the actual total fish catch from NAFO area 2J averaged for the 1990s of 3.8 t/km^2yr. The fish catch for the remainder of the periods were quite high compared to the primary production and did not fit the correlation from Harrison and Parsons (2000).

In Hamilton Inlet there are many factors that can influence plankton dynamics other than climate, such as regulation of river flow and ice cover. This makes it difficult to determine whether changes in plankton dynamics are caused by climate changes or regulation of river flow. Before the 1970s, when the NAO index was negative and the river flow was unregulated, there was a small population of Z, but after 1976 the Z population diminished. After 1976, relative to pre-1970, the timing of the P bloom remained unchanged and the biomass decreased, unlike the Labrador Sea and Shelf. The primary production in the Inlet decreased after 1976 by about 25%, while for the Shelf there was little difference between the time periods. The primary production was correlated with sustainable fish catch using the correlation from Harrison and Parsons (2000). The fish catch decreased from 1.6 to 1.4 t/km^2yr from before 1970 compared to after 1976. The data for Hamilton Inlet before 1970 was quite sparse and to fill in the gaps, data combined from the whole period was used. This may have resulted in fewer changes between the two periods. Also, the light and ice cover were not specific for the time periods investigated.

Comparing all the regions, the spring P bloom timing was earliest on the Shelf. The Inlet P bloom timing was similar to the late timing of the Sea in the 1990s. The Z bloom timing was also earliest on the Shelf. The Inlet was much later. The late timing of the spring blooms in the Inlet can be explained by the ice cover, which remains until June and decreased the mixed-layer depth and solar radiation. The Z annual biomass was greatest in the Sea and decreased from the Sea to the Inlet. The P annual biomass during the 1990s for the Sea was much higher than the other regions. In the 1960s the Sea had

comparable annual P biomass to the Shelf and the Inlet had the lowest P biomass. The nutrient levels in the Sea were the highest and the Shelf and Inlet had progressively less nutrients.

Climate, in addition to affecting bloom timing and phytoplankton abundance could also change certain rate parameters. Li *et al.* (2000) found that model results for the Strait of Georgia and Juan de-Fuca Estuary was sensitive to biological rate parameters. This is similar to the model in the Labrador Sea, which was most sensitive to the zooplankton maximum grazing rate. The model may respond to climate variability by changes in these parameters. For example, an increase in average water temperature may result in faster phytoplankton growth rate.

The NPZD model used is a simple ecosystem model. In order to investigate further plankton response to climate change it would be more realistic to include other state variables in the model such as bacteria or ammonia. Also the zooplankton modeled are mainly microzooplankton. To improve the accuracy, a larger zooplankton parameter could be included that considers life stages and development. However, this simple model used is a necessary first step in understanding the plankton dynamic responses to climate change and anthropogenic effects before pursuing more complex food web models. The physical model is also a simple 1-D model which can also be made more accurate by considering vertical and horizontal advection.

Most importantly for any model study, there is a great need for observations to both force the model and compare the results. The biological data must be more intensive than the bi-monthly measurements provided by satellites images. More

advanced modeling will certainly require more detailed and regular biological and physical observations.

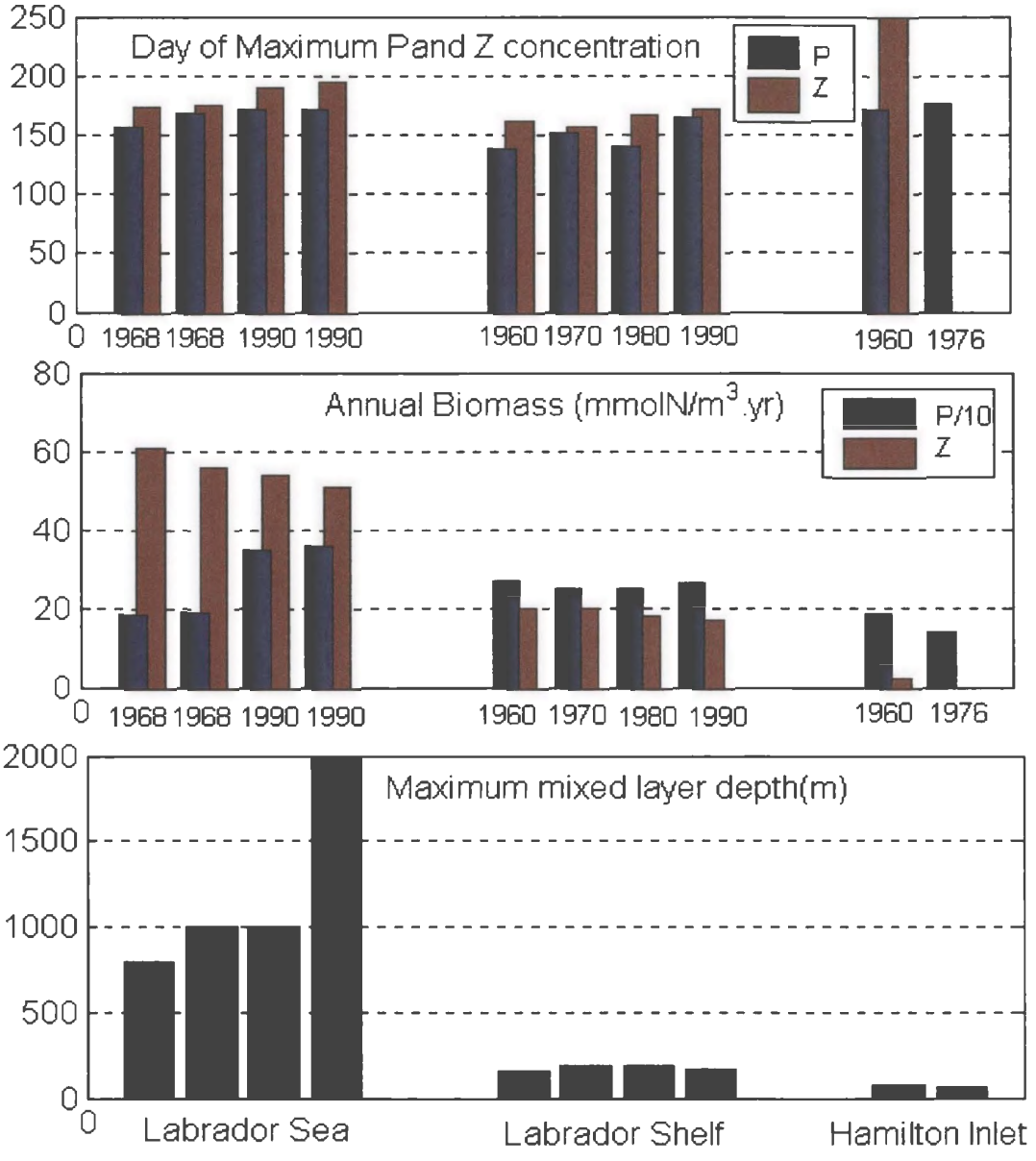

Figure 5.1: Comparison of A) day of maximum P(blue) and Z (red) concentration, B) annual P and Z biomass (mmol N/m^3) and C) maximum mixed-layer depth for the Labrador Sea, Shelf and Hamilton Inlet.

References

Aebischer, N. J., J. C. Coulson and Colebrook J. M. 1990. Parallel long-term trends across four marine trophic levels and weather. Nature 347: 753-755.

Afanasyev, Y. D., N. P. Nezlin and Kostianoy A. G. 2001. Patterns of seasonal dynamics of remotely sensed chlorophyll and physical environment in the Newfoundland region. Remote Sensing Env. 76: 268-282.

Aiken, J., G. F. Moore, D. K. Clark and Trees C. C. 1995. The SeaWiFS CZCS-Type pigment algorithym. NASA Tech. Memo. 104566, vol. 29. S. B. Hooker, E. R. Firestone, Eds. NASA Goddard Space Flight Center, Greenbelt, Maryland, 34pp.

Anderson, L. G., A. R. Coote and Jones E. P. 1985. Nutrient and alkalinity in the Labrador Sea. J. Geophys. Res. 90: 7355-7360.

Anderson, T. R. 1993. A spectrally averaged model of light penetration and photosynthesis. Limnol. Oceanogr. 38: 772-775.

Bobbitt, J. and Akenhead S. 1982. Influence of controlled discharge from the Churchill River on the oceanography of Groswater Bay, Labrador. Can. Tech. Report of Fish. Aquat. Sci. 1097, 43pp.

Buchanan, R. A. and Foy M. S. 1980. Plankton, Nutrients, Chlorophyll, Phytoplankton and Ichthyoplankton. OLABS Program Report (Offshore Labrador Biological studies) prepared by Atlantic Biological Services Ltd., St. John's, NF for Total Eastcan Explorations Ltd., Calgary, AB., 293pp.

Campbell, J. W. and Aarup T. 1992. New production in the North Atlantic derived from seasonal patterns of surface chlorophyll. Deep-Sea Res. 39: 1669-1694.

Campbell, R. W. and Head E. J. H. 2000. Egg production rates of *Calanus finmarchicus* in the western North Atlantic: effect of gonad maturity, female size, chlorophyll concentration, and temperature. Can. J. Fish. Aquat. Sci. 57: 518-529.

Cardoso, D. and deYoung B. 2002. Historical hydrographic data from Goose Bay, Lake Melville and Groswater Bay, Labrador: 1950-1997. Department of Physics and Physical Oceanography, Data Report 2002-2, Memorial University of Newfoundland, St. John's, Newfoundland.

Carlotti, F. and Radach G. 1996. Seasonal dynamics of phytoplankton and *Calalnus finmarchicus* in the North Sea as revealed by a coupled one-dimensional model. Limnol. Oceanogr. 41: 522-539.

Coachman, L. K. 1953. River flow and winter hydrographic structure of the Hamilton Inlet-Lake Melville estuary of Labrador. Blue Dolphin Labrador Expedition – Winter Project 1953, unpublished manuscript, 19pp.

Colbourne, E. 2002. Physical oceanographic conditions on the Newfoundland and Labrador Shelves during 2001. Canadian Science Advisory Secretariat, Research Document 2002/023, 26pp.

Colbourne, E. and Fitzpatrick C. 2002. Physical oceanographic conditions in NAFO subareas 2 and 3 on the Newfoundland and Labrador Shelves during 2001. NAFO SCR Doc. 02/41, 23 pp.

Colbourne, E. 2000. Interannual variations in the stratification and transport of the Labrador Current on the Newfoundland Shelf. ICES CM 2000/L:02, 20pp.

Colebrook, J. M. 1978. Continuous Plankton Records: zooplankton and environment, North-East Atlantic and North Sea, 1948-1975. Oceanologica Acta 1: 9-23.

Conkright, M. E., S. Levitus and Boyer T. P. 1994. World Ocean Atlas 1994. Vol.1: nutrients. NOAA Atlas NESDIS 1, Washington, DC, 150pp.

Conover, R. J. 1968. Zooplankton-life in a nutritionally dilute environment. Amer. Zoologist 8: 107-118.

Cushing, D. H. 1990. Recent studies on long-term changes in the sea. Freshwater Biology 23: 71-84.

Denman, K. L., and Powell T. M. 1984. Effects of physical processes on planktonic ecosystems in the coastal ocean. Oceanogr. Mar. Biol. Ann. Rev. 22: 125-168.

Denman, K. L. and Gargett A. E. 1995. Biological-physical interactions in the upper ocean: The role of vertical and small scale transport processes. Annu. Rev. Fluid Mech. 27: 225-255.

Denman, K. L., M. A. Peña and Haigh S. P. 1998. Simulations of marine ecosystem response to climate variation with a one-dimensional coupled ecosystem/mixed-layer model. Biotic impacts of extratropical climate change: the Pacific, Proceedings 'Aha Huliko'a Hawaiian Winter Workshop, University of Hawaii at Manoa: 141-147.

Denman, K. L. and M. A. Peña. 1999. A coupled 1-D biological/physical model of the northeast subarctic Pacific Ocean with iron limitation. Deep-Sea Res. II 46: 2877-2908.

deYoung, B., and Rose G. A. 1993. On recruitment and distribution of Atlantic cod (*Gadus morhua*) off Newfoundland. Can. J. Fish. Aquat. Sci. 50: 2729-2741.

DFO, 2003. Newfoundland and Labrador snow crab. DFO Science Stock Status Report, 2003/021, 15 pp.

Dickson, R. R., P. M. Kelly, J. M. Colebrook, W. S. Wooster and Cushing D. H. 1988a. North winds and production in the eastern North Atlantic. J. Plank. Res. 10: 151-169.

Dickson, R. R., J. Meincke, S. A. Malmberg and Lee A. J. 1988b. The "great salinity anomaly" in the northern North Atlantic 1968-1982. Prog. Oceanogr. 20:103-151.

Doney, S. C., D. M. Glover, and Najjar R. G. 1996. A new coupled, one-dimensional biological-physical model for the upper ocean: applications to the JGOFS Bermuda Atlantic Time Series (BATS) site. Deep-Sea Res. II 43: 591-624.

Doronin, Y. P. and Kheisin D. E. 1977. Sea-ice. Amerind Publishing Co. Pvt. Ltd., New Deli., 323pp.

Drinkwater, K. F. 1994. Environmental changes in the Labrador Sea and some effects on fish stocks. ICES C.M. Mini: 4., 19pp.

Drinkwater, K. F. and Harding G. C. 2001. Effects of the Hudson Strait outflow on the biology of the Labrador Shelf. Can. J. Fish. Aquat. Sci. 58: 171-184.

Dyer, K. R. 1979. Estuarine hydrography and sedimentation. Cambridge University Press, GB., 230pp.

Edwards, A. M. and Brindley J. 1996. Oscillatory behaviour in a three-component plankton population model. Dynamics and Stability of Systems 11: 347-370.

Edwards, A. M. and Brindley J. 1999. Zooplankton mortality and the dynamical behaviour of plankton population models. Bulletin of Mathematical Biology 61: 303-339.

Edwards, C. A., T. A. Powell and Batchelder H. P. 2000. The stability of an NPZ model subject to realistic levels of vertical mixing. J. Mar. Res. 58: 37-60.

Evans, G. T. and Parslow J. S. 1985. A model of annual plankton cycles. Biol. Oceanogr. 3: 327-347.

Fasham, M. J. R. 1995. Variations in the seasonal cycle of biological production in subarctic oceans: A model sensitivity analysis. Deep-Sea Res. I 42: 1111-1148.

Fasham, M. J. R., H. W. Ducklow and McKelvie S. M. 1990. A nitrogen-based model of plankton dynamics in the oceanic mixed-layer. J. Mar. Res. 48: 591–639.

Fenco Newfoundland Limited 1981. Lake Melville freeze up study 1980: final report. Newfoundland and Labrador Department of Industrial Development report., 128pp.

Fenco Newfoundland Limited 1981. Lake Melville/offshore Labrador winter navigation study 1979-1980: final report. Department of Industrial Development report., 116pp.

Fenco Newfoundland Limited 1982. Lake Melville freeze up and winter navigation study 1981-1982: final report. Newfoundland and Labrador Department of Industrial Development report. Vol. I: chap. 1-7, Vol. II: chap. 1-14.

Franks, P. J. S., J. S. Wroblewski and Flierl G. R. 1986. Behaviour of a simple plankton model with food-level acclimation by herbivores. J. Mar. Biol. 91: 121-129.

Franks, P. J. S. 1995. Coupled physical-biological models in oceanography. Rev. Geophys. Supp. July: 1177-1187.

Franks, P. J. S. and Walstad L.J. 1997. Phytoplankton patches at fronts a model of formation and response to transient wind events. J. Mar. Res. 55: 1-30.

Franks, P. J. S. 2002. NPZ models of plankton dynamics: Their construction, coupling to physics, and application. J. Oceanogr. 58: 379-387.

Frost, B. W. 1993. A modeling study of processes regulating plankton standing stock and production in the open subarctic Pacific Ocean. Prog. Oeanogr. 32: 17-56.

Harrison, P. J. and Parsons T. R. 2000. Fisheries oceanography: An integrative approach to fisheries ecology and management. Blackwell Science Ltd., MA USA. 347pp.

Hooker, S. B., W. E. Esaias, G. C. Feldman, W. W. Gregg and McClain C. R. 1992. An overview of SeaWiFS and Ocean colour. NASA Tech. Memo. 104566, vol. 1. S. B. Hooker, E. R. Firestone, Eds. NASA Goddard Space Flight Center, Greenbelt, Maryland, 24pp.

Hutchings, J. A. 1996. Spatial and temporal variation in the density of northern cod and a review of hypotheses for the stock's collapse. Can. J. Fish. Aquat. Sci. 53: 943-962.

Hutchings, J. A., and Myers R. A. 1994. What can be learned from the collapse of a renewable resource? Atlantic cod, *Gadus Morhua*, of Newfoundland and Labrador. Can. J. Fish. Aquat. Sci. 51: 2126-2146.

Hydro Lower Churchill Development Corporation Limited, 1980. Lower Churchill Project Generation Facilities Enviornmental Impact Statement (Volume II), 383pp.

Ikeda, M. 1987. Salt and heat balances in the Labrador Sea using a box model. Atmos.-Ocean 25: 197-223.

Iqbal, M. 1983. Introduction to solar radiation. Academic Press, Toronto, 390pp.

Irwin, B., C. Caverhill, C. Mossman, E. Horne and Platt T. 1989. Primary productivity on the Labrador Shelf during July 1985. Can. Rep. Fish. Aquat. Sci. 760: 115pp.

Irwin, B., C. Caverhill, P. Dickie, E. Horne and Platt T. 1986. Primary productivity on the Labrador Shelf during June and July 1984. Can. Rep. Fish. Aquat. Sci. 577: 162pp.

Irwin, B., J. Anning, C. Caverhill and Platt T. 1990. Primary production on the Labrador Shelf and in the Strait of Bell Isle in May 1988. Can. Rep. Fish. Aquat. Sci. 784: 96pp.

Irwin, B., P. Evans and Platt T. 1978. Phytoplankton productivity experiments and nutrient measurements in the Labrador Sea from 15 October to 31 October 1977. Fish. Mar. Serv. Data Rep. 83: 40pp.

Irwin, B., W. G. Harrison, C. L. Gallegos and Platt T. 1978. Phytoplankton productivity experiments and nutrient measurements in the Labrador Sea and Davis Strait, Baffin Bay, and Lancaster Sound from 26 August to 14 September 1978. Can. Rep. Fish. Aquat. Sci. 213: 103pp.

Lavender, K. L. and Davis R. E. 2002. Observations of open-ocean deep convection in the Labrador Sea from subsurface floats. J. Phys. Oceanogr. 32: 511-526.

Lazier, J. R. N. 1980. Oceanographic conditions at Ocean Weather Ship Bravo, 1964-1974. Atmos. Ocean 18: 227-238.

Lazier, J. R. N. and D. G. Wright, 1993. Annual velocity variations in the Labrador Current. J. Phys. Oceanogr. 23: 659-678.

Lazier, J. R. N. 1982. Seasonal variability of temperature and salinity in the Labrador Current. J. Mar. Res. 40: 341-356.

Lazier, J. R. N. and D. G. Wright, 1988. Temperature and salinity changes in the deep Labrador Sea. 1962-1986. Deep-Sea Res. 35: 1247-1253.

Lazier, J. R. N, R. Hendry, A. Clarke, I. Yashayaev and Rhines P. 2002. Convection and restratification in the Labrador Sea, 1990-2000. Deep-Sea Res. I 49: 1819-1835.

Li, M., A. E. Gargett and Denman K. L. 2000. What determines seasonal and interannual variability of phytoplankton and zooplankton in strongly estuarine systems? Application to the semi-enclosed estuary of strait of Georgia and Juan de Fuca Strait. Estuarine, Coastal and Shelf Sci. 50: 467-488.

Loder, J. W., B. Petrie and Gawarkiewicz G. 1995. The coastal ocean off northeastern North America: A large scale view. The Sea: The global coastal ocean processes and methods, K. H. Brink and A. R. Robinson, eds. John Wiley & Sons, Inc., vol. 10: 604pp.

Loder, J. W., W. C. Boicourt and Simpson J. H. 1998. Western ocean boundary shelves coastal segment (W). The Sea: Ideas and observations on progress in the study of the seas, K. H. Brink and A. R. Robinson, eds. John Wiley & Sons, Inc., vol. 11: 3-28.

Longhurst, A., S. Sathyendranath, T. Platt and Caverhill C. 1995. An estimate of global primary production in the ocean from satellite radiometer data. J. Plank. Res. 17: 1245-1271.

Louanchi, F. and Najjar R. G. 2001. Annual cycles of nutrients and oxygen in the upper layers of the North Atlantic Ocean. Deep-Sea Res. II 48: 2155-2171.

Maclaren Atlantic Ltd. 1976. Preliminary summary of results of Imperial Oil environmental cruise program. Halifax, 57 pp.

Mann, K. and Lazier J. 1996. Dynamics of marine ecosystems: Biological-Physical interactions in the oceans. Blackwell Science Inc, 2nd ed., MA, US. 394 pp.

Marra, J. and Ho C. 1993. Initiation of the spring bloom in the northeast Atlantic (47°N, 20°W): a numerical simulation. Deep-Sea Res. II 40: 55-73.

McClain, C. R, W. E. Esaias, W. Barnes, B. Guenther, D. Endres, S. Hooker, G. Mitchell and Barnes R. 1992. Calibration and validationplan for SeaWiFS. NASA Tech. Memo. 104566, vol. 3. S. B. Hooker, E. R. Firestone, Eds. NASA Goddard Space Flight Center, Greenbelt, Maryland, 41pp.

McGillicuddy, D. J. 1995. One dimensional numerical simulation of new primary production: Lagrangian and Eulerian formulations. J. Plank. Res., 17, 405-412.

Memorial University of Newfoundland, Faculty of Engineering and Applied Science 1974. Lake Melville ice research, 1973-1974, report no. III. Ocean Engineering Group, Memorial University of Newfoundland, 145pp.

Memorial University of Newfoundland, Faculty of Engineering and Applied Science 1973. Lake Melville ice research, 1972-1973, Appendices Vol. I. Ocean Engineering Group, Memorial University of Newfoundland, 154pp.

Memorial University of Newfoundland, Faculty of Engineering and Applied Science 1973. Lake Melville ice research, 1972-1973, Appendices Vol. II. Ocean Engineering Group, Memorial University of Newfoundland, 51pp.

Myers, R. A., G. Mertz and Helbig J. A. 1990. Long period changes in the Salinity of Labrador Sea Water. ICES C.M. C:21: 8pp.

Myers, R. A., N. J. Barrowman, G. Mertz, J. Gamble and Hunt H. G. 1994. Analysis of continuous plankton recorder data in the Northwest Atlantic 1959-1992. Can. Tech. Rep. Fish. Aquat. Sci. 1966: 246pp.

Newfoundland Fisheries Research Station 1952. Report of the Newfoundland Fisheries Research Station for 1952. The Station, 1951-1955, St John's, NF. 15pp., Appendix (3): Investigator II-Lake Melville, 2-3.

Newfoundland Fisheries Research Station 1953. Report of the Newfoundland Fisheries Research Station for 1953. The Station, 1951-1955, St John's, NF. 12pp., Appendix: Exploration of the Hamilton Inlet Bank, Labrador, 11-13. Appendix (35): Hydrography-Lake Melville, 53-54.

Nutt, D. C. 1950. The Blue Dolphin Labrador Expedition; field report 1950. Unpublished manuscript, 11pp.

Nutt, D. C. 1951. The Blue Dolphin Labrador Expeditions, 1949 and 1950. Arctic 4, (1): 3-11.

Nutt, D. C. 1952. The Blue Dolphin Labrador Expedition; field report 1952. Unpublished manuscript, 9pp.

Nutt, D. C. 1953. The Blue Dolphin Labrador Expedition, Winter Project; field report 1953. Unpublished manuscript, 4pp.

Parsons, T. R., M. Takahashi and Hargrave B. 1984. Biological Oceanographic Processes. Pergamon Press, New York, 330 pp.

Pavshtiks, E. A. 1968. The influence of currents upon seasonal fluctuations in the plankton of the Davis Strait. 2nd European Sym. Mar. Biol. 34: 383-392.

Pepin, P. and Maillet, G. L. 2002. Biological and chemical oceanographic conditions on the Newfoundland Shelf during 2001 with comparisons with earlier observations. Canadian Science Advisory Secretariat, Research Document 2002/052, 60pp.

Petrie, B., P. Yeats and Strain P. 1999. Nitrate, Silicate and Phosphate Atlas for the Scotian Shelf and the Gulf of Maine. Can. Tech. Rep. Hydrogr. Ocean Sci. 203, vii-96pp.

Petrie, B., J. W. Loder, S. Akenhead and Lazier J. 1992. Temperature and Salinty variabilility on the eastern Newfoundland Shelf: the residual field. Atmos.-Ocean 30: 120-139.

Pickart, R. S., and Emery W. J. 1982. Descriptive physical oceanography an introduction. Pergamon Press Canada Ltd., Ontario. 249pp.

Pickart, R. S., S. Fiammetta and Moore G. W. K. 2003. Is Labrador Sea water formed in the Irminger basin?. Deep-Sea Res. I, 50: 23-52.

Planque, B. and Taylor A. H. 1998. Long-term changes in zooplankton and the climate of the North Atlantic. ICES J. Mar. Sci. 55:644-654.

Platt, T., S. Sathyendranath, and Ravindran P. 1990. Primary production by phyto-plankton: analytic solutions for daily rates per unit area of water surface. Proc. R. Soc. Lond. Ser. B 241: 101-111.

Raymont, J. E. G. 1980. Plankton and productivity in the oceans. Vol. 1, Oxford; New York: Pergamon Press, 489pp.

Riley, G. 1946. Factors controlling phytoplankton populations on Georges Bank. J. Mar. Res. 6: 54-73.

Rose, G. A., B. deYoung, D. W. Kulka, S.V. Goddard, and Fletcher G. L. 2000. Distribution shifts and overfishing the northern cod (*Gadus morhua*): a view from the ocean. Can. J. Fish. Aquat. Sci. 57: 644-664.

Sarmiento, J. L., R. D. Slater, M. J. R. Fasham, H. W. Ducklow, J. R. Toggweiler, and Evans G. T. 1993. A seasonal three-dimensional ecosystem model of nitrogen cycling in the North Atlantic euphotic zone. Global Biogeochem. Cycles 7: 379-415.

Sathyendranath, S., and Platt T. 1988. The spectral irradiance field at the surface and in the interior of the ocean: A model for applications in oceanography and remote sensing. J. Geophys. Res. 93: 9270-9280.

Saunders, D. 1981. The absence of Codfish in Groswater Bay, with emphasis on the Pack's Harbour fishery. Department of Fisheries and Oceans Canada.

Shuby, J. L 1969. Oceanographic Observations. North Atlantic Ocean Station Bravo United States Coast Guard Oceanographic Report No. CG 373-20, 450pp.

Shuby, J. L 1974. Oceanographic Observations. North Atlantic Ocean Station Bravo United States Coast Guard Oceanographic Report No. CG 373-63, 160pp.

Siegel, D. A., S. C. Doney and Yoder J. A. 2002. The North Atlantic spring phytoplankton bloom and Sverdrups critical depth hypothesis. Science 296: 730-733.

Smith, S. D. and Dobson, F. W. 1984. The heat budget at Ocean Weather Station Bravo. Atmos.-Ocean 22: 1-22.

Steele, J. H. 1998. From carbon flux to regime shift. Fish Oceanogr. 7: 176-181.

Steele, J. H. and Henderson E. W. 1992. The role of predation in plankton models. J. Plankton Res. 14: 157–172.

Stuart, V., S. Sathyendranath, E. J. H. Head, T. Platt, B. Irwin and Maass H. 2000. Bio-optical characteristics of diatom and prymnesiophyte populations in the Labrador Sea. Mar. Ecol. Prog. Ser. 201: 91-106.

Sutcliffe, W. H. 1983. Nutrient flux onto Labrador Shelf from Hudson Strait and its biological consequences. Can. J. Fish. Aquat. Sci. 40: 1692-1701.

Sutcliffe, W. H. 1972. Some relations of land drainage, particulate material and fish catch in two eastern Canadian bays. Can. J. Fish. Aquat. Sci. 29: 357-362.

Sutcliffe, W. H. 1973. Correlations Between Seasonal River Discharge and Local Landings of American Lobster (*Homarus americanus*) and Atlantic Halibut (*Hippoglossus*) in the Gulf of St Lawrence. Can. J. Fish. Aquat. Sci. 30: 856-859.

Sverdrup, H. U. 1953. On Conditions for vernal blooming of phytoplankton. J. Cons. Int. Explor. Mer. 18: 287-295.

Taggart, C.T., J. Anderson, C. Bishop, E. Colbourne, J. Hutchings, G. Lilly, J. Morgan, E. Murphy, R. Myers, G. Rose, and Shelton P. 1994. Overview of cod stocks, biology, and environment on the Newfoundland Shelf. Cod and Climate Changes. ICES mar. Sci. Symp. 198:140-157.

Tang, C. L. and DeTracey B. M. 1998. Space-time variation ofmixed-layer properties, heat and salt fluxes, and ice melt in the Newfoundland marginal ice zone. J. Geophys. Res. 103, no. C1: 1177-1191.

Tang, C. L., Q. Gui, and DeTracey B. M. 1999. A modeling study of upper ocean winter processes in the Labrador Sea. J. Geophys. Res. 104, no. C10: 23,411-23,425.

Taylor, A. H. 1995. North-South shifts of the Gulf Stream and their climatic connection with the abundance of zooplankton in the UK and its surroundings seas. ICES J. Mar. Sci. 52: 711-721.

Taylor, A. H., A. J Watson, M. Ainsworth, J. E. Robertson and Turner D. R. 1991. A modeling investigation of the role of phytoplankton in the balance of carbon at the surface of the North Atlantic. Global Biogeochem. Cycles 5: 151-171.

The Labrador Sea Deep Convection Experiment. 1998. Bulletin of the American Meteorological Society: Vol. 79, pp. 2033–2058.

Tian, R. C., D. Deibel, R. B. Rivkin and Vezina A. F. 2004. Sensitivity of Biogenic carbon export to ocean climate in the Labrador Sea, a deep-water formation region. Global Biogeochem. Cycles 17: 1-11.

Tian, R. C., A. F. Vezina, M. Starr and Saucier F. 2001. Seasonal dynamics of coastal ecosystems and export production at high latitudes: A modeling study. Limnol. Oceanogr. 46: 1845-1859.

Tolmazin, D. 1985. Changing coastal oceanography of the Black Sea. I: Northwestern Shelf. Prog. Oceanog. 15: 217-276.

Trela, P. 1996. Effect of spatial and temporal variability in oceanic processes on air-sea fluxes of carbon dioxide. PhD thesis, Dalhousie University, Halifax, 221pp.

Walsh, J. J. 1983. Death in the Sea: Enigmatic phytoplankton losses. Prog. Oceanogr. 12: 1-86.

Webb, W. L., M. Newton and Starr D. 1974. Carbon dioxide exchange of *Alnus rubra*: A mathematical model, Oceologia 17: 281-291.

Welschmeyer, N. A, S. Strom, R. Goericke, G. R. DiTullio, M. Belvin, and Peterson W. 1993. Primary production in the subarctic Pacific: Project SUPER. Prog. Oceanogr. 32: 101-135.

Wroblewski, J. S. 1977. A model of phytoplankton plume formation during variable Oregon upwelling. J. Marine Res. 35: 357-394.

Wroblewski, J. S. 1989. A model of the spring bloom in the North Atlantic and its impact on ocean optics. Limnol. Oceanogr. 34: 1563-1571.

Wroblewski, J. S., J. L. Sarmiento and Flierl G. R. 1988. An ocean-basin scale model of plankton dynamics in the North Atlantic. Part I. Solutions for the climatological oceanographic conditions in May. Global Biogeochem. Cycles 2: 199-218.

Yashayaev, I. 2002. Oceanographic conditions in the Labrador Sea in the 1990s and in the context of interdecadal variability. NAFO SCR Doc. 02/51, 1pp.

Appendix 1: Calculation of Incoming Solar Radiation

The incoming solar radiation is computed based on equations from Iqbal (1983) as follows:

Correction for sun-earth distance due to earth's elliptical orbit:

$\Gamma = 2 * \pi * (day - 1)/365$ (equation 1.2.2, pp.3 (Iqbal 1983))

$E_o = 1.000110 + 0.034221*\cos(\Gamma) + 0.001280*\sin(\Gamma) + 0.000719*\cos(2 * \Gamma)$

$+ 0.000077*\sin(2*\Gamma)$ (equation 1.2.1, pp.3 (Iqbal 1983))

Solar declination (δ) is the angle of the line joining the centers of the sun and earth to the equatorial plane in units of degrees:

$\delta = (0.006918 - 0.399912*\cos(\Gamma) + 0.070257*\sin(\Gamma) - 0.006758*\cos(2*\Gamma) +$

$0.000907*\sin(2*\Gamma) - 0.002697*\cos(3*\Gamma)+0.00148*\sin(3*\Gamma)) * (180/\pi)$

(equation 1.3.1, pp.7 (Iqbal 1983))

Convert to units of radians: $\delta\_rad = \delta*\pi/180;$

Calculate sunrise hour angle (w_s) in units of degrees:

$w_s = \cos^{-1}(-\tan(lat\_rad) * \tan(\delta\_rad))$ (equation 1.5.4, pp. 16, (Iqbal 1983))

Convert to units of radians: $w_s\_deg = w_s * 180/\pi$

Calculate incoming radiation for particular day on a horizontal surface (Ho) in units of MJ/m^2*day:

$Ho = (24/\pi) * Isc * E_o *((\pi/180) * w_s\_deg * (\sin(\delta\_rad) * \sin(lat\_rad)) +$

$(\cos(\delta\_rad) * \cos(lat\_rad) * \sin(w_s)))$ (equation 4.2.18, pp. 64, (Iqbal 1983))

where Γ is the day angle in units of radians, Isc is the solar constant 1367W/ m^2 and lat_rad is the latitude in radians.

Appendix 2: Parameter values reported in Literature

Parameter	Symbol	Units	Value	Reference	Location
PAR attenuation coefficient for sea water	k_w	m^{-1}	0.04	Fasham *et al.* (1990), Fasham (1995), Denman and Pena (1999), McGillicuddy (1995), Sarmiento *et al.* (1993)	Station S Bermuda, OWS P, OSP, N. Atlantic
			0.06	Sathyendranath and Platt (1988), Trela (1996)	OWS P, Labrador Sea
			0.08	Marra and Ho (1993)	N. East Atlantic
			0.10	Evans and Parslow (1985)	N. Atlantic and Pacific
			0.2, 0.04-0.2	Edwards and Brindley (1999)	
PAR attenuation coefficient for (P + D)	k_c	m^{-1} (mmol N/m^3)$^{-1}$	0.023	Sathyendranath and Platt (1988), Trela (1996)	OWS P, Labrador Sea
			0.03	Fasham *et al.* (1990), Sarmiento *et al.* (1993)	Station S Bermuda, N. Atlantic
			0.06	Fasham (1995), Denman and Pena (1999)	OWS P, OSP
			0.12	Evans and Parslow (1985)	N. Atlantic and Pacific
			0.4, 0.3 – 1.2 m^2 / g C	Edwards and Brindley (1999)	
Initial slope of P-I curve	α	d^{-1} (W/ m^2) $^{-1}$	0.025	Fasham *et al.* (1990), Sarmiento *et al.* (1993)	Station S Bermuda, N. Atlantic
			0.04	Sathyendranath and Platt (1988), Evans and Parslow (1985)	OWS P, N. Atlantic and Pacific
			0.05	Doney *et al.* (1996), Tian *et al.* (2004)	Station S Bermuda, Labrador Sea
			0.08	Denman and Pena (1999)	OSP
			0.14	Welschmeyer *et al.* (1993)	OWS P

Parameter	Symbol	Units	Value	Reference	Location
Initial slope of P-I curve	α	d^{-1} $(W/m^2)^{-1}$	0.025, 0.083, 0.14	Fasham (1995)	OWS P
			0.028, 0.048,0.06	Trela (1996)	Labrador Sea
		d^{-1} $(Ein/m^2)^{-1}$	0.35, 0.32, 0.272, 0.216	Welschmeyer *et al.* (1993)	OWS P
			0.35	Frost (1993)	OWS P
Maximum P growth rate			2.9	Fasham *et al.* (1990)	Station S Bermuda
			1.25, 2.0	Fasham (1995)	OWS P
			2.0	Evans and Parslow (1985), Denman and Pena (1999), Edwards *et al.* (2000)	N. Atlantic and Pacific, OSP
			2.1	Doney *et al.* (1996)	Station S Bermuda
			0.435, 0.217-1.3	Li *et al.* (2000)	Pacific
			1.0, 0.9, 0.64	Trela (1996)	Labrador Sea
			0.96	Tian *et al.* (2004)	Labrador Sea
			0.9	Marra and Ho (1993)	N. East Atlantic
N half saturation constant	k_n	mmol N/m^{-3}	0.1	Denman and Pena (1999), Frost (1993), Edwards *et al.* (2000)	OWS P, OSP
			0.2	Doney *et al.* (1996), Marra and Ho (1993)	Station S Bermuda, N. East Atlantic
			0.5	Evans and Parslow (1985), Fasham (1995), Fasham *et al.* (1990)	N. Atlantic and Pacific, OWS P
			1.5, 1-2	Li *et al.* (2000)	Pacific
			0.03, 0.02 – 0.15 gC/m^3	Edwards and Brindley (1999)	

Parameter	Symbol	Units	Value	Reference	Location
P mortality rate	m_{pd}	d^{-1}	0.045, 0.09	Fasham *et al.* (1990)	Station S Bermuda
			0.05, 0.06	Fasham (1995)	OWS P
			0.07	Evans and Parslow (1985)	N. Atlantic and Pacific
			0.075	Doney *et al.* (1996)	Station S Bermuda
			0.05	Denman and Pena (1999)	OSP
			0.15	Marra and Ho (1993)	N. East Atlantic
			0.0435, 0.087, 0.0217-0.109	Li *et al.* (2000)	Pacific
			0.1	Wroblewski *et al.* (1986), Edwards *et al.* (2000)	
Z maximum grazing rate	r_m	d^{-1}	1.0	Evans and Parslow (1985), Denman and Pena (1999), Fasham *et al.* (1990), Doney *et al.* (1996)	N. Atlantic and Pacific, Station S Bermuda, OSP
			0.2	Fasham (1995)	OWS P
			0.01- 0.6	Parsons *et al.* (1984)	
			0.6, 0.6 – 1.4	Edwards and Brindley (1999)	
			0.5	Trela (1996), Wroblewski *et al.* (1988), Marra and Ho (1993)	Labrador Sea, N. East Atlantic
			0.1, 0.25	Tian *et al.* (2004)	Labrador Sea
			0.174, 0.087, 0.0289-0.867	Li *et al.* (2000)	Pacific
			0.5, 4.0	Edwards *et al.* (2000)	

Parameter	Symbol	Units	Value	Reference	Location
Z assimilation efficiency	g_a		0.75, 0.5	Fasham (1995)	OWS P
			0.75	Fasham *et al.* (1990), Trela (1996), Wroblewski *et al.* (1988), Sarmiento *et al.* (1993)	Station S Bermuda, Labrador Sea, N. Atlantic
			0.7	Denman and Pena (1999), Doney *et al.* (1996), Wroblewski *et al.* (1986)	Station S near Bermuda, OSP
			0.5	Evans and Parslow (1985)	N. Atlantic and Pacific
			0.6 – 0.95	Conover (1968)	
			0.10 – 0.20	Parsons *et al.* (1984)	
			0.3, 0.7	Edwards *et al.* (2000)	
Z grazing half saturation constant	k_p	mmol N/m^3	0.4	Denman and Pena (1999)	OSP
			0.283	Frost (1993)	OWS P
			1.0	Fasham (1995), Evans and Parslow (1985), Fasham *et al.* (1990), Sarmiento *et al.* (1993)	OWS P, N. Atlantic and Pacific, Station S Bermuda
			1.5, 1-2	Li *et al.* (2000)	Pacific
			0.035, 0.02 – 0.1 gC/m3	Edwards and Brindley (1999)	
Z losses to nitrogen	m_{zn}	d^{-1}	0.2	Denman and Pena (1999)	OSP
Z losses to detritus	m_{zd}	d^{-1}	0.05	Denman and Pena (1999)	OSP
D sinking speed	w_s	$m\ d^{-1}$	0, 3, 6, 10	Denman and Pena (1999)	OSP
			5	Fasham (1995)	OWS P
			1, 10	Fasham *et al.* (1990)	Station S Bermuda
D remineralization rate	r_e	d^{-1}	0.1	Denman and Pena (1999), Doney *et al.* (1996)	Station S Bermuda, OSP
			0.05	Fasham (1995), Fasham *et al.* (1990)	OWS P
			0.05-0.07	Frost (1993)	OWS P

Appendix 3: Model Sensitivity

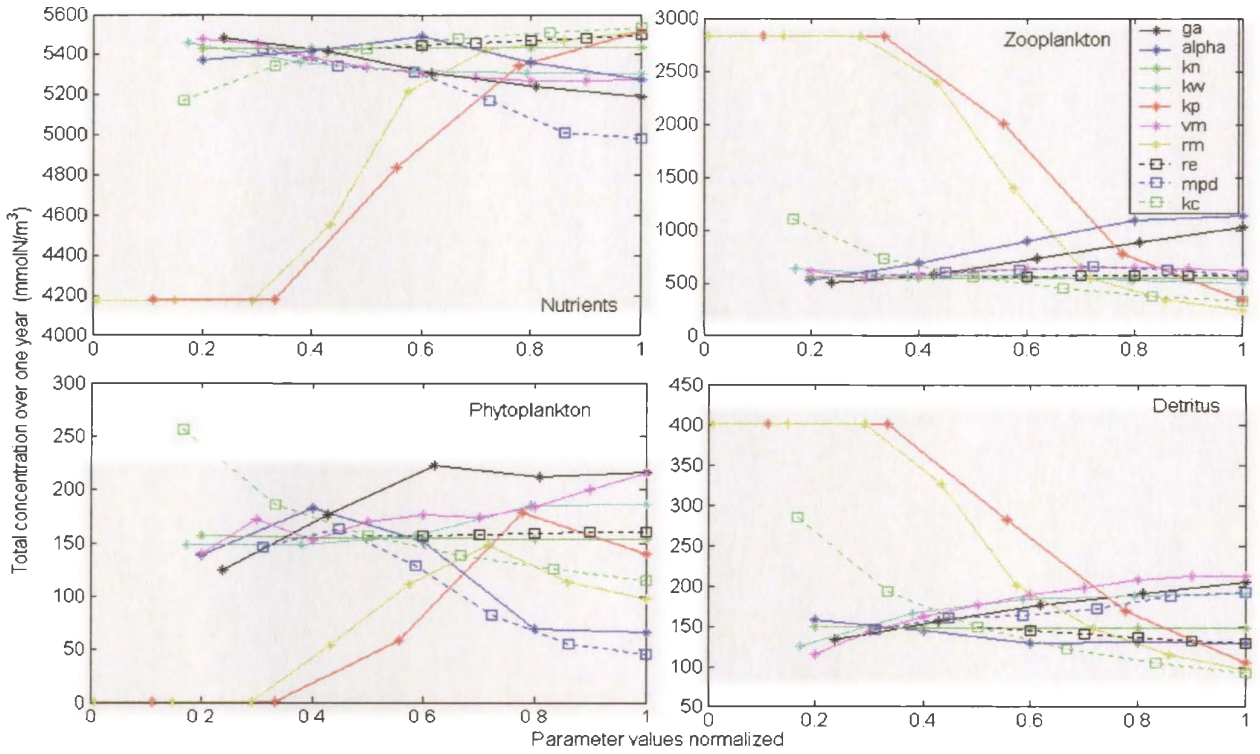

Figure A.0.1 Normalized range of each parameter and the corresponding total concentration over one year of N, P, Z and D from NPZD model simulations using Bravo station 1968 data.